Building and testing models of cosmic inflation with modified gravity

Chris Longden

Submitted for the degree of Doctor of Philosophy

School of Mathematics and Statistics

August 11, 2018

supervised by

Prof. Carsten van de Bruck

Abstract

Cosmic inflation, the idea that the very early universe underwent a dramatic accelerating expansion of space, has found great success in explaining aspects of the universe that were previously poorly understood. As a result, it has gained popularity and traction in the scientific mainstream in recent decades. However, it is still unclear exactly how inflation could have occurred; nothing in the established laws of physics can explain it. Now, in the modern era of precision cosmology, experimental data capable of probing and testing the details of this epoch has become available. With this, a deeper understanding of the physics of inflation may be possible, and it may prove to be the key to unlocking some of the greatest unsolved mysteries in theoretical physics.

In this thesis, models of beyond-standard-model physics, with a particular focus on those inspired by modified theories of gravity (those that extend Einstein's theory of General Relativity), are studied with the goal of understanding their inflationary consequences and hence establish how feasible these exotic theories are as descriptions of the early universe from this perspective. Additionally, some thought is given to present and future tests of inflation as well as how new data, or improvements in the presently available data, will increase cosmologists' ability to discriminate between different theories of inflation and hence move closer to answering the question of what caused it once and for all.

Preface to the thesis

This is a thesis consisting of research on the general theme of models of cosmic inflation and modifications of Einstein's theory of gravitation, general relativity. In an effort to be largely self-contained, this thesis is divided into two major parts. There will be a series of introductory chapters reviewing the background and key equations/results that will be used and referred to later in the subsequent series of chapters presenting my original research. To give an overview of the chapters comprising the thesis, we have:

- Background Review
    1. Introduction
    2. Gravity
    3. Cosmology
- Original Research
    4. Disformally Coupled Inflation
    5. Inflation and the Gauss-Bonnet term
    6. Testing Inflation with the Running of the Running of the Spectral Index

This will be followed with some brief concluding remarks.

7. Conclusions

The content presented in this thesis is based on the original work of the author except in a few specific cases where results produced by collaborators are used. In particular, it is noted that the derivation of equation (5.3.17) was done by Charlotte Owen of Lancaster University, as was the application of our results described in Chapter 5 to obtaining the data in Table 5.1.

Acknowledgements

I first give thanks to the scientists and fellow students I have collaborated with on research projects, as well as those with whom I have enjoyably discussed my work throughout my postgraduate studies. My interactions with Konstantinos Dimopoulos, Tomi Koivisto, Jurgen Mifsud, Charlotte Owen, Laura Paduraru and Mat Robinson have helped shape my growth as a researcher, as a physicist, and as a mathematician over the past four years. On a similar note, I thank all the lecturers and teachers who provided my formal education leading up to this, as well as my parents for providing the environment which allowed me the freedom to pursue and dedicate myself to my educational and intellectual goals, from childhood to adulthood.

To Marysia, I give my thanks for helping me find the mental strength needed to come this far, and for endlessly and unconditionally[1] supporting me with sound advice.

Finally, it is an understatement to say that these acknowledgements would not be complete without a mention of Carsten who I have been privileged to have as a supervisor and friend. On both a personal and professional level, I don't think I could have asked for anything better. Whether discussing the intricacies of cosmological perturbation theory, or simply talking about life in general, I have enjoyed and benefited from all our meetings and conversations, and as a result I have emerged from my postgraduate studies as a more capable, accomplished and confident person. Truly, thank you.

[1] At worst, subject to the occasional bribe with chocolate.

"*Much human ingenuity has gone into finding the ultimate Before. The current state of knowledge can be summarized thus: In the beginning, there was nothing, which exploded.* "

- Sir Terry Pratchett, *Lords and Ladies*, 1992

CONTENTS

CHAPTER 1

INTRODUCTION

Cosmology is the study of the whole universe as a physical system. Humanity has sought to answer fundamental questions about the universe, its beginning, and its end, for thousands of years and creation mythologies are often a key part of many cultures and religions. While, historically, cosmology firmly resided in the domains of theology and philosophy, with time, people came to apply the scientific method to the subject of the universe we inhabit, leading to the present day where physical cosmology is a well-established scientific field. The modern scientific approach to cosmology often involves working with the two main pillars of modern theoretical physics: General Relativity (GR),[1] which classically describes the nature of space, time and gravity, and the Standard Model of particle physics which describes all other known particles and forces within the framework of Quantum Field Theory.[2–4] Particle physics tells us what kinds of matter exist in the universe, and General Relativity tells us how that matter can cause spacetime to curve, expand, or contract. For the past century, these two paradigms have become increasingly more empirically supported by a growing body of experimental tests, culminating with the recent discoveries of gravitational waves[5,6] and the Higgs Boson.[7,8] Parallel to this, cosmologists have been applying ideas from these theories in order to understand the billions of years of our universe's history since its inception, and for the most part

this has been a successful scientific endeavour, leading to the establishment of the "Hot Big Bang" Cosmology.[9–12] In this framework, the early universe is immensely hot and dense, but cools as spacetime expands to approach the less extreme universe we live in today. The expansion of the universe is initially quite fast, but decelerates with time as it passes through the epochs of radiation domination and matter domination. It is under these initially hot, but expanding and hence cooling, conditions that the key quantitative predictions of modern cosmology have been made and subsequently had their veracity confirmed scientifically. This includes the theory of primordial nucleosynthesis,[13] which details the process of the initial formation of the chemical elements once the universe had cooled sufficiently to allow nuclei to stably exist, as well as the identification of Cosmic Microwave Background (CMB) radiation[14] with the newly free-streaming photons from the moment when the universe similarly became cool enough to allow neutral atoms to form. The consistency of many such details and observations established the Hot Big Bang model as the widely accepted scientific mainstream.

Despite the overwhelming success of the Hot Big Bang in explaining large parts of our universe's history, significant open problems remain. We find from observations of type Ia supernovae[15–17] that the expansion of the universe is currently accelerating due to the apparent presence of an unknown "dark energy". Similarly, the observed rotation profiles of galaxies suggest the presence of an invisible but gravitating "dark matter".[18–23] Together, this so-called "dark sector", which cannot be accounted for by the present mainstream understanding of particle physics and gravity, can be inferred to comprise some 95 %[24] of the contents of the universe. It is both astonishing and immensely interesting that even with theories as successful as General Relativity and the Standard Model in describing the physics we experience on and around the planet Earth, we only fully understand a small fraction of our wider universe. Nonetheless, by taking into account the empirical abundance of "dark" quantities, the cosmological model was refined to include them, resulting in the ΛCDM model of cosmology. While it posits the existence of dark matter and dark energy as needed, it does not explain where they come from or how the standard model of particle physics and/or GR would need to be improved to account for

them. Furthermore, because of this inability to explain the observed present state of the universe's expansion, we cannot answer one of the biggest questions in all cosmology that has drawn attention since ancient times: how will the universe come to an end? Will it expand forever until an eventual "heat death", or will it perhaps recollapse in a "big crunch" scenario?[25–28] Unless we come to understand more of *what* dark energy is and not just how much of it there is right now, we will not be able to make such future forecasts with certainty.

Equally as tantalising as our lack of an answer as to how the universe will end, is our lack of an answer to how it began. As the quote in the preface of this thesis wittily puts it, the Hot Big Bang has little more to say in response to this question than "at first there was nothing, which then exploded". It is, of course, not possible to simply walk up to the very early universe and directly study it. However, relics from the distant past of the universe that still exist today can provide us with important hints. In particular, the CMB radiation is homogeneous on scales that appear to violate causality. This is the so-called Horizon Problem[29] which cannot be resolved within the framework of the Hot Big Bang. Similarly, experiments suggest that space itself is geometrically flat, or at least indistinguishably close to flatness, despite the fact that the standard cosmology would require an immense fine tuning of the initial curvature of spacetime to achieve this, also known as the Flatness Problem.[30] Additionally, the non-observation of magnetic monopoles synthesised in the extremely hot early universe is known as the Monopole Problem,[31] completing the infamous trinity of problems with the Hot Big Bang. Inconsistencies such as these with the standard Big Bang cosmology have led to the proposition that in the distant past, during the first fraction of a second after the universe's beginning, it must have undergone an accelerating expansion. This early-universe accelerated expansion is known as *inflation*.[32–36] Note that while the expansion of the universe is also accelerating today, in order to not ruin the aforementioned successes of the Hot Big Bang model, the expansion of the universe would appear to need to tantalisingly stop accelerating before the epoch of e.g. primordial nucleosynthesis, and then resume acceleration at much later times.

While the hypothesis of an accelerating expansion at early times was first proposed

to solve these problems of the Hot Big Bang cosmology, the greatest success of inflationary cosmology is arguably its explanation of the initial formation of structures in the universe. That is, such an early-time accelerated expansion typically leads to the desirable property of a nearly (but not perfectly) scale-invariant power spectrum of overdensities in the matter content of the early universe. These initial overdensities can then go on to become seeds for the stars and galaxies that the universe is comprised of today to form via billions of years of gravitational collapse. The near-scale invariance of these fluctuations is a necessary condition to allow this collapse process to proceed in a way consistent with observations, a fact which has been repeatedly verified with ever-increasing precision by consecutive generations of CMB observation experiments such as WMAP[37,38] and Planck.[39,40] While it is widely understood and accepted that the early universe requires such a period of accelerating expansion (though alternative, albeit less popular, proposals such as Variable Speed of Light models do exist), it is much harder to explain how this came about. As with the dark energy problem, no form of conventional matter-energy (such as baryonic matter or radiation) can actually invoke such an expansion when described by General Relativity. There are hence two major classes of approaches to resolving this problem.

The first approach is to assume that General Relativity is not the ultimate theory of gravity, and that some theory of *modified* gravity is needed to explain anomalies like periods of accelerating expansion (inflation, dark energy) and dark matter. Despite the fact that it has passed every experimental test carried out in the preceding century,[41] and despite the difficulty in finding modifications of General Relativity which are free of pathologies, there are some hints that this may be the case; General Relativity is famously incompatible with quantum mechanics, which forms the basis of our understanding of all non-gravitational phenomena in nature.[42] One may argue that an ultimate goal of theoretical physics as a discipline is a "theory of everything" which encompasses scientific understanding of all fundamental aspects of nature in a single theory guided by a consistent set of physical principles, but it is hard to imagine how such a theory may be constructed when such contradictions between quantum theory and gravity remain unresolved. A reconciliation of quantum theory

and gravitation may lie in a modified theory of gravitation, and the implication that such a theory could simultaneously provide the means for inflation may be a key hint to its nature. A large class of modified gravity theories are so-called scalar-tensor theories, and there exists a vast body of work on finding the most general acceptable scalar-tensor theory[43–45] as well as investigating and applying their phenomenology to cosmological problems.[46]

The second approach is to assume we are describing gravity correctly (or at least correctly enough for present purposes), but that our comprehension of particle physics is incomplete. In theories beyond the standard model, there may exist exotic matter sources which can drive an accelerated expansion of spacetime even when described with classical gravity. Often, these two approaches - the modification of gravity and the extension of particle physics - are complementary or in some cases even mathematically equivalent (some theories of modified gravity may be mathematically recast in the form of General Relativity coupled to non-standard matter sources, and so on). Nevertheless, in this thesis, we are largely interested in the former approach of modifying gravity.

Cosmic inflation deals with energy scales unimaginably larger than those achievable with terrestrial experiments, and it is hence a highly useful probe of what kind of unknown physics, whether it be gravitational or particle-theoretical, remains undiscovered in this regime. Inflationary cosmologists hence construct and study models of inflation motivated by modified gravity, string theories, supersymmetry, and all other kinds of cutting edge ideas in fundamental physics. After decades of effort in this direction, there are now a plethora of models of inflation,[47,48] but many of them make similar predictions for the precise form of the primordial power spectrum of inhomogeneities, which is the main discriminator we have in comparing theories to data. While a handful of them have since been ruled out by the ever-more-restrictive constraints derived from CMB experiments, there are still numerous models which conform to the data and cannot yet be easily discriminated between or ruled out. To determine which, if any, of the scenarios realising an inflationary expansion actually corresponds to the way the early universe inflated, it is important that these efforts in model building are complemented with the development and implementation of

experimental tests of inflationary models, and an increasing amount of research is hence being focused in this direction. Such approaches involve looking at what information can be extracted from the CMB radiation, or other probes into the early universe, and how it could be used to further constrain the details of the inflationary period.

Aspects of both the ongoing endeavour to build and study interesting theoretical models of inflation to make links to fundamental theory, as well as the goal of testing and constraining those models to better scrutinise the resulting smorgasbord of models, are reflected in this thesis. Chapters 2 and 3 of this work will present a review of important ideas in gravity and cosmology, as the majority of the results presented here are derived and interpreted in the context of this knowledge. Chapter 4 then contains discussion of my work on the string-theory-inspired model of Disformally Coupled Inflation, comparing its predictions to established experimental measurements of the primordial power spectrum, as well as looking at how such a model affects the deviation from Gaussian statistics (the bispectrum), which will hopefully come to be precisely constrained by future experiments. Chapter 5 describes my research into Gauss-Bonnet Coupled Inflation, studying the phenomenology of this alternative theory of gravity, considering how it is constrained by the imprint left on the power spectrum by the details of post-inflationary reheating, and giving thought to the possibility of quintessential inflation, where the accelerating expansions of both inflation and dark energy are realised in a single model. Finally, in Chapter 6, contrary to the previous chapters where more emphasis was placed on model-building, greater attention is paid to the goal of testing inflation. It is here I detail the research conducted on a quantity known as the running of the running of the inflationary spectral index, and how measurements of this higher-order deviation from scale invariance could place powerful constraints on the details of the inflationary mechanism.

1.1. Conventions and Notation

We will largely work in Planck units where $\hbar = c = 8\pi G = 1$, such that the reduced Planck mass,

$$M_{\rm Pl}^2 = \frac{\hbar c}{8\pi G} \approx (2.44 \times 10^{18}\ \text{GeV})^2\,, \tag{1.1.1}$$

is also equal to unity, though occasionally we may reinstate it explicitly in equations when it may be helpful to do so.

Unless otherwise stated, Greek letters will be used to label indices in four-dimensional spacetime. Similarly, lower-case Roman letters will denote purely spatial indices (such as when referring to only the spatial coordinates in 4D, or when extra spatial dimensions are present.) Upper case Roman letters will be used when denoting spacetime in a total number of dimensions other than 4. Repeated indices in a single term indicate summation according to the usual Einstein summation convention.

We will make use of the notation $f_{,x}$ to succinctly represent the partial derivative of a function f with respect to the variable x. Similarly, the notation ∂_μ will be used to denote partial differentiation with respect to x^μ.

We will use a "mostly positive" metric signature $(-,+,+,+)$.

CHAPTER 2

GRAVITATION

On cosmological scales the dominant force of nature is gravitation. Unlike electromagnetism it has no opposite charges to cancel out over large scales, and unlike the nuclear forces it has unlimited range. While it is negligibly weak on scales of individual particles, unlike the other forces of nature, it is also universal - acting on anything with mass or energy. So, when large amounts of matter-energy are involved, such as in stars, galaxies and indeed, the universe as a whole, it often plays a key role. Furthermore, the relativistic principle of describing gravity as a manifestation of the geometry of spacetime itself is the very principle which allows cosmologists to discuss the expansion of the universe, which is the core of modern physical cosmology. The contents of this thesis will hence be heavily dependent on the physics of gravitation. In this chapter we shall therefore review some of the main ideas in both Einstein's established theory of General Relativity[1] as well as various proposed modifications of and alternatives to it, which will play a key role in the later chapters.

2.1. General Relativity

For hundreds of years, gravity was understood as an attractive force between all massive bodies, described by Newton's Universal Law of Gravitation, in which the force of attraction is proportional to the masses of objects and inversely related to the square of the distance between them. This can also be formulated as the Poisson equation[49]

$$\partial_i \partial^i \Phi(x^i) = 4\pi G \rho(x^i)\,, \tag{2.1.1}$$

where Φ is the gravitational potential and ρ is the mass density present. G is Newton's constant, which encodes the strength of the gravitational force. Equation (2.1.1) describes how the distribution of matter (on the right hand side) sources the gravitational potential. The force derived from this potential, using Newton's second law of motion for cartesian spatial coordinates x^i

$$\ddot{x}^i + \partial^i \Phi = 0\,, \tag{2.1.2}$$

correspondingly determines the motion of that matter due to gravity. This largely accounted for the orbital motion of Earth and the planets, validating the theory as the leading description of gravity for hundreds of years, but the problematic nature of some of its aspects have been known more-or-less since its inception. Newton himself stated that[50] no one "who has in philosophical matters any competent faculty of thinking" would believe in such an "absurdity" as an instantaneous force acting through a vacuum across great distances, with no apparent entity mediating the interaction. As well as such conceptual issues, experiments leading to more precise measurements of the orbit of Mercury were conducted and it was found that the orbit precessed in a way not accounted for by Newton's law.[51] Similarly, the observed bending of light rays by massive bodies like the Sun was inexplicable in this description of gravity as an attraction between masses due to the masslessness of light.

Einstein's theory of General Relativity (GR) solved these problems, and thus became accepted as the new paradigm. The idea of an unmediated force at a distance was

done away with, as gravity came to be understood as the curvature of spacetime. In this geometric picture of gravitation, the bending of light rays by massive objects was also now explicable as a consequence of light moving through this curved space, and the anomalies in the orbit of Mercury were accounted for by relativistic corrections to the dynamics. The success in explaining these phenomena, as well as many other experimental tests since, established General Relativity as the mainstream theory of gravity, where it has remained for more than a hundred years.[29,52–55]

General Relativity is a geometric theory in which the fundamental objects of interest are mathematically modelled as tensor fields,[1] as this allows the theory to be formulated in a coordinate-invariant manner. The quantity encoding the gravitation in a system is no longer the scalar gravitational potential function of eq. (2.1.1), but instead a four-dimensional symmetric metric tensor, $g_{\mu\nu}$, defined on a Lorentzian manifold that models spacetime. That is, the "proper distance" between neighbouring points in spacetime is given by

$$\mathrm{d}s^2 = g_{\mu\nu}\mathrm{d}x^\mu \mathrm{d}x^\nu \,, \tag{2.1.3}$$

where $\mathrm{d}x^\mu$ are tensors specifying the displacement in space and time between those points, such that x^0 is typically the time coordinate t and the remaining x^i are spatial coordinates. If one takes a diagonal metric with components $(-1, 1, 1, 1)$ - the Minkowski metric $\eta_{\mu\nu}$ - then one recovers the special theory of relativity. In general, however, the metric describes spacetime as possessing curved geometry, and this manifests as objects feeling a "force" due to this as they move through spacetime. Really, though, there is no force in the Newtonian sense; objects simply move along geodesics[2] of the spacetime described by the metric, just as a free particle in classical

[1] The usual abuse of terminology of referring to tensor fields as simply "tensors" will henceforth be used.

[2] Geodesics may be timelike, spacelike or null, depending on the nature of the object in question. Conventional objects all follow timelike geodesics ($\mathrm{d}s^2 < 0$) and hence obey the set of limitations we call causality, while some massless objects such as photons follow null geodesics ($\mathrm{d}s^2 = 0$) and travel at the speed of light.[3] Spacelike geodesics ($\mathrm{d}s^2 > 0$) violate causality and are usually not of interest.

[3] To make it more obvious how the speed of light comes into play in this discussion it is helpful to choose units in which $c \neq 1$. With units reinstated, we have $x^0 = ct$, and this makes it more apparent that a null geodesic obeys $\mathrm{d}x^i \mathrm{d}x_i = c^2 \mathrm{d}t^2$ - loosely that the space and time intervals an object traverses are in fixed proportion or "speed" - while a timelike geodesic is limited to

physics moves along geodesics of the geometry of its surroundings, which happen to be typically flat. The main difference is that in GR, space itself is not geometrically flat, and the geodesics involved are therefore not the familiar and intuitive straight lines of the Newtonian world. The spacetime location of a test particle described by coordinates x^μ can be shown to obey the geodesic equation

$$\ddot{x}^\mu + \Gamma^\mu_{\alpha\beta}\dot{x}^\alpha\dot{x}^\beta = 0\,, \tag{2.1.4}$$

where the dot signifies differentiation with respect to an affine parameter λ, which the spacetime coordinates $x^\mu(\lambda)$ are taken to be function of so that it parametrises the motion of the test particle from beginning to end. The Γ in this equation represents the Christoffel symbols,[52] which are, for a symmetric metric-compatible (Levi-Civita) connection on the manifold, derived from the metric via the definition

$$\Gamma^\mu_{\alpha\beta} = \frac{1}{2}g^{\mu\delta}\left(\partial_\alpha g_{\beta\delta} + \partial_\beta g_{\alpha\delta} - \partial_\delta g_{\alpha\beta}\right)\,. \tag{2.1.5}$$

Equation (2.1.4) can be interpreted as the relativistic analogue of Newton's second law in eq. (2.1.2), replacing the Newtonian concept of the gravitational potential with a "force" derived from the rate of change and gradients of the metric (Γ). It is also important to note that in this geometric theory, the usual flat-space concept of partial differentiation is unsuitable as partial derivatives of quantities do not transform as tensors and their result may be hence coordinate-dependent. The covariant derivative[56] is a generalisation of this to maintain the tensorial nature of objects under differentation, such that if one is interested in the conservation of a tensor quantity it is this derivative rather than the conventional partial derivative that one is interested in. It is defined for tensors with contravariant indices $(\mu_1 \dots \mu_m)$ and covariant indices $(\nu_1 \dots \nu_n)$ as

$$\begin{aligned}\nabla_\alpha T^{\mu_1\mu_2\cdots}{}_{\nu_1\nu_2\dots} = \partial_\alpha T^{\mu_1\mu_2\cdots}{}_{\nu_1\nu_2\dots} + \Gamma^{\mu_1}_{\alpha\lambda}T^{\lambda\mu_2\cdots}{}_{\nu_1\nu_2\dots} + \Gamma^{\mu_2}_{\alpha\lambda}T^{\mu_1\lambda\dots}{}_{\nu_1\nu_2\dots} + \dots \\ - \Gamma^\lambda_{\alpha\nu_1}T^{\mu_1\mu_2\cdots}{}_{\lambda\nu_2\dots} - \Gamma^\lambda_{\alpha\nu_2}T^{\mu_1\mu_2\cdots}{}_{\nu_1\lambda\dots} - \dots\,,\end{aligned} \tag{2.1.6}$$

speeds less than this as $\mathrm{d}s^2 < 0$ instead implies $\mathrm{d}x^i\mathrm{d}x_i < c^2\mathrm{d}t^2$.

such that there will be $m + n + 1$ terms.

In addition to this description of how objects move in curved spacetime, GR's other component is the analogue of the Newtonian statement that the distribution of mass sources the gravitational potential according to eq. (2.1.1). To begin to describe how the contents of spacetime set-up its curvature, it is first useful to define quantities which measure this curvature.[29,52–54] Such quantities include the Riemann tensor

$$R^{\rho}{}_{\sigma\mu\nu} = \partial_\mu \Gamma^{\rho}{}_{\nu\sigma} - \partial_\nu \Gamma^{\rho}{}_{\mu\sigma} + \Gamma^{\rho}{}_{\mu\lambda}\Gamma^{\lambda}{}_{\nu\sigma} - \Gamma^{\rho}{}_{\nu\lambda}\Gamma^{\lambda}{}_{\mu\sigma}\,, \tag{2.1.7}$$

the Ricci tensor

$$R_{\mu\nu} = R^{\lambda}{}_{\mu\lambda\nu}\,, \tag{2.1.8}$$

and the Ricci scalar

$$R = g^{\mu\nu} R_{\mu\nu}\,. \tag{2.1.9}$$

The construction of this scalar measure of curvature is important as it allows one to write an action functional[52] depending on the spacetime metric, known as the Einstein-Hilbert action

$$S_{EH}[g_{\mu\nu}] = \kappa \int \mathrm{d}^4x \sqrt{-g} R\,, \tag{2.1.10}$$

where g is the determinant of the metric and κ is an arbitrary constant (for now).[4] This is the simplest action one can construct from scalar geometric quantities describing curvature, and its variation with respect to the metric leads to Einstein's field equations in a vacuum:

$$G_{\mu\nu} = 0\,, \tag{2.1.11}$$

where $G_{\mu\nu} = R_{\mu\nu} - \frac{1}{2} R g_{\mu\nu}$ is called the Einstein tensor, and is a symmetric, divergence-free, matrix of functions of the metric and its first and second derivatives, as can

[4] The factor of $\sqrt{-g}$ is included as d^4x is not a tensor. As one must generalise the idea of differentiation in curved spacetimes, similarly the measure of integration must be modified in such a way to ensure covariance.

be seen from the definitions of the Christoffel symbols and curvature tensors in eqs. (2.1.5 – 2.1.9). While this system of ten independent partial differential equations describes relativistic gravitation in a vacuum, we are also interested in how matter plays a role and sources the curvature of spacetime in this picture. To understand this, consider a total action comprised of the above Einstein-Hilbert term and a minimally-coupled[5] matter Lagrangian $\mathcal{L}_m$ which is a function of some matter fields denoted ψ and the metric itself,

$$S = S_{\text{EH}}[g_{\mu\nu}] + S_m[\psi] = \kappa \int \mathrm{d}^4x\sqrt{-g}R + \int \mathrm{d}^4x\sqrt{-g}\mathcal{L}_m(\psi, g_{\mu\nu})\,, \tag{2.1.12}$$

whose variation leads to

$$G_{\mu\nu} = \frac{1}{2\kappa}T_{\mu\nu}\,, \tag{2.1.13}$$

where $T_{\mu\nu}$ is the energy-momentum tensor for the matter content of the theory.[52] It is derived from the Lagrangian $\mathcal{L}_m$ via the functional derivative

$$T_{\mu\nu} = -\frac{2}{\sqrt{-g}}\frac{\delta\sqrt{-g}\mathcal{L}_m}{\delta g^{\mu\nu}} = g_{\mu\nu}\mathcal{L}_m - 2\frac{\delta\mathcal{L}_m}{\delta g^{\mu\nu}}\,, \tag{2.1.14}$$

and is a covariantly conserved quantity ($\nabla_\mu T^\mu_\nu = 0$), generalising the Newtonian idea of conservation of energy. Eq. (2.1.13) quantifies how the amount and nature of the energy-momentum the matter possesses, specified by its energy-momentum tensor, determines the metric via second-order partial differential equations (recall that $G_{\mu\nu}$ contains second derivatives of the metric), analogously to how in Newtonian gravity the amount and distribution of mass determines the gravitational potential via a second-order partial differential equation in eq. (2.1.1).

The constant of proportionality in the Einstein equations, κ, is fixed by requiring that in the limit of perturbatively weak gravity and velocities much less than the speed of light, the Newtonian expression in eq. (2.1.1) is recovered. From this, it is found[29] (in units $\hbar = c = 1$) that $\kappa = (16\pi G)^{-1}$ and the Einstein field equations

[5] Here, minimal coupling means adding no explicit gravity-matter interactions, but instead simply taking a flat-space Lagrangian for the matter, promoting the Minkowski metric to the general metric $g_{\mu\nu}$, introducing the invariant integration measure and replacing partial derivatives with covariant ones to ensure compatibility with GR).

become

$$G_{\mu\nu} = 8\pi G T_{\mu\nu} = \frac{1}{M_{\rm Pl}^2} T_{\mu\nu} \,. \tag{2.1.15}$$

In the last expression here, we have defined the (reduced) Planck mass $M_{\rm Pl}^{-2} = 8\pi G \approx (2.44 \times 10^{18}\text{GeV})^{-2}$ for convenience as we will, for the majority of this thesis, work in units such that many quantities are measured in units of (some power of) $M_{\rm Pl}$ and/or set $M_{\rm Pl} = 1$ for simplicity.

One can also add a so-called *cosmological constant* term to General Relativity,[46,52,56] by taking instead the action (now with κ taking its true value)

$$S = \frac{M_{\rm Pl}^2}{2} \int \mathrm{d}^4x\sqrt{-g}\,(R - 2\Lambda) + \int \mathrm{d}^4x\sqrt{-g}\mathcal{L}_m(\psi, g_{\mu\nu})\,, \tag{2.1.16}$$

which leads to the field equations

$$G_{\mu\nu} + \Lambda g_{\mu\nu} = 8\pi G T_{\mu\nu} \,. \tag{2.1.17}$$

This extra term, Λ represents the vacuum energy of spacetime itself, which we have no reason to assume is zero and, like all other energy sources, will gravitate according to GR. This is important in cosmology as a possible source of dark energy as, unlike classical matter, vacuum energy gravitates in such a way that it can result in an accelerated expansion of spacetime. This approach, however, leads to the (in)famous Cosmological Constant Problem - sometimes called the greatest embarrassment in modern theoretical physics - where the value of Λ must be excessively fine-tuned (by tens if not hundreds of orders of magnitude of precision) to meet observational constraints.

The system of equations in eq. (2.1.15) or eq. (2.1.17) is highly non-linear in the metric and its derivatives, and so general and exact solutions (given that T takes some feasible form) are sparsely found.[57] Much analytical work with GR is hence based around either analysis of special cases, particularly those with considerable amounts of symmetry to simplify the equations, or approximation techniques such as perturbation theory.[29] Both of these approaches will be relevant for cosmological applications, as we will discuss in Chapter 3.

General Relativity, as described above, has passed many experimental tests on scales as small as a few microns and as large as the solar system[58] with astonishing precision. However on the smallest scales, where quantum effects reign supreme, and on the largest scales of galaxies and cosmology, unsolved problems remain. It is often said that General Relativity even predicts its own downfall - this refers to it permitting the existence of singularities, which are thought to be broadly unphysical. Black holes, in GR, are understood as objects containing point-like instances of infinite spacetime curvature, and if one extrapolates back to the beginning of the universe and the moment of the Big Bang itself, one finds a similar prediction of a singular point in spacetime. The undesirability of this alone is a strong motivation to consider GR as incomplete. Gravity as described by GR is also not suitable to be formulated as a quantum theory. Unlike the other known forces of nature, quantising GR leads to a non-renormalisable theory (meaning its predictions are once again divergent, in a way that cannot be handled by the techniques of quantum field theory, beyond the scope of this thesis).[59,60] It is thought and hoped that some high energy phenomena not accounted for by GR may be able to dispense of these incurable divergences and allow a unified description of all forces of nature in the framework of quantum mechanics. Just as the anomalies and pathologies of Newtonian gravity motivated the foundation of GR, the unsolved problems of today may be a sign that there is an *even better* theory of gravity waiting to be found. Realising such a theory may also bring answers to problems on the largest scales such as the nature of dark matter, the Cosmological Constant Problem, and the mechanism of cosmic inflation.

Nevertheless, finding a satisfactory extension of GR which does not spoil its successes in making highly precise predictions of phenomena on the scale of the solar system is not trivial. Many different approaches have been attempted, but to date none have transcended GR and gained wide acceptance as none have yet managed to simultaneously alleviate the problems of GR in its extreme limits of application and avoid the ruination of its successes in more familiar circumstances. Further tests of gravity, especially those on cosmological scales[61] where the greatest deviations from GR may be expected, are of course needed to settle the issue in the long run, but

in the mean time, much theoretical work has been done on finding and classifying the most promising and interesting ways that GR could be extended or modified. The following section will review some of these key theoretical ideas and models of modified gravity that are of relevance to the later chapters of this thesis.

2.2. Modified Gravity

To arrive at GR, we constructed the simplest action using a scalar measure of curvature, the Einstein-Hilbert action (from here we work in Planck units with $M_{\rm Pl} = 1$)

$$S = \frac{1}{2}\int \mathrm{d}^4x\sqrt{-g}R + S_m[\psi, g_{\mu\nu}]\,, \tag{2.2.1}$$

but this is not the *only* possible choice. We chose to construct an action in this way appealing only to the principles of relativity and simplicity. Both of these assumptions can be challenged.

Firstly, by relaxing the requirement for simplicity, one can also consider writing down an action containing curvature scalars other than the most elementary and minimalistic choice of R alone. These could be as simple as higher powers of the Ricci scalar such as R^2 or R^3, or perhaps other scalar contractions of the Ricci tensor such as $R_{\mu\nu}R^{\mu\nu}$. One could also write down a less simple theory of gravity by including additional degrees of freedom such as scalar fields, or terms with non-minimal coupling of matter fields to curvature. Many different ideas along these lines have been considered in the literature.[46,62–65] In this way, one can construct alternative geometric theories of gravity which retain the principle that the curvature of the spacetime metric manifests as what we call gravity, but the details of the dynamics and field equations of gravity, and the specific nature of the interactions between matter and gravity, can be different to those of GR.

As well as such direct modifications of GR, one can also consider approaches where a different idea guides the formulation of the theory from the beginning. Just as GR itself superseded Newtonian gravity by changing the fundamental object of concern from a potential sourced by mass to the metric of spacetime, it is possible that gravity could be better described by a different paradigm entirely, which introduces new

physics in regimes where GR appears insufficient. String Theory is such an approach, based on the idea that the fundamental objects of nature are one-dimensional objects called strings. This seemingly simple premise, surprisingly, gives rise to not only a theory of modified gravity but perhaps all other forces and matter, too. It will be discussed explicitly in Section 2.3 as some of the later chapters of this thesis use ideas derived from it.

Another way of thinking of modifications of gravity, which is complementary to the aforementioned strategies, is effective field theory.[66–69] This involves both a "bottom-up" approach in which physically-motivated additions to the low-energy theory (GR) are studied phenomenologically and tested, and a "top-down" approach in which the low-energy behaviour of a complete high-energy theory is considered to assess its suitability.

Some of the types of modified gravity that have been widely studied and that have relevance to the body of work in this thesis include:

2.2.1. $f(R)$ theories

A simple generalisation of GR is $f(R)$ theory,[70–72] where the action is given by

$$S = \int \mathrm{d}^4x\sqrt{-g}f(R) + S_m[\psi, g_{\mu\nu}]\,. \tag{2.2.2}$$

The action can now depend on any function of the scalar curvature. The Einstein-Hilbert action is clearly recovered when $f(R) = R/2$, linear in R. If one includes a term that is zeroth order in R, one essentially introduces a cosmological constant as in eq. (2.1.16). It is hence common for the functional form of f to include the Einstein-Hilbert linear term plus higher powers of R. The simplest and perhaps most well-studied example is Starobinsky Gravity, described by the action

$$S = \int \mathrm{d}^4x\sqrt{-g}\left(\frac{R}{2} + \alpha R^2\right) + S_m[\psi, g_{\mu\nu}]\,, \tag{2.2.3}$$

which is interesting as it provides a simple and feasible realisation of cosmic inflation,[73] as well as being of interest to the problem of dark matter.[74] The value of the parameter α must be small enough to not introduce excessively large corrections to

GR in familiar settings[75] and can hence be constrained by experiment[76] to have a value no greater than about $|\alpha| \lesssim 10^{-9}\mathrm{m}^2$. Theories with other powers of R have also been explicitly considered.[77]

2.2.2. Scalar-tensor theories

In addition to the spin-2 (tensor) degree of freedom in GR, one can consider theories of gravity with additional spin-0 (scalar) degrees of freedom, leading to the class of scalar-tensor theories of modified gravity.[65,78–82] The simplest realisation of this is if one minimally couples a canonical scalar field ϕ with potential V to GR, such that

$$S = \int \mathrm{d}^4x\sqrt{-g}\left(\frac{R}{2} + X - V(\phi)\right) + S_m[\psi, g_{\mu\nu}]\,, \tag{2.2.4}$$

where $X = -\partial_\mu\phi\partial^\mu\phi/2$ is the kinetic term for the field. This has equation of motion

$$\Box\phi + V_{,\phi} = 0\,, \tag{2.2.5}$$

known as the Klein-Gordon equation.

In the minimal example of eq. (2.2.4) , the scalar field could easily be reinterpreted as part of the S_m action, and treated like a normal minimally-coupled matter field, such as the Higgs field[83,84] or some other scalar in a fundamental theory. One can also however consider non-minimal scalar-tensor theories. For example, a more general theory would be of the form

$$S = \int \mathrm{d}^4x\sqrt{-g}\left(F(\phi)\frac{R}{2} + \omega(\phi)X - V(\phi)\right) + S_m[\psi, g_{\mu\nu}]\,. \tag{2.2.6}$$

Here the function $F(\phi)$ gives a non-minimal coupling to gravity, which means that the effective strength of gravity varies as a function of the field ϕ. A successful theory of this kind would need the behaviour of the field to be such that $F(\phi) \approx 1$ in the limits where GR works and is precisely correct. The term $\omega(\phi)X$ is a non-canonical kinetic term, which affects the dynamics of the scalar field, and hence how it plays a role in gravitation. One particular scalar-tensor theory of this form that has been widely studied is the case of $F(\phi) = \phi$, $\omega(\phi) = \omega_0/\phi$ and $V = 0$, known as

Brans-Dicke theory.[85] Again, experimental tests constrain the theory such that the parameter ω_0 must be at least $O(10^4)$.[86]

Non-minimal couplings such as $F(\phi)R$ also naturally arise in the context of quantum field theory in a curved spacetime background. When renormalising a scalar-tensor theory, one finds counterterms of this form are necessary,[87] such that they arise at the quantum level even if the classical theory does not explicitly contain them. The role of this non-minimal coupling is central to the idea of Higgs inflation,[84] which will be discussed in Section 5.1.

Equivalence with $f(R)$ theories

It is interesting to note that the action

$$S = \int \mathrm{d}^4x\sqrt{-g}\big[f(\phi) + x(R-\phi)\big] + S_m[\psi, g_{\mu\nu}]\,, \tag{2.2.7}$$

can be seen to be equivalent to the $f(R)$ action of eq. (2.2.2) by using the equation of motion for the auxiliary field x ($R = \phi$). Similarly, the ϕ equation of motion yields $x = f'(\phi)$, which, upon reinsertion into eq. (2.2.7) yields

$$S = \int \mathrm{d}^4x\sqrt{-g}\,(f'(\phi)R + f(\phi) - \phi f'(\phi)) + S_m[\psi, g_{\mu\nu}]\,, \tag{2.2.8}$$

which is a scalar-tensor theory of the form given by eq. (2.2.6). $f(R)$ theories are hence a subset of scalar-tensor theories with $\omega(\phi) = 0$, $F(\phi) = f'(\phi)$ and $V(\phi) = f(\phi) - \phi f'(\phi)$.[88,89]

2.2.3. Conformal and disformal transformations

If one considers two metrics related by a conformal rescaling, where the conformal multiple depends on a scalar field ϕ, in general,

$$\hat{g}_{\mu\nu} = e^{2A(\phi)}g_{\mu\nu}\,, \tag{2.2.9}$$

then the Ricci Scalar for the two metrics are related via[90]

$$\sqrt{-\hat{g}}R(\hat{g}) = \sqrt{-g}e^{2A(\phi)}\left[R(g) - 6\Box A(\phi) - 6\nabla_\mu A(\phi)\nabla^\mu A(\phi)\right] . \tag{2.2.10}$$

This suggests that a scalar-tensor theory of the form (2.2.6), which contains a term like $F(\phi)R$, could be re-written in terms of such a different metric to instead contain the term $e^{2A(\phi)}F(\phi)R$, as well as several new scalar field terms. Consequently, under a conformal transformation with $e^{2A} = F^{-1}$, the new action would have the usual Einstein-Hilbert gravity term of $R/2$, but different structure in the scalar sector of the action. The choice of metric for which this occurs is called the Einstein Frame (EF). The total action of a scalar-tensor theory of the form (2.2.6) in the Einstein Frame can be written,

$$S_{\rm EF} = \int \mathrm{d}^4x\sqrt{-g}\left(\frac{R}{2} + X - V(\chi)\right) + S_m[\psi, \hat{g}_{\mu\nu}] , \tag{2.2.11}$$

where we have performed a field redefinition $\chi = \chi(\phi)$ to canonically normalise[83] the kinetic term $X = -\partial_\mu\chi\partial^\mu\chi/2$. This EF action is then largely equivalent to eq. (2.2.4) - a scalar field minimally coupled to GR - albeit on different metrics related by eq. (2.2.9). The physical difference is that the matter action is now minimally coupled not to the gravitational metric $g_{\mu\nu}$, but the conformally related $\hat{g}_{\mu\nu} = e^{2A}g_{\mu\nu}$. The matter energy-momentum tensor is hence not covariantly conserved with respect to the gravitational metric ($\nabla_\mu(g)T^\mu_\nu(\hat{g}) \neq 0$) in the Einstein Frame, or indeed any conformally related frame except the original frame where the metric in the matter action is the same as the metric of the gravity sector, known as the Jordan Frame (JF).

Transformation to the Einstein Frame hence amounts to replacing a scalar field that doesn't interact directly with matter, but is non-minimally coupled to gravity, with a scalar field that explicitly interacts with matter, but minimally couples to gravity. One consequence of this interaction between the scalar field and matter sector is that quantities such as particle masses become dependent on the scalar field.[6] Alternatively, this means that matter does not follow geodesics of the metric

[6] However, ratios of particle masses remain unchanged, unless multiple matter sectors are coupled to different metrics. What one does have to be careful of, however, is time-varying particle masses.

g, but instead those of $\hat{g}$, which depends on ϕ. While there was once considerable debate in the literature surrounding the issue of whether this means the two frames represent physically distinct theories or not, it is now widely accepted, at least at the classical level, that conformally related theories are simply different parametrisations of the same physics.[91–96]

Given the interest and applicability of conformal transformations in understanding scalar-tensor theories, the question of whether other useful transformations akin to this may play an interesting role has of course been asked. It has been shown that the most general metric transformation including a scalar field which maintains physical requirements such as causality is the so-called disformal transformation,[97] generalising conformal transformations to

$$\hat{g}_{\mu\nu} = C(\phi, X) g_{\mu\nu} + D(\phi, X) \phi_{,\mu} \phi_{,\nu} \,. \tag{2.2.12}$$

Unlike conformal transformations which only rescale the metric by a spacetime-dependent function, thus preserving the angle between objects, disformal transformations do not preserve angles and introduce non-minimal kinetic interactions via the metric's dependence on derivatives of the field. The inverse metric under a disformal transformation is[98]

$$\hat{g}^{\mu\nu} = \frac{1}{C(\phi, X)} \left(g^{\mu\nu} - \gamma^2 \phi^{,\mu} \phi^{,\nu} \right) \,, \tag{2.2.13}$$

where

$$\gamma = \left(1 + 2 \frac{D}{C} X \right)^{-\frac{1}{2}} \,. \tag{2.2.14}$$

This γ factor is ubiquitous in disformally transformed theories, appearing in the equations of motion and with many physically relevant quantities depending on it, and it should therefore generally be real, finite, and so on. Its form and function are reminiscent of the Lorentz factor of Special Relativity in that it begins at unity for $X = 0$ but then increases as the "speed" of the field increases ($X \to -\infty$), affecting its evolution, until eventually diverging at a certain value of X. This essentially imposes a limit on the rate of change of ϕ, depending on the functions D and C,[99] and

also has interesting effects on the behaviour of disformally coupled matter fields.[100] As with conformal transformations, the invariance of disformally transformed theories[101–107] and their phenomenology[44,108–112] has been widely studied.

2.2.4. Further Modifications of GR

In this section we will conclude our review of modifications of GR by touching on some extensions of the basic ideas presented in Sections 2.2.1 and 2.2.2.

Beyond the scope of simple $f(R)$ theories are those which also depend on contractions such as $R_{\mu\nu}R^{\mu\nu}$, $R_{\rho\sigma\mu\nu}R^{\rho\sigma\mu\nu}$ or even terms with derivatives of these curvature tensors. In general, unlike the $f(R)$ theories, however, these terms often induce ghost degrees of freedom and higher than second derivatives in the equation of motion, leading to pathological Ostrogradsky instabilities.[113–118]

The most general scalar-tensor theory with at most second order equations of motion is Horndeski's theory,[43] which was rediscovered in recent years[119–121] and has seen a surge of interest in its application to cosmological problems.[122–129] The full Horndeski theory Lagrangian is

$$\begin{aligned} L_H = {} & G_4(\phi, X)R_4 + P(\phi, X) - G_3(\phi, X)\,(\Box\phi) + G_{4,X}\left[(\Box\phi)^2 - (\partial_\alpha\partial^\beta\phi)(\partial^\alpha\partial_\beta\phi)\right] \\ & + G_5(\phi, X)G_{\alpha\beta}\partial^\alpha\partial^\beta\phi - \frac{1}{6}G_{5,X}\big[\,(\Box\phi)^3 - 3\,(\Box\phi)\,(\partial_\alpha\partial^\beta\phi)(\partial_\beta\partial^\alpha\phi) \\ & + 2(\partial_\alpha\partial^\beta\phi)(\partial_\beta\partial^\gamma\phi)(\partial_\gamma\partial^\alpha\phi)\big]\,, \end{aligned} \tag{2.2.15}$$

where P and G_n are arbitrary functions of the scalar ϕ and its kinetic term, X.

More general "beyond Horndeski" scalar-tensor theories which are free of pathologies of have since been found.[44,130] Furthermore, higher-derivative and even infinite-derivative theories of gravity have been considered, and possess properties useful for the removal of singularities and achieving tameable quantum behaviour.[116,117,131–134]

One special case of particular interest to this thesis (see Chapter 5) is Einstein-Gauss-Bonnet gravity,[46,135–137] where the action is

$$S = \int \mathrm{d}^4x\sqrt{-g}\left[\frac{R}{2} + G\left(R^2 - 4R_{\mu\nu}R^{\mu\nu} + R_{\rho\sigma\mu\nu}R^{\rho\sigma\mu\nu}\right)\right] + S_m[\psi, g_{\mu\nu}]\,, \quad (2.2.16)$$

where G is a constant, and the combination of curvature scalars in round parenthesis $R^2 - 4R_{\mu\nu}R^{\mu\nu} + R_{\rho\sigma\mu\nu}R^{\rho\sigma\mu\nu}$ is the Gauss-Bonnet (GB) term and will be denoted as E_{GB}. While the quadratic curvature scalars appearing in the GB term individually contain the higher order derivatives of the metric associated with unstable extra degrees of freedom, the GB term is special because all of these terms cancel out for this specific combination of R^2, $R_{\mu\nu}R^{\mu\nu}$ and $R_{\rho\sigma\mu\nu}R^{\rho\sigma\mu\nu}$, or indeed any constant multiple, G, of it. In four dimensions, however, it is a total derivative due to the generalised Gauss-Bonnet theorem, and hence does not contribute to the equations of motion. If one promotes the constant G to a function of a field ϕ, however, the combination $G(\phi)E_{\mathrm{GB}}$ is not a total derivative, and will contribute non-trivially to the theory. We can hence write down a theory containing a scalar field which couples to the Gauss-Bonnet combination in this way:

$$S = \int \mathrm{d}^4x\sqrt{-g}\left[\frac{R}{2} + X + V(\phi) + G(\phi)E_{\mathrm{GB}}\right] + S_m[\psi, g_{\mu\nu}]\,. \quad (2.2.17)$$

Actions of this form can be shown to be equivalent to a subset of Horndeski models, thus ensuring their good behaviour.[122]

Horndeski's theory also allows for arbitrary dependence on X. So called $P(X)$ theories,

$$S = \int \mathrm{d}^4x\sqrt{-g}\left[\frac{R}{2} + P(X, \phi)\right] + S_m[\psi, \hat{g}_{\mu\nu}]\,, \quad (2.2.18)$$

also known as k-essence[138,139] have been studied for their properties, particularly in inducing a sub-luminal propagation speed in ϕ.[140] Another particular type of kinetic term that has received considerable interest is the Dirac-Born-Infeld (DBI) kinetic term[99,141]

$$S = \int \mathrm{d}^4x\sqrt{-g}\left[\frac{R}{2} + \frac{1}{f(\phi)}\left(1 - \sqrt{1 - 2f(\phi)X}\right)\right] + S_m[\psi, g_{\mu\nu}]\,, \quad (2.2.19)$$

which has links to String Theory, to be discussed more in Section 2.3.

Finally, let us note that scalar-tensor theories need not have just one scalar field.[142–145] Especially in scenarios motivated by high energy particle theory where many scalar fields can typically exist, it is not unthinkable that more than one would play some role in alleviating the problems with GR. This leads to an expanded range of interactions to consider, such as mixed kinetic terms of the form $\partial_\mu\phi\partial^\mu\chi$. A very general description of this is the action, generalising the single-field $P(X)$ case of eq. (2.2.18) is the $P(\phi^I, X^{IJ})$ class of theories,

$$S = \int \mathrm{d}^4x\sqrt{-g}\left[\frac{R}{2} + P(\phi^I, X^{IJ})\right] + S_m[\psi, g_{\mu\nu}]\,, \tag{2.2.20}$$

where field indices (I, J) run from $1 \ldots N$ where N is the number of fields and $X^{IJ} = -\partial_\mu\phi^I\partial^\mu\phi^J/2$ are the generalised kinetic terms. These are especially interesting as each scalar field can, in principle, have a different propagation speed (as we will see in Chapter 4), leading to enriched phenomenology.[146–148]

2.3. String Theory

In this section we take a brief excursion into one of the most prominent theories of quantum gravity, String Theory, to touch on some themes that motivate and inspire the original work in the later chapters of this thesis. This is not intended to be a comprehensive review of String Theory, as the technical details are largely beyond the scope and purpose of this thesis. Many results will therefore simply be quoted without explanation beyond what is required to set the scene for the subsequent research presented. The reader is directed to the books and lecture notes cited in this section for a more rigorous induction into the field.

Much of physics is based on the concept of particles - zero-dimensional objects like electrons and quarks. Classically, these objects move through spacetime to trace out a world line $x^\mu(\sigma)$ which describes where the particle is as a function of the affine parameter σ. Relativistically, the world-line of a massive particle is determined via extremisation of the proper-time $\mathrm{d}\tau^2 = -\mathrm{d}s^2 = -g_{\mu\nu}\mathrm{d}x^\mu\mathrm{d}x^\nu$ - essentially the length of its world line. This is equivalent to the statement that objects follow geodesics

according to eq. (2.1.4).

String theory[149–154] is a fundamental theory of quantum gravity which begins instead from the principle that the basic objects of nature are strings, which are one-dimensional in extent, unlike the point-like particles of conventional physics. In this picture, particles are understood as different vibrating excitations of the fundamental and extremely small strings, and interactions are related to the joining and splitting of strings.

As a result of their one-dimensionality, a string moving through time traces out a two-dimensional "world sheet" rather than a world line. Hence, the object which must now be extremised to describe the dynamics of the string is not the length of a world line, but the *area* of a world sheet. Let us define coordinates on the world sheet $\sigma^a = (\tau, \sigma)$ where τ is timelike and σ is spacelike. The world sheet is then parametrisable as a function $x^M(\tau, \sigma)$, where we embed the world sheet as a two-dimensional hypersurface in a D-dimensional target spacetime such that M runs from 0 to $D-1$. The induced metric on the worldsheet is then given by[56]

$$\gamma_{ab} = \frac{\partial x^M}{\partial \sigma^a} \frac{\partial x^N}{\partial \sigma^b} g_{MN} \,, \tag{2.3.1}$$

where g is the metric of the D-dimensional target spacetime. Let us assume for simplicity that this is Minkowski spacetime with $g_{MN} = \eta_{MN}$. The area of the world sheet (strictly, something proportional to the area) is then given by the action integral

$$S = -T \int \mathrm{d}^2\sigma \sqrt{-\gamma} = -T \int \mathrm{d}^2\sigma \sqrt{(\dot{x} \cdot x')^2 - (\dot{x})^2 (x')^2} \,, \tag{2.3.2}$$

where γ is the determinant of the world sheet metric, $\dot{x} = \partial_\tau x$, $x' = \partial_\sigma x$, $A \cdot B = \eta_{MN} A^M B^N$ and $A^2 = A \cdot A$. This is known as the Nambu-Goto action, describing the relativistic dynamics of a string. The constant of proportionality T represents the tension of the string. Its variation with respect to x yields equations of motion. These are very inconvenient to work with because of the square root in the action, and so a related action called the Polyakov action and defined by[155]

$$S = -\frac{1}{4\pi\alpha'}\int \mathrm{d}^2\sigma\sqrt{-h}h^{ab}\partial_a x^M \partial_b x^N \eta_{MN}\,, \tag{2.3.3}$$

is instead used. This can be shown to have the same equations of motion as eq. (2.3.2) by eliminating the extra field h_{ab} with its equation of motion.[154] One finds that $h_{ab} = 2f\eta_{MN}\partial_a X^M \partial_b X^n = 2f\gamma_{ab}$ with $f^{-1} = h^{ab}\partial_a X^M \partial_b X^N \eta_{MN}$. Substituting this back in to eq. (2.3.3) recovers eq. (2.3.2), if $(2\pi\alpha') = T^{-1}$.

The Polyakov action is invariant under local conformal transformations $h_{ab} \to \Omega(\tau,\sigma)h_{ab}$ and general coordinate transformations, meaning one can always choose a frame in which the world sheet metric is flat, $h_{ab} = \eta_{ab}$, reducing eq. (2.3.3) to

$$S = -\frac{1}{4\pi\alpha'}\int \mathrm{d}^2\sigma\partial_a x^M \partial^A x_M\,. \tag{2.3.4}$$

This now looks like an action for D free scalar fields living on the two-dimensional worldsheet metric, though we also keep in mind the original motivation of a worldsheet of a string embedded in a D-dimensional target spacetime.

Upon quantisation of the theory in Minkowski space, one finds that preservation of the conformal symmetry of the classical theory is dependent on the choice of $D = 26$ free fields on the world sheet, which has the startling alternative interpretation of a 26 dimensional target spacetime. That is, the theory described here requires spacetime to have 26 dimensions, rather than the 4 we are familiar with. Furthermore, the ground state of the quantised theory has a negative mass-squared, leading to an unresolved tachyonic instability in the theory. The spectrum predicted by the Polyakov action also fails to account for the existence of fermions. This is hence called Bosonic String Theory. Why do we concern ourselves with a theory containing such pathologies and oddities, then? This is because String Theory is surprisingly, despite all of this, a quantum theory of gravitation unified with other forces. This is because the quantised Polyakov action also leads to a massless, symmetric spin-2 field, G_{MN}, whose equations of motion at lowest order in a series expansion of powers of α' are the Einstein Equations (2.1.11). That is, GR emerges from String Theory at the lowest order of approximation, and higher orders introduce modifications of gravity. That this is a consequence of the initial supposition that quantised one-dimensional

strings are the fundamental objects in the universe is staggering, providing extensive motivation to search for further refinements of the idea which better match reality - perhaps having a smaller number of excess spacetime dimensions, or maybe even some fermions.

Other fields such as the scalar dilaton, Φ, which dynamically controls the effective coupling constants in the theory, and an antisymmetric tensor field B_{MN} (a 2-form) are also part of the quantised bosonic string spectrum. String theories give rise to, and hence also give a top-down physical motivation for, corrections to GR such as the Gauss-Bonnet term[156–160] as described in eq. (2.2.16) and studied in Chapter 5.

2.3.1. Supersymmetry and Superstrings

The absence of fermions in String Theory can be alleviated by the introduction of supersymmetry. Supersymmetry[161,162] is a symmetry between bosons and fermions that is of considerable interest even outside the context of String Theory as an interesting extension of standard model particle physics. In supersymmetric scenarios, all bosons have fermionic analogues ("superpartners") and vice-versa, leading to a whole spectrum of additional particles to alleviate or explain problems with the standard model such as dark matter. Mathematically, one arrives at supersymmetry by extending the Poincaré symmetry group of Special Relativity to the Super-Poincaré group which contains both commuting (bosonic) and anticommuting (fermionic) generators, leading to the idea of "superspace" in which both conventional coordinates x^μ and fermionic coordinates $\theta^\alpha\,, \bar{\theta}_{\dot{\alpha}}$ are present.[163]

The absence of fermions in the spectrum of the Polyakov action can be cured by making a superstring theory - that is, a string theory like the Polyakov action but with supersymmetry, such that the action is

$$S = -\frac{1}{4\pi\alpha'}\int \mathrm{d}^2\sigma \left(\partial_a x^M \partial^A x_M - i\bar{\psi}^M \rho^a \partial_a \psi_M\right)\,, \tag{2.3.5}$$

where ρ^a are Dirac matrices in two dimensions, and ψ^M is a spinor.

Superstring Theory not only contains both bosonic and fermionic states, allowing one to potentially account for all the known matter in the standard model and grav-

ity, but also cures the tachyonic instability of the Polyakov action. The requirement of $D = 26$ is also reduced to $D = 10$.

There are multiple consistent ways of introducing fermions to construct a superstring theory, which vary in the details of how one applies boundary conditions to the fermions, for example. These choices each lead to different additional field content upon quantisation, on top of those of Bosonic String Theory. The different superstring theories are: Heterotic $SO(32)$ and $E_8 \times E_8$ which take their names from the symmetry group of the non-Abelian gauge field that arises in each theory, Type IIa String theory which has a 1-form C_1 and a 3-form C_3 called Ramond-Ramond fields, Type IIb String Theory which similarly has Ramond-Ramond fields consisting of a scalar C, a 2-form C_2 and a 4-form C_4, and finally Type-I String Theory which is equivalent to Heterotic $SO(32)$ theory under the so-called S-duality transformation in the string coupling constant $g_s \to 1/g_s$.

In all of these theories, the supersymmetry imposes that the graviton has a fermionic superpartner called the gravitino. In the low-energy limit, superstring theories hence reduce to theories of supergravity. Just as General Relativity as a theory of gravity is constructed by making the symmetries of Special Relativity local, supergravity is the local-symmetry version of supersymmetric theory. In any case, in superstring and supergravity theories, there exist many fields, including scalar fields, which can be used to physically motivate and construct particular scalar-tensor theories.

To resolve the apparent incompatibility of the 10-dimensionality of superstring theories and the four dimensions of spacetime we observe in reality, compactifications of the 6 extra dimensions are invoked. That is, one looks for specific configurations of the fields in the superstring theory of interest which solve the equations of motion for geometries that only contain four macroscopic dimensions, with the rest much smaller than any scale probed in experiments to date (but could be found and tested by future microscopic tests of gravity or on cosmological scales where their influence may be greater). Such compactifications have been widely studied and form the basis of realistic applications of String Theory.

2.3.2. Open strings, and D-branes

Strings can be classified as "closed" or "open". Closed strings are periodic in their spacelike world sheet coordinate σ such that $x^M(\sigma,\tau) = x^M(\sigma + 2\pi, \tau)$, and hence represent loops of string. Open strings on the other hand have two end points. The behaviour of these end points, however, is constrained by the requirement that a boundary term in the variation of the Polyakov action vanishes. Two types of boundary conditions achieve this. First, Neumann boundary conditions in which the end points of the string are free to move, and do so at the speed of light. Secondly, Dirichlet boundary conditions, which fix the end points of the string to particular points. An open string can have Neumann boundary conditions in some directions (say, for $M = 0 \dots p$), and Dirichlet boundary conditions in others ($M = p+1 \dots D-1$), such that in general, the endpoints of open strings are confined to p-dimensional hypersurfaces. The hypersurface they are confined to is called a Dp-brane or just D-brane.[164]

D-branes are not just constructions which conveniently describe the possible boundary conditions of strings, however, as they are in their own right dynamical objects describing the collective end-points of strings; String Theory is hence not just a theory of one-dimensional strings but also, in this fashion, naturally contains higher-dimensional hypersurfaces which can dynamically fluctuate and move through spacetime, sweeping out generalised world volumes. The endpoints of open strings that reside on D-branes, upon quantisation, lead to the presence of various matter fields on the brane, including effective scalar fields which parametrise the motion and fluctuation of the brane, and gauge fields. Hence, in addition to the large field content of superstring theories, D-branes also give rise to a range of additional fields which may play interesting roles in high energy theory. The action describing a D-brane (excluding effects due to their interactions with the additional C_n fields in superstring theories, which is dealt with by a so-called Chern-Simmons term) is a Dirac-Born-Infeld type action, motivating scalar-tensor theories with kinetic terms like eq. (2.2.19). In superstring theories, the stability of D-branes is related to the presence of the Ramond-Ramond (R-R) fields, such that in Heterotic theories there are no stable D-branes because there are no R-R fields, while in Types IIa and IIb

superstring theories, there are Dp-branes with p even and odd, respectively.
So-called "braneworld" scenarios have been widely studied as high energy theories of gravity in which one can investigate various cosmological phenomena.[165] The presence of matter fields on a brane, which has its own induced metric different from the metric of the target spacetime they exist in, also motivates bimetric scenarios where additional fields are coupled to a metric that is conformally (2.2.9) or disformally (2.2.12) related to the gravitational metric. Such a scenario will form the basis of the original research presented in Chapter 4, where a D3-brane in Type IIb Superstring Theory forms the basis of a non-trivial scalar-tensor model of inflation.

CHAPTER 3

COSMOLOGY

In this chapter we review the present state of knowledge in cosmology, as the models and techniques here form the foundations of the majority of ongoing research in the field. We will describe the successes of the ΛCDM model and the Hot Big Bang, but also their drawbacks. A main point of focus will be inflation, as this is a central theme of the thesis which the original research chapters will be primarily based on.

3.1. The Expanding Universe

3.1.1. The Cosmological Principle

While early and mythical descriptions of the universe often placed Earth as the centre of space, later and more scientific approaches tended more to the assumption that our position in space is not particularly special. This is partly a philosophical statement, but it is also supported by observation. Heliocentrism is a more sensible model of the solar system than geocentrism, when one appeals to a rudimentary understanding of gravitation and orbital mechanics. Further advances in astronomy confirmed this way of thinking; our planet is just one of many bodies around a typical star in a galaxy that is largely unremarkable when compared to others. Cosmology today still starts from this axiom that, at least to first approximation, our position

in the universe is not special or unique. In particular, we as humans are taken to be typical observers in a universe that is homogeneous and isotropic. That is, from any particular point in space one would see the universe the same way we do, on the whole, and that on average the universe looks about the same no matter which way you look from that point. Of course, a cosmologist in a different galaxy would have a different local environment - they might count a few more stars in their galaxy than in ours, or a handful more or less galaxies nearby - but beyond this we expect that they would perceive the average properties of the whole universe - its density or its temperature, say - to be about the same that we do.

3.1.2. Cosmology, Relativity and Gravitation

The axiom that the universe is homogeneous and isotropic is codified and formalised in how one represents it in a General Relativistic framework. While solving the full and untempered Einstein field equations is a monumental task, if one instead posits some physical principles or symmetries that a system is to obey, the simplified field equations are typically found to be more tractable. If the universe is to be homogeneous, then its metric should not depend on spatial coordinates x^i. Similarly, isotropy implies that the spatial part of the metric should not behave differently in different directions. Consequently, the simplest metric satisfying these assumptions that one can imagine, is

$$\mathrm{d}s^2 = g_{\mu\nu}\mathrm{d}x^\mu \mathrm{d}x^\nu = -\mathrm{d}t^2 + a(t)^2 \delta_{ij}\mathrm{d}x^i \mathrm{d}x^j \,. \tag{3.1.1}$$

This is often called the FLRW or FRW metric, after the initials of the authors credited[166–169] with the conception and proof of this. There is hence only one free function, $a(t)$ that specifies the metric entirely, and the Einstein field equations reduce to a much simpler form which will be shown in due course. First, though, let us consider the physical interpretation of the function $a(t)$. Inspection of the above line element indicates that it is a time-dependent scale factor multiplying the spatial part of the metric. This has a clear interpretation for cosmology; it is the expansion of space with time. While mathematically, one could simply set $a = 1$ and have a

static spacetime, experimental evidence suggests that we may not wish to do this. Since the early 20th century, observations of distant galaxies have revealed that they appear to be moving away from us. More dramatically, further away galaxies appear to be receding faster (as determined by e.g. doppler shifting of spectroscopic lines). A concise explanation for this is that the galaxies are not coincidentally arranged with such velocities by pure chance, but rather that the space between our Milky Way and each of these galaxies is expanding in physical size. In this way, the inferred "speed" of a galaxy at distance $R(t) = a(t)r$ would be

$$v = \dot{R} = \frac{\mathrm{d}}{\mathrm{d}t}(a(t)r) = \frac{\dot{a}}{a}R\,, \tag{3.1.2}$$

where $R(t)$ is the physical distance to the galaxy, and r is the "comoving" distance. This latter comoving distance does not change due to the expansion of the universe, but would change due to, say, the intrinsic motion of the galaxy itself, which we neglect here. Equation (3.1.2), in any case, is known as Hubble's Law, and explains the apparent recession velocities of galaxies as due to expansion of space. The ratio between the recession velocity and the physical distance is referred to as the Hubble parameter, $H(t)$, defined by

$$H(t) = \frac{\dot{a}}{a}\,. \tag{3.1.3}$$

It is hence a convenient quantity that represents the rate of expansion of the universe. By convention, a's value today is denoted a_0 and is taken to have a value of 1. Similarly other quantities measured at the present time are subscripted with a 0, such as H_0, which is experimentally found[24] to be around 70 $\mathrm{km\,s^{-1}\,Mpc^{-1}}$, meaning that a galaxy around one megaparsec away from us will appear to recede at around 70 km/s. Due to the experimental uncertainty in its precise value, it is oftentimes written as $H_0 = 100h\ \mathrm{km\,s^{-1}\,Mpc^{-1}}$, such that the factor $h \approx 0.7$ can appear in many derived expressions and separate the uncertainty in H_0 from any uncertainty in the derived quantity itself.

As hinted above, Einstein's equations simplify considerably if the FRLW metric of eq. (3.1.1) is used as an ansatz. The *Friedmann equations* resulting from this allow

one to determine the details of the expansion rate a's evolution in time for a given energy-momentum tensor. Their explicit form is, in terms of the expansion rate H,

$$3H^2 = -T^0_0\,, \tag{3.1.4}$$

$$-(2\dot{H} + 3H^2)\delta^i_j = T^i_j\,. \tag{3.1.5}$$

All other energy-momentum components must be zero (otherwise, the assumptions of the FRW metric are violated). Such an energy-momentum tensor is usually parametrised as a perfect fluid with energy density ρ, pressure p such that,

$$T^\mu_\nu = \mathrm{diag}\left(-\rho(t), p(t), p(t), p(t)\right)\,. \tag{3.1.6}$$

These quantities are also explicitly homogeneous and isotropic (depending only on t), else they would gravitationally affect the spacetime around them and disturb these symmetries. Explicitly, then the Friedmann equations are

$$3H^2 = \rho\,, \tag{3.1.7}$$

$$-(2\dot{H} + 3H^2) = p\,. \tag{3.1.8}$$

Either one of these differential equations specifies a for a given matter content. Similarly, covariant conservation of energy momentum ($\nabla_\mu T^\mu_\nu = 0$) relates ρ and p via the fluid equation

$$\dot{\rho} + 3H(\rho + p) = 0\,. \tag{3.1.9}$$

This can also be derived by combining the two Friedmann equations. It is also convenient to represent the pressure of a perfect fluid via the equation of state $p(t) = w\rho(t)$, where w is a constant, such that the fluid equation would be

$$\dot{\rho} + 3(1 + w)H\rho = 0\,. \tag{3.1.10}$$

We can solve this by rewriting eq. (3.1.10) in the form

$$\frac{\dot{\rho}}{\rho} = -3(1+w)\frac{\dot{a}}{a}\,, \tag{3.1.11}$$

which implies

$$\rho(t) = \rho_0 a^{-3(1+w)}\,. \tag{3.1.12}$$

This can then be substituted back in to the first Friedmann equation (3.1.7) to obtain a differential equation solely in a,

$$\dot{a} \propto a^{-(1+3w)/2}\,, \tag{3.1.13}$$

which has solution

$$a(t) = a_0 \left(\frac{t}{t_0}\right)^{\frac{2}{3(1+w)}}\,. \tag{3.1.14}$$

In general, we thus see that General Relativity predicts that a homogeneous universe containing a perfect fluid of equation of state w, will expand as a power-law in time, and the exponent is determined by that equation of state. The exception to this result is the special case where $w = -1$, where the above procedure is invalid and instead the correct solution takes the form

$$a(t) = a_0 e^{H_0 t}\,. \tag{3.1.15}$$

Where $H = H_0$ is now a constant as when $w = -1$, the fluid equation tells us that ρ is constant and thus by the Friedmann equation H is too. Note that for the power law solutions when $w \neq -1$, we instead have $H \propto 1/t$.

Matter in the standard model of particle physics can be largely grouped into two classes. In the cosmological context these are often call dust (or sometimes simply matter) and radiation. Dust refers to massive particles which, at the given temperature, move significantly slower than the speed of light and behave non-relativistically. A cosmologically dilute fluid of non-interacting dust will be pressureless, and hence it has $w = 0$. Radiation refers to either massless particles like photons, or suffi-

ciently low-mass particles that at the given temperature, they move at $v \approx c$ and behave analogously. As a fluid of photons behave as a black body gas with radiation pressure $p = \rho/3$, this has $w = 1/3$. These observations imply that a universe filled with dust would obey $a \propto t^{2/3}$ and a radiation-filled universe would instead follow $a \propto t^{1/2}$. In either case, the expansion of the universe slows down with time. It is also interesting to explicitly note that from eq. (3.1.12), we can say that cosmic dust will dilute as $\rho \propto a^{-3}$, which is as expected - essentially this states that the energy density is inversely proportional to the volume. Radiation, however, goes as $\rho \propto a^{-4}$, which can be thought of as dilution both with volume, and loss of energy due to red-shifting of the photon's wavelength ($\rho \propto E/V \propto \lambda^{-1}V \propto a^{-1}V \propto a^{-4}$). In any case, one implication of this that will become important later is that during an expansion, radiation dilutes in energy density faster than non-relativistic matter.

3.1.3. Curvature and Density of the Universe

While we have thus far ignored this by using the Cartesian-like form of eq. (3.1.1), the FRLW metric is also permitted to have global curvature. This does not break homogeneity so long as the curvature is a constant throughout space. This is more readily described if one transforms to spherical polar coordinates, in which the metric can be written,

$$\mathrm{d}s^2 = g_{\mu\nu}\mathrm{d}x^\mu \mathrm{d}x^\nu = -\mathrm{d}t^2 + a(t)^2\left(\frac{\mathrm{d}r^2}{1-kr^2} + r^2\mathrm{d}\Omega^2\right), \tag{3.1.16}$$

where $\mathrm{d}\Omega^2$ is the metric on a 2-sphere and k is the curvature, which can be $k = 0$ for flat geometry, or $k = \pm 1$ for spherical/hyperbolic geometry.[1] When accounted for in this way, the curvature appears in the Friedmann equations as

$$3H^2 = \rho - \frac{3k}{a^2},, \tag{3.1.17}$$

$$-(2\dot{H} + 3H^2) = p + \frac{k}{a^2}. \tag{3.1.18}$$

[1] An alternative normalisation where a is fixed and k varies can be used, but will not be described here.

Curvature can be eliminated in a combination of these equations, most often known as the acceleration equation,

$$\frac{\ddot{a}}{a} = -\frac{1}{6}(\rho + 3p) \ , \tag{3.1.19}$$

which is useful in making curvature-independent statements about the expansion of the universe.

Equations (3.1.17 – 3.1.18), upon inspection, reveal that curvature contributes to the expansion of the universe analogously to a fluid with $\rho \propto a^{-2}$ or equivalently $w = -1/3$, albeit with a negative contribution to the effective energy density if k is positive. Equation (3.1.17) implies one can define[170] a critical density $\rho_c = 3H^2$ for which $k = 0$, such that a condition for the universe being spatially flat is that $\rho = \rho_c$ exactly, while a closed (spherical) universe or an open (hyperbolic) universe would respectively have larger and smaller densities. That is, one can determine the curvature of the universe by measuring its density. With reinstated units, the critical density takes the value today of,

$$\rho_{c,0} = 3H_0^2 M_{\rm Pl}^2 \approx 1.9h^2 \times 10^{-26} \text{ kg m}^{-3}. \tag{3.1.20}$$

Alternatively, if one writes this in terms of solar masses, it takes the value

$$\rho_{c,0} \approx 2.8h^2 \times 10^{11} M_\odot \text{Mpc}^{-3} \, . \tag{3.1.21}$$

As a rough Fermi estimation, astronomical observations suggest galaxies weigh some 10^{11} solar masses, and are separated from one another by about a megaparsec in space, so we can see that the density of the universe is at least around the same order of magnitude as the critical density. As we will later discuss, however, merely counting galaxies in this way is insufficient to precisely determine the density of the universe as dark matter and dark energy play a central role. More refined observations and experiments accounting for such factors reveal that $|\rho_0 - \rho_{c,0}| \ll \rho_{c,0}$ suggesting the geometry of the universe is consistent with flatness, typically to sub-percent precision[171] (varying a little depending on the method).

3.1.4. Realistic, Multi-Fluid Models

While a universe containing only matter or only radiation, for example, can be easily understood via the above prescription, the real universe contains multiple fluids (dust and radiation, as well as dark energy which we will later see does not fit into either class) as well as possibly a small amount of curvature. It is hence useful when studying models of the universe to decompose the density and pressure in the Friedmann equations into non-interacting components for each fluid, for example given some non-relativistic matter, radiation and curvature, the first Friedmann equation could be understood as

$$3H^2 = \rho = \rho_{\mathrm{m}} + \rho_{\mathrm{r}} + \rho_{\mathrm{k}} \,, \tag{3.1.22}$$

where $\rho_{\mathrm{k}} = -k/a^2$ is an effective curvature energy density, and the matter and radiation densities obey the fluid equation for their respective equations of state of 0 and 1/3. However, as we know from the solution of the fluid equation in eq. (3.1.14), each non-interacting ρ_i has its own dependence on a. We can hence recast the Friedmann equation as

$$3H^2 = \rho_{\mathrm{m},0} a^{-3} + \rho_{\mathrm{r},0} a^{-4} + \rho_{\mathrm{k},0} a^{-2} \,. \tag{3.1.23}$$

This gives us a differential equation for a in terms of a multi-component universe, and can be numerically (or in some special cases, analytically) solved. Qualitatively, however, one can see that as a increases, eventually the radiation term will become smaller than the matter term, which will in term become smaller than the curvature term, no matter the hierarchy of their initial densities; some fluids/densities simply dilute faster than others and this gives rise to a key observation. That is, in the distant future it is the curvature of the universe which determines its fate.[2] A flat universe would, at late times, be matter-dominated and behave like $a \propto t^{2/3}$; it would expand forever, but at an ever-decreasing rate. A hyperbolic universe with $k < 0$ would at late times be dominated by the curvature term, and behave as $a \propto t$, expanding forever, but now at a constant rate. If $k > 0$ and the universe has closed,

[2] Or, it would be if not for dark energy, which will be introduced shortly.

spherical, geometry, then eventually the matter and curvature terms would become equal and $H = 0$ would occur, at which point the expansion would reverse in a time-symmetric fashion (the Friedmann equation is invariant under $t \to -t$) and recollapse.

This can also be written in terms of density parameters, defined for each fluid as $\Omega_i = \rho_i/\rho_c$, such that

$$H^2 = H_0^2 \left[\Omega_{\mathrm{m},0} a^{-3} + \Omega_{\mathrm{r},0} a^{-4} + \Omega_{\mathrm{k},0} a^{-2}\right] . \tag{3.1.24}$$

This is convenient as it often easier to work with the density parameters evaluated today (correspondingly denoted with a 0 in the subscript), which are numbers between 0 and 1, and whose sum is equal to unity. Furthermore, the relationship between scale factor and redshift, z,

$$a(z) = \frac{1}{1+z} , \tag{3.1.25}$$

which tells us what the scale factor of the universe was at the time from which we are seeing an object at a redshift of z[3], allows us to write this in the form

$$H(z)^2 = H_0^2 \left[\Omega_{\mathrm{m},0}(1+z)^3 + \Omega_{\mathrm{r},0}(1+z)^4 + \Omega_{\mathrm{k},0}(1+z)^2\right] , \tag{3.1.27}$$

which is useful for observational purposes. As z can be measured by astronomical observation for a range of distant objects, and the value of $H(z)$ can also be calculated using Hubble's Law (3.1.2) on a galaxy at redshift z, one can use measurements from many distant objects in this fashion to determine the parameters in the H-z relationship of eq. (3.1.27). In this way, one reconstructs the history of $H(z)$ and hence gains a greater understanding of the composition of the universe both in the past and today.[172]

[3]Note that redshift is defined such that $(1+z)$ is the ratio of the wavelengths observed today (λ_0) and emitted by an object in the past (λ_{em}). The scale factor of the universe at the times of observation and emission are in direct proportion to these wavelengths. Combining these facts gives us

$$\frac{a(t_0)}{a(t_{\mathrm{em}})} = \frac{\lambda_0}{\lambda_{\mathrm{em}}} = (1+z) , \tag{3.1.26}$$

which leads to the result (3.1.25) as $a_0 = 1$ today

A convenient way of observationally studying the H-z relationship above is via measurement of the luminosity distance of standard candles such as type Ia supernovae[15,17] and using the data from this to fit the cosmological density parameters in eq. (3.1.27). When this was done, the data was found to be consistent with an accelerating expansion, one in which $\ddot{a} > 0$. One can infer from the data that this requires the presence of an extra fluid, which dominates the expansion profile of the universe, consistent with an equation of state of (close to) -1.[24] As exposed in eq. (3.1.15), such a fluid induces an exponentially accelerating expansion of space. Additionally, studying the acceleration equation (3.1.19), it is clear that the condition for an accelerating expansion $\ddot{a} > 0$ is $p < -\rho/3$, or $w < -1/3$, which is inconsistent with a model containing just dust, radiation and curvature. This is shocking as it implies the existence of a "dark energy" - a component of the universe's contents which corresponds to no substance formed from standard model particles.

3.1.5. Cosmological Constant and Dark Energy

Perhaps the simplest extension of the cosmology discussed thus far that would meet some of the descriptors of dark energy is the cosmological constant introduced in eq. (2.1.16). The cosmological constant, Λ, can be thought of as the vacuum energy of spacetime itself. Deriving a modified set of Friedmann equations from the Λ-containing Einstein field equations (2.1.17) reveals that

$$3H^2 = \rho_{\mathrm{m}} + \rho_{\mathrm{r}} - \frac{3k}{a^2} + \Lambda, , \tag{3.1.28}$$

$$-(2\dot{H} + 3H^2) = p_{\mathrm{m}} + p_{\mathrm{r}} + \frac{k}{a^2} - \Lambda\,. \tag{3.1.29}$$

Evidently from the form of the contribution of Λ in these two equations, it is like a perfect fluid with $w = -1$. From eq. (3.1.12), we see this means that its energy density scales as $\rho \propto a^0$ - hence the name "cosmological constant". It is an energy density component which remains constant despite the expansion of the universe. Unlike matter or radiation or curvature, it does not dilute, and hence would be the dominant component of the universe at late times when all other fluids are negligible,

and in its presence, the fate of the universe would be one of eternal, accelerating expansion. Including it in the picture described above, the H-z relation becomes

$$H(z)^2 = H_0^2 \left[\Omega_{\mathrm{m},0}(1+z)^3 + \Omega_{\mathrm{r},0}(1+z)^4 + \Omega_{\mathrm{k},0}(1+z)^2 + \Omega_{\Lambda,0}\right] , \tag{3.1.30}$$

where $\Omega_\Lambda = \Lambda/3H^2$. Experiments suggest the present day values[24] of the density parameters in this model are

$$\Omega_{\mathrm{m},0} \approx 0.3 \tag{3.1.31}$$

$$\Omega_{\mathrm{r},0} \ll 1 , \tag{3.1.32}$$

$$\Omega_{\mathrm{k},0} \approx 0 , \tag{3.1.33}$$

$$\Omega_{\Lambda,0} \approx 0.7 . \tag{3.1.34}$$

The average equation of state of the universe is then $w \approx -0.7$, firmly in the range needed for accelerating expansion. We can also give a value for the cosmological constant by noting from the definition of Ω_Λ that then $\Lambda \approx 0.7 \times 3H_0^2$. This paints a picture of a flat universe whose radiation content has diluted to a fraction of a percent of the energy contained in the universe as it dilutes faster than the other components. Meanwhile, there is still a non-negligible component of non-relativistic matter, but it will inevitably become less important as the universe continues to expand, leaving only dark energy. This changes the discussion above in which we said that curvature determines the ultimate fate of the universe; dark energy supersedes this for as long as it continues to behave as it does today with $w \approx -1$, and will cause the universe to expand exponentially forever. If instead, dark energy does not remain this way for all time and it later takes on a different behaviour, the fate of the universe will correspondingly be determined by this, though we do not fully understand dark energy well enough to confirm or deny this possibility at present.

Dark energy is not the only "dark" component of our universe of which we know little. Of the non-relativistic matter contained in the universe (with $\Omega_\mathrm{m} \approx 0.3$), the majority of this is found to be not the conventional atomic matter that makes up

the intuitive and observable world of stars and planets, but instead a mysterious "dark matter" which is optically invisible. Unlike atoms and conventional matter that interact with light and hence can be seen in large enough quantities such as galaxies, dark matter is completely invisible and we can only infer its presence via its gravitational influence. In fact, one finds that some 85% or so of the matter component of the universe is dark,[24] leaving only a few percent of the universe's mass and energy behind to make up the atoms of conventional matter. In essence, one of the most interesting results of modern cosmology is hence that the proportion of the universe's contents we know and understand well is tiny. The leading model of cosmology, based on a universe containing cold[4] dark matter and a cosmological constant (as well as the small amount of normal dust/radiation), is known as the ΛCDM model. And while this model describes the majority of phenomena in the universe very well, we lack a fundamental explanation of what dark matter is made of, and whether dark energy is a cosmological constant or something else entirely.

The Cosmological Constant's Problem

The possibility that dark energy is something more complex than a mere cosmological constant remains open. First, this is because of conceptual problems in interpreting the value of the cosmological constant. In the above discussion, we neglected that, according to standard model particle physics and quantum field theory, vacuum energy is also produced by quantum effects in matter fields. The actual value of Λ gravitating and appearing in the Friedmann equations, is then comprised of a bare cosmological constant Λ_{cc} from the gravitational action, and a contribution coming from quantum effects Λ_{q}. The problem with this is that quantum field theory predicts that this latter contribution to the vacuum energy relative to the inferred value of the vacuum energy today (Λ) is approximately $\Lambda_{\mathrm{q}} \approx 10^{120}\Lambda$. This would require us to choose the gravitational vacuum energy Λ_{cc} such that it cancels out the quantum contribution to hundreds of digits of precision in order to achieve the desired value of Λ.[46] This degree of fine-tuning alone seems unnatural enough

[4] Cold dark matter differs from warm or hot dark matter in that it is assumed to be entirely non-relativistic, and hence $w \equiv 0$.

to be a concern, and is often said to be the "greatest embarrassment of theoretical physics", but the problem runs deeper still than this. The value of Λ_q is also highly sensitive to the details of new physics, and simply taking into account the existence of new particles beyond the standard model, or even just computing it to a higher degree of accuracy within the framework of perturbative QFT, changes the value we expect it to take, and would hence require order-by-order re-tuning of the cosmological constant. This is simply not acceptable from a theoretical standpoint. While approaches such as the sequester[173,174] have been proposed to alleviate this immense fine-tuning issue, an entirely satisfactory framework in which to reconcile quantum mechanics and gravity/cosmology in this way has not yet been proposed. The future solution may depend on the details of beyond-standard-model physics or those of the unification of gravity with the other forces (e.g. String Theory).
In the mean time, this motivates consideration of alternative explanations of the accelerating expansion, beyond the simple (or evidently not so simple!) cosmological constant.

Scalar Field Cosmology and Dark Energy

An alternative proposition for the nature of dark energy is an exotic scalar field, in a scenario that is often known as quintessence - the introduction of a fifth force of nature mediated by this scalar to solve the dark energy problem. A canonical scalar field with arbitrary potential V has the Lagrangian

$$\mathcal{L}_\phi = -\frac{1}{2}\partial_\mu\phi\partial^\mu\phi - V(\phi)\,, \tag{3.1.35}$$

and its addition to the usual gravitational action forms the simplest scalar-tensor theory of gravity as set out in eq. (2.2.4) of Section 2.2.2. Its variation yields the energy-momentum tensor

$$T_{\mu\nu} = \partial_\mu\phi\partial_\nu\phi + g_{\mu\nu}\mathcal{L}_\phi\,, \tag{3.1.36}$$

leading to the identification of a scalar field with a perfect fluid, via eq. (3.1.6), with effective energy density and pressure

$$\rho_\phi = \frac{1}{2}\dot{\phi}^2 + V\,, \tag{3.1.37}$$

$$p_\phi = \frac{1}{2}\dot{\phi}^2 - V\,. \tag{3.1.38}$$

Unlike the fluids of dust and radiation considered previously, the equation of state parameter $w = p/\rho$ for the scalar field fluid is non-constant and dynamical. This motivates the possibility that w could change in future and affect the ultimate fate of the universe. In fact, w for a scalar field can take any instantaneous value in $[1, -1]$ depending on the ratio of kinetic and potential energy densities it carries. In particular, in a potential-dominated regime, we find $w \approx -1$ which makes it suitable to imitate a cosmological constant and hence serve as a dark energy candidate. In this approach, the scalar field typically evolves in time somewhat too, leading to an equation of state that differs slightly from -1 (as allowed by the experimental bounds on w), and possibly also changes with time. This could hence in principle be distinguished from a cosmological constant with precise enough measurements. This possible answer to the dark energy problem, however, leads to a host of its own questions. As a scalar-tensor theory, a quintessence model of dark energy may interfere with the successes of General Relativity by modifying the behaviour of gravity. Much work has gone into finding extended scalar-tensor theories to achieve quintessence without causing overly large deviations in GR's highly accurate predictions of usual phenomena. One example of this is the idea of screening mechanisms,[175–177] whereby a coupling between the scalar field and matter mellows and suppresses the gravitational effect of the scalar field in high-density, small-scale regions such as Earth and the solar system where GR has been most precisely verified, while still allowing it to produce more pronounced effects such as dark energy on global scales where constraints are more liberal. This remains an active area of research, and one that we will be largely uninterested in for the purposes of this thesis, but we will revisit the applications of scalar-tensor theories later in this chapter when we come to look at inflation.

3.1.6. History of the Universe and Thermodynamics

Present knowledge suggests that the universe is approximately[24] 14 billion years old, which can be roughly estimated as $t \approx H_0^{-1} \approx 10^{10}$ years, and in the Hot Big Bang model it begins at this time in a state of extreme temperature where the matter-energy content is super-relativistic and hence behaving as radiation. With the tools and theoretical framework described above, we can go on to understand many of the details of how this evolved to the universe we see today and explain some of the more striking results of the last 100 years of breakthroughs in cosmology.

We now have an idea that the universe contains dust, radiation and dark energy (and possibly curvature), and that by GR the densities of these fluids evolve differently as the universe expands, and in turn cause the universe's expansion rate to change. ("Spacetime tells matter how to move; matter tells spacetime how to curve." [178]) One consequence of this, as mentioned previously, is that the dominant component of the universe changes with time. Radiation scales as $\rho \propto a^{-4}$ while dust scales as $\rho \propto a^{-3}$ so if one starts off with an excess of radiation as in the Hot Big Bang, but with a small amount of dust nonetheless present, and lets the universe evolve for some time, eventually there will be more dust than radiation. Alongside this change, however, the universe also cools as it expands, which changes the microphysical behaviour of these fluids - reactions and interactions and other physical processes occurring between particles depend on the temperature they are carried out at. Of particular relevance is that as the universe cools in this way, massive particles will gradually become non-relativistic and behave not as radiation but as dust.

It is intuitive enough that the universe cools as it expands in this way, but how much does it cool with time? This can be answered by considering the temperature of the universe to be the temperature of a radiation bath with a thermal spectrum that fills it, which has energy density $\rho \propto T^4$ by the well known Stefan-Boltzmann relation. Combining this with eq. (3.1.12) yields

$$T \propto a^{-1}\,, \tag{3.1.39}$$

or that the temperature of the universe scales in inverse proportionality with its

size, whose evolution with time is given by (3.1.14). For a given cosmological history, this tells us $T(t)$. This has several useful applications in more quantitatively understanding the history of the universe. In what follows we will list some of the key phases in the universe's history and where they fit in to the thermal history $T(t)$.

Firstly, at very high temperatures, or in the very early universe, it is thought that the microphysics of the universe is described not by the standard model of particle physics, but instead by a so-called GUT (Grand Unified Theory) which unifies the electromagnetic and nuclear forces in terms of a more fundamental description of nature whose consequences are not apparent at the relatively pedestrian energy scales our present experience and technology can access. In the standard ΛCDM model, the time at which GUT physics control the universe can be estimated[9,36] as a tiny fraction of a second after the Big Bang when $T \approx 10^{28}$ K, when radiation still dominates. Following this, the universe continues to cool and gradually approach the standard model which we perceive today.

When the universe cools further over the first second or so of its existence to a more "moderate" temperature of $T \approx 10^{10}$ K, a major milestone is reached. Typical photons in the universe's radiation bath cooled to an energy comparable to the binding energy of atoms.[11] That is, nucleon-photon collisions begin to be too weak to break apart nuclei that form via the strong nuclear force. This time in the history of the universe thus represents the birth of matter as we know it; from this moment, nuclei of the lightest few elements of the periodic table were able to stably exist to later go on to form stars and fuse into the substances that form planets and living organisms. This is known as the epoch of Nucleosynthesis, and the precise rate at which different elements and isotopes were produced in the radiation-dominated cosmological background of the ΛCDM model is one of the key confirmations of its success. Without this, there would not be a concise explanation for the initial conditions for the abundances of primordial elements, and hence the prevalence of them and their derivatives today. While nuclei were at this point able to form in this way, they still could not form neutral atoms as the photon sea was still plenty energetic enough to rapidly ionise atoms if any formed.

Some time after this, estimated around a few thousand years into the universe's existence, with temperatures now in the realm of some tens of thousands of Kelvins, the density of dust/matter finally outgrew the initially dominant radiation density and the universe began its matter-dominated epoch in which the expansion rate is now $a \propto t^{2/3}$. After this when the universe was 350,000 years old, the photons finally cooled enough to allow neutral atoms to stably exist and the beginning of atomic matter and the laws of chemistry naturally followed. The universe at this time was some 3000 K in temperature, and it is in these conditions that one of the most significant and interesting events in the history of the universe occurred: decoupling.[36,179] Prior to this, as the universe consisted of photons and a plethora of charged particles (nuclei and electrons), those photons strongly interacted with the charged matter in their presence, maintaining a thermal equilibrium. When matter became neutral due to the expansive cooling of the universe in this way, the interaction rate dropped off sharply and suddenly, leaving the atoms decoupled from the photons, and the photons more-or-less freely streaming. The photons of the epoch of decoupling are still around today some billions of years later, cooled and stretched out even further, and can be detected as microwave-frequency radiation, permeating space in every direction, known as the Cosmic Microwave Background (CMB).

Some time after this period of matter domination, the expansion inevitably dilutes the conventional fluids to a point where instead the constant-density dark energy fluid comes to dominate. This brings us to the state of the universe today, where we have observed and measured the CMB radiation with a temperature of just 2.73 K.[14] The detection and explanation of this forms another cornerstone of the Hot Big Bang cosmology's success, but it is also an immensely useful probe of the state of the early universe. As the pre-decoupling photons were in thermal equilibrium with the matter distribution of the universe at that time, the slight anisotropies of the CMB radiation in different parts of space reveal precisely how inhomogeneous the universe was in the early matter-dominated epoch. That is, some regions of space were denser and hence slightly hotter than their surroundings in the early universe, producing CMB radiation of ever so slightly different temperature.

These differences, while minute, are detectable and have a magnitude of $\Delta T \approx 10^{-5}T$. One interesting footnote of this is that it confirms to high accuracy the validity of the FRLW metric as a metric for the universe, with inhomogeneities small enough to be often neglected or, when necessary for more precise questions, treated perturbatively. This is of ultimate relevance, however, as it is those slight overdensities and inhomogeneities which, via gravitational collapse, later formed stars and galaxies and the structure-rich universe we observe today. The CMB radiation thus gives us otherwise inaccessible information about the state of the universe in its early life, and provides us with data on the initial conditions of the subsequent growth of structure via initially tiny gravitational instabilities. One can of course ask the question though, what gave rise to that initial distribution of inhomogeneity in the structure of the universe and why did it take the precise form it did, a question which will be addressed in some detail in the next chapter.

3.2. Inflation

3.2.1. Problems with the Hot Big Bang

With time, it became apparent that despite the Hot Big Bang model's success in describing the history of the universe as a series of epochs of radiation, matter and accelerating dark energy domination, there were some inconsistencies and issues that could not be satisfactorily resolved without an extension of the physics discussed above. These include:

The Horizon Problem

As mentioned previously, we can observe in any direction out in space a background of microwave-frequency thermal radiation (the CMB) originating from the epoch of decoupling when neutral atoms first formed. Furthermore, this radiation is highly isotropic, exhibiting the same temperature across all space to within a few millionths of a degree. This implies that radiation coming from two opposite sides of the observable universe was, at the time of decoupling, in thermal equilibrium. However,

an approximate calculation suggests that information propagating at the speed of light (hence following a null geodesic where, in the radial direction in flat spacetime, $\mathrm{d}r = ca^{-1}\mathrm{d}t$) since the Big Bang will have travelled a distance

$$R(t) = a(t)\int_0^t \frac{c\,\mathrm{d}t'}{a(t')} \approx ct \approx cH^{-1}\,. \tag{3.2.1}$$

In this, we have assumed that the scale factor is constant for simplicity, but this is sufficient for a back-of-envelope, order of magnitude estimate. The maximum distance a light-speed signal could have travelled since the Big Bang at the time of decoupling would then be approximately (using $H \propto t^{-1}$ during the radiation and matter-dominated epochs involved and the approximate values for the age of the universe today and the time of decoupling)

$$R_{\mathrm{dec}} \approx cH_0^{-1}\left(\frac{t_{\mathrm{dec}}}{t_0}\right) \approx 10^{-1}\ \mathrm{Mpc}\,. \tag{3.2.2}$$

This is the maximum size a patch of space could be causally connected over, and hence in thermal equilibrium across, at the time of decoupling. Since the time of decoupling and until the present day, assuming matter domination (hence $a \propto t^{2/3}$), this patch of space will have expanded in size to

$$R_{\mathrm{dec}}\frac{a_0}{a_{\mathrm{dec}}} = 0.1\ \mathrm{Mpc} \times \left(\frac{t_0}{t_{\mathrm{dec}}}\right)^{\frac{2}{3}} \approx 10^2\ \mathrm{Mpc}\,, \tag{3.2.3}$$

which, on cosmological scales, is very small indeed. The isotropy of CMB radiation over more than a few degrees of the sky is hence apparently in violation of causality, in the Hot Big Bang cosmology. This is known as the Horizon Problem.

The Flatness Problem

Observations[171] suggesting that the curvature density parameter of the universe is presently consistent with 0 ± 10^{-2} or so present two possibilities. Firstly, the universe could be perfectly flat with $k = 0$. Alternatively, if $k \neq 0$, then the curvature density parameter is presently non-zero and will not be identically zero at any point in the universe's history. However, should this latter scenario be the case, this presents a

problem. Noting that

$$\Omega_k = -\frac{k}{a^2 H^2}\,, \tag{3.2.4}$$

we see that in a radiation-dominated background

$$a \propto t^{\frac{1}{2}}\,, \quad H \propto t^{-1} \;\rightarrow\; \Omega_k \propto t\,, \tag{3.2.5}$$

while in a matter-dominated background

$$a \propto t^{\frac{2}{3}}\,, \quad H \propto t^{-1} \;\rightarrow\; \Omega_k \propto t^{2/3}\,. \tag{3.2.6}$$

In either case, it grows. For $|\Omega_k| = 10^{-2}$ today, it would have to have been much smaller in the early universe. Putting some numbers in we find, more specifically, that at some early time, such as nucleosynthesis (1 second after the Big Bang), this would imply

$$\Omega_k(t_{\rm nuc}) = 10^{-2} \times \left(\frac{t_{\rm nuc}}{t_{\rm eq}}\right) \times \left(\frac{t_{\rm eq}}{t_0}\right)^{\frac{2}{3}} \approx 10^{-17}\,, \tag{3.2.7}$$

where the first bracket accounts for the radiation-dominated phase between nucleosynthesis and equality, and the second bracket accounts for the matter-dominated epoch between equality and today (we neglect the existence of dark energy for simplicity). Essentially, this shows that for the universe to have a non-zero, but permissibly small curvature today, the primordial curvature must have been immensely fine-tuned to be close to zero. The further back in time one looks, the more severely fine-tuned the early-time curvature must be. This fine tuning problem is called the Flatness Problem and is also not resolved within the standard Big Bang cosmology.

The Monopole Problem

In the first tiny fraction of a second after the Big Bang when the temperature is huge (e.g. $T \approx 10^{28}$ K), the laws of physics are thought to be described by so-called Grand Unified Theories instead of the usual Standard Model of particle physics. In these theories, particles and objects with masses only a few orders of magnitude below the

Planck mass may be produced. These "relics" include monopoles, supersymmetric particles and topological defects and are a problem in the foundations of the Hot Big Bang expansion. Their immense mass would cause them to quickly become non-relativistic and resultingly dominate the universe, should they be sufficiently long-lived (as non-relativistic particles scale in density as a^{-3} while the background radiation scales as a^{-4}). This would interfere with the success of the Hot Big Bang model, which requires the radiation-dominated epoch to persist through until at least the time of Nucleosynthesis in order to correctly replicate the primordial abundances of the chemical elements. A mechanism which avoids this is likely necessary to allow the correct cosmology to proceed in the context of a typical high energy theory of particle physics.

Primordial Structure Formation

We mentioned previously how structures in the universe such as galaxies and so on formed due to slight overdensities and inhomogeneities in the early universe which grew through gravitational instability and subsequent collapse over billions of years. This can be probed by looking at anisotropies in CMB radiation, with a magnitude of around one part in 10^5. The question is: where did these inhomogeneities initially come from (e.g. what kind of initial conditions are needed in order to lead to this at the time of decoupling, and what mechanism generates them) and why did they have the amplitude and statistical distribution they did. Addressing this question will be of central importance later in this thesis, but it requires the tools of cosmological perturbation theory which will be introduced in due course.

3.2.2. Inflationary Cosmology

3.2.3. Resolving the HBB Problems: Accelerating Expansion

A proposed solution to the inconsistencies and problems of the Hot Big Bang cosmology was developed in the early 1980s. What if, in the extremely early universe, there was a period of accelerating expansion of space? That is, preceding the usual radiation-dominated epoch, what if there were an epoch - which we now call *infla-*

tion - in which the expansion of the universe underwent a rapid acceleration and hence grew in size by a large factor. Let us see how this assumption relates[179] to the problems listed above:

The Horizon Problem Revisited

In the Hot Big Bang model, light could not have travelled far enough in the time before decoupling for a patch of space that expanded into the size of our observable universe today to be in thermal equilibrium, and so the apparent isotropy of CMB radiation today is not possible. If, however, in the very early universe, a period of substantial expansion occurred, then a much larger patch of space today could have been in causal contact in the distant past due to this. The early universe is re-envisaged such that a much smaller initial patch of space expanded into the observable universe today, hence explaining how it could have ever been in causal contact; the horizon beyond which patches of space were never in causal contact is pushed out to beyond the size of the observable universe.

The Flatness Problem Revisited

In an accelerating expansion $\ddot{a} > 0$, which, corresponds to $w < -1/3$ via eq. (3.1.19). In combination with eq. (3.1.14), this implies that in such cases the density parameter of curvature (3.2.4) is decreasing with time, rather than increasing as in the matter and radiation-dominated expansions. This means that, qualitatively, it is possible to alleviate the fine-tuning issue of the Flatness Problem by having an accelerating expansion of space in the early universe, as this would drive Ω_k closer to 0, rather than away from it, making the very small value allowed today much more natural. This also lets us simply estimate how much the universe would need to have expanded in this fashion to counteract the growth of Ω_k at later times. Extending the calculation in eq. (3.2.7) back to an inflationary epoch taking place between times t_1 and t_2, we would find that

$$\Omega_k(t_0) = \Omega_k(t_1) \times \left(\frac{a_1 H_1}{a_2 H_2}\right)^2 \left(\frac{t_{\rm eq}}{t_{\rm f}}\right) \times \left(\frac{t_0}{t_{\rm eq}}\right)^{\frac{2}{3}}, \tag{3.2.8}$$

where the terms in brackets from left to right represent the inflationary period, the radiation-dominated period from after inflation up until equality, and the matter-dominated period from equality up to today (again, neglecting the present dark energy epoch for simplicity). Let's say we take the value of Ω_k at the beginning of inflation ($t = t_1$) to be $O(1)$ for argument's sake, then, assuming that inflation is driven by a cosmological constant-like fluid with equation of state $w = -1$ so that $H_1 = H_2$, and taking a typically assumed time of inflation's end of $t_2 \approx 10^{-34}$ s, one finds that eq. (3.2.8) implies that to achieve a suitably small $\Omega_k(t_0)$ one would need

$$\frac{a_2}{a_1} \approx 10^{26}\,, \tag{3.2.9}$$

that is, the universe would need to increase in size by a factor 10^{26} during the inflationary expansion. This amount is usually written instead in terms of the number of e-folds of expansion - the number of times the universe has multiplied in size by a factor e, or

$$N = \log_e\left(\frac{a_2}{a_1}\right) \approx 60\,. \tag{3.2.10}$$

The Monopole Problem Revisited

Unwanted stable relics of the early universe's particle theory would be diluted away to essentially zero density by an inflationary expansion, thus preventing them from coming to dominate. It is important, however, that following the inflationary epoch these particles are not reproduced. This will be important later when we come to discuss the particulars of inflation and specifically how (and at what temperature) its end comes about.

Primordial Structure Formation Revisited

Inflation ameliorates the Horizon, Flatness and Monopole Problems essentially by brute force; have enough expansion occur quickly enough and these issues go away. How this relates to primordial inhomogeneities seeding subsequent growth of structure in the universe is considerably more subtle, but we will shockingly see in due

course that inflation does indeed give rise to a possible solution of this issue too.[179]

3.2.4. How to Inflate a Universe

It is fine to state that a period of inflation is necessary, but we have no physical mechanism to explain how it comes about. As discussed, no matter in the standard model can drive an accelerating expansion of spacetime. We need a new field or fluid, which we will call the *inflaton*, which can fulfil this role. Fortunately, how to go about answering this has already been hinted at in Section 3.1.5 - the premise of an accelerating expansion is exactly the same as the dark energy problem. We can't, however, just use a cosmological constant term as while this would most definitely drive inflationary expansion of space, inflation would not be able to stop, either. We previously saw that a cosmological constant behaves as its name suggests and maintains a constant energy density while other fluids dilute via expansion of spacetime - once it dominates, it dominates forever, which is not desirable.

It is therefore natural to consider that the inflationary fluid begins with an equation of state close to -1 then later changes equation of state to something larger, stopping the accelerating expansion of space and giving way to the usual and well-understood radiation-dominated epoch of the Hot Big Bang. How we precisely go about this will be discussed later in Section 3.2.5, but for now, we note that the ability to change the equation of state is naturally possible in scalar fields, which we also mentioned in the context of dark energy previously. As we have an equation of state, using eqs. (3.1.37 – 3.1.38), of

$$w = \frac{\frac{1}{2}\dot{\phi}^2 - V}{\frac{1}{2}\dot{\phi}^2 + V}\,, \tag{3.2.11}$$

we can see that if $2V \gg \dot{\phi}^2$ then $w \approx -1$. If $\dot{\phi} \equiv 0$ then this is identical to a cosmological constant (cf. the Lagrangian in eq. (3.1.35) for example) but if $\dot{\phi}$ instead varies, then so does w. In fact, since the opposite limit of $2V \ll \dot{\phi}^2$ implies $w \approx 1$, we can see that any equation of state between ± 1 is possible in this model. We hence have a reasonable starting point for our discussion of how to drive a sustained but not unending period of inflation; scalar fields. Particularly, we want a scalar

field which is initially close to static, but later begins to roll down its potential[179] such that the equation of state departs from the accelerating regime and can allow inflation to terminate. To understand this better, let us study the equation of motion of the field ϕ. Using either the fluid equation (3.1.9) with the appropriate density (3.1.37) and pressure (3.1.38) or by directly applying the variational principle to the scalar-tensor action (3.1.35) and specialising to a cosmological background, we find the Klein-Gordon equation in an expanding spacetime

$$\ddot{\phi} + 3H\dot{\phi} + V_{,\phi} = 0\,. \tag{3.2.12}$$

This, in addition to one of the Friedmann equations (as the other Friedmann equation can be derived from it and the fluid equation) specifies the evolution of the universe. For simplicity we take the G_{00} equation:

$$3H^2 = \frac{1}{2}\dot{\phi}^2 + V\,. \tag{3.2.13}$$

To solve the system of eqs. (3.2.12) and (3.2.13) exactly is not trivial. Note in particular the term $3H\dot{\phi}$, which can be rewritten using the Friedmann equation as

$$\ddot{\phi} + \sqrt{\frac{3}{2}\dot{\phi}^2 + 3V}\dot{\phi} + V_{,\phi} = 0\,,$$

which is rather nonlinear and hence does not typically admit any obvious solutions even for simple potentials. Numerically this poses no problem but this does not facilitate a deeper understanding. An approximation scheme is hence in order to make some analytical headway to this end.

As we already have the condition $2V \gg \dot{\phi}^2$ during inflation, we can apply this to understanding the approximate behaviour of the system in this limit. This will be very accurate in the early stages of inflation, but break down as it comes to an end. Proceeding along this line of thought, the Friedmann equation is approximated by

$$3H^2 \approx V\,. \tag{3.2.14}$$

This alone makes solving the system more tractable as it does away with the non-

linearity in $\dot{\phi}$, but we can do a little bit better. This approximation so far has not simplified the Klein-Gordon equation as $\dot{\phi}^2$ does not appear as part of it. To progress, we further note that, in addition to the requirement that $2V \gg \dot{\phi}^2$ to make the expansion of spacetime inflationary, we also need inflation to be somewhat sustained in order for there to be enough inflationary expansion (60 e-folds to achieve 3.2.9, typically) to solve the problems associated with the Hot Big Bang model. This is significant because even if $\dot{\phi}^2$ is small initially, a large $\ddot{\phi}$ will quickly change this and terminate inflation early. We hence also require the condition $\ddot{\phi} \ll 3H\dot{\phi}$. A good approximation of the Klein-Gordon equation during inflation, then is

$$3H\dot{\phi} + V_{,\phi} \approx 0 \tag{3.2.15}$$

This is often simpler to solve for a given potential than the full Klein-Gordon equation and so is widely used in understanding inflation. This type of approach is known as the slow-roll approximation (SRA). We will now formalise the technology of this slow-roll approximation.

Slow-Roll Inflation

Let us define a parameter

$$\epsilon_0 = -\frac{\dot{H}}{H^2}\,. \tag{3.2.16}$$

Using the Friedmann equations (for any background, not just the scalar field case) it is possible to see more generally that

$$\epsilon_0 = \frac{3}{2}\left(1+w\right)\,. \tag{3.2.17}$$

That is, when $w = -1$, $\epsilon_0 = 0$ and when $w = -1/3$ (the end of inflation, as expansion ceases to be accelerating), we instead have $\epsilon_0 = 1$. The parameter ϵ_0 hence runs from 0 to 1 from beginning to end of an inflationary expansion, and is useful to parametrise the progress of inflation as a result. Values of this parameter exceeding 1 represent non-inflationary expansion. However, using the Friedmann equations in the special case of the inflationary scalar field, we also see that

$$\epsilon_0 = \frac{3\dot{\phi}^2}{\dot{\phi}^2 + 2V} \approx \frac{3\dot{\phi}^2}{2V}\,. \tag{3.2.18}$$

By inspection one finds from this that ϵ_0's smallness is also linked to the validity of the slow-roll approximation; when SRA is fulfilled, $\epsilon_0 \approx 0$. The slow-roll parameter is hence also a useful tracker and order parameter in which to express the slow-roll approximation. One could, for example, write the Friedmann equation in the form

$$3H^2 = V(1 + O(\epsilon_0))\,, \tag{3.2.19}$$

specifically showing where the terms that are linear (or higher) order in the small number ϵ_0 arise.

As the slow-roll approximation also deals with ensuring that higher time derivatives of ϕ are sufficiently small, we can extend this idea to parametrise this too. In fact, we can use quantities related to derivatives of ϵ_0 to formalise this. While many competing definitions exist in books and literature on the subject, the author finds some of the more common ones rather arbitrary and lacking systematic structure and will hence define and use a less-common (related to approaches such as that of[180]) but more structured variation of this.[5] Additional slow-roll parameters are hence defined to follow the recursion relation

$$\epsilon_0 = -\frac{\dot{H}}{H^2}\,, \quad \epsilon_n = \frac{\dot{\epsilon}_{n-1}}{H\epsilon_{n-1}}\ (n > 0)\,. \tag{3.2.20}$$

Here, for example, ϵ_1's smallness implies $\ddot{\phi} \ll H\dot{\phi}$, and higher slow-roll parameters in turn imply smallness of subsequent derivatives of the field. During early inflation, then, $\epsilon_n \ll 1$ to ensure a state of accelerating and sustainable expansion. When expressing a term's order in slow-roll parameters, we will collectively refer to them as just ϵ with no subscript, such that e.g. $O(\epsilon)$ means that a term is linear in one or more ϵ_n without specifying which.

[5] For example, ϵ_0 is usually defined this way as the first slow-roll parameter, and is usually denoted as just ϵ with no subscript. But, one definition for the second slow-roll parameter found in textbooks is, for example, $\delta = \epsilon - \frac{\dot{\epsilon}}{2H\epsilon}$, and the next one after that is called $\xi = \frac{\dot{\epsilon}-\dot{\delta}}{H}$. With this it becomes increasingly hard to generalise to higher orders and succinctly refer to slow-roll parameters, hence the preference here for the recursive definition presented.

Duration and number of e-folds of inflation

It is useful to further note that eq. (3.2.18) can be rewritten using eq. (3.2.15) to take the form

$$\epsilon_0 \approx \frac{1}{2}\left(\frac{V'}{V}\right)^2 . \tag{3.2.21}$$

For a given potential, we can now compute ϵ_0 approximately. One use of this is determining when inflation ends (solving for $\epsilon_0 = 1$). Take, for example, an arbitrary monomial potential

$$V(\phi) = A\phi^n \,, \tag{3.2.22}$$

for which

$$\epsilon_0 \approx \frac{n^2}{2\phi^2} \;\rightarrow\; \phi_{\text{end}} \approx \frac{n}{\sqrt{2}} \,. \tag{3.2.23}$$

If we hence know approximately when inflation ends, we can also consider how large ϕ must be at the beginning of inflation to produce around 60 e-folds of expansion before reaching ϕ_{end}. We can write the e-fold number N by rewriting its definition in terms of an integral as

$$N = \ln\left(\frac{a_2}{a_1}\right) = \int_{t_1}^{t_2} H(t)\,\mathrm{d}t \;, \tag{3.2.24}$$

which, upon further manipulation, can be written

$$N(\phi) = \int_{\phi_{\text{end}}}^{\phi} \frac{1}{\sqrt{2\epsilon_0}}\,\mathrm{d}\phi' = \int_{\phi_{\text{end}}}^{\phi} \frac{V(\phi')}{V'(\phi')}\,\mathrm{d}\phi' \;. \tag{3.2.25}$$

Taking again the monomial potential above, we find [179]

$$N(\phi) = \frac{\phi^2}{2n} - \frac{n}{4} \,, \tag{3.2.26}$$

or that for a given N we require an initial field value of

$$\phi_{\text{ini}} \approx \sqrt{2n\left(N + \frac{n}{4}\right)} \,, \tag{3.2.27}$$

which, for say $n = 2$ and $N = 60$, gives $\phi_{\text{ini}} \approx 16 M_{\text{Pl}}$.[6] In this way, for a given inflationary model, we can determine the initial state necessary to produce the desired amount of inflation within the slow-roll approximation. This has its limitations; certain potentials or more complicated models involving more than just a minimal scalar field may not be analytically tractable in this way. Such extended models may also be able to violate the conditions of the slow-roll approximation yet still produce viable inflation, too, and would need to be treated with a different set of assumptions. Nevertheless, this example using a simple model demonstrates how we can, in principle, learn about the physics of inflation from some simple constraints. Let us finish this discussion of slow-roll inflation by solving the approximate Klein-Gordon and Friedmann equations (3.2.14) and (3.2.15) for the time evolution of the scalar field and the scale factor in this model. By direct integration and some algebra, one comes to

$$\phi(t) = \phi_{\text{ini}} \left(1 + \frac{n(n-4)}{2} \sqrt{\frac{A}{3}} \phi_{\text{ini}}^{\frac{n-4}{2}} (t - t_{\text{ini}}) \right)^{\frac{2}{4-n}} , \tag{3.2.28}$$

and

$$a(t) = a_{\text{ini}} \exp \left[\frac{\phi_{\text{ini}}^2 - \phi(t)^2}{2n} \right] , \tag{3.2.29}$$

where the former expression is valid for all $n \neq 4$, which instead yields the special case

$$\phi(t) = \phi_{\text{ini}} \exp \left[-4 \sqrt{\frac{A}{3}} (t - t_{\text{ini}}) \right] . \tag{3.2.30}$$

As a visual aid, we plot the case of $n = 2$ in Figure 3.1, to demonstrate some of these results and compare them to a numerical solution of the exact equations of motion.

We can see that the slow-roll solutions are a remarkably accurate approximation of the numerical solutions, and only begin to differ significantly in the last couple of

[6] In this prototypical example, this large initial condition raises questions of the stability of the potential to UV completion above the Planck scale. This remains a problem in a subset of inflationary models, but may just be a symptom of our incomplete understanding of high energy physics.

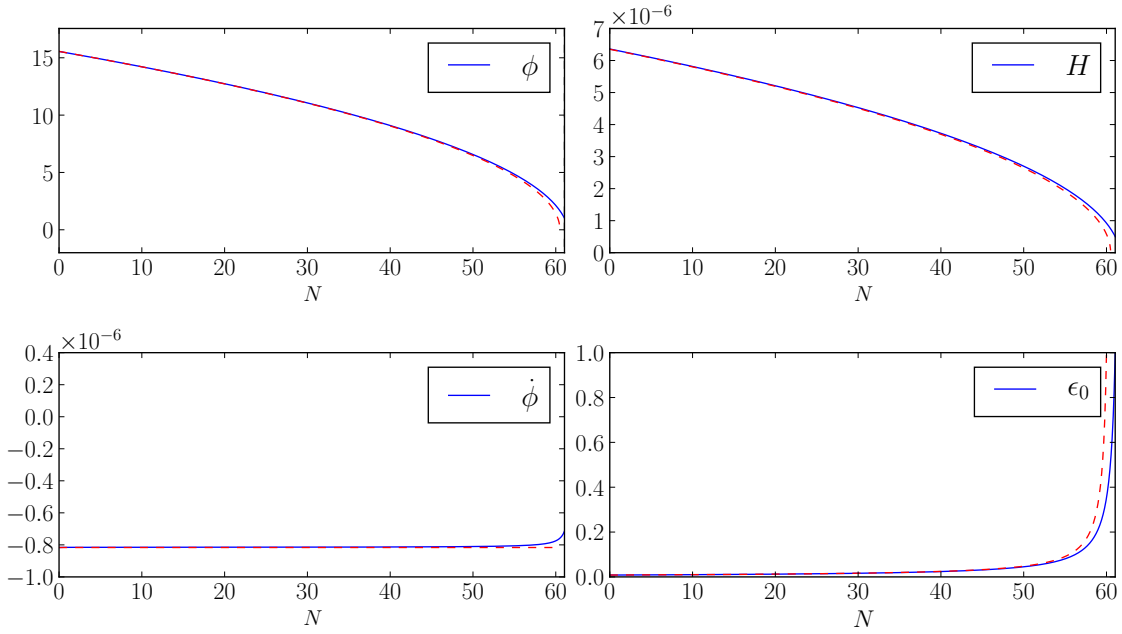

Figure 3.1.: Solutions of the slow-roll equations of motion (in blue) and their exact numerical values (dashed red), as a function of e-fold number N. An initial condition to produce 60 e-folds of inflation of $\phi_{\text{ini}} = \sqrt{242}$ was chosen in accordance with (3.2.26). We can see in the top-left panel that the approximate solution for ϕ matches the exact solution well until the last few e-folds, as does $H \approx \sqrt{V(\phi)/3}$ in the top-right panel. The slow-roll solution (3.2.28) implies $\dot{\phi}$ is constant, and this is shown to be, again, largely true until the last few e-folds in the bottom left panel. Finally, the slow-roll parameter ϵ_0 as given by (3.2.23) is shown in the bottom-right panel, and shows that inflation terminates in reality at $N \approx 61$, again matching the slow-roll analytics to a very good accuracy.

e-folds of inflation where $\epsilon \to 1$ and the $O(\epsilon)$ corrections to the equations of motion become comparable in size to the leading order terms.

While we can hence calculate the background evolution of an inflaton field and its resulting expansion history $a(t)$, and we have seen how this would solve some of the problems with the Hot Big Bang cosmology if it occurred in the very early universe, it remains to be seen how the usual cosmological history can play out following such a period of inflation. This will be addressed in a later section. Additionally, we have little to say thus far with regards to experimental tests and measurements of inflation via perturbation theory, which will be addressed in more detail later also. First, though, we take a swift review of some of the prominent ideas in inflationary

model building that go beyond the prototypical power law potential discussed thus far.

Models of Inflation

The type of model we have considered above is a member of the class of "large field" inflationary models. The field starts at some typically super-Planckian displacement as in eq. (3.2.27) and rolls towards the minimum of the potential, occurring at a smaller field value. To fulfil the slow-roll conditions and sustain a period of inflationary expansion, the potential should not be excessively steep. It is worth mentioning that while this is the most conventional realisation of inflation, other possibilities do exist. Consider instead a potential like

$$V(\phi) = V_0(\phi^2 - \nu^2)^2\,, \tag{3.2.31}$$

where the field could instead start at $\phi \approx 0$ and roll away from this unstable maximum towards one of the minima at $\phi = \pm\nu$. Such "small field" inflationary models also exist as a feasible class of model. Beyond simple differences in the shape and general type of potential being used, though, inflationary models can vary in at least as many ways as the general scalar-tensor theories described in Section 2.2.2. Couplings to other gravitational terms in the action, the presence of more terms containing derivatives of the scalar field, and so on will all change the behaviour of the inflaton.[181,182] Indeed, there also need not be just one scalar field in an inflationary scenario. The interactions between two scalar fields can change the shape of the effective potential each field experiences as a function of the other field's value and hence give rise to a much wider range of phenomenology (and we will see later that the presence of multiple fields has unique implications at the perturbative level). Some of these possibilities will motivate the work presented in the later chapters of this thesis.

Inflation has been criticised, resultingly, for having so many possible variations that it can essentially "predict anything". Additionally, that the rapid expansion of spacetime has been shown to lead to a so-called multiverse scenario where countless

different outcomes occur simultaneously in unobservable patches of the universe has yielded similar criticisms. Critics espousing such views typically argue that these concerns push the idea of inflation into unscientific territory due to a lack of falsifiability or testability.[183,184] This has become a topic of some controversy and contention in recent years and many scientists in the field have also published work seeking to address these criticisms.[185,186] The debate has even appeared in popular scientific publications, suggesting a certain degree of public interest and engagement with the topic.

3.2.5. How to Stop a Universe Inflating

We have already seen in the previous section that in slow-roll inflation, the parameter ϵ_0 measures the progress of inflation, and the expansion of spacetime only crosses the acceleration-deceleration threshold once $\epsilon_0 = 1$. The point at which this occurs hence marks the end of inflation, but it does not alone promise that the expansion will remain non-inflationary in the future, nor that the subsequent cosmological expansion will recover the successes of the Hot Big Bang model. On this first point, note that an inflationary potential could have such a shape that ϵ_0 increases to above 1 but then later would revert to a second period of inflation as it drops below 1 again. On the second point, the later stages of the universe's history are strongly consistent with radiation and dust fluids, so we somehow need to recover this scenario after inflation. This is difficult because after 60 e-folds of expansion any matter which may have existed in the pre-inflationary universe is indiscriminately diluted and cooled by tens, if not hundreds, of orders of magnitude by the extreme expansion that occurred. If left unchanged from this low-temperature, low-density state, the universe could never develop the rich structure we observe today and would remain a cold and lifeless void. To make progress in addressing this, we first need to look at what the inflaton is doing during and after the end of inflation.

Continuing with the example of the monomial potential and slow-roll inflation from the previous section, we choose to first look at the case of $n = 2$. In such cases of even values of n, the inflaton potential has a minimum at $\phi = 0$ and one would typically expect the solution of the Klein-Gordon equation to result in oscillations

about this minimum. By contrast, odd power potentials would not have this feature and the inflaton might be expected to instead to plummet towards $\phi = -\infty$ with ever-lower energy as the potential is unbounded from below in such examples. This is intuitively not a desirable late-time (post-inflationary) behaviour for the inflaton. We hence stick with even powers, for which the $n = 2$ case is both the simplest example to mathematically discuss as well as a physically-meaningful and useful prototype for a wide range of inflationary potentials which have a more general shape but possess a minimum at say $\phi = \nu$, around which the Taylor series of the potential would look like

$$V(\phi) \approx V(\nu) + \frac{1}{2} m_\phi^2 (\phi - \nu)^2 \,, \tag{3.2.32}$$

where m_ϕ is the effective mass of the field at that minimum. This is a typical post-inflationary scenario, in which the inflaton violates slow-roll as it reaches an effective minimum in the potential and the Klein-Gordon equation becomes

$$\ddot{\phi} + 3H\dot{\phi} + m_\phi^2 \phi = 0 \,, \tag{3.2.33}$$

where, for simplicity, we have implicitly performed a field redefinition $\phi \to \phi + \nu$. This is now the differential equation for a damped harmonic oscillator, where the expansion of space encoded in $H(t)$ is the source of damping. A general solution of this will look like

$$\phi(t) \propto e^{\int k(t) \mathrm{d}t} \,, \tag{3.2.34}$$

where the Klein-Gordon equation implies that the function k should have the approximate form

$$k(t) \approx \frac{-3H(t) \pm \sqrt{9H(t)^2 - 4m_\phi^2}}{2} \,. \tag{3.2.35}$$

We can see that the relative size of m_ϕ and H determine whether the integrand is real or complex, and hence set the severity of the damping. After inflation, however, $H \ll m_\phi$ is a good approximation, which one can see by considering eq. (3.2.21)

and eq. (3.2.14) to reveal that around the end of inflation

$$\epsilon_0 \approx \frac{m_\phi^2}{3H^2} \approx 1 \quad \rightarrow \quad H \sim m_\phi \,. \tag{3.2.36}$$

As H strictly decreases with time during a decelerating expansion, it is clear that post-inflation, $m_\phi > H$ and so the behaviour of the inflaton in eq. (3.2.34) will be dominated by this and hence be complex, yielding solutions of the form

$$\phi(t) = \Phi(t) \sin\left(m_\phi t\right) \,, \tag{3.2.37}$$

where the prefactor function Φ, encoding the damping, behaves as

$$\Phi(t) \propto e^{-\frac{1}{2}\int 3H(t)\mathrm{d}t} \,. \tag{3.2.38}$$

As the field oscillates, its equation of state parameter w will similarly oscillate. However, over several oscillations, the time-averaged equation of state can be worked out as

$$\langle w \rangle = \frac{\langle p \rangle}{\langle \rho \rangle} \approx \frac{\langle \cos^2\left(m_\phi t\right) \rangle - \langle \sin^2\left(m_\phi t\right) \rangle}{\langle \cos^2\left(m_\phi t\right) \rangle + \langle \sin^2\left(m_\phi t\right) \rangle} \approx 0 \,, \tag{3.2.39}$$

where we have neglected terms proportional to $\dot{\Phi}$ as we assume the time evolution due to the oscillatory factor is faster than that due to the damping of the amplitude in Φ. This is justified, again, by noting that the oscillations occur with a frequency of m_ϕ while the damping occurs on a time-scale determined by H which we have established is sub-dominant in the post-inflationary regime. What we have shown, with this, is that the average equation of state of the oscillating scalar field is close to zero, and hence the post-inflationary expansion of the universe will look like that of a dust-dominated background on sufficiently long time-scales. That is, $a \propto t^{2/3}$ and $H \approx 2/3 \times t^{-1}$. Inserting this latter result into the form of the damping factor in eq. (3.2.38) reveals that during this time, $\Phi \propto t^{-1}$. We hence see by combining this with the oscillatory term that post-inflation, $\phi \sim \sin\left(m_\phi t\right)/t$. Some of these results are shown in Figure 3.2, in which we compare these analytical predictions to a numerical integration of the exact equations of motion in the post-inflationary

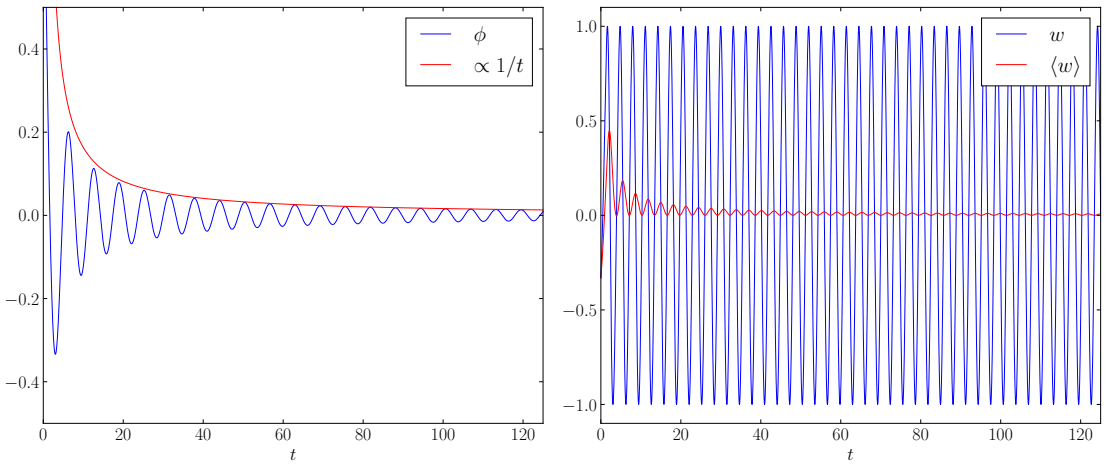

Figure 3.2.: Post-inflationary oscillations of the inflaton. This is the continuation of the trajectory in Figure 3.1. The field (left panel) oscillates with an amplitude decreasing in inverse proportion with time (measured in units of $1/m_\phi$) due to expansion of the universe, while the equation of state w (right panel, blue line) also oscillates such that its effective value averaged over several oscillations (red line) is zero, causing the inflaton to behave as pressureless dust.

regime using the same trajectory as the inflationary solution shown in Figure 3.1. As expected, Figure 3.2 shows that the envelope of the field's oscillations scales approximately as t^{-1}, with this approximation improving as time goes on. Similarly, the average equation of state, while of course fluctuating due to individual oscillations, clearly converges towards $\langle w \rangle = 0$.

To understand this more formally, we note that the instantaneous equation of state is related to the slow-roll parameter ϵ_0 via eq. (3.2.17), which implies that we can calculate the average equation of state over a given number of e-folds $(N_2 - N_1)$ as[187]

$$\begin{aligned}\langle w \rangle = \frac{1}{N_2 - N_1} \int_{N_1}^{N_2} w(N') \mathrm{d}N' &= \frac{1}{N_2 - N_1} \int_{N_1}^{N_2} \left(\frac{2}{3} \epsilon_0(N') - 1 \right) \mathrm{d}N' \\ &= -\frac{2}{3} \times \frac{1}{N_2 - N_1} \int_{N_1}^{N_2} \frac{H'(N')}{H(N')} \mathrm{d}N' - 1 \\ &= \frac{2}{3} \times \frac{\ln(H_2/H_1)}{\ln(a_1/a_2)} - 1 \,, \end{aligned} \tag{3.2.40}$$

where we have used $\mathrm{d}N/\mathrm{d}t = H$ to rewrite ϵ_0 in terms of a derivative with respect to N, and then directly integrated the resulting expression. As a sanity check, for an expansion dominated by a single perfect fluid of constant equation of state w, we can use the result (3.1.14) and $H \propto t^{-1}$ to find that $\langle w \rangle \equiv w$, as one would expect. Conversely, when the energy-momentum content of the universe is described by a varying equation of state the instantaneous and average equations of state are not generally equal, and in the case of a rapidly oscillating instantaneous w, this average is often a more suitable descriptor of the broad dynamics of the universe. Interestingly, it can be shown to only depend on the scale factor and its first derivative (within H) at the beginning and end of the period over which one would like to calculate the average.

These results we have found are evidently not the desired behaviour of the universe, however. The inflaton's late time behaviour allows the universe to mimic a matter-dominated epoch, but this does not explain where all the actual matter that exists at the times of nucleosynthesis and decoupling comes from. It also fails to account for the radiation-dominated epoch. It is clear that to end the domination of the inflaton and allow the universe to transition into a Hot Big Bang-like period of expansion, a further mechanism is needed.

Perturbative Reheating

We need a mechanism, in particular, that generates conventional radiation and/or matter from an oscillatory scalar field. This is called *reheating*, as it takes the supercooled post-inflationary universe and returns it to a Hot Big Bang-like state. The idea behind it is to couple the inflaton to other fields and hence allow it to decay into them. If the decay products are considerably less massive than the inflaton then they will be relativistic, behaving as radiation and thus meeting the first criteria needed to recover the desired post-inflationary behaviour. Furthermore, it is important that the reheating temperature - the temperature of these decay products at the end of the reheating procedure - is sufficiently small that GUT relics cannot be re-produced (e.g. below the GUT scale) as we invoked inflation partly

to avoid these in the first place (the Monopole Problem). Similarly, the resulting temperature after reheating should be large enough to sustain the usual processes of the Hot Big Bang, such as nucleosynthesis. Lastly, as we know that during an inflationary expansion, any other forms of matter-energy are rapidly diluted away, we can say that this mechanism must do its job after inflation has ended, during the oscillatory phase described in the previous section.

We approach this problem using the techniques of Quantum Field Theory, where an appropriate minimalistic interaction Lagrangian between the inflaton and its decay products might look something like

$$\mathcal{L}_{\text{int}} = -\frac{1}{2}g^2\phi^2\chi^2 - h\phi\bar{\psi}\psi\,, \tag{3.2.41}$$

where χ is another scalar field (though higher spin bosons could, of course, also be considered) and ψ is a fermionic spinor field, which each have their own Lagrangians dealing with their kinetic and mass terms as usual (but will not need to be directly considered here and are hence not shown). Under the kind of field redefinition we applied to eq. (3.2.32) where the minimum of the inflationary potential occurs at $\phi = \nu$, the quartic term in eq. (3.2.41) would additionally generate a cubic interaction vertex of the form

$$\mathcal{L}_{\text{int}} \supset -\nu g^2\phi\chi^2\,, \tag{3.2.42}$$

as well as modifications to the mass terms of the decay products. With this series of interaction terms in the Lagrangian, decays such as $(\phi\phi \to \chi\chi)$, $(\phi \to \chi\chi)$ and $(\phi \to \psi\bar{\psi})$ are possible. Considering the Feynman diagrams for these interactions allows one to calculate perturbative loop corrections order-by-order to the effective mass of ϕ due to quantum field theory effects. While the process of this calculation is beyond the scope of this thesis, the well-established result[188,189] is that one obtains a modified Klein-Gordon equation

$$\ddot{\phi} + 3H\dot{\phi} + (m_\phi^2 + \Pi(m_\phi))\phi = 0\,, \tag{3.2.43}$$

where Π is known as the self-energy and is a complex quantity. Its real part describes

corrections to the bare mass of the ϕ field, while the imaginary part encodes the decay rate of ϕ particles into the products above. This decay rate is denoted Γ, and is given to leading order by

$$\Gamma = \Gamma(\phi \to \chi\chi) + \Gamma(\phi \to \psi\psi) \tag{3.2.44}$$

where the $(\phi\phi \to \chi\chi)$ process is seen to not contribute at this level, and the decay rates are given by[188]

$$\Gamma(\phi \to \chi\chi) = \frac{\nu^2 g^4}{8\pi m_\phi}\,, \text{ and } \Gamma(\phi \to \psi\psi) = \frac{m_\phi h^2}{8\pi}\,. \tag{3.2.45}$$

Seeking solutions to eq. (3.2.43) of the form (3.2.34)we find, in the limit where m_ϕ dominates over the real part of the self energy, that

$$\phi(t) \propto e^{-\frac{1}{2}\int (3H(t)+\Gamma)\mathrm{d}t} \sin(m_\phi t)\,. \tag{3.2.46}$$

Comparing to eq. (3.2.38) we see that the effect of ϕ's decay is to increase the amount of damping of the post-inflationary oscillations. Now, following the same logic as before, the envelope function Φ can be seen to take the shape

$$\Phi(t) \propto \frac{e^{-\Gamma t}}{t}\,, \tag{3.2.47}$$

which indeed drops off more steeply than the $\Phi \propto 1/t$ we found when decays were absent. The decay rate Γ, phenomenologically, is equivalent to the replacement $3H \to 3H + \Gamma$, and the same physical behaviour would hence arise from the Klein-Gordon equation

$$\ddot{\phi} + (3H + \Gamma)\dot{\phi} + m_\phi^2 \phi = 0\,. \tag{3.2.48}$$

This additional damping term has a clear physical interpretation; the energy in ϕ is being lost not only to the expansion of the universe, but also via decay pathways. From this kind of behaviour, we can see that decay will become significant once $3H \approx \Gamma$. During inflation itself, $3H$ is approximately constant and may be larger than Γ, but once it begins to decrease more significantly after inflation, this will

inevitably come about once H decreases sufficiently. An inflaton coupled to matter fields that oscillates about an effective minimum is thus generally expected to decay in this fashion.

This is exactly the kind of thing we need to reheat the universe; the oscillating inflaton's energy is sequestered and is converted into radiation. Thus, the universe ceases to be dominated by ϕ and a radiation-dominated epoch will follow once sufficient amounts of decay occur, allowing the conventional Big Bang cosmology to proceed as desired.

The universe now, hence, contains both a scalar field, ϕ, obeying the modified Klein-Gordon equation (3.2.48), and a radiation fluid consisting of relativistic χ and ψ particles. The Friedmann equation hence looks like

$$3H^2 = \rho = \rho_\phi + \rho_\mathrm{r}\,, \tag{3.2.49}$$

and we expect that the equation of state will, once radiation comes to dominate, tend to the usual value of $w = 1/3$, though not before a period of oscillation while ϕ remains a significant contributor to the energy content of the universe. To dynamically study the behaviour of the radiation fluid here, the fluid equation (3.1.9) needs modifying to account for the interaction with ϕ. We know that the total energy density ρ should obey the normal fluid equation due to covariant conservation of the energy-momentum tensor, so the individual fluid equations for the inflaton and radiation should take the form

$$\dot{\rho_\phi} + 3H(\rho_\phi + p_\phi) = -Q\,, \tag{3.2.50}$$

$$\dot{\rho_\gamma} + 4H\rho_\gamma = Q\,, \tag{3.2.51}$$

where Q is some non-conservation term. The sum of the non-conserved parts in each fluid equation must be 0 to ensure total conservation, hence the equal and opposite-sign values in each case. As the fluid equation for ϕ is equivalent to its Klein-Gordon equation, we can by direct comparison identify the form of Q as

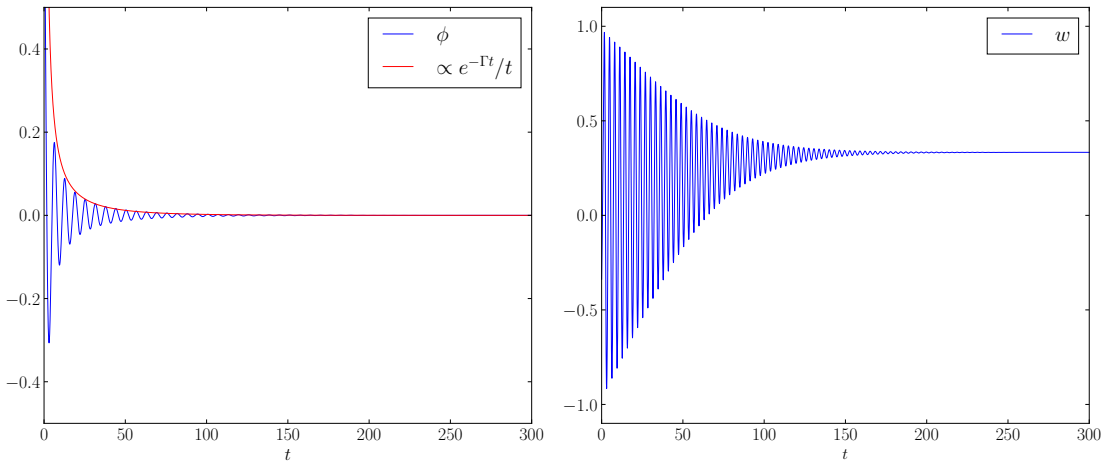

Figure 3.3.: Post-inflationary oscillations of the inflaton as it decays into other particles with decay rate Γ given by eq. (3.2.44) with $g = 10^{-3}$, $h = 5 \times 10^{-4}$, $m_\phi = 10^{-6}$ and $\nu = 1$. The field (left panel) oscillates with an amplitude decreasing according to (3.2.47) as predicted, while the equation of state w (right panel) initially oscillates as in Figure 3.2 before settling down at $w = 1/3$ as radiation domination begins due to the decay products coming to dominate over the inflaton.

$$Q = \Gamma \dot{\phi}^2 = \Gamma(\rho_\phi + p_\phi) \approx \Gamma \rho_\phi \,, \tag{3.2.52}$$

which is of course equivalent again to the replacement $3H \to 3H + \Gamma$. In the last approximate equality we note that the oscillating inflaton has $p_\phi \approx 0$ because $\langle w_\phi \rangle \approx 0$ (regardless of the modified shape of the envelope function). We hence have an equation of motion for the radiation

$$\dot{\rho}_\gamma + 4H\rho_\gamma \approx \Gamma \rho_\phi \,. \tag{3.2.53}$$

We can then numerically solve this along with the Klein-Gordon equation and the Friedmann equation (3.2.49), and show exactly this in Figure 3.3, comparing again to analytical predictions. We use the same set-up as in Figure 3.2 to directly contrast the post-inflationary behaviour of the universe with and without inflaton decays. Finally, we can calculate the reheat temperature from the energy density of radiation produced by the time that the universe is radiation-dominated using

$$\rho_{\rm r} = \frac{\pi^2}{30} g_* T_{\rm reh}^4 \,, \tag{3.2.54}$$

where $g_* \approx 10^3$ is the number of relativistic degrees of freedom one might expect from a typical high energy particle theory. Numerically we find the resulting temperature in this simple example is $T_{\rm reh} \approx 10^{13} - 10^{14}$GeV. This is both low enough to avoid pathological relic reproduction ($m \approx 10^{16}$GeV) and significantly higher than the temperature at which nucleosynthesis must later occur, as desired.

As we will see, the details of reheating can influence the quantities that we measure to test theories of inflation, making the reheating phase also possibly within the realm of empirical testing.

Beyond Perturbative Reheating

Non-perturbative effects can also play a role in the reheating process. Here we briefly review two of the main manifestations of this. Firstly, the phenomenon of parametric resonance which is complementary to the oscillatory perturbative reheating described above, and secondly the mechanism of instant preheating, which can occur even in non-oscillatory (NO) scenarios and provide an alternative route to a reheated universe in such cases.

Parametric Resonance Consider the quartic coupling in eq. (3.2.41). Starting from the equation of motion (2.2.5) for a canonical scalar field, it can be shown that the Fourier modes of the scalar field χ will obey a wave equation[188]

$$\ddot{\chi_k} + 3H\dot{\chi_k} + \left(\frac{k^2}{a^2} + m^2_{\chi,\rm eff}\right)\chi_k = 0 \,, \tag{3.2.55}$$

where the effective mass-squared of the χ field, incorporating a bare mass term as well as interactions with ϕ is given by,

$$m^2_{\chi,\rm eff} = m^2_{\chi,0} + g^2\phi^2 \,. \tag{3.2.56}$$

Inserting eq. (3.2.37) for the post-inflationary behaviour of ϕ, we can rewrite the equation of motion as

$$X_k'' + \omega_k^2 X_k = 0\,, \tag{3.2.57}$$

where

$$\omega_k^2 = A_k - 2q\cos(2z) + \Delta\,. \tag{3.2.58}$$

In this, we are working with the redefined mode function $X_k = a^{3/2}\chi_k$. Priming denotes differentiation with respect to a new time coordinate $z = m_\phi t$. The parameters in the ω_k are defined, in terms of model parameters and the inflaton envelope function Φ, as

$$A_k = \frac{k^2}{m_\phi^2 a^2} + 2q\,, \quad q = \frac{g^2\Phi^2}{4m_\phi^2}\,, \text{ and } \quad \Delta = \left(\frac{m_\chi}{m_\phi}\right)^2 + \frac{3}{4}(2\epsilon_0 - 3)\left(\frac{H}{m_\phi}\right)^2\,. \tag{3.2.59}$$

In the limit of negligible Δ,[7] this equation becomes the well-known Mathieu equation, which is notable for having highly unstable solutions of the form $X_k \propto e^z$ for certain values of the parameters defined above.

As the parameters A_k and q vary in time as a function of a and Φ, the modes X_k will move in and out of the instability bands of the Mathieu equation, leading to short periods of rapid growth. This is known as parametric resonance, and is a non-perturbative effect that occurs in addition to the description of perturbative reheating above.

We note that the occupation number of each k mode can be expressed[188]

$$n_k = \frac{1}{\omega_k}\left[\frac{1}{2}|\dot{X}_k|^2 + \frac{1}{2}\omega_k^2|X_k|^2\right] - \frac{1}{2}\,, \tag{3.2.60}$$

and that the resulting energy density of produced χ particles, integrating over all k values, is

[7] We expect Δ to be small for three reasons. Firstly, $m_\chi \ll m_\phi$ to suppress the first term, else the inflation could decay into sufficiently heavy particles to once again cause the Monopole Problem. Secondly, $H \ll m_\phi$, which as previously argued is typical of reheating, suppresses the second term. Lastly, since $w \approx 0$, we expect $\epsilon_0 \approx 3/2$, further suppressing the second term.

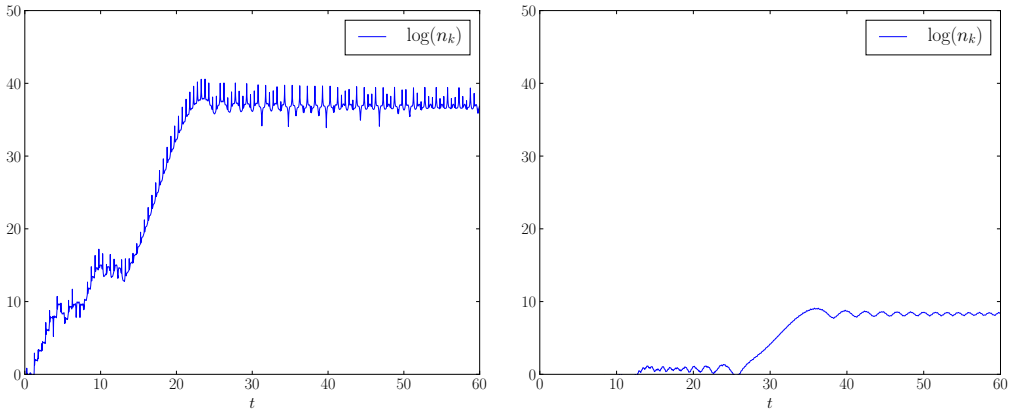

Figure 3.4.: Exponential growth of n_k (3.2.60) for $k = 4.0\times10^{-6}$ (left) and $k = 1.0\times10^{-4}$ (right) , showing varying degrees of parametric resonance. Time here is shown in units of $m_\phi/2\pi$ which roughly equates to the number of oscillations the inflaton field has undergone. In the former case, we find that $n_k \sim e^{38}$ while in the latter case this value is many orders of magnitude smaller. This illustrates the sensitivity of this process to the momentum of the produced particles. This gives us some idea that the total energy density (3.2.61) will be dominated by a small range of k values . The theory parameters used are $m_\phi = 100m_\chi = 5.0\times10^{-6}$ and $g = 5.0\times10^{-4}$. The left panel is based on Figure 6 in[188] as this was shown to be a particularly interesting case.

$$\rho_\chi = \frac{m_\chi}{2\pi^2}\int_0^\infty k^2 n_k \mathrm{d}k\,, \tag{3.2.61}$$

One generally expects, then, that such a rapid increase of the χ_k modes would lead to non-perturbative growth in the energy density of decay products. In Figure 3.4 we show a numerical analysis of this for some specific k values, showing the exponential growth of n_k in each case. Particularly in the left panel of this figure, we can see periods of exponential growth such as $t \approx 15 - 25$ corresponding to an instability of the Mathieu equation for the values of A_k and q at that time.

While the explosive particle production made possible by these non-perturbative effects is rather striking, it turns out that, particularly for larger g values, the backreaction this has on ϕ and the expansion of the universe somewhat curtails its effect. In reality a more careful analysis of this, supported by results from lattice simulations, shows that the majority of the energy density transferred to decay products during reheating is in the perturbative mechanism.[188,190] Parametric

resonance primarily occurs in the early stages of reheating[8] and is an important part of understanding of exactly how decay products are created on a microscopic level, but does not drastically change e.g. the reheating temperature predicted by the perturbative analysis.

Instant Preheating So far, all of our discussion of reheating has depended upon an oscillatory late-time inflaton, typically achieved by a local minimum in $V(\phi)$. In more general situations, such as where the potential tails off after a period of inflation and the field continues to roll, an alternative to perturbative and parametric reheating is needed.[191] For example, with an exponential potential $V \propto e^{\phi}$, the field would continue to roll towards $\phi \to -\infty$ after inflation. While this non-oscillatory (NO) type of behaviour is inappropriate for perturbative reheating or parametric resonance, it can still be used to our advantage. During this period, $\dot{\phi}^2 \gg V$ as the potential is now exponentially suppressed and the field is rolling quickly, meaning that $w \approx 1$ and its energy density scales as $\rho \propto a^{-6}$. This makes it very easy for even a relatively small amount of decay products, should we find a way to make them, to dominate the universe as both dust-like and radiation-like fluids do not dilute this rapidly. Additionally, with a general quartic coupling between the inflaton and a χ field, such as $\mathcal{L} \supset g^2\chi^2(\phi^2 - \nu^2)$, the effective mass of decay products is

$$m^2_{\chi,\text{eff}} = m^2_{\chi} + g^2(\phi - \nu)^2 \,. \tag{3.2.62}$$

Such interactions terms are further motivated by supergravity scenarios with superpotentials of a compatible form such as $W \propto \chi^2(\phi - \nu)$[192,193] and enhanced symmetry points in A-term inflation.[194–197] We see from this expression that as $|\phi| \to \infty$ the decay products will have a large mass and hence more energy, meaning we need to produce fewer of them to end the domination of the inflaton. One consequence of this, however, is that to stop excessively massive particles dominating the universe (due to behaving like dust) and re-introducing the Monopole Problem, we must assume the decay products χ further decay into smaller-mass and hence relativistic particles very quickly and efficiently with an interaction like

[8] Hence the popularity of referring to parametric reheating by the portmanteau *preheating*.

$$\mathcal{L}_{\text{int}} \supset \lambda\chi\bar{\psi}\psi\,. \tag{3.2.63}$$

This also has the advantage of avoiding any complications to do with backreaction of the produced χ particles on ϕ's behaviour. To proceed, we assume $g|\phi| \gg m_\chi$ such that $m_{\chi,\text{eff}} \approx g|\phi|$. Particle production occurs when the adiabaticity condition $|\dot{m}_{\chi,\text{eff}}| \ll m^2_{\chi,\text{eff}}$ is violated. Using

$$\dot{m}_{\chi,\text{eff}} \approx g|\dot{\phi}|\,, \tag{3.2.64}$$

we can see that particle production would hence occur for $g|\dot{\phi}| > g^2(\phi^2 - \nu^2)$. This would be satisfied for a band of values centered around ν, e.g. when $\phi = \nu \pm \phi^*$, where

$$\phi^* = \sqrt{\frac{|\dot{\phi}|_{(\phi=\nu)}}{g}}\,. \tag{3.2.65}$$

Given this, the approximate time scale over which particle production would occur would be $\Delta t \approx \phi^*/|\dot{\phi}|_{(\phi=\nu)}$, which is a rather short time-scale compared to typical reheating procedures, hence the name Instant Preheating for this process. One finds that,[188,191] in these conditions with momentum scale given hence by $k^* \sim 1/\Delta t = \sqrt{g|\dot{\phi}|_{(\phi=\nu)}}$, the occupation number of each Fourier mode would sharply increase over the time-scale Δt around the point where $\phi = \nu$, such that

$$n_k = \exp\left(-\frac{\pi(k^2 + m^2_{\chi,\text{eff}})}{(k^*)^2}\right) = \exp\left(-\frac{\pi(k^2 + m^2_{\chi,\text{eff}})}{g|\dot{\phi}|_{(\phi=\nu)}}\right)\,, \tag{3.2.66}$$

which implies that when $|\dot{m}_{\chi,\text{eff}}| \gg m^2_{\chi,\text{eff}}$ in the middle of instant preheating, we produce a total density of χ particles via eq. (3.2.61) of

$$\rho_\chi \approx \frac{g^{5/2}|\dot{\phi}|^{3/2}_{(\phi=\nu)}|\phi - \nu|}{8\pi^3}\,. \tag{3.2.67}$$

Thus, as ϕ rolls past ν, the decay products will grow in effective mass and hence total energy density, allowing them to easily dominate over the inflaton (before quickly decaying to radiation). For sufficiently large g (typically at least $O(10^{-4})$ or so) this

produced density is already significant for a relatively small ($O(M_{\rm Pl})$ or less) field displacement after inflation. We hence see that such non-perturbative considerations can feasibly be used reheat the universe in the context of runaway potentials where the previous oscillatory reheating mechanisms cannot be employed.

Finally we point out that in such NO scenarios, even in the absence of instant preheating, it has been shown that gravitational particle production[87,198] can reheat the universe.[199,200] That is, because in a general curved spacetime particle number is not conserved, the indirect gravitational interaction between the inflaton and other matter fields can lead to production of radiation. Because this does not require any assumptions about the coupling of the inflaton to other fields, but only that everything couples to gravity, its wide applicability and generality is noteworthy. The indirectness of this makes it rather inefficient, however, so it is possible that not all inflationary scenarios will be able to gravitationally reheat with a sufficiently large temperature to recover a feasible Hot Big Bang scenario. This inefficiency is also why, despite these effects technically being present alongside the discussed mechanisms of reheating, they are comfortably negligible when just about any other mechanism is feasible.

3.3. Cosmological Perturbations and Inflation

In the preceding discussion, we discussed a perfectly homogeneous universe and its inflationary expansion driven by a scalar field ϕ. However, the real universe is not perfectly homogeneous, and this is something to be thankful for in that it enables galaxies, planets and eventually life to come into existence. We know, however, that in the early universe homogeneity was a good approximation as, for example, the spectrum of CMB photons reveals in its tiny fluctuations of one part in 10^5. Due to this, our cosmological models can assume homogeneity and obtain valid and useful results for the most part. However, we have measured these tiny fluctuations in the CMB and this gives us a useful probe of the early universe. We can exploit this to more deeply understand the physics that led to this state of affairs. In particular, we can learn something of inflation in this way.[179]

By applying perturbation theory to the homogeneous inflationary solution in a model, we can find its predictions for the spectrum of inhomogeneities generated at the end of inflation.[201] Then, by modelling how these inhomogeneities evolve from that point until the time of CMB formation, at which point they become measurable, we can test and constrain models of inflation. The key result of this approach is that the primordial power spectrum of inhomogeneities - immediately after inflation - must be nearly (but not exactly) scale-invariant in order to successfully evolve into something compatible with the observed CMB fluctuations. As we will see soon, this slight departure from scale invariance is typical of inflationary models, which is the reason why we believe that inflation is a good theory of the early universe. Furthermore, the exact degree to which an inflationary model predicts deviation from scale-invariance is then a testable prediction of that model, and it is in this way that the CMB anisotropies provide us a window into the physics of the early universe. In what follows we shall formalise this idea and detail the mathematical techniques and objects that will be of central importance in the majority of the later chapters of this thesis.

3.3.1. Perturbation Theory

Fluctuations in the CMB occur due to density variations in the fluid of nuclei and electrons that CMB photons were in equilibrium with before decoupling. These density variations are assumed to come about due to fluctuations in the inflaton field as inflation ends and produces conventional matter via reheating, thus transferring its inhomogeneity to it. An object of interest, then, is the spatial variation in the inflaton, ϕ. We can model this as a linear perturbation

$$\phi = \bar{\phi}(t) + \delta\phi(t, x^i)\,, \tag{3.3.1}$$

where $\bar{\phi}$ (and other barred quantities to follow) denote the homogeneous solution detailed in the previous sections, and $\delta\phi$, which depends on spatial coordinates x^i is the inhomogeneous correction to this. Motivated by the observed smallness of the CMB anisotropies that we are ultimately interested in, we can comfortably treat

this as a small perturbation obeying $|\delta\phi| \ll |\bar{\phi}|$.

These fluctuations in the inflaton will lead to fluctuations in the energy momentum tensor $T_{\mu\nu} = \bar{T}_{\mu\nu} + \delta T_{\mu\nu}$, which then in turn source small perturbations in the Einstein Tensor $G_{\mu\nu} = \bar{G}_{\mu\nu} + \delta G_{\mu\nu}$ via the Einstein equations such that $\delta G_{\mu\nu} = \delta T_{\mu\nu}$. It is therefore necessary that the metric also has perturbative corrections to generate the terms on the left hand side of this. As the metric is symmetric, in four dimensions it has ten degrees of freedom and we expect the perturbation δg to be the same in this regard. To study this further, it is useful to first decompose the metric perturbation into scalar, vector and tensor components such that

$$g_{\mu\nu} = \bar{g}_{\mu\nu} + \delta g_{\mu\nu} \,, \tag{3.3.2}$$

where $\bar{g}_{\mu\nu}$ is, again, the homogeneous metric (FRLW-type in our case), and the symmetric perturbation of the metric can be written in the general form[179]

$$\delta g_{\mu\nu} = \begin{pmatrix} -2A & a(t)B_i \\ a(t)B_i & a(t)^2 h_{ij} \end{pmatrix} \,, \tag{3.3.3}$$

where A is a scalar, B_i is a three-vector, and h_{ij} is a symmetric $(0,2)$ tensor with $9 - 3 = 6$ independent components, summing to the ten expected free functions in δg.

By writing the vector part of the perturbed metric B_i as the sum of a divergenceless vector β_i and the gradient of a scalar B ($B_i = \partial_i B + \beta_i$ with $\partial^i \beta_i = 0$) and similarly decomposing the tensor

$$h_{ij} = 2C\bar{g}_{ij} + 2\partial_i\partial_j E + (\partial_i E_j + \partial_j E_i) + E_{ij} \tag{3.3.4}$$

into a scalar C, a vector (which again has a scalar part, E, and a divergenceless vector part E_i) and a transverse and traceless 2-tensor E_{ij} ($\partial^j E_{ij} = \delta^{ij} E_{ij} = 0$), we can decompose the 10 perturbations into into 4 scalars (4×1 d.o.f), 2 divergence-free vectors (2×2 d.o.f) and one transverse and traceless tensor (2 d.o.f). The significance of this is that the scalar, vector and tensor modes defined in this way cannot interact with one another at leading order in perturbations. Consider, for

example, an equation consisting of 0-tensors relating some of these perturbations. The four scalars (A, B, C, E) could clearly be present, as could scalar derivatives of them, but in order to make a vector mode contribute to this equation, one would have to take its divergence to form a 0-tensor from it. However, we have constructed these vectors (B_i, E_i) as divergence-free such that any such constructions would be automatically zero. Similarly, the tensor mode E_{ij}'s tracelessness forbids it from sourcing a scalar perturbation, while its transverse constraint inhibits it from appearing in an equation of 1-tensors. Thus, we can decouple the scalar, vector and tensor perturbations constructed in this way.

However, not all of these ten degrees of freedom are physical due to the gauge symmetry associated with reparametrisation invariance in General Relativity. As we are free to make an infinitesimal coordinate redefinition $x^\mu \to x^\mu + y^\mu$, there are four arbitrary functions y^μ associated with this symmetry which leave the system with only six physical degrees of freedom. For our purposes, we will choose to work in *Newtonian* gauge,[52] in which our four free functions are used to set $B = E = 0$ and $B_i = 0$. In this gauge, the remaining two scalar potentials are often renamed such that $A = \Phi$ and $C = -\Psi$ due to their close relation to the Newtonian gravitational potential in classical theory, hence the naming of this gauge choice. Our Newtonian Gauge perturbed metric, then, has a scalar part

$$\delta g^{(S)}_{\mu\nu} = \begin{pmatrix} -2\Phi & 0 \\ 0 & -2a(t)^2\Psi\delta_{ij} \end{pmatrix} , \tag{3.3.5}$$

and a tensor part

$$\delta g^{(T)}_{\mu\nu} = \begin{pmatrix} 0 & 0 \\ 0 & a(t)^2 E_{ij} \end{pmatrix} . \tag{3.3.6}$$

Formally, a part containing the vector E_i also remains, but in the context of cosmology these vector modes are essentially vanquished by the expansion of spacetime (one would eventually just find that their amplitude decreases as a^{-2} in a cosmological background), leaving them negligible for most purposes, and certainly all purposes that will be addressed in this thesis. We will henceforth ignore them, and

treat only the two scalar perturbations and the two degrees of freedom included in the tensor mode in what follows.

3.3.2. Inflationary Perturbations and the Primordial Power Spectrum

Having categorised the perturbations of the metric, we shall now consider the other ingredient in the Einstein Equations - the matter content. In particular, in inflation we are interested in a perturbed scalar field. The Einstein equations will then let us relate the scalar field perturbation $\delta\phi$ to the metric perturbations and determine their state and evolution. For a perturbation of the form (3.3.1), the energy-momentum tensor of a scalar field (3.1.36) transforms such that

$$\begin{aligned}\delta T_{\mu\nu} = (\partial_\mu\phi\partial_\nu + \partial_\nu\phi\partial_\mu)\delta\phi - \left(\frac{1}{2}\partial_\mu\phi\partial^\mu\phi + V\right)\delta g_{\mu\nu} \\ - \left(\frac{1}{2}\partial_\rho\phi\partial_\sigma\phi\ \delta g^{\rho\sigma} + \partial^\sigma\phi\partial_\sigma\delta\phi + \frac{\mathrm{d}V}{\mathrm{d}\phi}\delta\phi\right)\bar{g}_{\mu\nu}\,. \end{aligned} \tag{3.3.7}$$

The other necessary ingredient is the perturbed Einstein Tensor $\delta G_{\mu\nu}$, which can be computed from the above perturbed metric the usual way while neglecting terms quadratic or higher order in perturbations. After a tedious but straightforward calculation, we obtain equations of motion for the scalar modes and tensor modes as follows:

Scalar Equations

From the off-diagonal spatial components ($\mu = i$, $\nu = j \neq i$) of the Einstein Equations we find first that as the spatial part of $\delta T_{\mu\nu}$ is diagonal

$$\Psi = \Phi\,, \tag{3.3.8}$$

so in what follows we will hence not distinguish between these two scalar potentials. Using this, the other scalar equations we obtain are

$$\partial_i\partial^i\Phi - 3H\dot{\Phi} = \frac{1}{2}\dot{\phi}\dot{\delta\phi} + \frac{1}{2}V_{,\phi}\delta\phi + V\Phi\,, \tag{3.3.9}$$

from the $\mu = \nu = 0$ equation. Then, from the integral over x^i of the $\mu = 0$, $\nu = i$ equation we have

$$\dot{\Phi} + H\Phi = \frac{1}{2}\dot{\phi}\delta\phi\,, \tag{3.3.10}$$

and finally from the $\mu = \nu = i$ equations one can show

$$\ddot{\Phi} + 4H\dot{\Phi} + 2\left(2\dot{H} + 3H^2\right)\Phi = \frac{1}{2}\dot{\phi}\dot{\delta\phi} - \frac{1}{2}V_{,\phi}\delta\phi + V\Phi - \dot{\phi}^2\Phi\,. \tag{3.3.11}$$

The covariant conservation of the perturbed energy momentum tensor then yields a further scalar perturbation equation

$$\ddot{\delta\phi} - \partial_i\partial^i\delta\phi + 3H\dot{\delta\phi} + V_{,\phi\phi}\delta\phi = 2(\ddot{\phi} + 3H\dot{\phi})\Phi + 4\dot{\phi}\dot{\Phi}\,. \tag{3.3.12}$$

These four (or five counting the $\Phi = \Psi$ constraint) equations are not all independent as there are only two functions to solve for (the Newtonian gauge metric perturbation Φ and the field perturbation $\delta\phi$). We also note that the metric perturbations are not independently dynamical (in this gauge) and are instead entirely specified by the field perturbation and the background cosmology (evolution of a, ϕ, etc). It is useful to define a gauge-invariant combination of the field and metric perturbations, which is widely known as the Sasaki-Mukhanov[202,203] variable

$$Q = \delta\phi + \frac{\dot{\phi}}{H}\Phi\,. \tag{3.3.13}$$

A final scalar quantity of interest that we shall define here is the scalar Ricci Curvature on the three-dimensional spatial part of the spacetime manifold, ${}^{(3)}R$. More specifically, we are interested in a gauge-invariant[204] relative of it denoted $\mathcal{R}$, and known as the comoving curvature perturbation. As space is taken to be homogeneous at the background level, the Ricci curvature is of perturbative smallness and this quantity will hence be expressable in terms of our scalar perturbations at leading order. It is found,[179] beginning from eq. (3.3.1) that after another lengthy

computation one arrives at

$$\mathcal{R} = -\Psi - \frac{H}{\dot{\phi}}\delta\phi = -\frac{H}{\dot{\phi}}Q\,. \tag{3.3.14}$$

It is these fluctuations in spatial curvature (and hence energy density) that we are interested in for later generating CMB anisotropy.

A notable property of $\mathcal{R}$ is its conservation on large scales.[9] That is, a Fourier mode $\mathcal{R}_k$ with wavenumber k behaves approximately as a constant in the limit $k \ll aH$. The lowest frequency modes, those with wavelengths sufficiently longer than the horizon size, are all but frozen.

Tensor Equations

Meanwhile the tensor equation of motion is

$$\ddot{E}_{ij} + 3H\dot{E}_{ij} - \partial_k\partial^k E_{ij} = 0\,. \tag{3.3.15}$$

This is a wave equation in an expanding spacetime and hence establishes the idea of gravitational waves. We interpret the tensor metric fluctuations as propagating waves in spacetime itself, analogous to spin-2 particles travelling on the background metric. However, they do not directly affect field perturbations or vice versa - they only indirectly associate via the gravitational waves' dependence in the above equation on a and H. Again, we see the usefulness of the scalar-tensor decomposition in that we have broken the perturbation equations up into a scalar part that determines how scalar curvature is sourced by field fluctuations, and a tensor part which describes the freely-propagating gravitational waves.

The primary generation of CMB anisotropies later comes from direct density/curvature fluctuations coming from the scalar modes in Section 3.3.2 and their nature is determined by the solutions of the equations therein. However, the presence of gravitational waves does also influence the CMB (albeit weakly), so we can also study them in this way. In what follows, we will go on to calculate the spectrum of infla-

[9] That is, when perturbations are purely adiabatic. As we will come to see when we generalise things later, the non-conservation of $\mathcal{R}$ occurs, for example, when multiple inflationary fields are considered.

tionary scalar and tensor fluctuations according to conventions that are appropriate for comparison to experimental constraints.

3.3.3. Quantisation

We need to account for the quantum nature of the microscopic fluctuations in the inflaton field. This means identifying the canonically quantisable variable and promoting it to a quantum operator. This can be simply achieved by finding the variable for which the action for the perturbations looks like that of a canonical scalar field which can then be quantised according to usual procedure. It turns out that if one defines the variable

$$v = aQ\,, \tag{3.3.16}$$

where Q is the Sasaki-Mukhanov variable (3.3.13) and works in *conformal time*, η, defined by $\mathrm{d}t = a\mathrm{d}\eta$, then the second order action for the perturbations takes the form

$$S_2 = \frac{1}{2}\int \mathrm{d}\eta\ \mathrm{d}^3x \left[(v')^2 - \delta^{ij}\partial_i v \partial_j v + \frac{z''}{z}v^2\right]\,. \tag{3.3.17}$$

Here, primed variables represent derivatives with respect to conformal time (obeying $F' = a\dot{F}$) and $z = a\dot{\phi}/H$. Note that by definition $v = -zR$ also, relating it more directly to the scalar curvature. In this form, the action for v is equivalent to a scalar field in Minkowski space with a time dependent mass term. Really, this time dependence arises from the effect of the spacetime evolution, but this repackaging into a mass term is useful for mathematical manipulation. We perform a standard quantisation process[87] on v, expanding it in terms of creation and annihilation operators obeying the usual commutation relations,

$$\hat{v} = \int \mathrm{d}^3k \left[v_k(\eta)\hat{a}_k + v_k^*(\eta)\hat{a}_k^\dagger\right]\,, \tag{3.3.18}$$

where v_k is a Fourier mode function whose time-dependence is determined by the equation

$$v_k'' + \left[k^2 - \frac{z''}{z}\right] v_k = 0\,, \tag{3.3.19}$$

which can also be written in the form[179]

$$v_k'' + \left[k^2 - \frac{1}{\eta^2}\left(\nu^2 - 1/4\right)\right] v_k = 0\,, \quad \nu^2 = \frac{1}{4} + \eta^2 \frac{z''}{z}\,. \tag{3.3.20}$$

The solution of this can be written in terms of standard Hankel Functions of the first and second kind, assuming (as will later be justified) that ν is constant, as

$$v_k(\eta) = \sqrt{-\eta}\left[A_k H_\nu^{(1)}(-k\eta) + B_k H_\nu^{(2)}(-k\eta)\right]\,, \tag{3.3.21}$$

where A_k and B_k are arbitrary constants to be set by boundary conditions. In this case, we obtain these by noting that in the limit of $k \to \infty$ the modes are high frequency enough that the expansion of spacetime is approximately constant over many oscillations of the wave, meaning that they behave essentially as in Minkowski space. Our solution should hence look asymptotically like the evolution of a scalar field in Minkowski space, which is well known,[87] and allows us to impose the condition

$$\lim_{k\to\infty} v_k \to \frac{1}{2k} e^{-ik\eta}\,, \tag{3.3.22}$$

which, using the asymptotic behaviour of the Hankel functions in the general solution, lets us impose $B_k = 0$ and find A_k such that

$$v_k(\eta) = \frac{\sqrt{-\eta\pi}}{2} e^{i(\nu+1/2)\pi/2} H_\nu^{(1)}(-k\eta)\,. \tag{3.3.23}$$

3.3.4. Power Spectrum of Curvature Perturbations

We can now calculate from this canonical field, invoked for mathematical convenience, more readily physically-interpretable quantities such as the curvature perturbation $\mathcal{R}_k = -v_k/z$ as defined previously. From this, we can subsequently go on to compute a power spectrum for such quantities. By power spectrum, we mean a function of k which describes the variation in a field, let us call it f for now. It is conventionally defined in terms of the statistical two-point correlation function of f

as[179]

$$\langle f(\mathbf{k}_1) f^*(\mathbf{k}_2) \rangle = \delta(\mathbf{k}_1 - \mathbf{k}_2) P_f(k) \,, \tag{3.3.24}$$

where, because of assumed isotropy, the power spectrum depends only on the magnitude of the wavenumber vector and not its direction. It is conventional to further define a rescaled power spectrum

$$\mathcal{P}_f(k) = \frac{k^3}{2\pi^2} P_f(k) \ . \tag{3.3.25}$$

Using our result from above for the canonical field, and its relationship with $\mathcal{R}$, this definition results in a power spectrum for the comoving curvature $\mathcal{R}$ of

$$\mathcal{P}_\mathcal{R} = \frac{k^3}{2\pi^2} |\mathcal{R}|^2 = \frac{k^3}{2\pi^2} \left| \frac{v_k}{z} \right|^2 \ . \tag{3.3.26}$$

This is the quantity we wish to calculate for an inflationary model, in order to test it experimentally. As we can for now treat $\mathcal{R}$ as a conserved quantity on superhorizon scales, computing its value at the end of inflation can be reduced to the problem of computing it, for each value of k, at the horizon-crossing point $k = aH$. Similarly, going through an equivalent process for tensor perturbations reveals that the spectrum of gravitational waves is

$$\mathcal{P}_\mathcal{T} = \frac{4k^3}{\pi^2} \left| \frac{u_k}{a} \right|^2 \ , \tag{3.3.27}$$

where u_k is a Fourier mode of another canonical variable, u, and it obeys the same equation (3.3.19) as the scalar mode but with $z \to a$ (reflecting how gravitational waves are affected only by the expansion of space and not the dynamics of the scalar field perturbation). The additional numerical factor present in this expression arises due to a sum over the polarisations of the gravitational waves.

Each inflationary model will predict different power spectra at the end of inflation due to the different evolutions of a and $z = a\dot{\phi}/H$. Note that a and z appear not only directly in the above expressions explicitly but also indirectly in v (and u) via the Hankel function's parameter ν in eqs. (3.3.23) and (3.3.20). We will shortly

move on to the topic of calculating a and z and thus $\mathcal{P}_\mathcal{R}$ and $\mathcal{P}_\mathcal{T}$ for a sample model, after a short detour to describe how we compare these spectra to experiment.

3.3.5. Testing Inflation with the Primordial Power Spectrum

The primordial power spectrum $\mathcal{P}_\mathcal{R}$ is typically parametrised in a log-log series expansion of the form

$$\log\left(\mathcal{P}_\mathcal{R}\right) = \log\left(A_s\right) + \left(n_s - 1\right)\log\left(\frac{k}{k^*}\right) + \frac{\alpha_s}{2}\log^2\left(\frac{k}{k^*}\right) + \frac{\beta_s}{6}\log^3\left(\frac{k}{k^*}\right) + \dots . \tag{3.3.28}$$

Here, A_s is the scalar amplitude which gives the value of the power spectrum at $k = k^*$, the so-called pivot-scale (an arbitrary k value to expand around, chosen for convenience typically[171] as 0.05 Mpc^{-1}). Further parameters in the expansion above are called the spectral index or the tilt (n_s), the running of the spectral index (α_s), the running of the running (β_s) and so on, each encoding a higher-order deviation from a constant, or scale-invariant, spectrum. CMB measurements typically indicate (varying slightly depending on the method) that the power spectrum is very close to scale-invariant, with values generally[39] close to $A_s \approx 2.2\times10^{-9}$ and $n_s \approx 0.96\pm0.01$. Of course, $n_s = 1$ and all higher order terms identically zero would represent a perfect scale invariant spectrum, and while we are now fairly sure that n_s is not exactly 1, we are considerably less certain of the extent of scale dependence from other terms. Precise values for the higher order terms (the runnings) are still a matter of some debate, with large error bars and multiple inconsistent approaches casting significant uncertainty on their negligibility or lack thereof. This will be the topic of the research presented in Section 6.

Similarly, the tensor power spectrum is expanded in this way, though with a slightly different historical convention to take note of

$$\log\left(\mathcal{P}_\mathcal{T}\right) = \log\left(A_t\right) + n_t\log\left(\frac{k}{k^*}\right) + \dots , \tag{3.3.29}$$

but as tensor perturbations have a comparatively less pronounced effect on the CMB

than the scalars, this is less well constrained and we only have a reliable upper limit on A_T, which is usually expressed in terms of the tensor-to-scalar ratio r as

$$r = \frac{\mathcal{P}_\mathcal{T}}{\mathcal{P}_\mathcal{R}} \lesssim 0.1\,, \tag{3.3.30}$$

which is conventionally defined at a different pivot scale of $k^* = 0.002\text{Mpc}^{-1}$. In a typical scenario, it is known that $r(0.05\ \text{Mpc}^{-1}) \approx 1.08 \times r(0.002\ \text{Mpc}^{-1})$, for the sake of comparison.[24]

It is useful to note that for a given power spectrum, the expansion parameters (n_s, etc) can be obtained via either a numerical fit to this parametrisation, or analytically via suitable derivatives of a known form of $\mathcal{P}_\mathcal{R}$ evaluated at $k = k^*$. That is, one can define using eq. (3.3.28), for example,

$$n_s = 1 + \left.\frac{\mathrm{d}\log\mathcal{P}_\mathcal{R}}{\mathrm{d}\log k}\right|_{k=k^*}\,, \tag{3.3.31}$$

which can be easily extended to higher orders as needed.

3.3.6. Primordial Spectra in Slow-Roll Inflation

To give an example of how the power spectra arise in inflation, we will do so assuming that the field is undergoing slow-roll. This is the most prototypical and fiducial example of practical interest, and so we proceed to note that from the definition of the slow-roll parameters (e.g. eq. (3.2.18) and other related forms) that[179]

$$z \approx \sqrt{2\epsilon_0}a + O(\epsilon^2)\,, \tag{3.3.32}$$

and the conformal time (treating H as constant)

$$\eta = \int \frac{1}{a}dt \approx \frac{1}{H}\int \frac{1}{a^2}da \approx -\frac{1}{aH} + O(\epsilon)\,, \tag{3.3.33}$$

so that ν in eq. (3.3.20) is approximately (treating H and ϵ_0 as constants)

$$\nu^2 = \frac{1}{4} + \eta^2\frac{z''}{z} \approx= \frac{1}{4} + \frac{2a^2H^2 + O(\epsilon)}{a^2H^2 + O(\epsilon)} = \frac{9}{4} + O(\epsilon)\,. \tag{3.3.34}$$

This justifies our previous assumption in solving (3.3.20) that ν is constant, as $O(\epsilon)$ corrections are small. In these results, the assumptions made generate errors that are encompassed in the $O(\epsilon)$ corrections. This is a strength of the slow-roll approach in that one can systematically handle such error terms. In any case, our main result of this is that the Hankel function parameter ν is approximately equal to 3/2 during inflation, with the deviation from this being comparable in magnitude to the slow-roll parameters.

Plugging the value $\nu = 3/2$ into the solution for v_k (3.3.23) and taking the asymptotic behaviour of the Hankel function in the limit[10] $\eta \to 0$ to compute the behaviour of the perturbation modes as inflation ends, we find

$$v_k \approx \frac{-i}{\sqrt{2k^3}\eta} \approx \frac{iaH}{\sqrt{2k^3}}\,, \tag{3.3.35}$$

where we have again used eq. (3.3.33) in the second approximate equality. Then, using eq. (3.3.26) and evaluating at $k = aH$ (owing to the superhorizon conservation of $\mathcal{R}$) we obtain a power spectrum

$$\mathcal{P}_\mathcal{R} \approx \frac{H^2}{8\pi^2\epsilon_0}\,. \tag{3.3.36}$$

We can then calculate things like the spectral index as in eq. (3.3.31) as

$$n_s \approx 1 - 2\epsilon_0 - \epsilon_1 + O(\epsilon^2)\,. \tag{3.3.37}$$

Repeating a very similar process for the tensor spectrum then yields

$$\mathcal{P}_\mathcal{T} = \frac{2H^2}{\pi^2}\,, \tag{3.3.38}$$

which immediately implies a tensor-to-scalar ratio $r = 16\epsilon_0$.

While it is not directly constrained at present, we can also show that the tensor spectral index $n_t = -2\epsilon_0$ in this simple example. This is primarily of interest because one can see from this that $r = -8n_t$ when a slowly rolling, minimal scalar field drives inflation. This will not generally be true for other models, and is hence

[10] Note that during inflation, η begins large and negative (cf. the above slow-roll approximation in eq. (3.3.33) of η) and approaches zero from below as inflation comes to an end.

an example of a consistency relation which requires two or more parameters to be related in a certain way if a particular explanation of inflation is taken to be correct, which has obvious uses in testing and constraining inflationary models.
These expressions are correct to lowest order in the slow-roll expansion, but higher order corrections can of course be computed by following the same calculation with fewer assumptions (e.g. accounting for time dependence of H and ϵ_0 when relevant).

3.3.7. Observable modes

Different wavenumbers k of the power spectrum, physically, represent fluctuations on a typical length scale of size $1/k$. Hence the maximum observable scale, set by the size of the visible universe, and the minimum observable scale, set by experimental precision of measuring devices used to probe CMB radiation, impose limits on the range of k values for which we can measure the power spectrum. Additionally, the expansion of the universe since inflation has stretched out each k mode so that scales observable today are much larger in physical size than they were at the time they were generated. Assuming a typical history of the post-inflationary universe (e.g. reheating with effective/average equation of state $\langle w \rangle \approx 0$, then radiation- and matter-dominated epochs as usual), a careful consideration of these factors allows us to determine when, during inflation, the scales we can observe today were leaving the horizon and hence setting up the initial conditions for the generation of observable CMB anisotropies, resulting in the well-known relationship[39]

$$N_* \approx 67 - \ln\left(\frac{k_*}{a_0 H_0}\right) + \frac{1}{4}\ln\left(\frac{V_*^2}{\rho_{\rm end}}\right) + \frac{1-3\langle w\rangle}{12(1+\langle w\rangle)}\ln\left(\frac{\rho_{\rm th}}{\rho_{\rm end}}\right) - \frac{1}{12}\ln\left(g_{\rm th}\right), \quad (3.3.39)$$

where N_* is the number of e-folds before the end of inflation at which the wavenumber k_* (measured today) leaves the horizon (when it is equal to the horizon scale aH during inflation), and V_* is the inflaton potential at this time. Parameters a_0 and H_0 are the scale factor (typically normalised as unity) and measured Hubble parameter at present. It also depends on $\rho_{\rm end}$ and $\rho_{\rm th}$ - the energy density of the universe immediately after inflation and reheating, respectively (in the latter case,

this is typically taken to be at some time when $\rho_{\rm r} \gg \rho_\phi$). Lastly, $g_{\rm th}$ is the number of relativistic degrees of freedom post-reheating which, for a typical temperature and assuming a fiducial GUT of some kind, is maybe $O(10^3)$ and is thus typically taken to be so.

In normal circumstances, one finds that for $k_* \in [10^{-3}, 10^1]$ Mpc^{-1} or so, representing the cosmic and experimental bounds on k_* values we can probe in CMB experiments, this relation implies $N_* \approx 50-60$. That is, it is typically 50 or more e-folds before the end of inflation that the observed k modes are generated, and then remain frozen until the end of inflation due to the discussed conservation of $\mathcal{R}$. At this time, still many e-folds before the end of inflation, the slow-roll approximation is still strongly held. That is, the observable modes are determined at a time when slow-roll parameters are small such that $O(\epsilon)$ corrections are much less than unity. This justifies the use of the slow-roll approximation up until this point, and also ensures that the spectral index in eq. (3.3.37) obeys $n_s \approx 1$. This is exactly the prediction of a nearly but not entirely scale-invariant spectrum of primordial fluctuations that we promised at the beginning of this chapter as the final and most significant piece of evidence for the feasibility of inflationary theory (as discussed in Section 3.3.5). Similarly, we saw above that $r \approx 16\epsilon_0$ which in this regime will also typically be small, as required by more modern experimental results.

The exact amount of departure from scale invariance is also hence set by the size of slow-roll parameters $50-60$ e-folds prior to the cessation of inflationary expansion, and this will differ a bit from model to model. To further illustrate this we return the example of a monomial potential with exponent n that we began to study in Section 3.2.4. Following eqs. (3.2.26) and (3.2.23), we find after some calculation that

$$\epsilon_{0*} = \frac{n}{4N_*}\,, \quad \epsilon_{1*} = \frac{1}{N_*}\,. \tag{3.3.40}$$

This implies that for the $n = 2$ model (omitting now the asterisks for brevity, though being careful to recall that these quantities are evaluated at $N \approx 50-60$)

$$n_s \approx 1 - 2\epsilon_0 - \epsilon_1 = 1 - \frac{n+2}{2N}\,, \tag{3.3.41}$$

and

$$r \approx 16\epsilon_0 = \frac{4n}{N}\,. \tag{3.3.42}$$

This means for, say, $n = 2$ and $N = 60$, we have $n_s \approx 0.967$ and $r \approx 0.13$. The former is nicely within the typical 1σ bounds for the experimentally measured value for the spectral index[39] discussed in Section 3.3.5, though the latter exceeds the more recently discovered bound of $r \lesssim 0.1$. This model of inflation specifically, is hence ruled out due to overproduction of gravitational waves, but it still serves as a simplistic introduction to the key ideas at hand. Other models - perhaps with a different potential or some extra terms in the action altering the dynamics - which may predict a smaller value of r while still keeping a spectral index close to that of this simple example are of present interest as feasible inflationary models. The original research presented in the forthcoming chapters of this thesis will address issues including this for some more complex but physically-motivated inflationary models.

3.3.8. Extensions

As previously mentioned, many variations and extensions of the basic inflationary model are possible. Here we will briefly detail some of the key model-building ideas and further tests possible that are well established and not uncommon within the literature, as they will come in handy later.

Power Spectra in Multi-field Scenarios

An important result in the single-field case was that the quantity $\mathcal{R}$ was conserved on superhorizon scales. The presence of an additional field in inflation breaks this conservation law, however, as in addition to adiabatic curvature perturbations $\mathcal{R}$ there are now entropy or isocurvature perturbations $\mathcal{S}$.[142,205–210] In general, an isocurvature perturbation is one such that two quantities can be simultaneously perturbed

while not affecting the overall curvature due to a cancellation between their individual effects on spacetime. In general, these occur whenever multiple distinct fluids are present (e.g. radiation and matter) but this is of no concern in the single-field inflationary scenario where the only non-negligible source of energy-momentum is ϕ. If instead we had two fields, ϕ and χ, this would no longer be the case, though. In fact, it is convenient in such scenarios to consider re-defined fields[205] σ and s:

$$\dot{\sigma} = \cos(\theta)\,\dot{\phi} + \sin(\theta)\,\dot{\chi}\,, \tag{3.3.43}$$

$$\dot{s} = \cos(\theta)\,\dot{\chi} - \sin(\theta)\,\dot{\phi}\,, \tag{3.3.44}$$

where

$$\tan(\theta) = \frac{\dot{\chi}}{\dot{\phi}}\,. \tag{3.3.45}$$

This implies physically that σ moves parallel to the trajectory in (ϕ, χ) field space while s is perpendicular to it. Perturbations of the σ and s fields (or rather the Sasaki-Mukhanov variables derived from them; Q_σ and Q_s), then, it turns out, respectively source the curvature and isocurvature perturbations in the model.[211] That is,

$$\mathcal{R} = \frac{H}{\dot{\sigma}} Q_\sigma\,, \tag{3.3.46}$$

$$\mathcal{S} = \frac{H}{\dot{\sigma}} Q_s\,. \tag{3.3.47}$$

With these definitions in hand we can go on to talk about how $\mathcal{R}$ is no longer a conserved quantity on superhorizon scales. Analysis of the equations of motion for the perturbed fields reveals that on superhorizon scales[212]

$$\dot{\mathcal{R}} \approx AH\mathcal{S}\,, \tag{3.3.48}$$

$$\dot{\mathcal{S}} \approx BH\mathcal{S}\,, \tag{3.3.49}$$

where A and B are model-dependent functions whose particular forms we are not presently interested in. Of course, in the single-field case $\mathcal{S} \equiv 0$ so $\dot{\mathcal{R}} \approx 0$ as expected. This system can be solved by introducing the transfer functions:

$$\mathcal{T}_{\mathcal{S}\mathcal{S}}(t) = \exp\left(\int_{t^*}^{t} B(t')H(t')\mathrm{d}t'\right)\,, \tag{3.3.50}$$

and

$$\mathcal{T}_{\mathcal{R}\mathcal{S}}(t) = \int_{t^*}^{t} A(t')H(t')\mathcal{T}_{\mathcal{S}\mathcal{S}}(t')\mathrm{d}t'\,. \tag{3.3.51}$$

The solution then takes the form

$$\begin{pmatrix}\mathcal{R}\\ \mathcal{S}\end{pmatrix} = \begin{pmatrix}1 & \mathcal{T}_{\mathcal{R}\mathcal{S}}\\ 0 & \mathcal{T}_{\mathcal{S}\mathcal{S}}\end{pmatrix}\begin{pmatrix}\mathcal{R}^*\\ \mathcal{S}^*\end{pmatrix}\,. \tag{3.3.52}$$

As these equations are valid on large scales, the first time t^* from which we can use them to determine the future state of the system is when $k = aH$. Prior to this, on subhorizon scales, the general structure of the single-field calculation remains valid, so we can say that the final power spectrum in a multi-field scenario is related to the usual horizon-crossing power spectrum $\mathcal{P}^*_{\mathcal{R}}$ via

$$\mathcal{P}_{\mathcal{R}} = \mathcal{P}^*_{\mathcal{R}} \times (1 + \mathcal{T}^2_{\mathcal{R}\mathcal{S}})\,, \tag{3.3.53}$$

where $\mathcal{T}_{\mathcal{R}\mathcal{S}}$ is computed between horizon-crossing and the end of inflation. This represents an enhancement in power over the standard case, and is due to the superhorizon transfer of power from isocurvature to curvature. Similar expressions can be found to describe the isocurvature power spectrum but these are beyond the scope of this thesis. We also note that this amplification of the scalar power spectrum breaks the usual single-field consistency relation, such that now $r = -8n_t/(1+\mathcal{T}^2_{\mathcal{R}\mathcal{S}})$,

such that an observed inequality of r and $-8n_t$ could be used to infer the presence of additional fields. As this would require a precise measurement of n_t, which is difficult given the relative inertness of tensor perturbations on the CMB, we cannot yet make this distinction.

Sound speeds

In the minimal single-field case above, we considered quantisation of the variable v with action given by eq. (3.3.17). In a wide class of more general theories with non-standard kinetic terms such as the DBI form (2.2.19) or equivalent results arising from e.g. non-standard gravity, the action for v may instead take a form like[213]

$$S_2 = \frac{1}{2}\int \mathrm{d}\eta\ \mathrm{d}^3x \left[(v')^2 - c_s^2 \delta^{ij}\partial_i v \partial_j v + \ldots\right] . \tag{3.3.54}$$

Here, the presence of a coefficient in front of the action's spatial gradient term implies a ratio between the sizes of temporal and spatial changes in the field that is not unity; a non-standard (and possibly variable) speed of propagation or "sound speed". Our minimal single-field case has $c_s = 1$, such that disturbances in v propagate at the speed of light, but more general actions such as the $P(X)$ action in eq. (2.2.18) instead have[214]

$$c_s^2 = \frac{P_{,X}}{P_{,X} + 2P_{,XX}X} , \tag{3.3.55}$$

such that when $P_{,XX} \neq 0$ (i.e. there are terms at least of quadratic order in X in the action), $c_s \neq 1$.

A key implication of this is that quantisation is affected. The additional factor of c_s^2 in the action manifests in a modification of the equation of motion (3.3.19) such that

$$v_k'' + \left[c_s^2 k^2 - \frac{z''}{z}\right] v_k = 0 . \tag{3.3.56}$$

Now, when applying the boundary condition of asymptotic matching with the Minkowski quantum scalar field, the correct limit for each mode of v is

$$\lim_{k\to\infty} v_k \to \frac{1}{2c_s k} e^{-ic_s k\eta} \,. \tag{3.3.57}$$

This in turn, following the same calculation route as previously presented but with this difference, modifies the slow-roll scalar spectrum of perturbations to take the form

$$\mathcal{P}_\mathcal{R} \approx \frac{H^2}{8\pi^2 \epsilon_0 c_s} \,, \tag{3.3.58}$$

such that parameters like the spectral index now depend on the rate of change of c_s, and the tensor-to-scalar ratio is suppressed to $r \approx 16\epsilon_0 c_s$. Once again, this modifies the consistency relation so that we now would have $r = -8c_s n_t$. Measurement of the consistency relation could hence also constrain the propagation speed of the perturbations.

Note that while here we have discussed a non-trivial scalar sound speed c_s, it is also possible for tensor perturbations to have a different propagation speed, c_t. The same mathematics as above applies, of course, such that one would have a tensor-to-scalar ratio of $16\epsilon_0 c_s/c_t$ if both were present.

Non-Gaussianity

The power spectrum encodes the two-point statistical correlation of the curvature perturbation field. Higher order correlators can also, in principle, be measured. This is however difficult, and only weak constraints on the bispectrum (which encodes the three-point function) are available at present. The three-point function measures how strongly the spectrum of perturbations deviates from a Gaussian profile, and is as a result called the non-Gaussianity. Once again, observationally, we know that CMB primordial anisotropies are very close to Gaussian, but as with the two point statistics we could potentially use the size of this deviation to test and constrain inflationary theories. To begin to formalise this, and analogously to eq. (3.3.24), we define the bispectrum B as

$$\langle \mathcal{R}(\mathbf{k}_1)\mathcal{R}(\mathbf{k}_2)\mathcal{R}(\mathbf{k}_3)\rangle = (2\pi)^3 \delta(\mathbf{k}_1 + \mathbf{k}_2 + \mathbf{k}_3) B(k_1, k_2, k_3) \,, \tag{3.3.59}$$

Convention dictates that we derive a value f_{NL} from the bispectrum, e.g. via the relation,[212]

$$\langle \mathcal{R}(\mathbf{k}_1)\mathcal{R}(\mathbf{k}_2)\mathcal{R}(\mathbf{k}_3)\rangle = -(2\pi)^7\delta(\mathbf{k}_1+\mathbf{k}_2+\mathbf{k}_3)\frac{\sum k_i^3}{\prod k_i^3}\left(\frac{3}{10}f_{NL}\mathcal{P}_{\mathcal{R}}^2\right), \qquad (3.3.60)$$

and seek to compute this derived parameter. Since the bispectrum formally depends on three momenta, its size can depend on the relative values of them, which is also called the shape or configuration of non-Gaussianity. Some models may predict a large f_{NL} in some configurations while predicting a smaller one in others. This is essentially a consequence of the fact that while there is only one way for a distribution to be Gaussian, it can deviate from Gaussianity in a multitude of ways which are mutually distinct. A common shape of non-Gaussianity to test for is the equilateral configuration for which the three momenta are equal.[215] Also of interest is the so-called squeezed limit of non-Gaussianity where one of the wavenumbers is considerably smaller than the other two, though such considerations will be of little importance for this thesis.

For single-field, minimal slow-roll inflation, it is found that $f_{NL} \sim O(\epsilon)$[216] which is far smaller than present experimental constraints (at best, for the most well constrained shape, the error bars are around ± 5 and consistent with zero[217] while for equilateral shapes the constraint reads $f_{NL} = -4 \pm 43$), but introduction of e.g. multiple fields[218,219] or significantly sub-luminal propagation speeds can generate large non-Gaussianity (typically proportional to c_s^{-2}, it is found[220]) and come into the realm of experimental falsifiability on these grounds. It is hoped that future experiments will further narrow these constraints, of course. The theory discussed in Chapter 4 contains several aspects that have the potential for producing notable non-Gaussianity and so it is primarily to that end that we are interested in this topic. Calculation of the bispectrum is significantly more involved than the two-point power spectrum as it depends on second order curvature perturbations for which the equations become unsurprisingly messy, but the modern In-In formalism approach is typically used to make this more tractable. The key result is that, at

leading order, one can take the third order action in perturbations, with Lagrangian $\mathcal{L}_3$, and compute correlation functions via the integral[221]

$$\langle \hat{F}(t) \rangle = -i \int_{t_0}^{t} \left\langle \left[\hat{F}(t'), H_{\rm int}(t') \right] \right\rangle \mathrm{d}t' \,, \tag{3.3.61}$$

where square brackets represent the commutator, the triangular brackets on the right hand side now represent computation of the quantum expectation value of the arbitrary operator inside (here denoted $\hat{F}(t)$), and $H_{\rm int}$ is the interaction picture Hamiltonian, which at leading order can actually be replaced with $-\mathcal{L}_3$. The lower integration limit t_0 is taken to be some sufficiently early time that fluctuations are deeply subhorizon. Then, following suitable application of Wick's Theorem, this can be evaluated with a (still rather involved) calculation that will be omitted here.

CHAPTER 4

DISFORMALLY COUPLED INFLATION

In this chapter original research by the author on the topic of disformally coupled fields in cosmic inflation is presented. This work was carried out in collaboration with Carsten van de Bruck and Tomi Koivisto. The results of this have been published in the Journal of Cosmology and Astroparticle Physics in two papers.[222,223] A further publication in Physical Review D,[148] based on research solely by the author, covers particular mathematical procedures that were developed in order to complete this work, and will be discussed below, but have more general applicability.

4.1. The model

Consider a theory of modified gravity with an Einstein-Hilbert term and two scalar fields, ϕ and χ, with potentials U and V respectively. The field ϕ is minimally coupled to the gravitational metric g, but χ is minimally coupled to a different metric $\hat{g}(g, \phi)$, as described by the action functional (noting that units are such that $M_{\rm Pl} = 1$)

$$S = \int \mathrm{d}^4x\sqrt{-g}\,\frac{R}{2} - \int \mathrm{d}^4x\sqrt{-g}\left[\frac{1}{2}g^{\mu\nu}\phi_{,\mu}\phi_{,\nu} + U(\phi)\right] - \int \mathrm{d}^4x\sqrt{-\hat{g}}\left[\frac{1}{2}\hat{g}^{\mu\nu}\chi_{,\mu}\chi_{,\nu} + V(\chi)\right]. \tag{4.1.1}$$

As the most general physically desirable form that the function $\hat{g}(g,\phi)$ is the disformal relation (2.2.12), we can rewrite the action (4.1.1) in terms of just the metric g as

$$S = \int \mathrm{d}^4x\sqrt{-g}\left[\frac{1}{2}R + X^{\phi\phi} - U + \frac{C}{\gamma}\left(X^{\chi\chi} - CV\right) + 2\gamma D(X^{\phi\chi})^2\right], \tag{4.1.2}$$

where γ is the disformal factor in eq. (2.2.14). We are now using the shorthand notation $X^{IJ} = -g_{\mu\nu}\partial^\mu\phi^I\partial^\mu\phi^J/2$ where I and J are field indices taking values from (ϕ,χ). Note that the χ kinetic terms are now those with respect to the g metric, but they appear non-canonically in the action to reflect the change in metric. We have hence transformed a bimetric theory of minimally coupled scalars to a single-metric theory with one minimal and one non-minimal field as well as non-trivial kinetic interactions via terms like $(X^{\chi\chi} - CV)/\gamma$ and $\gamma(X^{\phi\chi})^2$. Note that γ depends on $X^{\phi\phi}$. We shall subsequently refer to this theory as *disformally coupled inflation*. It is entirely specified by the forms of four arbitrary functions; the two potentials U and V as well as the coupling functions C and D. Our primary motivation for studying this is that disformal couplings are highly general and it is interesting to find out more about the range of phenomena this might give rise to when applied to a two-field theory.

As well as the general motivation to study theories with two fields on disformally related metrics, this kind of model is realised in the context of braneworlds, where in a Type IIb String Theory scenario the second metric $\hat{g}$ could be the induced metric on a D3-brane in the compactified extra dimensions, and matter fields on this brane such as χ are thought of as parametrising the motion of the end points of strings attached to that brane.[104,110,224–226] Meanwhile, the metric of our 3+1 macroscopic dimensions is g, and the field ϕ is a parametrisation of the radial motion of the

D3-brane. With this motivation in mind, one would expect the kinetic term of ϕ to instead take DBI form,[227–229] as in eq. (2.2.19), which leads us to define another action reflecting this

$$S = \int \mathrm{d}^4x\sqrt{-g}\left[\frac{1}{2}R + \frac{C}{D}\left(1-\frac{1}{\gamma}\right) - U \right. \\ \left. + \frac{C}{\gamma}\left(X^{\chi\chi} - CV\right) + 2\gamma D(X^{\phi\chi})^2\right] . \tag{4.1.3}$$

The inflationary properties of a DBI term like this in isolation have been well studied and it is known to have interesting effects.[230–232] In this scenario, both the DBI kinetic term and the disformally-coupled second field originate from the dynamics of a brane and its strings. It is therefore interesting to think of this version of the theory as a generalisation of DBI inflationary models, now accounting for the possibility of this second field χ. The common origin of the disformal coupling and the DBI kinetic term is reflected in how the DBI warp function in (2.2.19) is found to be $f = D/C$. The theory hence still depends on just four free functions, due to this relation. One could consider another scenario in which the DBI kinetic term's origin is different to that of the disformality, in which case f could be a fifth free function, but we will not concern ourselves with this possibility in this work.

To distinguish between the two actions (4.1.2) and (4.1.3) we shall name the former one as the *canonical* model of disformally coupled inflation, and the latter shall be referred to as the DBI model. We are interested in both realisations with different motivations, but the mathematics are similar enough in each case that we can largely proceed in generality in what follows.

4.2. Inflationary Dynamics

When written in terms of one metric but non-minimal fields, both the canonical (4.1.2) and DBI (4.1.3) models are special cases of the general $P(X^{IJ}, \phi^K)$ action in eq. (2.2.20), which has been well studied.[148,212,233] To describe both canonical and DBI models at once in the following calculations, we will write results first in terms

of the $P(X^{IJ}, \phi^K)$ Lagrangian and its derivatives, only specialising to the particular forms of P in (4.1.2) and (4.1.3) when it is instructive to do so.

While one could in principle take the modified gravity representation of the theory in which the disformal metric $\hat{g}$ is left in that form, and analyse the system in this way, the transformation of the theory into $P(X^{IJ}, \phi^K)$ form enables us to study it using the usual Einstein equations (2.1.15), albeit with a highly non-standard energy-momentum tensor derived from the ϕ and χ fields' action. This is explicitly given by

$$T^{\mu\nu} = Pg^{\mu\nu} + P_{<IJ>}\partial^\mu\phi^I\partial^\nu\phi^J\,, \tag{4.2.1}$$

where we have defined a symmetrised derivative with respect to kinetic combinations

$$P_{<JK>} = \frac{1}{2}\left(\frac{\partial P}{\partial X^{JK}} + \frac{\partial P}{\partial X^{KJ}}\right)\,, \tag{4.2.2}$$

for convenience. Throughout this work we will be referring to and using this notation extensively, including as second and even third order symmetrised derivatives of this kind such as $P_{<IJ><KL><MN>}$ which are constructed by recursive application of the above definition. Many of the possible combinations of indices in these derivatives of P give rise to non-unique expressions due to factors such as the defined symmetrisation, the commutation of partial derivatives, and the coincidental symmetries of the Lagrangian of this model, and so for easy reference we have catalogued them appendix A.1.

4.2.1. Background cosmology

Specialising to a flat FRW background, the Einstein equations reduce to the usual form

$$3H^2 = \rho = 2P_{<IJ>}X^{IJ} - P\,, \tag{4.2.3}$$

$$2\dot{H} = -(\rho + p) = -2P_{<IJ>}X^{IJ}\,. \tag{4.2.4}$$

Note that the pressure p is equivalent to the Lagrangian P evaluated on the background. The energy density and pressure can also be thought of as a sum of terms coming from the two fields. The field ϕ, being either a canonical scalar or a DBI field, will have its usual (canonical or DBI) contribution to ρ and p. That is, for canonical ϕ we just have eqs. (3.1.37 – 3.1.38), whereas for the DBI case we have (following the definition above and some manipulation)

$$\rho_\phi = \frac{C}{D}(\gamma - 1) + U\,, \tag{4.2.5}$$

$$p_\phi = \frac{C}{D}\left(1 - \frac{1}{\gamma}\right) - U\,. \tag{4.2.6}$$

Meanwhile, the χ field with its non-minimal kinetic structure will have an unusual energy density and pressure profile, also depending on ϕ and $\dot{\phi}$. It will be useful to explicitly note the forms of these expressions, which are

$$\rho_\chi = \gamma C\left(\gamma^2 X^{\chi\chi} + CV\right)\,, \tag{4.2.7}$$

$$p_\chi = \frac{C}{\gamma}\left(\gamma^2 X^{\chi\chi} - CV\right)\,, \tag{4.2.8}$$

where, in the FRW background, the γ parameter (2.2.14) takes the form

$$\gamma = \frac{1}{\sqrt{1 - 2\frac{D}{C}X^{\phi\phi}}} = \frac{1}{\sqrt{1 - \frac{D}{C}\dot{\phi}^2}}\,. \tag{4.2.9}$$

The non-standard energy density and pressure of χ hence lead to an equation of state for the χ field of

$$w_\chi = \frac{1}{\gamma^2}\frac{\gamma^2 X^{\chi\chi} - CV}{\gamma^2 X^{\chi\chi} + CV}\,, \tag{4.2.10}$$

such that during potential domination (now defined by $CV \gg \gamma^2 X^{\chi\chi}$) the equation of state approaches not -1 as for a canonical scalar, but $-1/\gamma^2$. That is, if γ is large, the χ field begins to act like dust. Furthermore, even in the moderate case of $\gamma > \sqrt{3}$ the χ field will not be able to individually drive an accelerating expansion

as its equation of state crosses the acceleration threshold of $-1/3$. It is therefore generally expected that ϕ is the primary inflaton in these models except in the limit of small γ (weak disformality and slow-roll), which is largely uninteresting as disformal effects will yield little more than small corrections to fiducial two-field inflation scenarios. We will typically consider ϕ to be the "inflaton" while χ is a secondary field whose primary effect upon inflation is to dynamically alter ϕ's behaviour via their disformal interactions.

The generalised Klein-Gordon equations can be shown take the form:

$$K_{IJ}\ddot{\phi}^J + 3HP_{<IJ>}\dot{\phi}^J + 2P_{<IJ>,K}X^{KJ} - P_{,I} = 0\,, \tag{4.2.11}$$

where the kinetic matrix K_{IJ} is defined by,

$$K_{IJ} = P_{<IJ>} + 2P_{<MJ><IK>}X^{MK}\,. \tag{4.2.12}$$

For $I = \chi$, in both canonical and DBI models, this reduces to

$$\ddot{\chi} + 3H\dot{\chi} + \gamma^2\frac{D}{C}\dot{\phi}\dot{\chi}\ddot{\phi} - \frac{1}{2}\left[(\gamma^2-3)\frac{C'}{C} - (\gamma^2-1)\frac{D'}{D}\right]\dot{\phi}\dot{\chi} + \frac{C}{\gamma^2}V' = 0\,, \tag{4.2.13}$$

Here we see some key differences with minimal inflationary scenarios. First, the non-standard kinetic terms in the action manifest via nonlinearities such as $\dot{\phi}\dot{\chi}\ddot{\phi}$ that are amplified as the disformality increases ($\propto \gamma^2$). Also, a large value of γ suppresses the role of the potential derivative term that would usually be the driving force for inflation in a minimally-coupled setting, both curtailing its steepness and allowing the modified kinetic terms to play a larger role. For $I = \phi$, the equation of motion derived is different in the canonical and DBI models. To express these differences succinctly, we introduce the symbol γ_d, defined as

$$\gamma_d = \begin{cases} 1 & \text{in the canonical case (4.1.2)} \\ \gamma & \text{in the DBI case (4.1.3)} \end{cases} \tag{4.2.14}$$

with which the ϕ field's equation of motion for both canonical and DBI cases can be unified in one expression as

$$\left(\gamma_d^3+\gamma^2\frac{D}{C}\rho_\chi\right)\ddot{\phi}+3H\dot{\phi}\left(\gamma_d-\gamma^2\frac{D}{C}p_\chi\right)+U' \\ +\frac{1}{2}(\gamma^2-1)\rho_\chi\frac{D'}{D}-\frac{1}{2}\left[(\gamma^2-2)\rho_\chi+3\gamma^2p_\chi\right]\frac{C'}{C} \\ +\frac{1}{2}\frac{C}{D}\left(\frac{D'}{D}-\frac{C'}{C}\right)(\gamma-1)^2(\gamma+2)=0\,, \tag{4.2.15}$$

such that for canonical models, the third line vanishes as this term arises purely due to the DBI kinetic term. Furthermore, the prefactors of the kinetic terms on the first line differ slightly between the two models, slightly altering the way in which disformality manifests itself. Interestingly, the extra terms due to the disformal interaction with χ on the first and second lines are neatly expressible in terms of the energy density and pressures of χ defined in (4.2.7 – 4.2.8).

Another quantity defined on the background that is of importance in theories like this is the sound speed. In a single-field theory, one finds this by looking at the second order action of the perturbations of the fields and taking the ratio of the prefactors of the gradient and kinetic terms, but in multi-field theories this is complicated by the presence of terms proportional to derivatives of two different fields. For a general $P(X^{IJ},\phi^K)$ theory, the second order action in terms of Sasaki-Mukhanov variables (3.3.13) is

$$S_{(2)}=\frac{1}{2}\int \mathrm{d}t\mathrm{d}^3x a^3\Big[K_{IJ}\dot{Q}^I\dot{Q}^J-\frac{1}{a^2}P_{<IJ>}\partial_iQ^I\partial^iQ^J \\ -N_{IJ}\dot{Q}^IQ^J-M_{IJ}Q^IQ^J\Big]\,. \tag{4.2.16}$$

where K_{IJ} is the kinetic matrix in eq. (4.2.12), and M_{IJ} and N_{IJ} are mass and interaction terms whose particular forms are well known in the literature[140,212] but not needed for the present discussion. The terms where $I\neq J$, if present, inhibit taking simple ratios of the relevant terms to determine propagation speeds, so instead one

takes the matrix product $(K^{-1})^{IK}P_{<KJ>}$, whose eigenvalues are the sound speeds of the fields. This, of course, allows for the possibility that each field will have a different sound speed, and indeed, this happens to be the case in disformally coupled inflation, as can be seen by directly evaluating the eigenvalues of the aforementioned matrix for the particular form of P. One identifies sound speeds,

$$c_s^{(1)} = \sqrt{\frac{\gamma_d C - \gamma^2 D p_\chi}{\gamma_d^3 C + \gamma^2 D \rho_\chi}}\,,$$
$$c_s^{(2)} = \frac{1}{\gamma}\,.$$

Note, however, that we have labelled these simply "1" and "2", rather than assigning them to the fields ϕ and χ. That is because, in cases such as this with two different propagation speeds, more care than usual has to be taken when quantising perturbations and this introduces some subtlety into precisely what we think of as propagating with these speeds. We will now take a short detour in explaining why this is before returning to analysis of the model.

4.2.2. A short detour: the kinetic structure of multi-field theories

In multi-field theories, one has the freedom to rewrite the theory in terms of any linear combination of the fields (or rather, their perturbations, which are more pertinent to the discussion),

$$\delta\phi^I = e^I_{I'}\delta\phi^{I'}\,, \tag{4.2.17}$$

where e is a change-of-basis matrix relating the initial fields (labelled with I') to the new fields (labelled with I). However, there are particular field combinations which lend themselves well to physical interpretation. A particularly common and useful basis to work in is the adiabatic/entropy representation, discussed in Section 3.3.8, ϕ^n, where $n = (\sigma, s)$, in which fields that are

- Orthonormal to one another,
- Parallel and perpendicular (respectively) to the trajectory in field space,

are defined. The orthogonality constraint can be generally imposed at the level of the second order action in Sasaki-Mukhanov (see eq. (3.3.13) for definition) perturbations such that the gradient term in (4.2.16) becomes the identity matrix, that is, the components of e satisfy the system of equations:

$$P_{<IJ>}e^I_{I'}e^J_{J'} = \delta_{I'J'}\,. \tag{4.2.18}$$

However, due to the symmetry $P_{<IJ>} = P_{<JI>}$, this does not entirely specify the basis transformation matrices. For example, in the two-field case there are four free functions in e but only three are specified by the above system, leaving one degree of freedom. This freedom is the ability to make a subsequent rotation with a new basis transformation $\bar{e}^{I'}_n$ without spoiling the orthonormality of the gradient terms. This degree of freedom is used to meet the second condition in the definition of the adiabatic/entropy basis; a rotation to orient the $Q^{I'}$ fields parallel and perpendicular to the field space trajectory of the $\phi^{I'}$s is made. In the two-field case, this amounts to a rotation by angle $\tan\theta = \dot{\phi}'/\dot{\chi}'$. This is especially useful to do as it then turns out that the curvature power spectrum depends only on the adiabatic σ field's perturbations, while the s field encodes the power in isocurvature perturbations.
Typically, it is hence useful to quantise the adiabatic/entropy fields. However, consider what quantisation means in the context of cosmological perturbations; it amounts to solving the perturbed equation of motion for each Fourier mode k of each field ϕ^I, v^I_k (where v^I is a convenient quantity defined as the scale factor a multiplied by the relevant Sasaki-Mukhanov variable), then setting the boundary conditions for this solution by imposing that it asymptotically looks like a free Minkowski space field at large frequencies. That is, for a field with sound speed c^I_s, as in eq. (3.3.57)),

$$v^I_k \to \frac{1}{2c^I_s k}e^{-ic^I_s k\eta}\,. \tag{4.2.19}$$

However, when transforming between different basis representations of the field per-

turbations, each newly defined field is a linear combination of the previous fields, that is

$$v_k^{I'} = e_I^{I'} v_k^I \,, \tag{4.2.20}$$

and this summation no longer takes the form of eq. (4.2.19) unless all the c_s^I values are the same (that is, it does not have a linear dependence on c_s). If all fields have the same c_s then all linear combinations of fields' perturbations can be written in this form and it is easy to quantise any linear combination of fields with the same procedure, but if different fields have different c_s values then a linear combination of two such perturbations will no longer have this form and it is difficult to see how to interpret this as not all combinations of fields can mathematically follow the normal canonical quantisation procedure. Physically, what this means is that if one cannot write the Fourier modes in this form then there is not a well-defined propagation speed, suggesting that the field under consideration is a composite of separate degrees of freedom with different speeds, and is hence not fundamental.

To solve this, one needs to identify a basis in which both the kinetic and gradient matrices in (4.2.16) are diagonal, as the fields in this basis do have separate and well-defined sound speeds. In general, none of the fields we have thus considered such as the $\phi^{I'}$ fields, or the adiabatic and entropy fields will be identifiable as fundamental. This is because the kinetic matrix in each case (e.g. $K_{I'J'} = e^I_{I'} e^J_{J'} K_{IJ}$) is not guaranteed to be diagonal by the given transformation. We instead consider a new field rotation $\phi^a = \hat{e}^{I'}_a \phi^{I'}$, where $\hat{e}$ is a rotation matrix with angle Θ, which, to ensure diagonality of the kinetic matrix K_{ab} in this basis, must be defined in the two-field case as[148]

$$\tan 2\Theta = \frac{2K_{\phi'\chi'}}{K_{\chi'\chi'} - K_{\phi'\phi'}} \,. \tag{4.2.21}$$

The adiabatic and entropy fields are hence only canonically quantisable when $\theta = \Theta$ (as this amounts to $\phi^a = \phi^n$), and the $\phi^{I'}$ fields are only canonically quantisable when $\Theta = 0$ (as this amounts to $\phi^a = \phi^{I'}$).

4.2.3. Kinetic structure of disformally coupled inflation: sound speeds

Based on this discussion, our fundamental degrees of freedom are not going to be the "physical" fields ϕ and χ, nor the adiabatic/entropy fields σ and s fields as in many simpler models. It is instead found, that the angle (4.2.21) is $\Theta = 0$ in our case. That is, the fundamental degrees of freedom are the $\phi^{I'}$ fields that are found via the basis transformation $\delta\phi^I = e^I_{I'}\delta\phi^{I'}$, where $P_{<IJ>}e^I_{I'}e^J_{J'} = \delta_{I'J'}$. Explicitly computing the change of basis yields

$$\begin{aligned} e^{\phi}_{\phi'} &= 1\,, \\ e^{\phi}_{\chi'} &= 0\,, \\ e^{\chi}_{\phi'} &= -\gamma^2\frac{D}{C}\dot{\phi}\dot{\chi}\,, \\ e^{\chi}_{\chi'} &= 1\,. \end{aligned}$$

That is $\phi = \phi'$ and is hence a fundamental degree of freedom, while χ is not, but instead the combination (which we will call θ instead of χ' for less crowded notation)

$$\delta\theta = \delta\chi - \gamma^2\frac{D}{C}\dot{\phi}\dot{\chi}\delta\phi\,, \tag{4.2.22}$$

is. After some algebra, one can see that at the background level, these fields are related by the differential equation $\dot{\theta} = \gamma^2\dot{\chi}$.
By writing the second order action in terms of this basis, we then identify the sound speeds for ϕ,

$$c_s^{(\phi)} = \sqrt{\frac{\gamma_d C - \gamma^2 D p_\chi}{\gamma_d^3 C + \gamma^2 D\rho_\chi}}\,, \tag{4.2.23}$$

and θ,

$$c_s^{(\theta)} = \frac{1}{\gamma}\,. \tag{4.2.24}$$

Note that we have rediscovered the same sound speeds we initially uncovered by

finding the eigenvalues of the appropriate matrix in the second order action, but we have now clearly identified which degrees of freedom actually possess these sound speeds. These are therefore the most natural fields to quantise, and they hence obey

$$v_k^\phi \to \frac{1}{2c_s^{(\phi)}k} e^{-ic_s^{(\phi)}k\eta}\,, \tag{4.2.25}$$

$$v_k^\theta \to \frac{1}{2c_s^{(\theta)}k} e^{-ic_s^{(\theta)}k\eta}\,. \tag{4.2.26}$$

However, if one were to quantise and set initial conditions for χ, it would be using the boundary condition

$$v_k^\chi \to \frac{1}{2c_s^{(\theta)}k} e^{-ic_s^{(\theta)}k\eta} - \gamma^2 \frac{D}{C}\dot{\phi}\dot{\chi}\frac{1}{2c_s^{(\phi)}k} e^{-ic_s^{(\phi)}k\eta}\,, \tag{4.2.27}$$

and as discussed in the previous section, this is not immediately compatible with the usual prescription for quantisation of field perturbations, indicating that the degree of freedom we call χ is composite and does not propagate with a single sound speed. In the limit of sufficiently weak disformal coupling,[1] the two fundamental sound speeds become approximately equal and close to 1 (as $\gamma(D=0)=1$). Similarly, in the limit of very strong disformal coupling, the sound speed for ϕ obeys

$$c_s^{(\phi)} \approx \sqrt{-w_\chi}\,, \tag{4.2.28}$$

such that the difference in sound-speeds can be written

$$(c_s^{(\theta)})^2 - (c_s^{(\phi)})^2 \approx \frac{1}{\gamma^2} + w_\chi\,, \tag{4.2.29}$$

and as noted above, w_χ approaches $-1/\gamma^2$ when χ is potential-dominated. In the limit of very strong disformal effects and potential-dominated χ we would hence also

[1] The precise mathematical meaning of strong/weak disformal effects in these expressions differs depending on whether a DBI kinetic term is present. For the canonical model, weak disformal coupling here means when $D \ll C/(\gamma^2 p_\chi)$ while in the DBI case it means $D \ll C/(\gamma p_\chi)$. In different expressions, different inequalities will be relevant, of course, so to save the tedium of repeatedly stating the precise definitions of "strong" and "weak" in all cases we will generally take these phrases to mean "when the term containing D is much smaller/larger than the competing term(s)".

expect to see approximately equal sound speeds for the two fields. In more typical cases of intermediate disformal coupling strength and/or a more general equation of state for χ, the two sound speeds would be expected to manifestly differ.

4.2.4. Results

Given the complex nonlinearity of the equations of motion, and the fact that disformal contributions to these equations of motion are dependent on the value of $\dot{\phi}$, the usual slow-roll approximation techniques will largely fail to account for the new effects in this theory.[222,223] When D is large, even slow-rolling solutions may differ significantly compared to conventional two-field models. Therefore, to understand the dynamics of this model in more detail, we perform a full numerical integration of the system of equations (4.2.3 – 4.2.4) and (4.2.11). To focus on the interesting features due to the disformal interaction, we make the simplest choice of potential for both fields; just a mass term, albeit with the possibility that ϕ and χ have different masses

$$U(\phi) = \frac{1}{2}m_\phi^2\phi^2\,, \quad V(\phi) = \frac{1}{2}m_\chi^2\chi^2\,. \tag{4.2.30}$$

We look however at two choices of coupling functions C and D. First, there are the "stringy" couplings arising from the physically-motivated String Theory construction of the model[104,110]

$$C = \frac{\phi^2}{\sqrt{T_3}}\,, \quad D = \frac{1}{\sqrt{T_3}\phi^2}\,, \tag{4.2.31}$$

where T_3 is the tension of the D3-brane. We also have an alternative choice of exponential couplings

$$C = C_0 e^{c\phi}\,, \quad D = D_0 e^{d\phi}\,. \tag{4.2.32}$$

While the stringy couplings represent an explicitly constructed model in Type IIb String Theory, we also wish to understand the wider possibilities for phenomenology in disformally coupled models, accounting for both the potential for different

realisations within the framework of String Theory and any wider contexts in which one might consider disformal couplings. The free parameters c and d allow us to control the rate of change of the coupling with respect to changes in ϕ (including the special case of constant couplings when these parameters are zero) which may serve as a prototype for a wide range of types of coupling for the sake of our investigation. In the remainder of this section, we present numerical solutions of eqs. (4.2.3 – 4.2.4) and (4.2.11) with the potentials and couplings specified above. While many sets of parameters were investigated during the course of this research, here we present seven examples to illustrate the overall qualitative trends and behaviours we witnessed.

Case 1: Stringy Couplings

The main parameter which defines the deviation of the inflationary dynamics from the standard case is γ in eq. (2.2.14). With the stringy couplings (4.2.31), γ takes the form

$$\gamma = \left(1 - \frac{\dot{\phi}^2}{\phi^4}\right)^{-\frac{1}{2}} , \tag{4.2.33}$$

which, for a slowly-rolling ϕ, obeys $\dot{\phi}^2 \ll \phi^4$ and hence implies negligible deviation from the case of $\gamma \approx 1$ for any brane tension T_3 and for either canonical or DBI variants of the model. It is hence difficult to construct trajectories where the field ϕ behaves as a conventional inflaton without rendering the disformal coupling negligible, and therefore uninteresting. Numerical studies confirm that this means that the result barely differs from conventional two-field inflation for a wide range of parameter space. One way to avoid this fate would be to consider non-slow-roll inflation where not the slow-rolling of the field, but kinetic or other effects drive inflation, but we will not explore this possibility here.

Similarly, it is difficult to have χ behave as an inflaton in the presence of significant disformality, because as noted in eq. (4.2.10), a large γ will make χ behave akin to a dust-like fluid with w_χ close to zero, not suitable for driving an accelerated expansion of space. Furthermore, we numerically observe that even if we set up a

situation with χ as the inflaton and $\gamma < \sqrt{3}$ but still above 1, the evolution of the system quickly approaches the trivial $\gamma = 1$ case.

Given these problems with achieving inflation with the stringy couplings, we will henceforth work only with the exponential couplings (4.2.32), which avoid the γ suppression problem in the slow-roll limit by instead having γ take the form

$$\gamma = \left(1 - \frac{D_0}{C_0} e^{(d-c)\phi} \dot{\phi}^2\right)^{-\frac{1}{2}} , \tag{4.2.34}$$

which for sufficiently large D_0/C_0 and not excessively negative $(d-c)$ could feasibly deviate from 1 even in a slow-rolling inflationary scenario. We can also see from this that we should take positive D_0 to impose $\gamma \geq 1$, and hence ensure subluminal propagation speeds (c.f. eqs. (4.2.23 – 4.2.24) and surrounding discussion) and a non-phantom equation of state for χ (4.2.10). While these restrictions are not strictly necessary, we can make further progress without appealing to these more problematic scenarios, and it will later prove phenomenologically desirable as we will show that ensuring $\gamma > 1$ is conducive to avoiding an excessive tensor-to-scalar ratio.

Case 2: Canonical Kinetic Term and Exponential Couplings, Example A

We now proceed to study inflationary dynamics of the exponentially coupled system in the canonical model. In our first example trajectory, shown in Figure 4.1, where the parameters are specified, the evolution has two parts. First, there exists a period of around 25 e-folds at the beginning where γ is increasing up to a maximum, before a second phase in which γ decreases to 1 and remains there. The enhancement of γ at early times is promising as, it is in this regime when the observable modes leave the horizon. This kind of behaviour is somewhat generically found in numerical simulations when a large positive value of $(d-c)$ is the primary source of γ's deviation from unity. At first, as ϕ begins to roll down the potential, $\dot{\phi}$ increases quickly and γ grows. However, as ϕ becomes smaller the steep exponential factor in γ sharply decreases and the value of $\dot{\phi}$ begins to stabilise, leading to an overall decrease in γ.

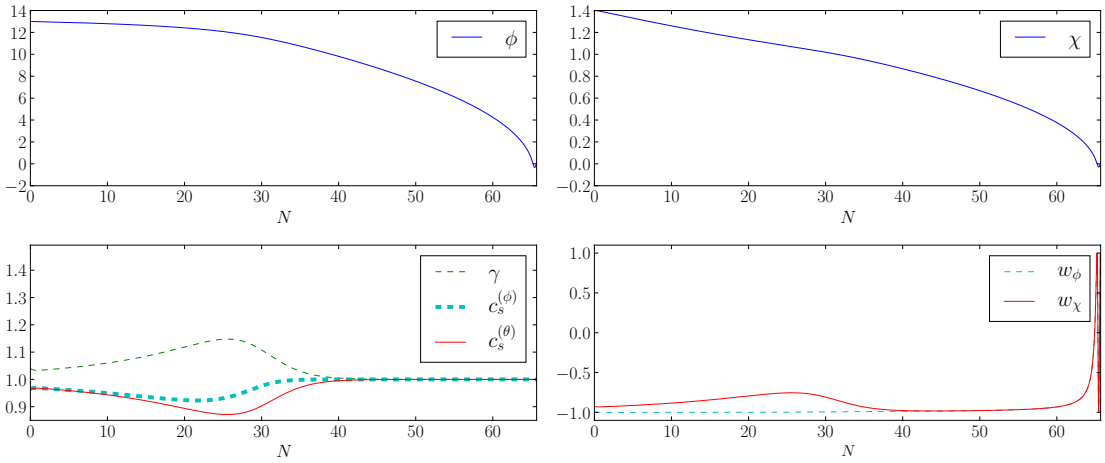

Figure 4.1.: Inflationary dynamics for the canonical model of disformally coupled inflation (4.1.2) with the potentials (4.2.30) and couplings (4.2.32). Parameters and initial conditions used are: $d = 2$, $c = 0$, $D_0 = 13.5$, $C_0 = 1$, $m_\phi = m_\chi = 1.8 \times 10^{-6}$, $\phi_0 = 13$, $\chi_0 = 1.4$, $\dot{\phi}_0 = -1.7 \times 10^{-7}$, $\dot{\chi}_0 = 0$.

Case 3: Canonical Kinetic Term and Exponential Couplings, Example B

Contrary to the previous example, in our next trajectory, shown in Figure 4.2, the major source of γ's evolution away from 1 is the large value of D_0/C_0. In such cases, numerical studies indicate that $\dot{\phi}$ remains fairly constant but the decrease in ϕ causes γ to drop from its initial large value to 1 at late times. Similarly, χ is held fairly constant due to the steepness of the conformal coupling, with a more negative value of c further inhibiting the evolution of χ. This raises the possibility of generating trajectories with sharp turns if the conformal coupling is large enough, which could lead to interesting features in the power spectrum.[234–237]

Case 4: Canonical Kinetic Term and Constant Couplings, Example C

In this example, shown in Figure 4.3, we explore the constant limit of the exponential couplings, $c = d = 0$. In the absence of an exponentially-enhanced deviation from unity, γ is made large by choosing a sufficiently large D_0. Also due to the lack of a ϕ-dependent term in γ, the value it takes remains constant through most of inflation. One can hence construct models where γ is incredibly large for an extended period of time, resulting in vanishingly small sound speeds, and χ behaving like dust to a

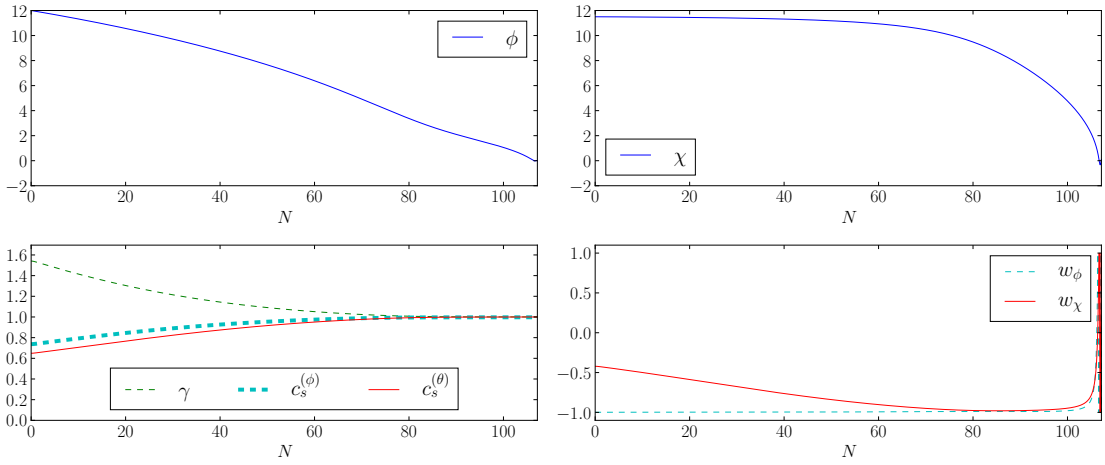

Figure 4.2.: Inflationary dynamics for the canonical model of disformally coupled inflation (4.1.2) with the potentials (4.2.30) and couplings (4.2.32). Parameters and initial conditions used are: $d = 0.19$, $c = -0.19$, $D_0 = 8 \times 10^9$, $C_0 = 1$, $m_\chi = 1.39 \times 10^{-6}$, $m_\phi = 2.78 \times 10^{-6}$, $\phi_0 = 12$, $\chi_0 = 11.5$, $\dot{\phi}_0 = -8.7 \times 10^{-7}$, $\dot{\chi}_0 = 0$

good approximation.

Case 5: Canonical Kinetic Term and Exponential Couplings, Example D

Here, a similar choice of parameters to Example B is made. The key difference is that c and d are somewhat larger, making the exponential disformal coupling vary considerably more with time. The system begins with a greater disformal influence, and w_χ close to 0, and γ more than double that of Example B. This also shortens inflation to have only 70 e-folds compared to B's 110, but γ still drops to 1, just with a steeper descent, as can be clearly seen in Figure 4.4. The point of this is to illustrate that similar models with different couplings can produce similar qualitative behaviour but with a faster or slower rate of change in γ. While the significance of this is not particularly apparent at the background level, we will see at the perturbative level when calculating primordial power spectra in the next section why this is important.

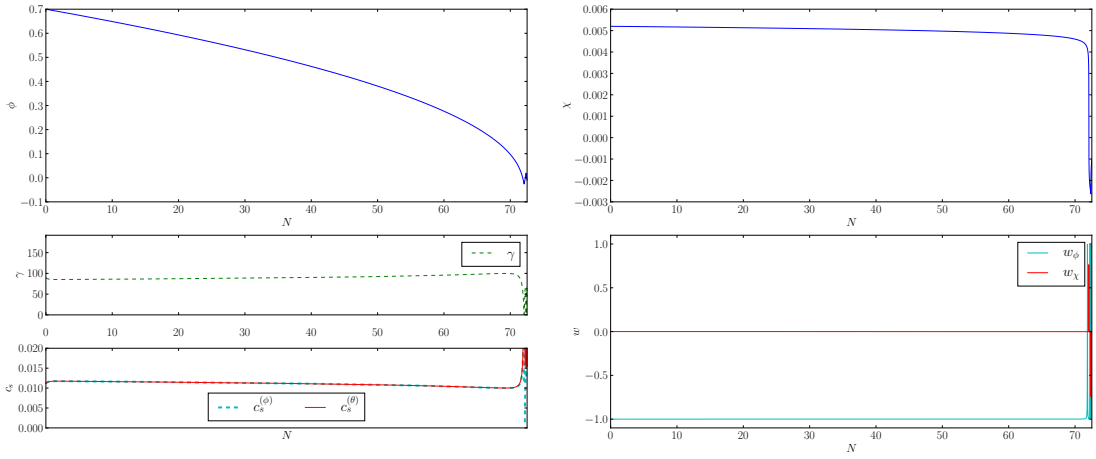

Figure 4.3.: Inflationary dynamics for the canonical model of disformally coupled inflation (4.1.2) with the potentials (4.2.30) and couplings (4.2.32).Parameters and initial conditions used are $d = 0$, $c = 0$, $D_0 = 5\times10^{21}$, $C_0 = 1$, $m_\phi = m_\chi = 1 \times 10^{-8}$, $\phi_0 = 0.7$, $\chi_0 = 0.0051$, $\dot{\phi}_0 = -1.414125 \times 10^{-11}$, $\dot{\chi}_0 = 0$.

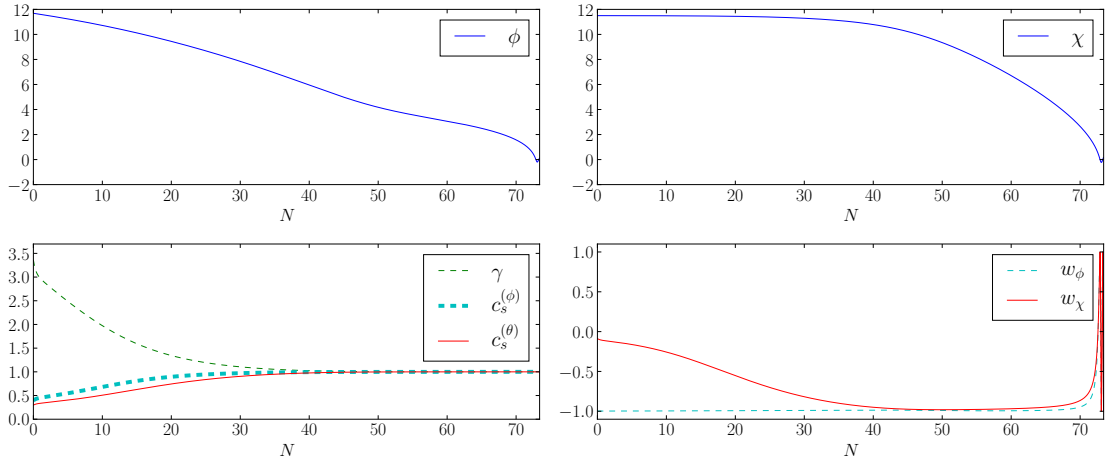

Figure 4.4.: Inflationary dynamics for the canonical model of disformally coupled inflation (4.1.2) with the potentials (4.2.30) and couplings (4.2.32).Parameters and initial conditions used are $d = 0.3$, $c = -0.3$, $D_0 = 5\times10^{9}$, $C_0 = 1$, $m_\phi = m_\chi = 1\times10^{-6}$, $\phi_0 = 11.689$, $\chi_0 = 11.0$, $\dot{\phi}_0 = -4.05\times10^{-7}$, $\dot{\chi}_0 = 0$.

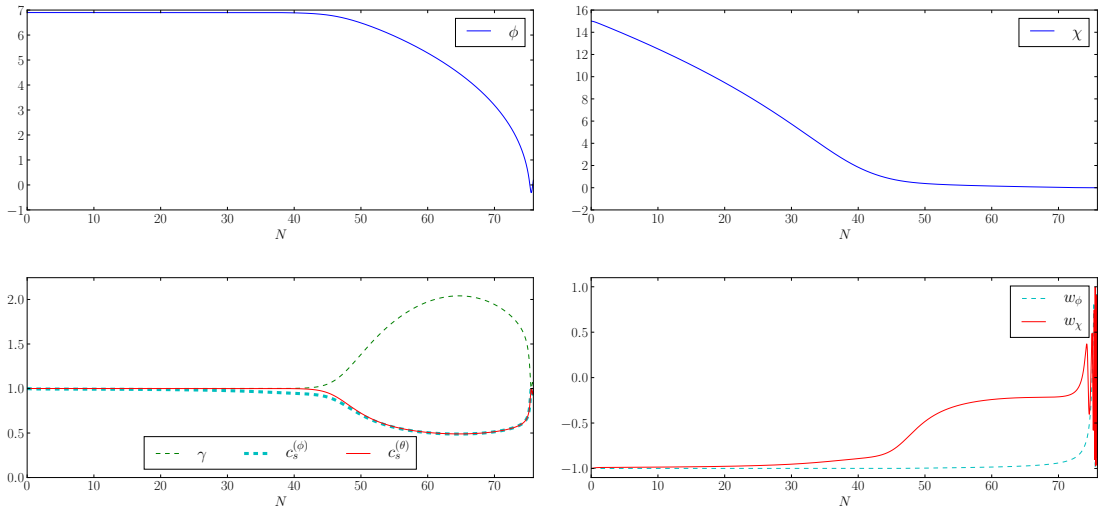

Figure 4.5.: Inflationary dynamics for the DBI model of disformally coupled inflation (4.1.3) with the potentials (4.2.30) and couplings (4.2.32). Parameters and initial conditions used are $m_\chi = 2.9 m_\phi = 2.286 \times 10^{-6}$, $C_0 = 1, D_0 = 3.8 \times 10^{12}$, $d = -c = 0.1$ and initial conditions are $\phi_0 = 6.9$, $\chi_0 = 15.0$.

Case 6: DBI Kinetic Term and Exponential Couplings, Example A

While it is possible to generate a similar range of trajectories in the DBI model as in the canonical model, the main regime in which they express a significant difference is in trajectories similar to canonical Example A of the canonical model, in which an initial increase and a subsequent decrease in γ occur. Unlike in the canonical trajectories where this largely happens at early times, in the DBI version of this trajectory, oftentimes the "bump" in γ is found to occur at the end of the inflationary phase, preceded by a phase of near-negligible disformal influence. DBI Example A, shown in Figure 4.5, realises this in such a way that during the observable window of inflation (around 50 or 60 e-folds prior to its end), γ has not yet begun its period of transient growth. The dynamics are therefore fairly conventional at early times, behaving like two co-operating inflatons, but at late times the growth in γ causes χ to behave like dust after horizon crossing.

Case 7: DBI Kinetic Term and Exponential Couplings, Example B

As in DBI Trajectory A, γ undergoes a transient growth, but this time it occurs much more gradually over a wider range of e-fold numbers. Most significantly, γ

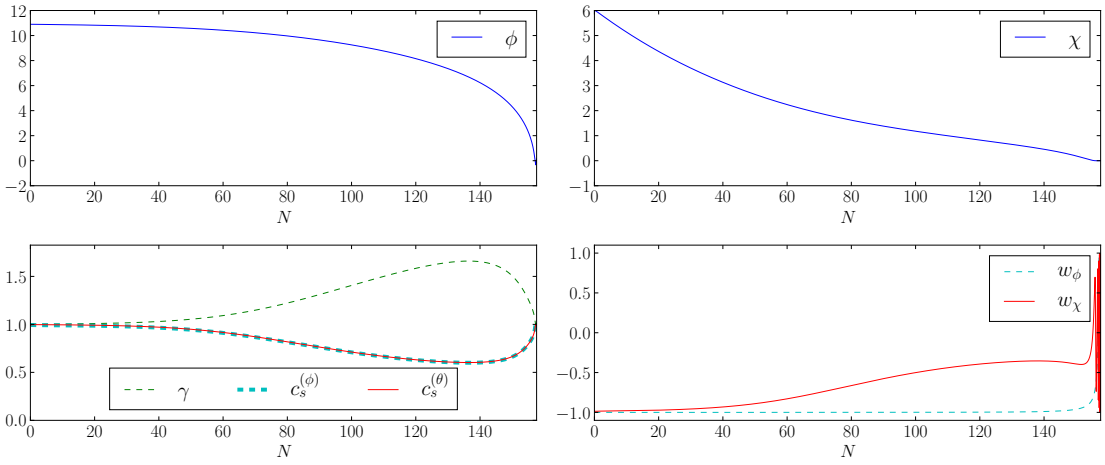

Figure 4.6.: Inflationary dynamics for the DBI model of disformally coupled inflation (4.1.3) with the potentials (4.2.30) and couplings (4.2.32). Parameters and initial conditions used are $m_\chi = 2.9 m_\phi = 2.286 \times 10^{-6}$, $C_0 = 1$,$D_0 = 3.8 \times 10^{12}$, $d = -c = 0.1$ and initial conditions are $\phi_0 = 6.9$, $\chi_0 = 15.0$.

is now changing throughout the observable window, and the dynamics are more affected by disformal effects even at early times. Unlike in Trajectory A where χ has two distinct phases of evolution, the transition between the two is now smoother, as seen in Figure 4.6.

4.3. Perturbations

The general expression in a $P(\phi^I, X^{JK})$ theory for the curvature perturbation $\mathcal{R}$ is[140]

$$\begin{aligned}\mathcal{R} &= \left(\frac{H}{2P_{<IJ>}X^{IJ}}\right) P_{<KL>}\dot{\phi}^K Q^L \\ &= \left(\frac{H}{\rho+p}\right)\left[\left(\gamma_d + \frac{D}{C}\rho_\chi\right)\dot{\phi}Q^\phi + \gamma C\dot{\chi}Q^\chi\right] \\ &= \left(\frac{H}{\rho+p}\right)\left[\left(\gamma_d - \gamma^2\frac{D}{C}p_\chi\right)\dot{\phi}Q^\phi + \gamma C\dot{\chi}Q^\theta\right] . \end{aligned} \tag{4.3.1}$$

To evaluate this and obtain a power spectrum, we hence numerically integrate the perturbed equations of motion for the Q^I.[238] The position of the observable window during inflation is determined via eq. (3.3.39) assuming efficient reheating ($\rho_{\rm th} \approx$

$\rho_{\rm end}$). The range of physical k values today taken to be observable for our purposes is $k \in [10^{-3}, 10^{1}]$ Mpc^{-1}. Similarly, we assume a pivot scale of $k_* = 0.05$ Mpc^{-1} for everything except the tensor-to-scalar ratio which is instead evaluated at $k_* = 0.002$ Mpc^{-1} according to usual conventions. Initial conditions are set using the canonical quantisation procedure discussed in Section 4.2.2, and by direct variation of the second order action (4.2.16) one obtains (Fourier transformed) equations of motion for the Sasaki-Mukhanov variables[222]

$$\alpha_1 \ddot{Q}_\phi + \alpha_2 \ddot{Q}_\chi - \alpha_3 \frac{k^2}{a^2} Q_\phi - \alpha_4 \frac{k^2}{a^2} Q_\chi + \bar{\alpha}_6 \dot{Q}_\phi + \bar{\alpha}_7 \dot{Q}_\chi + \bar{\alpha}_9 Q_\phi + \bar{\alpha}_{10} Q_\chi = 0\,, \quad (4.3.2)$$

$$\beta_1 \ddot{Q}_\phi + \beta_2 \ddot{Q}_\chi - \beta_3 \frac{k^2}{a^2} Q_\phi - \beta_4 \frac{k^2}{a^2} Q_\chi + \bar{\beta}_6 \dot{Q}_\phi + \bar{\beta}_7 \dot{Q}_\chi + \bar{\beta}_9 Q_\phi + \bar{\beta}_{10} Q_\chi = 0\,. \quad (4.3.3)$$

These are equivalent to what one would find if they began not from an action principle, but from the perturbed equations of motion for $\delta\phi^I$ using direct perturbation theory on the fields' energy momentum tensor, that is,

$$\begin{aligned} &\alpha_1 \delta\ddot{\phi} + \alpha_2 \delta\ddot{\chi} + \alpha_3 \partial_i\partial^i \delta\phi + \alpha_4 \partial_i \partial^i \delta\chi + \alpha_5 \dot{\Psi} \\ &\quad + \alpha_6 \delta\dot{\phi} + \alpha_7 \delta\dot{\chi} + \alpha_8 \Psi + \alpha_9 \delta\phi + \alpha_{10} \delta\chi = 0\,, \end{aligned} \quad (4.3.4)$$

$$\begin{aligned} &\beta_1 \delta\ddot{\phi} + \beta_2 \delta\ddot{\chi} + \beta_3 \partial_i\partial^i \delta\phi + \beta_4 \partial_i \partial^i \delta\chi + \beta_5 \dot{\Psi} \\ &\quad + \beta_6 \delta\dot{\phi} + \beta_7 \delta\dot{\chi} + \beta_8 \Psi + \beta_9 \delta\phi + \beta_{10} \delta\chi = 0\,, \end{aligned} \quad (4.3.5)$$

which are coupled to the Newtonian Gauge metric perturbation $\Psi = \Phi$ (via the off-diagonal spatial Einstein equations as in the standard case described in Section 3.3.2) and its derivative, which are determined by perturbed Einstein equations in the form

$$2\left(\partial_i\partial^i \Psi - 3H\dot{\Psi}\right) = \delta\rho = X_1 \Psi + X_2 \delta\phi + X_3 \dot{\delta\phi} + X_4 \delta\chi + X_5 \dot{\delta\chi}\,, \quad (4.3.6)$$

$$2\left(\dot{\Psi}+H\Psi\right) = -\delta q = -Y_1\delta\phi + -Y_2\delta\chi\,, \tag{4.3.7}$$

$$\begin{aligned} 2\left(\ddot{\Psi}+4H\dot{\Psi}+4\dot{H}\Psi+6H^2\Psi\right) &= \delta p \\ &= Z_1\Psi + Z_2\delta\phi + Z_3\dot{\delta\phi} + Z_4\delta\chi + Z_5\dot{\delta\chi}\,. \end{aligned} \tag{4.3.8}$$

The form of the various coefficients in these perturbation equations and their interrelations are given in appendix A.2. Note in particular that in the Sasaki-Mukhanov representation of the perturbed Klein-Gordon equations that barred coefficients such as $\bar{\alpha}_6$ are present and differ from unbarred coefficients in the $\delta\phi^I$ form of the equations. These differences arise due to the elimination of the gauge variable Ψ needed to make the Sasaki-Mukhanov form of the equations explicitly Gauge-invariant.

4.3.1. Results

Here we present power spectra calculated numerically via the above procedure for the six interesting cases (i.e. excluding the rejected stringy coupling case) studied at the background level in Section 4.2.4. For each model, the spectra are calculated at a series of k values in the observable range, then numerical fitting is used to calculate the amplitude of scalar and tensor perturbations at the pivot scale (and hence the tensor-to-scalar ratio), as well as the scalar spectral index and its runnings from this data. Each of the trajectories discussed was chosen to reflect and represent a different type of behaviour observed in numerical studies of the model, but we also chose a priori to present examples which produced an acceptable scalar amplitude, compatible with Planck 1σ bounds. While most absolute choices of parameters did not lead to a feasible scalar amplitude, by noting that $A_s \propto V$, the effective potential, it is easy to re-scale the parameters and initial conditions of a trajectory to normalise the scalar amplitude. We assume that each trajectory's spectral properties are representative of their class of trajectories with qualitatively similar dynamics, but given the size and complexity of parameter space we do not perform a detailed

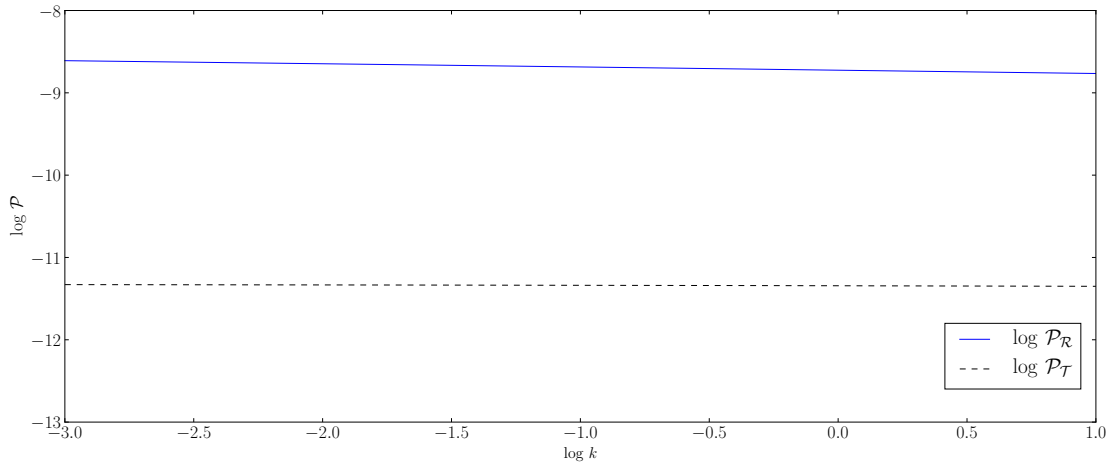

Figure 4.7.: The scalar ($\mathcal{P}_\mathcal{R}$, blue solid line) and tensor ($\mathcal{P}_\mathcal{T}$, black dashed line) power spectra for Canonical Trajectory A, discussed in Section 4.2.4 at the background level. A normalised amplitude of 2.12×10^{-9} is obtained, and the resulting spectrum has $n_s = 0.961$, $\alpha_s = -5.3 \times 10^{-4}$ and $\beta_s = 1.8 \times 10^{-4}$. The tensor-to-scalar ratio is found to be 1.7×10^{-2}.

statistical analysis of this.[222] Instead, we aim with this work to simply categorise the interesting types of behaviour and make an initial exploration of the spectral properties possible within this theory.

Canonical Trajectory A

This trajectory represents disformal effects driven by a large value of the disformal exponent d. Initially, ϕ rolls down its potential, causing $\dot{\phi}$ to increase quickly enough to boost the value of γ, but as ϕ decreases from this, the steep exponential in γ kicks in and causes it to decrease again. The early-time boosting of γ causes sound speeds to depart from unity and hence amplifies the scalar spectrum ($A_s \propto c_s^{-1}$). Resultingly, the tensor-to-scalar ratio is suppressed compared to the simplest models of inflation, with a calculated value of $r = 1.7 \times 10^{-2}$, well within present experimental bounds. Similarly, a feasible spectral index of $n_s = 0.961$ and typically small runnings of $O(10^{-4})$ are found. The power spectra are explicitly shown in Figure 4.7.

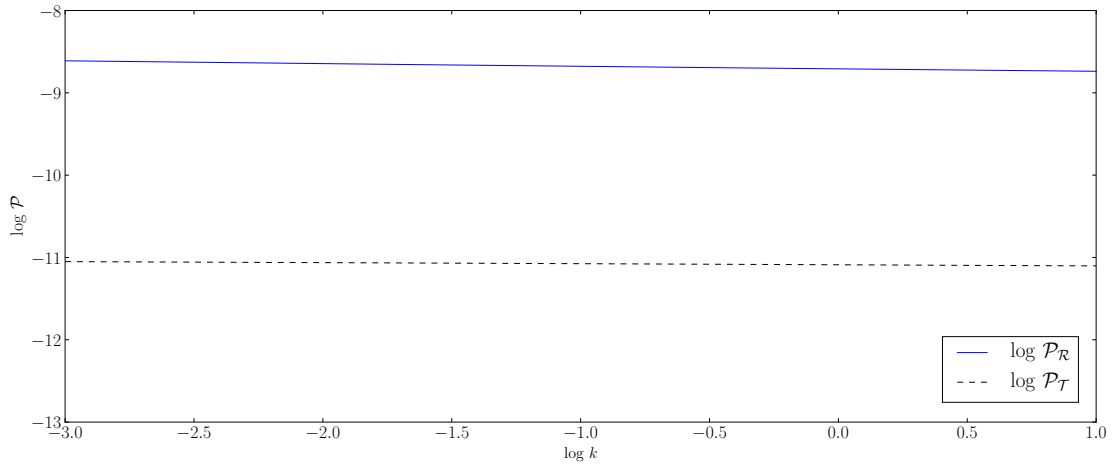

Figure 4.8.: The scalar ($\mathcal{P}_\mathcal{R}$, blue solid line) and tensor ($\mathcal{P}_\mathcal{T}$, black dashed line) power spectra for Canonical Trajectory B, discussed in Section 4.2.4 at the background level. A normalised amplitude of 2.15×10^{-9} is obtained, and the resulting spectrum has $n_s = 0.968$, $\alpha_s = 7.1 \times 10^{-4}$ and $\beta_s = -2.1 \times 10^{-5}$. The tensor-to-scalar ratio is found to be 1.7×10^{-2}.

Canonical Trajectory B

Here, instead of a large exponent in the disformal coupling, a large prefactor D_0 provides the disformality that affects the dynamics. Instead of a "bump" in γ we observe typically a smooth monotonic decrease from an initially large value. While this likely leads to some small differences with the previous case, the overall effect of the spectrum is comparable, with low sound speeds amplifying scalar perturbations and producing a small tensor-to-scalar ratio of $r = 3.1 \times 10^{-2}$, as well as $n_s = 0.968$ and, again, $O(10^{-4})$ runnings. The power spectra are explicitly shown in Figure 4.8.

Canonical Trajectory C

In a significant departure from the previous examples, Canonical Trajectory C has small initial conditions but an immensely large γ. This example of extreme disformal inflation somewhat surprisingly still can produce feasible spectra, with $n_s = 0.967$, and runnings of $O(10^{-3})$. As one would qualitatively expect, the extremely large γ (extremely small sound speeds) manifest through an incredibly small tensor-to-scalar ratio of $r = 1.2 \times 10^{-9}$, which is likely undetectably small. The spectra are shown in Figure 4.9.

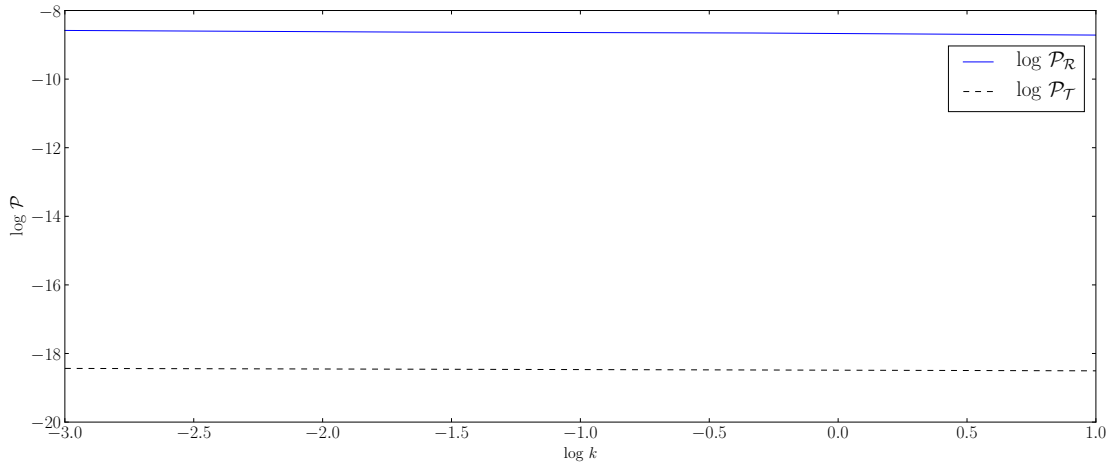

Figure 4.9.: The scalar ($\mathcal{P}_\mathcal{R}$, blue solid line) and tensor ($\mathcal{P}_\mathcal{T}$, black dashed line) power spectra for Canonical Trajectory C, discussed in Section 4.2.4 at the background level. A normalised amplitude of 2.15×10^{-9} is obtained, and the resulting spectrum has $n_s = 0.967$, $\alpha_s = 1.2 \times 10^{-3}$ and $\beta_s = -1.1 \times 10^{-3}$. The tensor-to-scalar ratio is found to be 1.2×10^{-9}.

Canonical Trajectory D

As discussed in the background results Section, Trajectory D is much like Trajectory B but with a steeper exponential coupling. This combination of a large disformal prefactor and exponential multiplier leads to steep and rapid variation in γ and sound speeds. At the level of the power spectrum, this unsurprisingly yields a yet-smaller tensor-to-scalar ratio due to the larger initial γ, but as can be seen clearly in the plot of the spectra in Figure 4.10, the scalar spectrum does not even look qualitatively scale-invariant compared to the previous examples. This is clearly explained when one considers that the dependence of the power spectrum on the sound speeds implies that the spectral index and runnings depend on derivatives of the c_s^I values. The presence of faster variation in γ, and hence the sound speeds, manifests as a large deviation from scale invariance with runnings now $O(10^{-2})$ or larger, violating the Planck bounds.[2]

[2]In Chapter 6 we will argue that these bounds on runnings are not necessarily valid, but even with the relaxations on this constraint discussed there, this trajectory is still difficult to reconcile with data

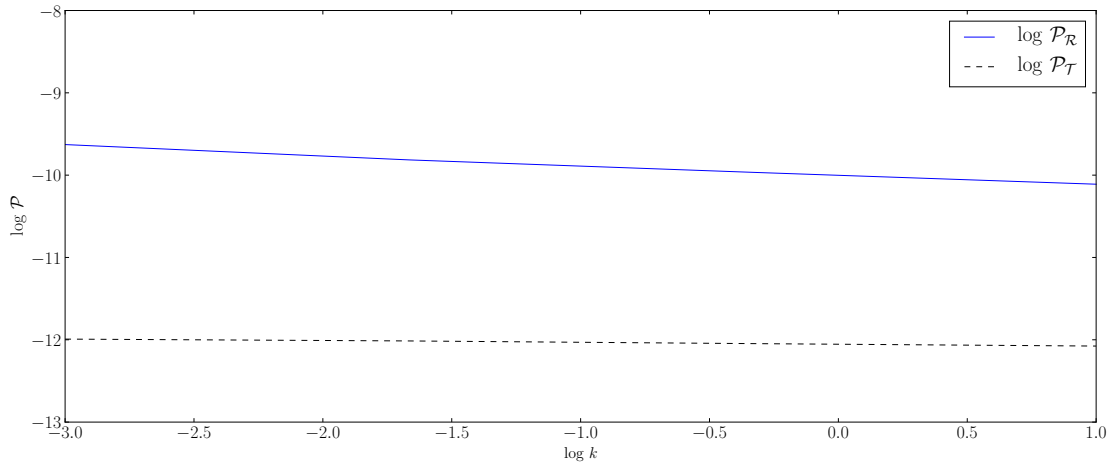

Figure 4.10.: The scalar ($\mathcal{P}_\mathcal{R}$, blue solid line) and tensor ($\mathcal{P}_\mathcal{T}$, black dashed line) power spectra for Canonical Trajectory D, discussed in Section 4.2.4 at the background level. The rather pronounced scale dependence in the scalar spectrum is qualitatively visible, and corresponds to running parameters α_s and β_s with magnitudes of around 10^{-2}, which exceeds the Planck bounds. The spectrum has not been normalised, owing to its inability to fulfil the constraints regardless.

DBI Trajectory A

As discussed previously, the main differences in the DBI model occur in "bump" scenarios like Canonical Trajectory A, where now the bump occurs at later times. In DBI Trajectory A, whose spectra are shown in Figure 4.11, the bump only begins after horizon crossing has occurred, so all the interesting dynamics are affecting the power spectrum via the late time entropy-adiabatic transfer. This produces a perhaps slightly surprisingly low tensor-to-scalar-ratio of $r = 7.2 \times 10^{-3}$, but this may be more due to coincidence from the choice of parameters and the complex superhorizon dynamics, rather than a generic effect. Beyond this, the spectrum has a respectable $n_s = 0.965$ and the usual runnings of $O(10^{-3})$.

DBI Trajectory B

The key difference between DBI Trajectories A and B is that in B (Figure 4.12), the growth in γ now begins on subhorizon scales, thus boosting the effects of horizon-crossing features on the spectrum, rather than in A where more convoluted superhorizon effects are the main source of disformality. Here, a clear point of under-

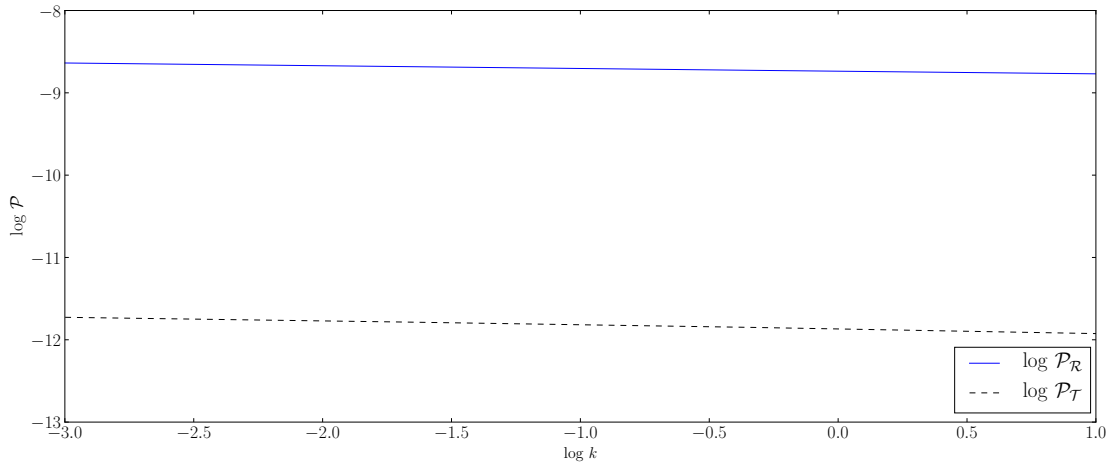

Figure 4.11.: The scalar ($\mathcal{P}_\mathcal{R}$, blue solid line) and tensor ($\mathcal{P}_\mathcal{T}$, black dashed line) power spectra for DBI Trajectory A, discussed in Section 4.2.4 at the background level. A normalised amplitude of 2.14×10^{-9} is obtained, and the resulting spectrum has $n_s = 0.965$, $\alpha_s = 2.4 \times 10^{-4}$ and $\beta_s = 2.1 \times 10^{-4}$. The tensor-to-scalar ratio is found to be 7.2×10^{-3}.

standing is that the suppressed sound speeds during horizon crossing mean that the amplitude is enhanced and a smaller tensor-to-scalar ratio of $r = 2.0 \times 10^{-3}$ is obtained. However, it seems the greater variation in disformal coupling effects in combination with the superhorizon effects also drives the spectral index and runnings farther from the typical values with $n_s = 0.973$ actually yielding a flatter spectrum at the linear deviation, but a higher second order deviation of $\alpha_s = -5.9 \times 10^{-3}$. β_s is then small again at -6.4×10^{-4}, curiously.

Effect of the size of disformal effects on the power spectrum

While the qualitative different types of behaviour possible in the context of this model are outlined in the previous Sections, it is also instructive to consider a series of similar trajectories with slightly differing parameters. For concreteness, we hence take Canonical Trajectory B as an example and in Figure 4.13 present spectra for several different values of D_0 in addition to the default one. We observe that as D decreases, the spectral index becomes steeper, the tensor-to-scalar ratio increases, and the scalar amplitude decreases, which is largely typical of the parameters that were numerically studied. This shows that for this model, the size of the disformal

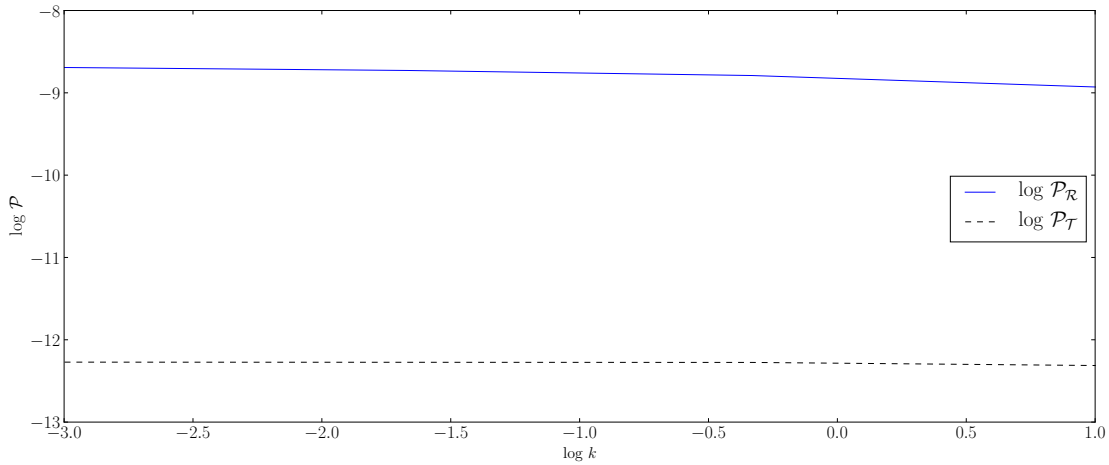

Figure 4.12.: The scalar ($\mathcal{P}_\mathcal{R}$, blue solid line) and tensor ($\mathcal{P}_\mathcal{T}$, black dashed line) power spectra for DBI Trajectory B, discussed in Section 4.2.4 at the background level. A normalised amplitude of 2.14×10^{-9} is obtained, and the resulting spectrum has $n_s = 0.973$, $\alpha_s = -5.9 \times 10^{-3}$ and $\beta_s = -6.4 \times 10^{-4}$. The tensor-to-scalar ratio is found to be 2.0×10^{-3}.

coupling is critical; were it much smaller we would be quickly departing the Planck 1σ bounds in n_s and r. These are very much "disformally driven" trajectories in that the choices of initial conditions and masses alone would not drive successful inflation with feasible spectra, and sufficiently large D is needed to correct this. The tensor spectra are affected somewhat less, as one might expect, though the deviation of the tensor spectra in the plot at large k show that the tensor tilt is being affected by a small amount.

Towards the epoch of reheating with disformal couplings

In all the trajectories considered here, it can be seen that as inflation ends, γ reduces towards 1 which would suggest post-inflationary concerns like reheating are still feasibly achievable in their usual form. However, as reheating usually involves oscillating fields, this implies that γ will still cyclically change during reheating, and may deform the typical behaviour of the field and hence the decay product densities from this process. However, it would be difficult to see exactly how this may manifest - consider in terms of the initial action the following modification, introducing bosonic decay products ψ and σ for each field, respectively

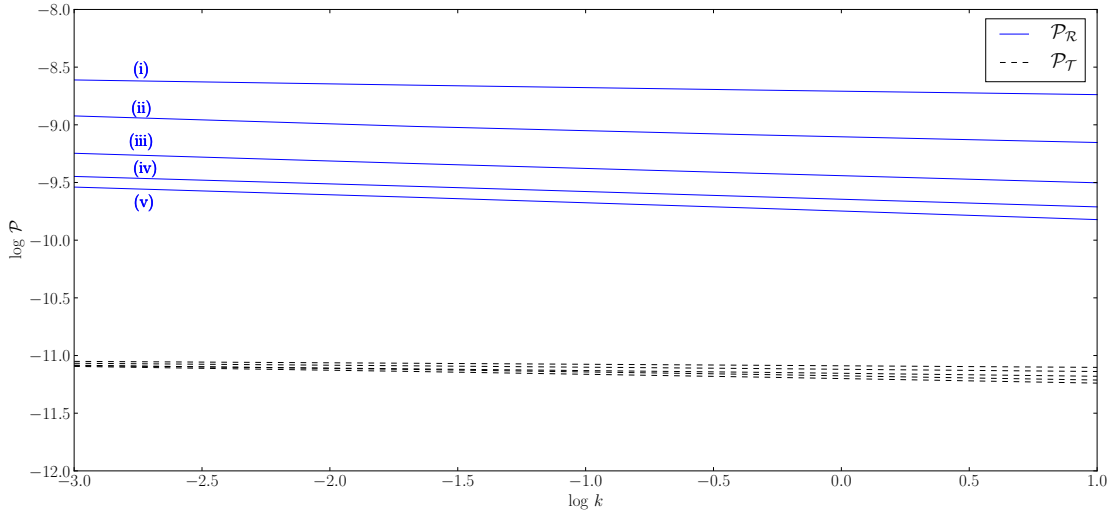

Figure 4.13.: Power spectra for Canonical Trajectory B with different choices for the parameter D_0. The blue curves show the scalar power spectra, the black (dashed) lines show the resulting tensor power spectra. The values of D_0 for the lines labelled (i-v) are (i) $D_0 = 8 \times 10^9$, (ii) $D_0 = 4 \times 10^9$, (iii) $D_0 = 2 \times 10^9$, (iv) $D_0 = 1 \times 10^9$ and (v) $D_0 = 0.5 \times 10^9$. The spectral indices for these choices of parameter are 0.9677, 0.9435, 0.9385, 0.9346 and 0.9306, respectively. The tensor-to-scalar ratio varies from 0.03 for $D_0 = 8 \times 10^9$ to 0.25 for $D_0 = 0.5 \times 10^9$.

$$S = \frac{1}{2}\int \mathrm{d}^4x\sqrt{-g}\; R - \int \mathrm{d}^4x\sqrt{-g}\left[\frac{1}{2}g^{\mu\nu}\phi_{,\mu}\phi_{,\nu} + U(\phi) + g_\phi^2\phi^2\psi^2\right] - \int \mathrm{d}^4x\sqrt{-\hat{g}}\left[\frac{1}{2}\hat{g}^{\mu\nu}\chi_{,\mu}\chi_{,\nu} + V(\chi) + g_\chi^2\chi^2\sigma^2\right]. \tag{4.3.9}$$

Each field can then decay into particles on its own metric ($\phi\phi \to \psi\psi$ and $\chi\chi \to \sigma\sigma$). This makes sense when considered in the brane-motivated case particularly. When transformed to the Einstein Frame as in eq. (4.1.3), one would obtain an additional decay term in the action

$$S \supset -\int \mathrm{d}^4x\sqrt{-g}\left[g_\phi^2\phi^2\psi^2 + \frac{C^2}{\gamma}g_\chi^2\chi^2\sigma^2\right] = -\int \mathrm{d}^4x\sqrt{-g}\left[g_\phi^2\phi^2\psi^2 + g_{\chi,\mathrm{EF}}^2\chi^2\sigma^2\right], \tag{4.3.10}$$

such that the effective coupling, between χ and its decay products σ, in the Einstein Frame $g_{\chi,\mathrm{EF}}^2 = C^2 g_\chi^2/\gamma$ depends on ϕ, reminiscent of modulated reheating.[239–247]

This would be tricky in itself, but the effective coupling also depends (via γ) on $\partial_\mu\phi$. Even normal modulated reheating significantly alters the details of reheating in a complex way,[248] so we expect the same to be true in our case, qualitatively speaking.

The reheating process will likely also vary considerably from trajectory to trajectory in our model. For example, even if the bare coupling constants in the bimetric action, g_ϕ and g_χ, are of similar magnitude initially, they will not remain this way once the field rolls significantly and disformality kicks in. Take Canonical Trajectory C, for example, where even a very slowly rolling field will easy generate large γ and thus heavily change the value of the $\chi \to \sigma$ decay constant.

An investigation into the dynamics of reheating, and hence its efficiency or average equation of state, in these models, would hence be interesting. Some limited work has been since done by other authors on this topic,[249] in which it was found to be feasible/promising that parametric resonance could occur even in extreme situations like Canonical Trajectory C.

A note on the stability of trajectories

One can also question how stable the model is under variation in the position of the observable window. (e.g. how many e-folds before the end of inflation do observable modes cross the horizon?) Variations like this could arise[223] due to inefficiencies in the post-inflationary reheating procedure (which, as we argue in the previous section, is not well understood and could hence have non-trivial behaviour). To address this, we plot in Figure 4.14 the spectral index and tensor-to-scalar ratio for the two DBI trajectories (as these prove most interesting for discussion's sake) under two different assumptions. First, our default assumption of efficient reheating with $\rho_{\rm th} = \rho_{\rm end}$, and secondly with $\rho_{\rm th} \ll \rho_{\rm end}$ (inefficient reheating). This affects the e-folding number of horizon-crossing via

$$\Delta N = \frac{1-3w}{12(1+w)} \ln\left(\frac{\rho_{\rm th}}{\rho_{\rm end}}\right) , \tag{4.3.11}$$

where we take an average equation of state during reheating of $w = 0$ for argu-

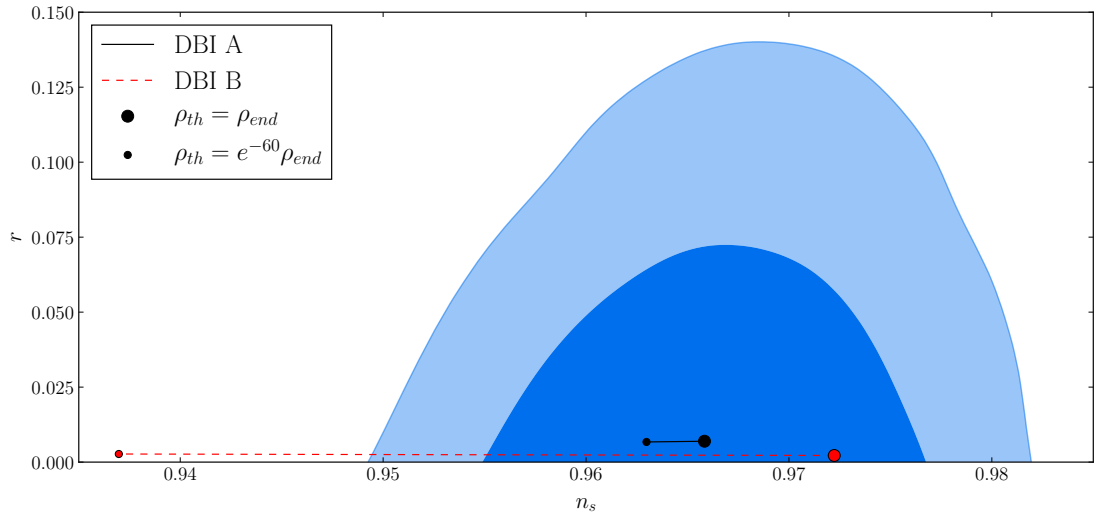

Figure 4.14.: Variation in the spectral index n_s and tensor-to-scalar ratio r as a function of reheating energy for DBI Trajectories A and B, overlaid on the Planck likelihood contours at 1σ and 2σ for these quantities. We see that Trajectory A is largely stable under such considerations and falls comfortably within the 1σ contour regardless of the efficiency of reheating, while Trajectory B is considerably more susceptible to being possibly ruled out subject to the size of this unknown parameter.

ment's sake. For the parameters considered this amounts to a different of 5 e-folds, parametrising essentially our ignorance in how reheating post-processes the location of the observable window.

One can see in Figure 4.14 that while DBI Trajectory A undergoes very little variation under a shift in the observable window, DBI Trajectory B undergoes a much more significant decrease to as low as $n_s \approx 0.94$, which from the overlaid Planck likelihood contours, we can see is comfortably (or perhaps uncomfortably) outside of the 2σ bounds. While in both cases the tensor-to-scalar ratio remains trivially unaffected, this large disparity in the behaviour of n_s in the two examples reveals that the stability of any prediction in this model is itself parameter-dependent and it is difficult to hence address this question fully without a more comprehensive analysis of the large available parameter space. This particular example is most likely due to the fact that in Trajectory A, γ is near-constant and ≈ 1 for a good while before and during horizon-crossing, a small shift in its location has no drastic effects. Meanwhile, as Trajectory B is constructed to allow a moderate change in γ across

the N values in which observable scales are leaving the horizon, its steeper variation over this interval means that a small shift in its location will have a pronounced change in the γ and hence c_s values determining the power spectra.

4.4. Non-Gaussianity

In contrast to the previous section, in which we numerically solved the first order perturbation equations for disformally coupled inflation and used this to determine the power spectra exactly, we will instead use approximate analytic methods in the following analysis of the bispectrum produced by the model. This is primarily due to the fact that to compute the non-Gaussianity/bispectrum, one needs to go to second order in perturbation theory, rendering the unapproximated equations of motion even more intractable and tedious to work with than the already rather extensive first order equations (4.3.2 – 4.3.8).

Instead, we work directly with the third order action from which one can derive the second order equations of motion. The derivation of even this is rather lengthy in $P(\phi^I, X^{JK})$ theories, but has been done.[212,233] We will only concern ourselves with a subset of this action for which it has been argued the dominant contributions to non-Gaussianity arise (that is, in an expansion of slow-roll and sound speed parameters, they produce the leading order terms). In terms of Q^ϕ and Q^χ, the terms we would in this sense be interested in, it turns out, would be[223]

$$\mathcal{L}_3 \supset a^3 g_{IJK}\dot{Q}^I\dot{Q}^J\dot{Q}^K + a h_{IJK}\dot{Q}^I\partial_i Q^J\partial^i Q^K \,. \tag{4.4.1}$$

with

$$g_{IJK} = \frac{1}{2}P_{<JK><AI>}\dot{\phi}^A + \frac{1}{6}P_{<AI><BJ><CK>}\dot{\phi}^A\dot{\phi}^B\dot{\phi}^C \,, \tag{4.4.2}$$

$$h_{IJK} = -\frac{1}{2}P_{<JK><AI>}\dot{\phi}^A \,. \tag{4.4.3}$$

We refer to the first term, which itself consists of eight permutations of ϕ and χ perturbations, as the kinetic vertices, and the second term's eight contributions as

the gradient vertices to distinguish them in future discussion.

Once again, to properly quantise this system according to the discussion of Section 4.2.2, we want to rewrite this in terms of the (ϕ, θ) basis we defined previously. To this effect, we perform the appropriate field redefinition $Q^I = e^I_{I'} Q^{I'}$ using the form of the e matrix given in Section 4.2.3 to obtain a new third order action in terms of the canonical variables:

$$\mathcal{L}_3 \supset a^3 g_{I'J'K'} \dot{Q}^{I'} \dot{Q}^{J'} \dot{Q}^{K'} + a h_{I'J'K'} \dot{Q}^{I'} \partial_i Q^{J'} \partial^i Q^{K'} \,, \tag{4.4.4}$$

where primed indices take values from (ϕ, θ) instead of (ϕ, χ) as usual, and we have neglected new terms depending on the derivatives of e as these would contribute at the next order in slow-roll, comparable to terms we have implicitly neglected already. The coefficients in this new action take the form

$$f_{I'J'K'} = e^I_{I'} e^J_{J'} e^K_{K'} f_{IJK} \,, \quad (f = g, h) \,. \tag{4.4.5}$$

By direct inspection of the expressions for the coefficients in the third order action, and noting that $\forall\ (A, B, C)$, $P_{<\chi\chi><A\chi>} = P_{<A\chi><B\chi><C\chi>} = 0$ as the Lagrangian contains terms of $O((X^{\phi\chi})^2)$ and $O(X^{\chi\chi})$ but no higher orders, we can immediately say that $g_{\theta\theta\theta} = g_{\chi\chi\chi} = 0$ and $h_{\theta\theta\theta} = h_{\chi\chi\chi} = 0$. This means that no non-Gaussianity is generated at this order purely due to the field on the disformal metric (i.e. $\langle Q^\theta(\mathbf{k}_1) Q^\theta(\mathbf{k}_2) Q^\theta(\mathbf{k}_3) \rangle \approx 0$), which is not unexpected as it is a canonical field whose only abnormal feature is living on a metric which is dependent on (derivatives of) ϕ. The non-zero terms at this order instead come from terms mixing ϕ and χ due to their interactions (e.g. the motion of ϕ distorting the metric that the otherwise canonical field χ feels), or purely from ϕ (which is non-standard in its kinetic structure due to the presence of γ in the equation of motion).

4.4.1. Relating non-Gaussianity of fields to non-Gaussianity of curvature

We can use the third order action in terms of Q^ϕ and Q^θ above to calculate three point correlation functions of these Sasaki-Mukhanov variables. We can then relate the three point correlation functions of the fields to that of the curvature perturbation $\mathcal{R}$ using

$$\begin{aligned}\langle \mathcal{R}(\mathbf{k}_1)\mathcal{R}(\mathbf{k}_2)\mathcal{R}(\mathbf{k}_3)\rangle = F_\phi^3 \langle Q^\phi(\mathbf{k}_1)Q^\phi(\mathbf{k}_2)Q^\phi(\mathbf{k}_3)\rangle + F_\phi^2 F_\theta \langle (Q^\phi)^2 Q^\theta\rangle \\ + F_\phi F_\theta^2 \langle Q^\phi (Q^\theta)^2\rangle + F_\theta^3 \langle Q^\theta(\mathbf{k}_1)Q^\theta(\mathbf{k}_2)Q^\theta(\mathbf{k}_3)\rangle \,, \end{aligned} \tag{4.4.6}$$

where for convenience we have used the shorthands:

$$\langle (Q^\phi)^2 Q^\theta\rangle = \langle Q^\phi(\mathbf{k}_1)Q^\phi(\mathbf{k}_2)Q^\theta(\mathbf{k}_3)\rangle + \text{perms.}\,, \tag{4.4.7}$$

$$\langle Q^\phi (Q^\theta)^2\rangle = \langle Q^\phi(\mathbf{k}_1)Q^\theta(\mathbf{k}_2)Q^\theta(\mathbf{k}_3)\rangle + \text{perms.}\,, \tag{4.4.8}$$

where '+perms.' indicates the inclusion of similar terms with all distinct permutations of the momenta $\mathbf{k}_n$.

In this expression F_ϕ and F_θ are, loosely speaking, the coefficients of Q^ϕ and Q^θ in the expression in eq. (4.3.1) relating $\mathcal{R}$ to these Sasaki-Mukhanov variables. More concretely, however, we really want to work with a modified version of this expression which instead of expressing the curvature and field perturbations in terms of each other at equal times, expresses the *final* curvature perturbation in terms of field perturbations at horizon crossing where their behaviour is well understood analytically from solutions of the first order perturbation equations (see e.g. eq. (3.3.20) and surrounding discussion). This involves making use of the transfer function formalism (Section 3.3.8) to parametrise the superhorizon evolution of the curvature perturbation in terms of the transfer function $\mathcal{T}_{\mathcal{RS}}$. We find, applying this, that the derived coefficients we want are given by

$$F_\phi = \frac{H}{P_{<IJ>}\dot{\phi}^I\dot{\phi}^J}\left[\left(\gamma_d - \gamma^2\frac{D}{C}p_\chi\right)\dot{\phi} + A\mathcal{T}_{\mathcal{RS}}\dot{\theta}\right], \tag{4.4.9}$$

$$F_\theta = \frac{H}{P_{<IJ>}\dot{\phi}^I\dot{\phi}^J}\left[\frac{C}{\gamma}\dot{\theta} - A\mathcal{T}_{\mathcal{RS}}\dot{\phi}\right], \tag{4.4.10}$$

where A is given by[223]

$$A = \frac{\gamma\left(\gamma_d - \gamma^2\frac{D}{C}p_\chi\right)\dot{\phi}\sqrt{c_s^{(\theta)}} + C\dot{\theta}\sqrt{c_s^{(\phi)}}}{\gamma\dot{\theta}\sqrt{c_s^{(\theta)}} - \gamma\dot{\phi}\sqrt{c_s^{(\phi)}}}. \tag{4.4.11}$$

These derived coefficients are the ones appearing in the equal-time expression (4.3.1) plus additional terms to handle the evolution $\mathcal{R}$ from horizon crossing to the end of inflation. All of the quantities in these expressions are the horizon-crossing values derived from background quantities at the time when $k = aH$, except for the transfer function $\mathcal{T}_{\mathcal{RS}}$ which encodes the superhorizon evolution. This can be obtained from our first order numerical simulations, as it is related to the ratio of the power spectrum at the end of inflation and horizon crossing.

With these tools now in place to derive the appropriate non-Gaussianity in curvature from the relevant field perturbations, we now turn our attention to the computation of the three point functions of the fields.

4.4.2. Three point functions of the fields

Using the standard In-In formalism approach (3.3.61) and our third order Lagrangian (4.4.4), we can proceed to compute the contributions to the bispectrum by computing a series of time integrals up until the end of inflation. As hinted above, at this level of approximation we can treat g and h coefficients in the action as constant, as their derivatives will be next order in slow-roll. We will work in conformal time $\mathrm{d}t = a\,\mathrm{d}\eta$ where the appropriate integration limits at this order are $[-\infty, 0]$. We will compute the contributions to the three point functions from the kinetic and gradient vertices separately and then sum them at the end.

Additionally, to make numerical predictions, we need to choose a particular shape of non-Gaussianity. For simplicity, we will be taking the equilateral configuration of non-Gaussianity ($k_1 = k_2 = k_3$) which has the constraint $f_{NL} = -4 \pm 43$. For other configurations, effects such as modes crossing the horizon at different times[216] can complicate matters, and our goal here is not to investigate the effect of this more general phenomenon, but instead how the parameters of disformally coupled inflation influence the bispectrum. It is emphasised that this choice is not an implication that the equilateral non-Gaussianity is the most significant or interesting for our model, but instead just a minimal choice intended to disentangle our results from some of the finer idiosyncrasies of non-Gaussianity which are not particular to our models. To maintain some generality we will present first the results without specifying a shape, but subsequently obtain the reduced expressions in the equilateral case for later use.[223]

Kinetic Vertices

For convenience in calculating contributions term by term, we rewrite the kinetic part of the third-order action (4.4.4), using the fact that $g_{\theta\theta\theta} = 0$ as we previously found, as

$$\mathcal{L}_3 \supset a^3 g_{\phi\phi\phi}(\dot{Q}^\phi)^3 + a^3(g_{\phi\phi\theta} + g_{\phi\theta\phi} + g_{\theta\phi\phi})(\dot{Q}^\phi)^2\dot{Q}^\theta + a^3(g_{\phi\theta\theta} + g_{\theta\phi\theta} + g_{\theta\theta\phi})\dot{Q}^\phi(\dot{Q}^\theta)^2 \,. \tag{4.4.12}$$

Doing the integral in eq. (3.3.61) term by term, then, and beginning with the vertex $a^3 g_{\phi\phi\phi}(\dot{Q}^\phi)^3$, we obtain a contribution to $\langle Q^\phi(\mathbf{k}_1)Q^\phi(\mathbf{k}_2)Q^\phi(\mathbf{k}_3)\rangle$,

$$\langle Q^\phi(\mathbf{k}_1)Q^\phi(\mathbf{k}_2)Q^\phi(\mathbf{k}_3)\rangle \supset (2\pi)^3\delta(\mathbf{k}_1 + \mathbf{k}_2 + \mathbf{k}_3) 3 g_{\phi\phi\phi} H^5 \frac{1}{\prod k_i^3}\frac{k_1^2 k_2^2 k_3^2}{K^3} \,. \tag{4.4.13}$$

With $a^3(g_{\phi\phi\theta} + g_{\phi\theta\phi} + g_{\theta\phi\phi})(\dot{Q}^\phi)^2\dot{Q}^\theta$, we find

$$\langle (Q^\phi)^2 Q^\theta \rangle \supset (2\pi)^3 \delta \left(\sum \mathbf{k} \right) (g_{\phi\phi\theta} + g_{\phi\theta\phi} + g_{\theta\phi\phi}) H^5 \frac{k_1^2 k_2^2 k_3^2 (c_s^\phi)^2 c_s^\theta}{\prod k_i^3} \times \left[\frac{1}{(\kappa^{\phi\phi\theta})^3} + \frac{1}{(\kappa^{\phi\theta\phi})^3} + \frac{1}{(\kappa^{\theta\phi\phi})^3} \right], \tag{4.4.14}$$

and finally, for $a^3(g_{\phi\theta\theta} + g_{\theta\phi\theta} + g_{\theta\theta\phi})\dot{Q}^\phi(\dot{Q}^\theta)^2$, the result is

$$\langle Q^\phi (Q^\theta)^2 \rangle \supset (2\pi)^3 \delta \left(\sum \mathbf{k} \right) (g_{\phi\theta\theta} + g_{\theta\phi\theta} + g_{\theta\theta\phi}) H^5 \frac{k_1^2 k_2^2 k_3^2 (c_s^\theta)^2 c_s^\phi}{\prod k_i^3} \times \left[\frac{1}{(\kappa^{\phi\theta\theta})^3} + \frac{1}{(\kappa^{\theta\phi\theta})^3} + \frac{1}{(\kappa^{\theta\theta\phi})^3} \right]. \tag{4.4.15}$$

We have used the shorthands $K = k_1 + k_2 + k_3$ and $\kappa^{IJK} = c_s^I k_1 + c_s^J k_2 + c_s^K k_3$ in these expressions.

Kinetic Vertices: Equilateral configuration Specialising to the equilateral configuration where $\kappa^{IJK} = k\left(c_s^I + c_s^J + c_s^K\right)$ and $K = 3k$, the three expressions above reduce to

$$\langle Q^\phi(\mathbf{k}_1) Q^\phi(\mathbf{k}_2) Q^\phi(\mathbf{k}_3) \rangle \supset (2\pi)^3 \delta \left(\sum \mathbf{k} \right) \frac{1}{9} g_{\phi\phi\phi} \frac{H^5}{k^6}, \tag{4.4.16}$$

$$\langle (Q^\phi)^2 Q^\theta \rangle \supset (2\pi)^3 \delta \left(\sum \mathbf{k} \right) 3(g_{\phi\phi\theta} + g_{\phi\theta\phi} + g_{\theta\phi\phi}) \frac{H^5}{k^6} \left(\frac{(c_s^\phi)^2 c_s^\theta}{(2c_s^\phi + c_s^\theta)^3} \right), \tag{4.4.17}$$

and

$$\langle Q^\phi (Q^\theta)^2 \rangle \supset (2\pi)^3 \delta \left(\sum \mathbf{k} \right) 3(g_{\phi\theta\theta} + g_{\theta\phi\theta} + g_{\theta\theta\phi}) \frac{H^5}{k^6} \left(\frac{(c_s^\theta)^2 c_s^\phi}{(2c_s^\theta + c_s^\phi)^3} \right). \tag{4.4.18}$$

Gradient Vertices

Again, decomposing the action into individual vertices for convenience, we have

$$\mathcal{L}_3 \supset a h_{\phi\phi\phi}\dot{Q}^\phi(\partial Q^\phi)^2 + a(h_{\phi\phi\theta}+h_{\phi\theta\phi})\dot{Q}^\phi\partial_i Q^\phi\partial^i Q^\theta + a h_{\theta\phi\phi}\dot{Q}^\theta(\partial Q^\phi)^2 + a(h_{\theta\phi\theta}+h_{\theta\theta\phi})\dot{Q}^\theta\partial_i Q^\phi\partial^i Q^\theta + a h_{\phi\theta\theta}\dot{Q}^\phi(\partial Q^\theta)^2 \,. \tag{4.4.19}$$

Once again, we methodically go through each term and compute the necessary integral. For the vertex $a h_{\phi\phi\phi}\dot{Q}^\phi(\partial Q^\phi)^2$ there is a contribution given by,

$$\langle Q^\phi(\mathbf{k}_1)Q^\phi(\mathbf{k}_2)Q^\phi(\mathbf{k}_3)\rangle \supset (2\pi)^3\delta\left(\sum \mathbf{k}\right)\frac{h_{\phi\phi\phi}H^5}{2(c_s^\phi)^2}\frac{1}{\prod k_i^3}\frac{1}{K^3} \times \left[k_1^2(\mathbf{k_2}\cdot\mathbf{k_3})F_1 + k_2^2(\mathbf{k_3}\cdot\mathbf{k_1})F_2 + k_3^2(\mathbf{k_1}\cdot\mathbf{k_2})F_3\right], \tag{4.4.20}$$

while for $a h_{\phi\theta\theta}\dot{Q}^\phi(\partial Q^\theta)^2$, one finds

$$\langle Q^\phi(Q^\theta)^2\rangle \supset (2\pi)^3\delta\left(\sum \mathbf{k}\right)\frac{h_{\phi\theta\theta}H^5}{2}\frac{1}{\prod k_i^3}\frac{c_s^\phi}{(c_s^\theta)^2} \times \left[k_1^2(\mathbf{k_2}\cdot\mathbf{k_3})\frac{F_1^{\phi\theta\theta}}{(\kappa^{\phi\theta\theta})^3} + k_2^2(\mathbf{k_3}\cdot\mathbf{k_1})\frac{F_2^{\theta\phi\theta}}{(\kappa^{\theta\phi\theta})^3} + k_3^2(\mathbf{k_1}\cdot\mathbf{k_2})\frac{F_3^{\theta\theta\phi}}{(\kappa^{\theta\theta\phi})^3}\right]. \tag{4.4.21}$$

Similarly, for $a h_{\theta\phi\phi}\dot{Q}^\theta(\partial Q^\phi)^2$, there is the contribution

$$\langle (Q^\phi)^2 Q^\theta\rangle \supset (2\pi)^3\delta\left(\sum \mathbf{k}\right)\frac{h_{\theta\phi\phi}H^5}{2}\frac{1}{\prod k_i^3}\frac{c_s^\theta}{(c_s^\phi)^2} \times \left[k_1^2(\mathbf{k_2}\cdot\mathbf{k_3})\frac{F_1^{\theta\phi\phi}}{(\kappa^{\theta\phi\phi})^3} + k_2^2(\mathbf{k_3}\cdot\mathbf{k_1})\frac{F_2^{\phi\theta\phi}}{(\kappa^{\phi\theta\phi})^3} + k_3^2(\mathbf{k_1}\cdot\mathbf{k_2})\frac{F_3^{\phi\phi\theta}}{(\kappa^{\phi\phi\theta})^3}\right]. \tag{4.4.22}$$

For the vertex $a(h_{\phi\phi\theta}+h_{\phi\theta\phi})\dot{Q}^\phi\partial_i Q^\phi\partial^i Q^\theta$, the result is

$$\langle (Q^\phi)^2 Q^\theta \rangle \supset (2\pi)^3 \delta\left(\sum \mathbf{k}\right) \frac{(h_{\phi\phi\theta}+h_{\phi\theta\phi})H^5}{4} \frac{1}{\prod k_i^3} \frac{1}{c_s^\theta} \times \left[\frac{k_2^2(\mathbf{k_3}\cdot\mathbf{k_1})F_2^{\theta\phi\phi} + k_3^2(\mathbf{k_1}\cdot\mathbf{k_2})F_3^{\theta\phi\phi}}{(\kappa^{\theta\phi\phi})^3} + \frac{k_3^2(\mathbf{k_1}\cdot\mathbf{k_2})F_3^{\phi\theta\phi} + k_1^2(\mathbf{k_2}\cdot\mathbf{k_3})F_1^{\phi\theta\phi}}{(\kappa^{\phi\theta\phi})^3} + \frac{k_1^2(\mathbf{k_2}\cdot\mathbf{k_3})F_1^{\phi\phi\theta} + k_2^2(\mathbf{k_3}\cdot\mathbf{k_1})F_2^{\phi\phi\theta}}{(\kappa^{\phi\phi\theta})^3} \right], \tag{4.4.23}$$

and finally, from the term $a(h_{\theta\phi\theta}+h_{\theta\theta\phi})\dot{Q}^\theta \partial_i Q^\phi \partial^i Q^\theta$ we find

$$\langle Q^\phi (Q^\theta)^2 \rangle \supset (2\pi)^3 \delta\left(\sum \mathbf{k}\right) \frac{(h_{\theta\phi\theta}+h_{\theta\theta\phi})H^5}{4} \frac{1}{\prod k_i^3} \frac{1}{c_s^\phi} \times \left[\frac{k_2^2(\mathbf{k_3}\cdot\mathbf{k_1})F_2^{\phi\theta\theta} + k_3^2(\mathbf{k_1}\cdot\mathbf{k_2})F_3^{\phi\theta\theta}}{(\kappa^{\phi\theta\theta})^3} + \frac{k_3^2(\mathbf{k_1}\cdot\mathbf{k_2})F_3^{\theta\phi\theta} + k_1^2(\mathbf{k_2}\cdot\mathbf{k_3})F_1^{\theta\phi\theta}}{(\kappa^{\theta\phi\theta})^3} + \frac{k_1^2(\mathbf{k_2}\cdot\mathbf{k_3})F_1^{\theta\theta\phi} + k_2^2(\mathbf{k_3}\cdot\mathbf{k_1})F_2^{\theta\theta\phi}}{(\kappa^{\theta\theta\phi})^3} \right]. \tag{4.4.24}$$

Gradient Vertices: Equilateral configuration Again, we specialise to the equilateral case where the F objects can be simplified such that

$$F^{IJJ}_{n(\mathrm{eq})} = F^{JIJ}_{n(\mathrm{eq})} = F^{JJI}_{n(\mathrm{eq})} = \left[(c_s^I)^2 + 10(c_s^J)^2 + 6c_s^I c_s^J\right] k^2\,,$$
$$F^{IIJ}_{n(\mathrm{eq})} = F^{IJI}_{n(\mathrm{eq})} = F^{JII}_{n(\mathrm{eq})} = \left[6(c_s^I)^2 + 2(c_s^J)^2 + 9c_s^I c_s^J\right] k^2\,,$$

and $F_n = 17k^2$ and the five above terms in the fields' three point functions then become

$$\langle Q^\phi(\mathbf{k}_1) Q^\phi(\mathbf{k}_2) Q^\phi(\mathbf{k}_3)\rangle \supset -(2\pi)^3\delta\left(\sum \mathbf{k}\right) \frac{17}{36} h_{\phi\phi\phi} \frac{H^5}{k^6} \frac{1}{(c_s^\phi)^2}\,, \tag{4.4.25}$$

$$\langle Q^{\phi}(Q^{\theta})^2\rangle \supset -(2\pi)^3\delta\left(\sum \mathbf{k}\right)\frac{3}{4}h_{\phi\theta\theta}\frac{H^5}{k^6}\left(\frac{c_s^{\phi}\left[(c_s^{\phi})^2+10(c_s^{\theta})^2+6c_s^{\phi}c_s^{\theta}\right]}{(c_s^{\theta})^2(2c_s^{\theta}+c_s^{\phi})^3}\right), \quad (4.4.26)$$

$$\langle (Q^{\phi})^2Q^{\theta}\rangle \supset -(2\pi)^3\delta\left(\sum \mathbf{k}\right)\frac{3}{4}h_{\theta\phi\phi}\frac{H^5}{k^6}\left(\frac{c_s^{\theta}\left[(c_s^{\theta})^2+10(c_s^{\phi})^2+6c_s^{\phi}c_s^{\theta}\right]}{(c_s^{\phi})^2(2c_s^{\phi}+c_s^{\theta})^3}\right), \quad (4.4.27)$$

$$\langle (Q^{\phi})^2Q^{\theta}\rangle \supset -(2\pi)^3\delta\left(\sum \mathbf{k}\right)\frac{3}{4}(h_{\phi\phi\theta}+h_{\phi\theta\phi})\frac{H^5}{k^6}\left(\frac{6(c_s^{\phi})^2+2(c_s^{\theta})^2+9c_s^{\phi}c_s^{\theta}}{c_s^{\theta}(2c_s^{\phi}+c_s^{\theta})^3}\right), \quad (4.4.28)$$

$$\langle Q^{\phi}(Q^{\theta})^2\rangle \supset -(2\pi)^3\delta\left(\sum \mathbf{k}\right)\frac{3}{4}(h_{\theta\theta\phi}+h_{\theta\phi\theta})\frac{H^5}{k^6}\left(\frac{6(c_s^{\theta})^2+2(c_s^{\phi})^2+9c_s^{\phi}c_s^{\theta}}{c_s^{\phi}(2c_s^{\theta}+c_s^{\phi})^3}\right). \quad (4.4.29)$$

4.4.3. Total Non-Gaussianity

Aggregating the contributions calculated term by term from the third order action in Section 4.4.2, our total three point functions for the fields in the equilateral configuration at leading order are

$$\langle Q^{\phi}(\mathbf{k}_1)Q^{\phi}(\mathbf{k}_2)Q^{\phi}(\mathbf{k}_3)\rangle = (2\pi)^3\delta\left(\sum \mathbf{k}\right)\frac{H^5}{k^6}\left(\frac{1}{36}\left[4g_{\phi\phi\phi}-\frac{17h_{\phi\phi\phi}}{(c_s^{\phi})^2}\right]\right), \quad (4.4.30)$$

$$\langle (Q^{\phi})^2Q^{\theta}\rangle = (2\pi)^3\delta\left(\sum \mathbf{k}\right)\frac{H^5}{k^6}\times\frac{3}{4}\frac{s}{(2+s)^3} \times\left[4g_1-h_{\theta\phi\phi}\frac{s^2+6s+10}{(c_s^{\phi})^2}-h_1\frac{2s^2+9s+6}{(c_s^{\theta})^2}\right], \quad (4.4.31)$$

$$\langle Q^{\phi}(Q^{\theta})^2\rangle = (2\pi)^3\delta\left(\sum \mathbf{k}\right)\frac{H^5}{k^6}\frac{3}{4}\times\frac{\bar{s}}{(2+\bar{s})^3} \times\left[4g_2 - h_{\phi\theta\theta}\frac{\bar{s}^2+6\bar{s}+10}{(c_s^{\theta})^2} - h_2\frac{2\bar{s}^2+9\bar{s}+6}{(c_s^{\phi})^2}\right], \tag{4.4.32}$$

where we have defined for convenience

$$g_1 = g_{\phi\phi\theta} + g_{\phi\theta\phi} + g_{\theta\phi\phi}\,, \qquad g_2 = g_{\phi\theta\theta} + g_{\theta\phi\theta} + g_{\theta\theta\phi}\,,$$
$$h_1 = h_{\phi\phi\theta} + h_{\phi\theta\phi}\,, \qquad h_2 = h_{\phi\theta\theta} + h_{\theta\phi\theta}\,,$$
$$s = \frac{c_s^{\theta}}{c_s^{\phi}}\,, \qquad \bar{s} = \frac{1}{s}\,.$$

with g and h coefficients as given in eq. (4.4.5). Using this, we can then evaluate the expression for $\langle\mathcal{R}(\mathbf{k}_1)\mathcal{R}(\mathbf{k}_2)\mathcal{R}(\mathbf{k}_3)\rangle$, given in eq. (4.4.6), using values from our numerical integration of the background (and first order perturbations for $\mathcal{T}_{\mathcal{RS}}$) and in turn define an f_{NL} value via comparison to eq. (3.3.60).

4.4.4. Results and Discussion

Finally, we present numerical results of the non-Gaussianity parameter f_{NL} for the five trajectories in Section 4.3.1 which were acceptable at the level of the power spectrum predictions (hence, excluding Canonical Trajectory D which was chosen to illustrate that excessive variation in γ produces too much scale dependence). The obtained f_{NL} values computed via the aforementioned method are compiled in Table 4.1 alongside the power spectrum properties obtained previously for the sake of comparison.[222,223]

We see that, given the present experimental bounds of $f_{NL} = -4 \pm 43$ on equilateral non-Gaussianity, it is only Canonical Trajectory C that is strictly and unambiguously ruled out. Meanwhile, Canonical Trajectory A is within these 1σ bounds but of a similar order to the present error in the constraint, making it likely that even moderate future tightening of this bound will rule it out. The remaining three

Table 4.1.: The calculated equilateral non-Gaussianity (f_{NL}) as well as the amplitude (A_s), tilt (n_s), tensor-to-scalar-ratio (r), running (α_s) and running of the running (β_s) for the studied trajectories of disformally coupled inflation

Trajectory	$10^9 A_s$	n_s	$10^4 \alpha_s$	$10^4 \beta_s$	$10^3 r$	f_{NL}
Canonical A (Fig. 4.1)	2.12	0.961	-5.3	1.8	17	-29.5
Canonical B (Fig. 4.2)	2.15	0.968	7.1	-0.21	31	-0.33
Canonical C (Fig. 4.3)	2.15	0.967	12	-11	1.2×10^{-6}	-2.4×10^6
DBI A (Fig. 4.5)	2.14	0.965	2.4	2.1	7.2	-0.59
DBI B (Fig. 4.6)	2.14	0.973	-59	-0.64	2.0	0.88

trajectories predict f_{NL} values of around $O(1)$ and are hence more feasible and harder to speculate about the validity of with the present data. Nevertheless, these non-Gaussianities are still rather pronounced compared to the typical $O(\epsilon) \ll 1$ non-Gaussianities in simplistic single-field models, which is not unexpected considering the presence of many factors generally capable of enhancing it above this level.

While we have not conducted a general trajectory-independent analysis of these results, which would be rather involved given the number of free parameters, we have examined the f_{NL} values for a subset of possible trajectories which have been selected by their compatibility with experimental constraints at the level of the power spectrum. We can also make further remarks based on the qualitative dependence of f_{NL} and parameters like the sound speeds and the transfer function, and use these to understand the possible variations in outcomes that we have observed and tabulated.

First, we note that while the five examples we have given here all produce negative f_{NL}, we have no reason from the structure of the analytical results to believe that this should be guaranteed, though this could be taken as evidence that it is at least unlikely.

By inspecting eqs. (4.4.30 – 4.4.32), we see that the typical relationship of $f_{NL} \propto c_s^{-2}$ is still present. Various terms in the total non-Gaussianity depend in this way on each of the sound speeds in the model separately, and so one or both of them being large may still typically be expected to amplify f_{NL}, though the presence of two sound speeds complicates this. This is not an unexpected generalisation of the well-studied case of how non-Gaussianities depend on a single sound speed (either

in single- or multi-field models). This also presents a reason as to why Canonical Trajectory C possesses such a prominent bispectrum, as it is in this trajectory where $c_s^{I'} \ll 1$, though we note that given the actual values of the sound speeds at horizon crossing that this only accounts for a factor of enhancement of $O(10^4)$ in f_{NL} and other effects must also be present to make it quite so large.

As well as the individual sound speeds, the ratio of the two sound speeds appears explicitly in the results (4.4.31) and (4.4.32), which give the contributions to the three point function involving both ϕ and θ perturbations. This is an effect arising purely from the presence of two different sound speeds, which as discussed is one of the key novel features of disformally coupled inflation. While it is hence interesting to point this out, we do not however find any evidence for this significantly influencing the results of the trajectories studied; the sound speeds remain either nearly equal or at best different by an $O(1)$ factor in these examples. In principle, though, changing the ratio of the sound speeds could shift which terms and which contributions are important in deciding the value of f_{NL}, leading to several different regimes where the dominant effects differ. In the case we have here, though, with nearly equal sound speeds, the three point functions are approximated by

$$\langle (Q^\phi)^2 Q^\theta \rangle = (2\pi)^3 \delta \left(\sum \mathbf{k} \right) \frac{H^5}{k^6} \left(\frac{1}{36} \left[4g_1 - \frac{17(h_{\theta\phi\phi} + h_{\phi\theta\phi} + h_{\phi\phi\theta})}{c_s^2} \right] \right) , \quad (4.4.33)$$

and

$$\langle Q^\phi (Q^\theta)^2 \rangle = (2\pi)^3 \delta \left(\sum \mathbf{k} \right) \frac{H^5}{k^6} \left(\frac{1}{36} \left[4g_2 - \frac{17(h_{\theta\theta\phi} + h_{\theta\phi\theta} + h_{\phi\theta\theta})}{c_s^2} \right] \right) . \quad (4.4.34)$$

Note that the approximate condition we derived in eq. (4.2.29) for there to be a significant difference in the sound speeds reveals that to robustly achieve a significant difference between the two sound speeds it would be desirable to investigate scenarios where the χ field rolls quickly, which could pave the way to interesting results in this direction.

Another factor of importance is the entropy-adiabatic power transfer encoded by $\mathcal{T}_{\mathcal{RS}}$. In a situation where the final curvature power spectrum is mostly of entropic origin ($\mathcal{T}_{\mathcal{RS}} \gg 1$), noting that $\langle \mathcal{R}(\mathbf{k}_1)\mathcal{R}(\mathbf{k}_2)\mathcal{R}(\mathbf{k}_3)\rangle \propto F_{I'}^3$ and $F_{I'} \propto \mathcal{T}_{\mathcal{RS}}$ in this limit due to eq. (4.4.9), we would expect $\langle \mathcal{R}(\mathbf{k}_1)\mathcal{R}(\mathbf{k}_2)\mathcal{R}(\mathbf{k}_3)\rangle \propto \mathcal{T}_{\mathcal{RS}}^3$ and hence from eq. (3.3.60)

$$f_{NL} \sim \frac{\langle \mathcal{R}(\mathbf{k}_1)\mathcal{R}(\mathbf{k}_2)\mathcal{R}(\mathbf{k}_3)\rangle}{\mathcal{P}_{\mathcal{R}}^2} \propto \frac{\mathcal{T}_{\mathcal{RS}}^3}{(1+\mathcal{T}_{\mathcal{RS}}^2)^2} \sim \mathcal{T}_{\mathcal{RS}}^{-1}\,. \tag{4.4.35}$$

This is particularly relevant, we find, for DBI Trajectory A, where the superhorizon evolution of the sound speeds is relatively pronounced compared to other trajectories and leads to a large $\mathcal{T}_{\mathcal{RS}} \approx 100$ that dominates the F coefficients as described above. This helps explain why this particular case exhibits a fairly small f_{NL}. Large $\mathcal{T}_{\mathcal{RS}}$ is also conducive to a small r, so one may expect these two quantities to correlate somewhat for spectra of highly entropic origin. The transfer function is also $O(10^2)$ in Canonical Trajectory C, however because γ is also $O(10^2)$, the coefficients $F_{I'} \propto \gamma^2 \gg \mathcal{T}_{\mathcal{RS}}$ are not dominated by superhorizon effects and instead, in this case, one can show that

$$f_{NL} \propto \gamma^6 \mathcal{T}_{\mathcal{RS}}^{-4}\,, \tag{4.4.36}$$

which also helps explain the size of f_{NL} in Trajectory C.

In summary there are many effects in play in determining the value of f_{NL} and for many trajectories a simple appeal to the values of c_s or $\mathcal{T}_{\mathcal{RS}}$ does not alone explain these values. Depending on the relative size of these quantities, the size of disformal factors like γ and D (influencing $F_{I'}$ and the g and h coefficients) and the ratio of the two sound speeds, the dominant term or terms in $\langle \mathcal{R}(\mathbf{k}_1)\mathcal{R}(\mathbf{k}_2)\mathcal{R}(\mathbf{k}_3)\rangle$ may differ greatly from example to example, creating some difficulty in making widely general statements about the results. Nonetheless, the sample of trajectories we have studied give us considerable hope that $O(1)$ non-Gaussianities may not be excessively rare in the regions of parameter space of the model where a feasible $\mathcal{P}_{\mathcal{R}}$ is produced, with the main counterexample being the rather non-conventional Canonical Trajectory C.

Finally, we conclude this chapter by noting that in this, we ignore the possibility that post-inflationary persistence of isocurvature perturbations could influence the processing of f_{NL} during reheating and hence technically change the mainstream Planck constraints which do not account for such specific effects. Future work on further understanding this would also be of potential interest.

CHAPTER 5

INFLATION AND THE GAUSS-BONNET TERM

The Gauss-Bonnet term is introduced in Section 2.2.4 as a modification of gravity motivated by its status as a special combination of quadratic curvature scalars which avoids the generation of unstable extra degrees of freedom often associated with such theories. This chapter will detail the original work in this area by the author in collaboration with Carsten van de Bruck, Konstantinos Dimopoulos and Charlotte Owen, leading to a number of papers[187,250,251] in Physical Review D.

5.1. Dynamics of the Gauss-Bonnet-coupled inflaton

We begin by stating the action of a Gauss-Bonnet coupled inflaton field as

$$S = \frac{M_{\rm Pl}^2}{2}\int \mathrm{d}^4x\sqrt{-g}\left[R - G(\phi)E_{\rm GB}\right] - \int \mathrm{d}^4x\sqrt{-g}\left[\frac{1}{2}(\partial\phi)^2 + V(\phi)\right], \qquad (5.1.1)$$

where $E_{\rm GB} = R^2 - 4R^{\mu\nu}R_{\mu\nu} + R^{\rho\mu\sigma\nu}R_{\rho\mu\sigma\nu}$ is the Gauss-Bonnet (GB) term. Compared to eq. (2.2.16) where we introduced this earlier, we have explicitly reinstated a factor of $M_{\rm Pl}^2$ in the action to make clear the dimensionality of the coupling function G;

as we have chosen to include the GB term in the gravitational part of the action proportional to $M_{\rm Pl}^2$ alongside the usual Ricci term, G must have a mass dimension of -2 to maintain the dimensionlessness of the action. Meanwhile the second term of the action just contains the normal scalar field terms. Varying this total action then gives us explicit equations of motion for the field and scale factor on an FRW background:

$$3M_{\rm Pl}^2H^2 = \frac{1}{2}\dot{\phi}^2 + V(\phi) + 12M_{\rm Pl}^2H^3\dot{G}\,, \tag{5.1.2}$$

$$2M_{\rm Pl}^2\dot{H} = -\dot{\phi}^2 + 4M_{\rm Pl}^2H^2(\ddot{G} - H\dot{G}) + 8M_{\rm Pl}^2H\dot{H}\dot{G}\,, \tag{5.1.3}$$

$$\ddot{\phi} + 3H\dot{\phi} + V_{,\phi} + 12M_{\rm Pl}^2H^2G_{,\phi}(\dot{H} + H^2) = 0\,. \tag{5.1.4}$$

Compared to the standard cosmological equations for a scalar field, several extra interesting features are present. It is clear that the equations of motion depend only on derivatives of G. This is expected as the GB term is by construction a total derivative in 4D and therefore only significant if a non-constant coupling function is present. Additionally, various complications arise due to the more complex structure of the system. In particular, the first Friedmann equation is no longer quadratic in H but cubic instead, making its solution less trivial. Futhermore, the generalised Klein-Gordon equation now depends on $\dot{H}$ and the gravitational field equation for $\dot{H}$ similarly depends on $\ddot{\phi}$ via $\ddot{G} = \ddot{\phi}\,G_{,\phi} + \dot{\phi}^2G_{,\phi\phi}$. Given this mixing of terms, it is useful to recast the two equations (5.1.4) and (5.1.3) in matrix form

$$\begin{pmatrix} M_{11} & M_{12} \\ M_{21} & M_{22} \end{pmatrix} \begin{pmatrix} \dot{H} \\ \ddot{\phi} \end{pmatrix} = \begin{pmatrix} V_1 \\ V_2 \end{pmatrix}\,, \tag{5.1.5}$$

with

$$
\begin{aligned}
M_{11} &= 2M_{\rm Pl}^2\left(1-4H\dot{G}\right)\,,\\
M_{12} &= -4M_{\rm Pl}^2H^2G_{,\phi}\,,\\
M_{21} &= -3M_{12}\,,\\
M_{22} &= 1\,,\\
V_1 &= -4M_{\rm Pl}^2H^3\dot{G}-\left(1-4M_{\rm Pl}^2H^2G_{,\phi,\phi}\right)\dot{\phi}^2\,,\\
V_2 &= -12M_{\rm Pl}^2H^4G_{,\phi}-3H\dot{\phi}-V_{,\phi}\,,
\end{aligned}
$$

such that one can easily solve for $\dot{H}$ and $\ddot{\phi}$ simultaneously by inverting the matrix of M coefficients. Note that when G is constant or zero and the GB coupling is resultantly inert, the matrix in question becomes diagonal, leaving the solution of the system obtainable via more straightforward means as usual. Before going on to study this system further, however, it will be useful to note some subtleties involved.

5.1.1. Gauss-Bonnet and Conformal Transformations

While the GB coupling is a well-motivated modification of gravity from the perspective of effective field theory as it is the simplest way of stably adding terms quadratic in curvature to GR, similar considerations would suggest that one could also expect a scalar coupling to the Einstein Hilbert term in such scenarios. In fact, it is found that such an $F(\phi)R$ coupling between a scalar and gravity is generated from quantum field effects in a curved background even if it is not explicitly included in the classical theory.[87] This is one of the key ideas in theories like Higgs Inflation[83,84,96,252–255] which uses such a non-minimal coupling between gravity and the standard model Higgs field h, typically with $F(h)=1+fh^2$. This is interesting because the Higgs field does not possess a suitable flat potential to drive inflation usually, but the effect of this coupling to gravity is to alleviate this problem at large h such that a period of inflation can be driven in the early universe before the usual Higgs physics are recovered at small h, when $F\approx 1$, so as to reconcile with usual particle physics.

In such $F(\phi)R$ theories, one typically uses a conformal transformation (2.2.9) to put the theory in the so-called Einstein Frame (EF) where on a rescaled metric the action looks like a minimally coupled scalar field again as in eq. (2.2.11), albeit with a different potential. This procedure is, however, problematic when additional terms are present in the action, such as in our case with the GB coupling. If one were to consider a theory contain both the F term and the G term, one could not simply conformally transform the F term away without causing the GB term to also transform and generate some new terms in the action, conversely rendering it even further from the appearance of a minimal scalar-tensor theory.
To see this, note that under a conformal transformation as in eq. (2.2.9), the specific behaviour of the Gauss-Bonnet term $E_{\rm GB}$ (in d dimensions for generality's sake) is[90]

$$\begin{aligned} E_{\rm GB} \to e^{-4A}\Big\{ & E_{\rm GB} - 8(d-3)R_{\mu\nu}\left(A^{;\mu}A^{;\nu} - A^{;\mu;\nu}\right) - 2(d-3)R\left(2\Box A + (d-4)\left(\nabla A\right)^2\right) \\ & + 4(d-2)(d-3)\left[\left(\Box A\right)^2 + (d-3)\left(\nabla A\right)^2\left(\Box A\right)\right] \\ & - 4(d-2)(d-3)\left(A_{;\mu;\nu}A^{;\mu;\nu} - 2A_{;\mu;\nu}A^{;\mu}A^{;\nu}\right) \\ & + (d-1)(d-2)(d-3)(d-4)\left(\nabla A\right)^4\Big\}, \end{aligned} \tag{5.1.6}$$

In particular we note from this that the full transformed action with both an F and a G term would contain things like (now returning to units where $M_{\rm Pl} = 1$ for brevity)

$$\begin{aligned} S &\supset \int d^dx\sqrt{-g}\Big\{Fe^{(d-2)A} + 4Ge^{(d-4)A}\left(\Box A\right)\Big\}\frac{R}{2} \\ &\overset{(4D)}{=} \int d^4x\sqrt{-g}\Big\{Fe^{-2A} + 4G\left(\Box A\right)\Big\}\frac{R}{2}\,. \end{aligned} \tag{5.1.7}$$

This evidently complicates the usual process of making a choice $A(\phi)$ such that the coefficient of $R/2$ is 1, particularly as the above expression includes objects such as $(\Box A)$. Additional terms such as

$$S \supset \int d^dx\sqrt{-g}\left[4(d-3)e^{(d-4)A}GR_{\mu\nu}\left(A^{;\mu}A^{;\nu}-A^{;\mu;\nu}\right)\right]$$
$$\overset{(4D)}{=} \int d^4x\sqrt{-g}\left[4GR_{\mu\nu}\left(A^{;\mu}A^{;\nu}-A^{;\mu;\nu}\right)\right]. \tag{5.1.8}$$

are also generated, and while these are all terms that are encompassed in the class of Horndeski scalar-tensor theories, it is comparatively easier to just remain in the Jordan Frame with action

$$S = \int \mathrm{d}^dx\sqrt{-g}\left[\frac{1}{2}F(\phi)R - \frac{1}{2}(\partial\phi)^2 - V(\phi) - \frac{1}{2}G(\phi)E_{\mathrm{GB}}\right], \tag{5.1.9}$$

and equations of motion

$$3H^2(F-4H\dot{G}) = \frac{1}{2}\dot{\phi}^2 + V(\phi) - 3H\dot{F}\,, \tag{5.1.10}$$
$$2(F-4H\dot{G})\dot{H} = -\dot{\phi}^2 - \ddot{F} + H\dot{F} + 4H^2(\ddot{G} - H\dot{G})\,, \tag{5.1.11}$$
$$\ddot{\phi} + 3H\dot{\phi} + V_{,\phi} - 3(\dot{H}+2H^2)F_{,\phi} + 12H^2G_{,\phi}(\dot{H}+H^2) = 0\,. \tag{5.1.12}$$

With this we can now generally treat cases where both F and G are important. Generalising the above matrix method (5.1.5) for determining $\dot{H}$ and $\ddot{\phi}$ in these coupled equations (5.1.11) and (5.1.12) we find the coefficients should now take the form

$$M_{11} = 2\left(F - 4H\dot{G}\right),$$
$$M_{12} = F_{,\phi} - 4H^2G_{,\phi}\,,$$
$$M_{21} = -3M_{12}\,,$$
$$M_{22} = 1\,,$$
$$V_1 = H\left(\dot{F} - 4H^2\dot{G}\right) - \left(1 + F_{,\phi,\phi} - 4H^2G_{,\phi,\phi}\right)\dot{\phi}^2\,,$$
$$V_2 = 6H^2\left(F_{,\phi} - 2H^2G_{,\phi}\right) - 3H\dot{\phi} - V_{,\phi}\,.$$

One application of this in particular is to study an $F(\phi)R$ theory like Higgs inflation with higher order corrections coming from a GB coupling.[250] We keep this motivation in mind as we proceed to derive results for this model in the next section.

5.1.2. Slow-roll power spectra

When considering theories with extra free functions or non-constant couplings, the slow-roll formalism is typically modified to include conditions on the rate of change of these objects in addition to the usual ϵ_n parameters in eq. (3.2.20). This is because if a function of the field grows too rapidly, this in turn implies that the field is growing rapidly enough that the slow-roll conditions would be violated at some order anyway. More practically speaking, it is useful to re-express equations of motion and other expressions in terms of analogues of the ϵ_n parameters so that an order-by-order expansion can be systematically carried out. To this end, we mimic the definition of the ϵ_n parameters in eq. (3.2.20) and define, first, slow-roll parameters derived from our non-minimal coupling function F

$$\zeta_0 = \frac{\dot{F}}{HF}\,, \quad \zeta_n = \frac{\dot{\zeta}_{n-1}}{H\zeta_{n-1}}\,, \tag{5.1.13}$$

where the slow-roll condition is, as usual, $\zeta_n \ll 1$. These ζ_n are interpretable as close relatives of the normal slow-roll parameters in the Jordan Frame, as we note that (in a theory with $G = 0$, for the moment) one finds that

$$\epsilon_0 \approx \frac{\dot{\phi}^2}{2H^2F} + \frac{\ddot{F}}{2H^2F} - \frac{\dot{F}}{2HF}\,, \tag{5.1.14}$$

which makes it clear that objects like $\zeta_0 = \dot{F}/(HF)$, up to $O(1)$ factors, must be kept small if the principle slow-roll parameters are to remain acceptably small. This is a similar approach to that taken by work in the literature[91,95] on the topic of inflationary calculations directly in the JF. Similarly, work on Gauss-Bonnet coupled fields in the literature[256] has on similar grounds defined slow-roll parameters derived from the function G coupled to a field in the EF such as

$$\delta_0 = 4\dot{G}H\,, \quad \delta_n = \frac{\dot{\delta}_{n-1}}{H\delta_{n-1}}\,, \tag{5.1.15}$$

again, with $\delta_n \ll 1$. However, our situation is slightly different in that we couple the Gauss-Bonnet term directly to the Jordan Frame field, not the Einstein Frame field, which as demonstrated by the above excursion into the nature of the GB term's conformal transformation, is a distinct theory. To see clearly the implications of this, we again move to compute ϵ_0 from eqs. (5.1.10 – 5.1.12) to find

$$\epsilon_0 = \frac{\frac{\dot{\phi}^2}{H^2F} + \frac{\ddot{F}}{H^2F} - \frac{\dot{F}}{HF} - \frac{4\left(\ddot{G} - H\dot{G}\right)}{F}}{2\left(1 - \frac{4H\dot{G}}{F}\right)} \,. \tag{5.1.16}$$

Note particularly that it is the combination $\delta_0/F = 4H\dot{G}/F$ rather than δ_0 by itself that appears in the resulting expression. From this, one might posit that the more appropriate slow-roll parameter for a GB-coupled field in the Jordan Frame is this combination which we will call $\Delta_0 = \delta_0/F$ with the usual recursive extension to higher orders, explicitly:

$$\Delta_0 = \frac{\delta_0}{F} = \frac{4H\dot{G}}{F} \,, \quad \Delta_n = \frac{\dot{\Delta}_{n-1}}{H\Delta_{n-1}} \,. \tag{5.1.17}$$

And indeed, if we now express some useful quantities in terms of the principle slow-roll parameters ϵ_n , the JF slow-roll parameters ζ_n and these new Jordan Frame Gauss-Bonnet slow-roll parameters Δ_n, we find, for example, that

$$\dot{\phi}^2 = H^2F\Big[2\epsilon_0 + \zeta_0 - \Delta_0 - \zeta_0\left(\zeta_1 + \zeta_0 - \epsilon_0\right) + \Delta_0\left(\Delta_1 + \zeta_0 - \epsilon_0\right)\Big] \,, \tag{5.1.18}$$

$$V(h) = \frac{H^2F}{2}\Big[6 - 2\epsilon_0 + 5\zeta_0 + \Delta_0 + \zeta_0\left(\zeta_1 + \zeta_0 - \epsilon_0\right) - \Delta_0\left(\Delta_1 + \zeta_0 - \epsilon_0\right)\Big] \,. \tag{5.1.19}$$

We see, then, that not only do the Δ_n parameters more appropriately capture the conditions for which the expansion of space is inflationary via their appearance in eq. (5.1.16) when considered in the Jordan Frame, but also that they appear on equal footing with the ϵ_n and ζ_n parameters, rather than appearing with an extra factor of F. Due to this, we consider it the most appropriate analogue of the conventional slow-roll parameters to use in what follows.

We also note that from eq. (5.1.10) it is clear that Δ_0 is also interpretable as the density parameter associated with the GB-coupling's contribution to the energy content of the universe, $\Omega_{\rm GB}$, as we can write the Friedmann equation in the form $\Omega_\phi + \Delta_0 = 1$.

We will now proceed to study the perturbation equations in this system

Scalar Perturbations

A careful study of the perturbation equations yields an equation of motion which can[257,258] be written in a form analogous to that shown in eq. (3.3.19)

$$v_k'' + \left[c_s^2 k^2 - \frac{z_s''}{z_s}\right] v_k = 0\,, \tag{5.1.20}$$

where $v = z_s\mathcal{R}/c_s$. The expression for the sound speed in this model, in terms of the coupling functions F and G, is

$$c_s^2 = 1 + 4\dot{G}\frac{\frac{1}{2}\left(\frac{\dot{F}-4H^2\dot{G}}{F-4H\dot{G}}\right)^2\left(\frac{\ddot{G}}{G} - H - 4\dot{H}\frac{F-4H\dot{G}}{\dot{F}-4H^2\dot{G}}\right)}{\dot{\phi}^2 + \frac{3}{2}\frac{\left(\dot{F}-4H^2\dot{G}\right)^2}{F-4H\dot{G}}}\,, \tag{5.1.21}$$

and as in the standard case (3.3.19) we can still express the quantity z_s in terms of a via $z_s = a\sqrt{Q_s}$. The function Q_s is then given by

$$Q_s = \frac{\dot{\phi}^2 + \frac{3}{2}\frac{\left(\dot{F}-4H^2\dot{G}\right)^2}{F-4H\dot{G}}}{\left(H + \frac{1}{2}\frac{\dot{F}-4H^2\dot{G}}{F-4H\dot{G}}\right)^2}\,. \tag{5.1.22}$$

It is clear that both of these expressions reduce to the standard case when the new couplings are trivial or neglected. Continuing to follow the logic presented in Chapter 3, we see that the power spectrum of curvature perturbations would be

$$\mathcal{P}_\mathcal{R} = \frac{k^3}{2\pi^2}\left|\frac{c_s v_k}{z_s}\right|^2\,. \tag{5.1.23}$$

Following an application of the slow-roll approximation to find that

$$Q_s = \frac{FA}{\left(1 + \frac{1}{2}x\right)^2}\,, \tag{5.1.24}$$

and

$$c_s^2 = 1 + \frac{xB}{2A}\,, \tag{5.1.25}$$

where A, B and x are the following combinations of slow-roll parameters

$$A = 2\epsilon_0 + \zeta_0 - \Delta_0 - \zeta_0\left(\zeta_1 + \zeta_0 - \epsilon_0\right) + \Delta_0\left(\Delta_1 + \zeta_0 - \epsilon_0\right) + \frac{3}{2}\left(\zeta_0 - \Delta_0\right)x\,, \tag{5.1.26}$$

$$x = \frac{\zeta_0 - \Delta_0}{1 - \Delta_0}\,. \tag{5.1.27}$$

$$B = \Delta_0\left(4\epsilon_0 - x + x\left[\Delta_1 + \zeta_0 + \epsilon_0\right]\right)\,, \tag{5.1.28}$$

we can arrive at the expression, correct at leading order in slow-roll, for the power spectrum

$$\mathcal{P}_\mathcal{R} \approx \frac{H^2}{4\pi^2 F\left|2\epsilon_0 + \zeta_0 - \Delta_0\right|}\,, \tag{5.1.29}$$

which yields a spectral index

$$n_s = 1 - 2\epsilon_0 - \frac{2\epsilon_0\left(\zeta_0 + \epsilon_1\right) + \zeta_0\left(\zeta_0 + \zeta_1\right) - \Delta_0\left(\zeta_0 - \Delta_1\right)}{2\epsilon_0 + \zeta_0 - \Delta_0}\,. \tag{5.1.30}$$

Note that for $F = 1$ and $\zeta_0 = \Delta_0 = 0$, these reduce to the standard case derived in Chapter 3 as one would expect. It is also interesting to note that, despite the usual result that $\mathcal{P}_\mathcal{R} \propto c_s^{-1}$ (3.3.58), eq. (5.1.25) shows in our case that $c_s^2 = 1 + O(\epsilon^2)$. Note that this arises because A and x are $O(\epsilon)$ and $B = O(\epsilon^2)$. As a result, at leading order, c_s will not appear in the power spectrum.[1] The main source of slow-roll-level deviation from the standard spectrum is therefore the effect of the F and G couplings on z_s which in turn sets the effective mass of the perturbations in eq. (5.1.20).

As in the standard case, slow-roll GB coupled inflation predicts an $O(\epsilon)$ deviation

[1] We use $O(\epsilon)$ to refer in brief to a term's order in all slow-roll parameters such as ζ_n and Δ_n, not just strictly the ϵ_n functions.

from a scale invariant curvature power spectrum and hence is a feasible model of inflation from this perspective.

Tensor Perturbations

The tensor perturbations also do not follow the standard results of Chapter 3 as we have a non-minimal gravity sector due to the presence of the GB term. This modifies the perturbation equation for gravitational waves such that the canonical variable u obeys[257,258]

$$u_k'' + \left[c_t^2 k^2 - \frac{z_t''}{z_t}\right] u_k = 0\,, \tag{5.1.31}$$

where now we have a $c_t \neq 1$ representing the possibility that gravitational waves may not travel at the speed of light, and $z_t = a\sqrt{Q_t}$. Here, Q_t depends on the scalar field and its coupling functions, because the dynamics of the gravitational waves are affected by not just the expansion of space (as in the minimal case of Chapter 3 where $z = a$) but also details of the field theory due to the non-minimal coupling; this is not General Relativity. In particular, we have for this theory that

$$c_t^2 = \frac{F - 4\ddot{G}}{F - 4H\dot{G}}\,, \tag{5.1.32}$$

and

$$Q_t = F - 4H\dot{G}\,. \tag{5.1.33}$$

The slow-roll expansions of these objects are then

$$Q_t = F\left(1 - \Delta_0\right)\,, \tag{5.1.34}$$

and

$$c_t^2 = \frac{1 - \Delta_0\left(\Delta_1 + \zeta_0 + \epsilon_0\right)}{1 - \Delta_0}\,. \tag{5.1.35}$$

We can then use eq. (3.3.27) and these expansions to express the tensor-to-scalar ratio (at leading order in slow-roll such that sound speeds, which deviate from unity

at second order, do not appear) for GB coupled inflation in the Jordan Frame as

$$r \approx \frac{\mathcal{P}_\mathcal{T}}{\mathcal{P}_\mathcal{R}} = 8 \times \left|\frac{Q_s}{Q_t}\right| = 8\frac{2\epsilon_0 + \zeta_0 - \Delta_0}{1 - \Delta_0} \,. \tag{5.1.36}$$

The role of the GB term here is particularly interesting as it can, for particular Δ_0 values at horizon crossing, suppress the tensor-to-scalar ratio below that of minimal slow-roll inflation.

It is also interesting at this point to consider the tensor spectral index, found to be

$$n_t = -2\epsilon_0 - \zeta_0 \,, \tag{5.1.37}$$

as this does not obey the usual consistency relation discussed in Chapter 3, that is $r \neq -8n_t$ due to the absence of a leading order GB contribution in n_t. This also occurs when the GB term is coupled to a scalar in the Einstein Frame,[256] but from these expressions clearly does not occur when considering an otherwise-minimal scalar in the Jordan Frame. This is an interesting signature of GB physics during inflation, and the exact amount of departure from $r = -8n_t$ could be used to measure Δ_0 (and hence the density parameter $\Omega_{\rm GB}$), given reasonably precise experimental values of n_t and r.

5.2. Effects on the end of inflation and reheating

We now move forward to complementing the former discussion of inflationary perturbations with a look at what happens as inflation ends in this class of theories. For much of what follows it will help to assume some particular form for the couplings to facilitate numerical evaluation. To that effect, we note that within the literature on GB-coupled inflation,[256] common choices of the functions V and G are power laws such as

$$V(\phi) = V_0\phi^n \,, \quad G(\phi) = G_0\phi^{-g} \,, \tag{5.2.1}$$

are found. Both n and g are taken to be positive, possibly equal, and often integers, such that the Gauss-Bonnet coupling is a negative power law and the potential is a

conventional positive power law of the kind discussed at length in Chapter 3. This is also partly motivated by the dimensions of these functions in the action; V must have a mass dimension of positive 4 while G's is negative 2. When studying such positive/negative power law forms for V and G, a useful quantity to define is

$$\alpha = \frac{4V_0G_0}{3}\,. \tag{5.2.2}$$

This is essentially a rescaling of G_0 by a convenient factor that appears in many derivations and often has a simple and pleasant value in physically-relevant cases, as we will soon see. We could also see how α appears in the results of the previous section by specialising to these specific functions (and assuming $F \approx 1$), where we would find that e.g. $r \propto (1-\alpha)$, revealing that the tensor-to-scalar ratio is most strongly suppressed when $\alpha \sim G_0V_0 \sim O(1)$. This is interesting as a minimal power-law potential model has been shown to exceed the constraints on r by itself, but this could be ameliorated by choosing a sufficiently large G_0 (α).

A minimal choice for $F(\phi)$ that we will also assume when needed is $F = 1 + f\phi^2$, with positive f assumed as this ensures the reality and positivity of quantities like a and H, which should remain such in the name of physical sensibility. This choice is simple, but additionally motivated by Higgs inflation and curved space renormalisation of a scalar field as mentioned before. It is also a decent prototype for many types of coupling as the leading order expansion of a function around a minimum.

5.2.1. Late time behaviour of the Gauss-Bonnet coupled inflaton

The full system of equations given above is rather complicated, and so to get a first impression of the behaviour of the system it is convenient to look towards a numerical solution. This reveals something striking; as shown in an example in Figure 5.1, the presence of the GB coupling (while neglecting F for now) inhibits the end of inflation.[259] We see the usual late-time behaviour of the field settling into its potential minimum when $\alpha = G_0 = 0$, but when $\alpha = 0.5$ (or generally $0 < \alpha < 1$) we instead see the field asymptotically approach the minimum as if heavily damped, not

even beginning to oscillate. Correspondingly, it is shown that ϵ_0 tends to a constant in the same limit.[187,250] Qualitatively, we observe in simulations that a smaller α corresponds to a larger final ϵ_0, but it always remains below 1 and hence does not ever represent the termination of inflationary expansion. Using the equations of motion, we can say that when ϵ_0 is constant, the GB slow-roll parameter δ_0 obeys to a good approximation

$$\delta_0 \left(t \to \infty\right) \approx \frac{2\epsilon_0}{1+\epsilon_0} \,, \tag{5.2.3}$$

and will hence also be constant. We also note that as α increases towards 1, the constant value that ϵ_0 approaches tends to 0, representing a perfect exponential expansion with a constant potential (and hence constant field), as shown in the figure. To understand these observations analytically, we consider that when ϵ_0 is well approximated by a constant value, the evolution of the Hubble parameter implied by the definition of the slow-roll parameter is

$$\dot{H} = -\epsilon_0 H^2 \quad \Rightarrow \quad H(t) = \left(c + \epsilon_0 t\right)^{-1} \,, \tag{5.2.4}$$

for some constant of integration c depending on the initial conditions. From the Friedmann equation, we can then say that the field's evolution should obey

$$\phi(t) = \left(\frac{\beta n}{V_0}\right)^{\frac{1}{n}} \left(c + \epsilon_0 t\right)^{-\frac{2}{n}} \,, \tag{5.2.5}$$

where β is a shorthand for the combination of slow-roll parameters given by an expansion of V/H^2 as in eq. (5.1.19), and hence effectively a constant in this regime. This is in good agreement with the numerics shown in Figure 5.1.

Note that this behaviour is not captured at any order in a slow-roll expansion. The leading order slow-roll expansion, for example, predicts $\epsilon_0 \propto \phi^{-2}$ and hence would predict that for small enough ϕ, inflation would always end. This detail is missed by much of the pre-existing literature on this topic. Only by analysing the equations of motion exactly - not perturbatively in slow-roll parameters - does one unveil the true behaviour of a gradual descent towards zero, when $0 < \alpha < 1$. Mathematically, this is related to the fact that the GB coupling diverges at $\phi = 0$. As the GB coupling

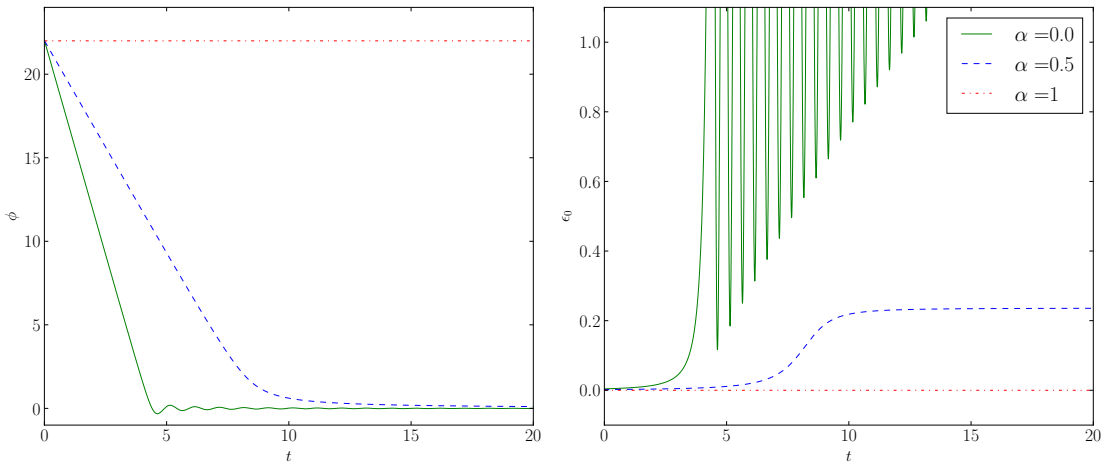

Figure 5.1.: Evolutions of ϕ and ϵ_0 in cosmic time for different given α values. Parameters are $n = g = 2$ and $V_0 = 3 \times 10^{-11}$. When $\alpha = 0$ (solid, green) standard inflation proceeds and ends (as $\epsilon_0 > 1$ eventually). On the other hand, when $\alpha = 0.5$ (blue, dashed), as stated in the main text, ϵ_0 takes a constant value at late times, and ϕ asymptotically tends to 0. Inflation continues forever. Lastly, for $\alpha = 1$ (red, dotted), ϕ is held constant at its initial condition and $\epsilon_0 \equiv 0$.

grows larger and larger with $\phi's$ descent towards 0, this influences the dynamics in such as way as to never let ϕ reach 0, slowing down the field and damping its usual oscillatory behaviour strongly.

It is also worth noting that for $\alpha > 1$ in this case (though not when the F coupling is also taken into account as will be shown later), the expansion of the universe is non-inflationary and the field rolls up its potential instead of down, making this case of little interest for present purposes. We are however still interested in exactly $\alpha = 1$, also shown in Figure 5.1, where the field freezes at its initial value and the slow-roll parameter is identically zero for all time. This, in contrast to the constant but non-zero ϵ_0 discussed above for intermediate α, *is* captured by slow-roll analysis which predicts $\epsilon_0 \propto (1 - \alpha)$. Analysis of the equation of motion in the limit of $\dot{\phi} = \ddot{\phi} = 0$ unveils that the constraint equation for a constant field in terms of the coupling functions is

$$V_{,\phi}F^2 - 2VFF_{,\phi} + \frac{4}{3}V^2G_{,\phi} = 0\,, \tag{5.2.6}$$

Using the forms of these functions described earlier in this section, and specialising

to an $n = 4$ potential for argument's sake (the JF Higgs potential is approximately this at early times), this reduces to

$$1 + f\phi^2 + \frac{\alpha g}{4}\phi^{g+4} = 0\,. \tag{5.2.7}$$

When $g = 0$ (corresponding to a constant and therefore trivial GB coupling) and $f \geq 0$, this has no real solutions, indicating the field cannot just freeze in place as expected. A particularly straightforward case to study further is when $g = -4$, though much of the following discussion is found numerically to still qualitatively apply, this is by far the easiest case to see why it works analytically. In this case, we have

$$1 + f\phi^2 - \alpha = 0\,. \tag{5.2.8}$$

That is, when $f = 0$, the field can only remain constant when $\alpha = 1$ (confirming the above result), but when $f \neq 0$ this has more possible solutions. One finds that the field can then freeze at a constant value of

$$\phi = \sqrt{\frac{\alpha - 1}{f}}\,, \tag{5.2.9}$$

such that if $\alpha \geq 1$ the field will be able to freeze with a positive f. We see this new behaviour in Figure 5.2.

It is interesting that the presence of the $F(\phi)$ coupling function enriches the phenomenology of the GB coupled inflaton. Now, $\alpha > 1$ does not preclude inflation from occurring and essentially, alongside the parameter f, allows one to build a model that approaches and freezes at any ϕ value, while the $\alpha = 1$, $f = 0$ model in Figure 5.1 remains frozen at the initial condition only. It is confirmed by numerical simulations that for a wide range of parameters, the field will approach the value predicted by eq. (5.2.9) and stabilise at it regardless of initial condition; the field will even increase from its initial condition to do this if necessary. Additionally, the transition between the early time behaviour and the late time freezing is less smooth when $f \neq 0$ as we observe in Figure 5.2 a local bump-like feature in the trajectory of ϵ_0 around $N = 60 - 70$ in the two $\alpha \neq 0$ cases.

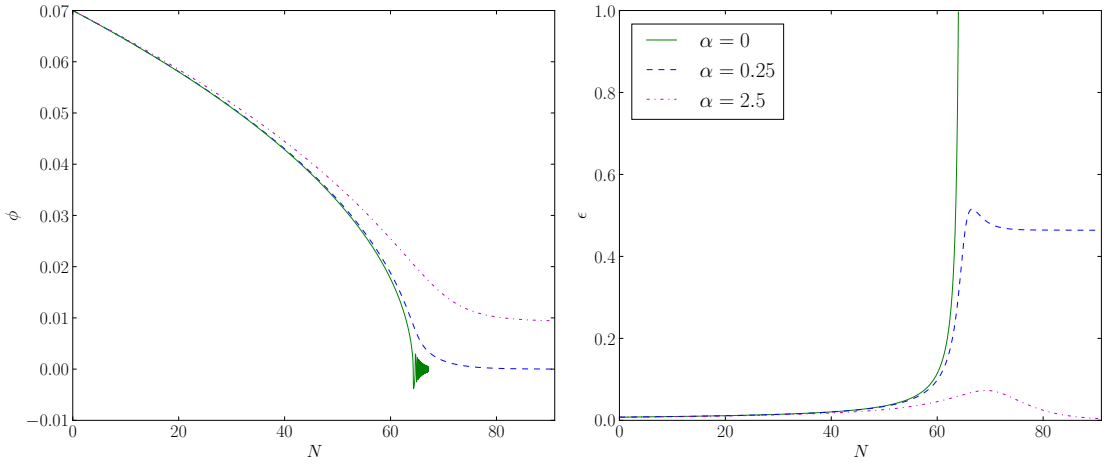

Figure 5.2.: Numerical solutions of ϕ and ϵ_0 as a function of e-fold number N, with $F = 1 + f\phi^2$ and $f = 17367.233$. The GB coupling is an inverse power-law ($g = -4$) while the potential is quartic. Parameters are chosen to mimic Higgs inflation specifically. The solid-green line corresponds to $\alpha = 0$ (standard inflation) and is shown for comparison with the other trajectories with non-trivial Gauss-Bonnet effects. Of these, the blue-dashed line has $\alpha = 0.25$ and shows late-time constant ϵ_0 as in the previously discussed case, while the purple-dotted line has $\alpha = 2.5$ which causes the scalar field to behave as a constant at late times. Finally, we see that this last trajectory also approaches the field value predicted by eq. (5.2.9) of ≈ 0.0093

This type of behaviour is not unique to (inverse) power law functions and is generally expected to occur whenever the GB coupling becomes large as the field rolls down its potential. Note for example that with exponential forms of the potential and GB coupling,

$$V(\phi) = V_0 e^{p\phi}\,, \quad G(\phi) = G_0 e^{-q\phi}\,, \tag{5.2.10}$$

that the solution of eq. (5.2.6) is found for $p \neq q$ to be

$$\phi = \frac{1}{q-p} \ln\left(\frac{4qV_0G_0}{3p}\right)\,, \tag{5.2.11}$$

and that numerically, late-time freezing of the field occurs (e.g. this possible solution is the one chosen by the dynamics) when q is sufficiently larger than p (typically $q/p \gtrsim 2$ is sufficient, making the prefactor in the above expression negative). For these potentials, the field rolls down its exponential potential indefinitely, rather

than towards a minimum, but once it has done so sufficiently, the GB coupling becomes exponentially large as the potential declines, and the same kind of impedance seen in the power law case is exhibited. The argument of the logarithm in the above expression can be considered the equivalent of the α parameter defined for the power laws (5.2.1), so we define

$$\alpha^* = \frac{4qV_0G_0}{3p} \tag{5.2.12}$$

and it is simple to see that when $q > p$, $\alpha^* > 1$ corresponds to the field freezing at positive values and $\alpha^* < 1$ to negative values. While the particulars vary depending on the precise forms of the functions, we see that a shrinking potential and quickly growing GB coupling are a recipe for inhibition of the inflaton's motion.

5.2.2. Implications for reheating

Of course, the lack of an end to inflation spells doom for the prospects of conventional reheating. Without oscillations about the minimum of the potential, perturbative reheating and parametric resonance will not be able to proceed. Worse yet, there is little to no hope of successfully achieving reheating via e.g. instant preheating either. To see this, consider eq. (3.2.67). For the power law coupling case described above, $\phi \to 0$, so the final density produced by instantaneous non-perturbative particle production would, with an interaction Lagrangian $\propto \lambda^2\phi^2\chi^2$, be

$$\rho_\chi \to \frac{\lambda^{5/2}|\dot{\phi}|^{3/2}_{\phi=\nu}\nu}{8\pi^3}\,. \tag{5.2.13}$$

Even assuming an optimistic set of parameters with $\lambda = O(1)$ and $\nu = O(1)$, using some typical numerical results from the simulations we previously carried out would suggest that $\dot{\phi}_{\phi=\nu} \approx 10^{-7}$ and therefore $\rho_\phi \approx O(10^{-13})$ which is comparable to the final inflation density ρ_ϕ also observed numerically. Now, unlike in the conventional case where the inflaton becomes kinetically-dominated and scales in density as a^{-6}, allowing the decay products χ to come to dominate as they scale as a^{-3} or a^{-4} instead, here the inflaton behaves differently. For a constant ϵ_0, one can show that the inflaton will scale as $a^{-2\epsilon_0}$, and $\epsilon_0 < 1$, such that the inflaton will eventually

dominate over the decay products even if they begin with comparable densities. The inability for inflation to end is therefore a significant problem with no clear and simple resolution in terms of how reheating can proceed following this. Despite the established successes of GB coupled inflation with e.g. power law potentials in producing feasible power spectra with suppressed tensor-to-scalar ratios at horizon crossing, in reality such models may not be able to exit the inflationary epoch via the usual period of reheating. One could add, for example, additional fields to deal with the problem of reheating here, but this would also likely ruin the successful power spectra generated at horizon crossing. We therefore consider how to minimally extend the model, preserving the early time behaviour when good power spectra are generated, and only altering the late-time behaviour enough to allow some kind of reheating to proceed.

5.2.3. Minimal extension of model

Consider again a power law potential and Gauss-Bonnet coupling, but with the extension of allowing the potential to possess a non-zero minimum ς. For simplicity we will consider the case where the exponents of V and G are equal but opposite in sign, and write this as

$$V(\phi) = V_0(\phi + \varsigma)^n\,, \quad G(\phi) = G_0\phi^{-n}\,. \tag{5.2.14}$$

For convenience, we perform a field redefinition to absorb this shift into the GB coupling function instead, so that we have a normal power law potential but a modified GB coupling. That is,

$$V(\phi) = V_0\phi^n\,, \quad G(\phi) = G_0(\phi - \varsigma)^{-n}\,, \tag{5.2.15}$$

as this makes the theory look more like normal inflation with the simplest potential but a non-standard correction coming from a coupling to modified gravity. Also for the sake of simplicity we will also omit the F function in the following discussion as we are mainly interested in overcoming the damping effect produced by the G coupling, which F only influences the smaller details of.

Essentially, this shift in the coupling means that instead of the theory proposing that the GB coupling tends to infinity as the potential minimum is approached, it will do one of two things depending on the sign of ς.[187]

- Positive ς: The GB coupling tends to infinity before the field can approach its minimum.
- Negative ς: The GB coupling will take on a finite but large value at the potential minimum.

Of these, the latter case sounds more promising. One can imagine that it will still allow the field to oscillate, but the large GB coupling can still affect the oscillatory behaviour. However, the former case is not to be immediately ruled out; while it does sound like it should only exacerbate the problem, it does provide a phenomenologically different result.

Positive shift

Now, as $\varsigma > 0$, the diverging GB coupling occurs at a point where there is a potential gradient, and this manifests in two ways, which we show in six examples of this model in Figure 5.3.
Firstly, we find that the new static solution occurs at a field value, marked as Λ on the figure, of

$$\phi = \Lambda = \varsigma \times \left(1 - \alpha^{\frac{1}{n+1}}\right)^{-1}, \tag{5.2.16}$$

where $\alpha \neq 1$. As can be seen in the six numerical examples given, the field approaches this static solution. There is hence an effective potential minimum at this point. Since $\alpha < 1$, as all other cases are uninteresting or ruled out, $\Lambda > \varsigma$ and the field always reaches this static solution before it can approach the divergence in the GB coupling. This differs from the $\varsigma = 0$ case where the field directly approaches the GB divergence at $\phi = 0$, rather than a point, Λ, somewhat before it. Secondly, depending on the strength of the GB coupling, various things can happen. For $\alpha = 0.1$, we see that the field just asymptotically approaches Λ as the GB

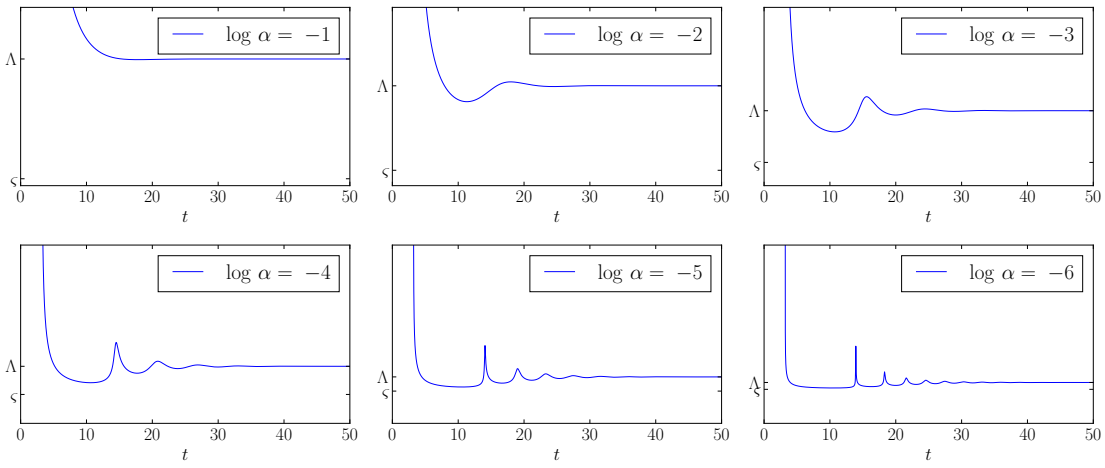

Figure 5.3.: Six examples of the $\varsigma > 0$ model with $\alpha = 10^{-x}$ for $x = 1 \ldots 6$ and $\varsigma = 0.05$ as a representative example of the different kinds of behaviour observed numerically. Oscillations occur about the point Λ defined in eq. (5.2.16) in general, but for sufficiently strong GB coupling ($\alpha \sim 0.1$) or sufficiently small distance between the GB divergence and this point ($\alpha < 10^{-3}$ or so) the oscillations are respectively either critically damped away or made highly irregular. For more intermediate values, somewhat normal oscillatory behaviour may briefly persist, but too transiently and with too little amplitude to facilitate reheating.

coupling is strong enough to damp it heavily. However, as α decreases and the GB coupling is weaker (by at least an order of magnitude or so), despite Λ now being closer to the divergence at $\phi = \varsigma$, some amount of oscillation is permitted to occur. This is only possible because $\Lambda > \varsigma$ such that the field is able to bypass its static solution without hitting the divergence. For the cases of $\alpha = 10^{-2}$ and to an extent also 10^{-3}, the oscillations are smooth, sinusoidal and decreasing in amplitude as in normal inflation, but once the effective minimum becomes prohibitively close to ς the GB force experienced by the field is very different depending on which side of the effective minimum it is on. As a result, non-sinusoidal oscillations occur. These distorted oscillations are sharp and short-lived. That is, once the field decreases below $\phi < \Lambda$, the suddenly very steep GB coupling now rapidly kicks it back to $\phi > \Lambda$. This is seen when $\alpha = 10^{-4}$ or less, in ever more extreme amounts.

The question, then, is whether this is suitable for perturbative reheating. Unfortunately, the answer is no, as the amplitude of the oscillations is far too small and they persist for too short a time, when they are even present at all, and a negligible

amount of radiation is produced in numerical simulations. Furthermore, the field settles at a point with positive-definite potential energy, and will hence continue to behave as vacuum energy. Any produced radiation would then be prevented from persisting as the dominant fluid thanks to its eventual dilution as the field holds constant. So while this case is intriguing, it is regrettably not useful to proceed with.

Negative shift

As stated, this case looks more promising. For a large enough negative ς, the GB coupling would be essentially zero throughout inflation and reheating, allowing things to proceed as normal, but this would also leave the inflationary spectra unmodified and basically trivialise the theory, so we need to instead consider more moderate or smaller ς values, closer to zero. We know from minimal slow-roll inflation and e.g. Figures 3.2 and 3.3 that the initial oscillations of the inflaton in, say, a quadratic potential will be of an amplitude $\Phi \approx 0.1$, so we expect that $|\varsigma|$ should be of a similar order to this, in order to have a pronounced effect on the oscillatory behaviour. This is shown in Figure 5.4, with two different α values for comparison.

Here we see that, for $\varsigma = -0.05$, the size of the resulting oscillations depends on α. For large α and hence a steep $G(\phi)$, in the left plot, the oscillations can only reach an amplitude of around half the size of ς. Meanwhile, for smaller α, shown in the right plot, oscillations nearly as large as ς may occur, suggesting that the GB coupling only becomes prohibitively strong when much closer to its divergent point. The oscillations are, however, in both cases, rather deformed at first when their amplitude is comparable to ς, exhibiting significant non-sinusoidal variation. This is, again, explained by the sharp variation in $G_{,\phi}$ breaking the usual symmetry of the restoring force on each side of the effective minimum. As the oscillations drop in amplitude due to the expansion of the universe, though, they feel the effect of the GB coupling less strongly due to being farther from the steepest part of the coupling function, and the oscillations relax towards a more sinusoidal waveform. This may be conducive to reheating. While the amplitude is smaller than normal, the oscillations persist for a comparable amount of time, and eventually begin to decrease in amplitude with

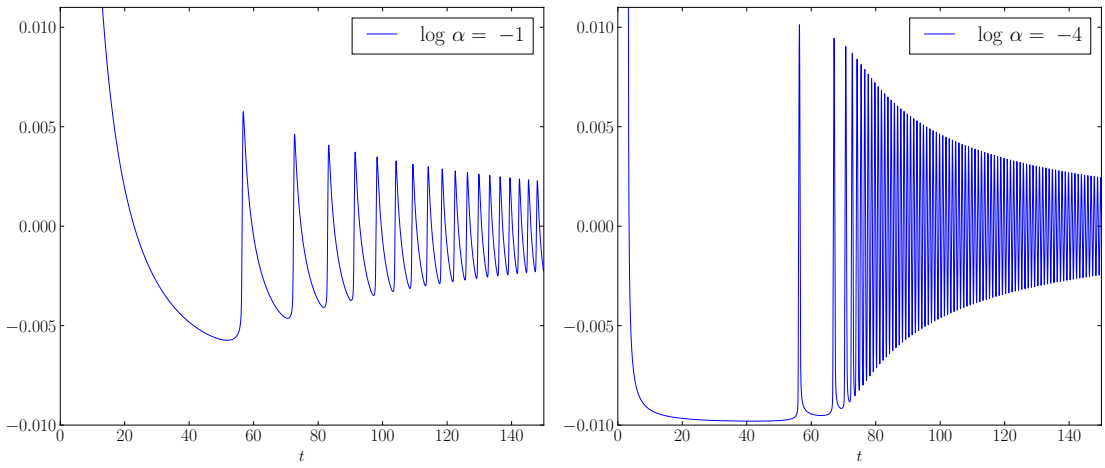

Figure 5.4.: Two examples of the $\varsigma < 0$ model with $\alpha = 10^{-1}$ and 10^{-4} for comparison, with ς taken to be -0.05. For the conservative former case, the displacement of the potential minimum from the GB divergence is comparable to the usual oscillatory amplitude, and this deforms the oscillations and reduces their amplitude (to around half of ς) due to the fairly strong GB coupling in this region. For a smaller α in the second case, the oscillations are more drastically deformed, higher frequency, and surprisingly higher in amplitude - now almost as large as ς allows - due to the less steep GB coupling, that only becomes significant closer to the divergence. As the oscillations persist for longer, decreasing in amplitude at a reasonable rate, and becoming less deformed with time, this may facilitate perturbative reheating, albeit with some changes.

time as approximately $1/t$. That is, something resembling usual post-inflationary oscillation is recovered, despite the initial period of modified behaviour.

There are some questions that arise from this, though. We can ask if the reheating temperature will be high enough to recover the Hot Big Bang's successes, given the less efficient reheating resulting from oscillations of a smaller amplitude (note that eq. (3.2.52) suggests that lower-amplitude oscillations directly cause a reduced rate of radiation production). Similarly, the non-uniformity and deformation of the oscillatory waveform may influence the equation of state during reheating, which, via eq. (3.3.39) may shift the observable window of inflationary perturbations and lead to measurable spectral changes. Similarly, reducing the efficiency of reheating will reduce the final energy density, having a similar effect. That is, if we take the term in eq. (3.3.39) which pertains to reheating and call this ΔN

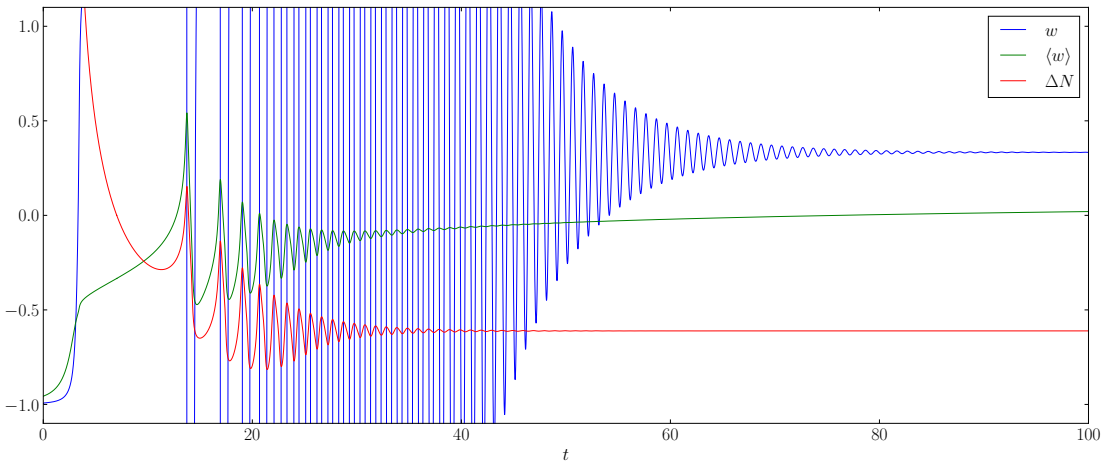

Figure 5.5.: Numerical calculation of the equation of state as a function of time for the trajectory with $n = 2$, $\alpha = 0.1$ and $\varsigma = -0.05$ (the left panel in Figure 5.4). Additionally show is the time-averaged equation of state (3.2.40) and the resulting change in the number of e-folds before the end of inflation that observable fluctuations are generated at, ΔN. The ΔN plot has the following interpretation; if one were to interpret the time $t_{\rm th}$ at which reheating is said to be completed as the time t in the graph, the observable window would be shifted by ΔN e-folds. The relatively constant nature of ΔN as reheating is completed ($w \to 1/3$, we can confidently predict this value independently on precisely when one takes reheating to have been finished.

$$\Delta N = \frac{1 - 3\langle w \rangle}{12(1 + \langle w \rangle)} \ln\left(\frac{\rho_{\rm th}}{\rho_{\rm end}}\right), \tag{5.2.17}$$

and find the relevant energy densities numerically, as well as use eq. (3.2.40) to find $\langle w \rangle$, we can compute the magnitude of these effects. An example is plotted in Figure 5.5.

From the figure we see that as in the standard case we have a successful decay process leading to a radiation-dominated ($w = 1/3$) universe at late times, just as in the minimal case shown in Figure 3.3. The earlier behaviour of w and hence $\langle w \rangle$, however, is rather distorted compared to the usual case as the oscillations in the negative ς model are initially non-sinusoidal (Figure 5.4). This even allows the equation of state to be spuriously larger than 1 or smaller than -1, as the GB-modified energy density and pressure derived from eqs. (5.1.10 – 5.1.11) can, in principle, when $\dot{G}$ is important, make the field behave as a fluid with such an

equation of state. The most important point to take away from this, however, is that $\Delta N(t)$ as defined in eq. (5.2.17) is very well approximated by a constant at late times, once reheating can be said to have completed. This means that we can compute ΔN accurately without worrying about formally defining the time when reheating ends, as the result is moderately agnostic of how, precisely, this is chosen. For the sake of argument, we take the end of reheating in future calculations to mean the point where $\Omega_{\rm r} = 2/3$, though we have also confirmed that our results are manifestly unchanged whether we take this value or, say, 0.9, for example. In this example, we see that a shift in the observable window of about half an e-fold arises, though this number varies for different parameter choices. We can also address the question of the reheating temperature from this calculation, by reading off the radiation energy density around this time, and find that is is reduced compared to a scenario in which we turn off the GB coupling, but still of a similar order ($\sim 10^{13}\,\mathrm{GeV}$) and thus nothing to worry about in terms of, say, facilitating a later period of nucleosynthesis ($\sim 10^{-3}\,\mathrm{GeV}$).

Range of α values

As a supplementary note, the usual result that inflationary behaviour occurs between $0 < \alpha < 1$ in GB coupled inflation is slightly modified for negative ς. Instead, an analysis of the equations of motion, supported by numerical evidence, yields the result that inflationary expansion occurs for $0 < \alpha < \alpha_{\rm max}$, with the upper limit given in terms of the shift parameter by

$$\alpha_{\rm max} \approx \left(1 - \frac{\varsigma}{\phi_0}\right)^{n+1} , \tag{5.2.18}$$

where ϕ_0 is the initial condition for ϕ. Typically we have $\alpha_{\rm max} \approx 1$, so we will ignore this effect in the present work, and restrict our parameter space to $\alpha < 1$ for simplicity.

5.2.4. Effects on spectra from non-standard reheating

The modified dynamics of the reheating oscillations will affect the total radiation density produced, and in turn the reheating temperature via eq. (3.2.54). We assume a fiducial decay rate of $\Gamma = 4 \times 10^{-8}$, for which the normal reheating temperature ($\alpha = 0$) would be $T_{\rm reh} \approx 10^{13}\,\text{GeV}$. We then calculate the new $T_{\rm reh}$ value as a fraction of this for a range of $\alpha \in [0, 1]$ and $\varsigma \in [-0.2, 0]$. The result is obtained numerically via direct integration of the cosmological equations for a scalar field (5.1.10 – 5.1.12) with the addition of a conventional radiation fluid of energy density $\rho_{\rm r}$. This is shown in Figure 5.6.

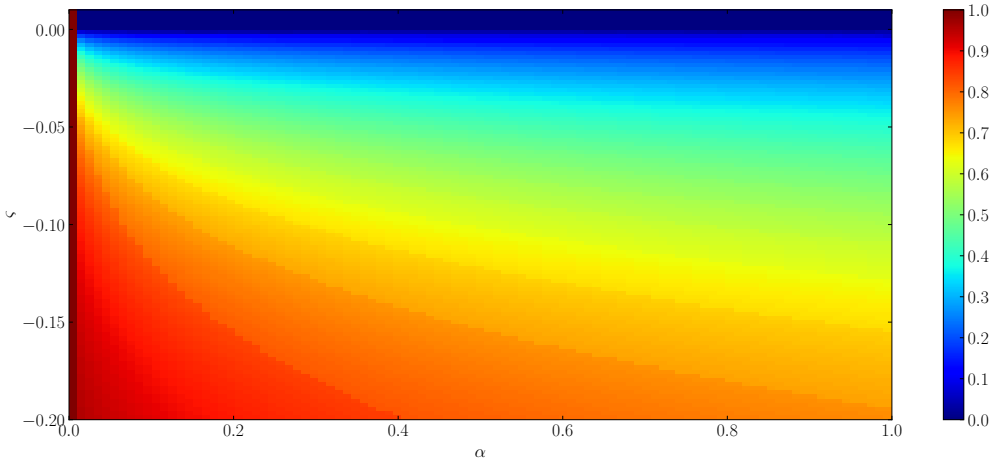

Figure 5.6.: The reheating temperature as defined by eq. (3.2.54), as a function of GB coupling strength α and potential minimum shift parameter ς, for the example case of $n = 2$ and a decay rate of $\Gamma = 4 \times 10^{-8}$. The calculated temperatures are displayed as a fraction of the Gauss-Bonnet-free case ($T_{\rm reh} \approx \mathcal{O}(10^{13}\text{GeV})$). For small α (weak GB coupling) and/or large negative ς (oscillations are hardly affected as $|\varsigma| > \Phi$) the reheating temperature is normal. For positive semi-definite ς, or for sufficiently small ς and very large α, reheating does not occur and the reheating temperature is given as zero. Even the least optimistic scenarios presented here, however, display a reheating temperature only an order of magnitude or two below the conventional case, which is still more than sufficient for e.g. nucleosynthesis.

Furthermore, using eq. (5.2.17) and the results of Figure 5.5, we can calculate the power spectrum for the range of α and ς, each one having a slightly different observable window position due to predicting a slightly different ΔN value, owing to

the difference in the oscillation dynamics that changing the GB coupling parameters brings about. In Figure 5.7 we show the ΔN value as a function of α and ς and the resulting spectral index n_s. This, along with a similar calculation of r, the tensor-to-scalar ratio, can be used to constrain our model parameters.

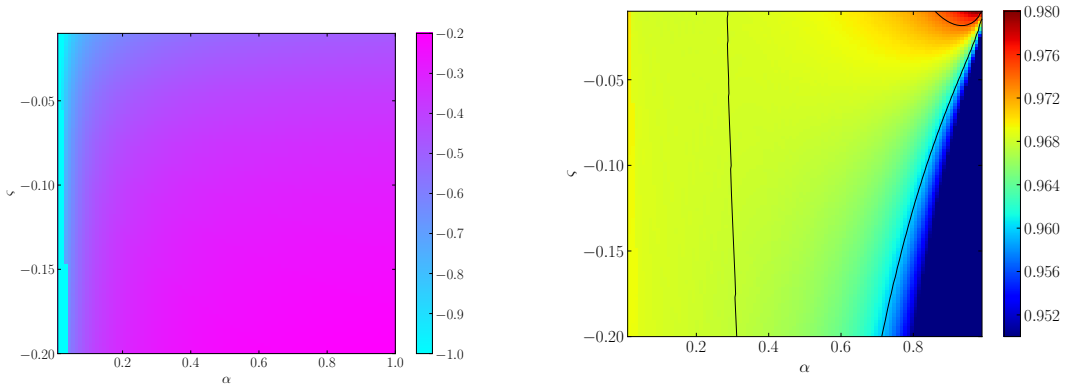

Figure 5.7.: Numerical results for ΔN (left) and the resulting variation in n_s (right), as a function of model parameters α and ς. The GB coupling modifies the dynamics of reheating, and in turn the average equation of state and final energy density, which via eq. (5.2.17) then move the observable window at which the spectral parameters are generated. On the plot of n_s we indicate the areas in tension with current data; the black line at around $\alpha = 0.3$ bounds the region to the left which predicts $r > 0.1$ and hence overproduces gravitational waves. The two contours on the right hand side of the graph bound regions with spectral index either above (upper,red) or below (lower, blue) the Planck 1σ range.[39] The remaining points are consistent with the Planck-measured amplitude of the power spectrum, and possess running parameters α_s and β_s of $O(10^{-3})$.

We have thus shown in some detail that while the simplest GB coupled inverse-power-law models in the literature impede reheating via the diverging G function at the potential minimum, this can be simply avoided by considering a minimal extension where the GB coupling and the potential are shifted by a relative value ς. For a reasonably wide range of values of this shift and the GB coupling strength parametrised by α, detailed in Figures 5.6 and 5.7, it is possible to perturbatively reheat the universe to an acceptable temperature. This does however lead to a non-standard equation of state during the reheating phase which affects inflationary predictions via displacement of the observable window given by eq. (3.3.39) and in turn the N-dependent slow-roll spectral parameters like n_s and r derived from

eq. (5.1.29), however the new values are often compatible with CMB constraints for moderate parameter values.

5.3. Towards Quintessential Inflation with the Gauss-Bonnet term

In the previous sections we took a negative view of the Gauss-Bonnet term's ability to freeze the motion of a scalar field as this impedes the end of inflation, preventing the recovery of the post-inflationary universe via reheating. However, to take a slightly different perspective, we ask what if this phenomenon could be used positively to instead construct a model of dark energy? In particular, what if we could achieve a so-called *quintessential inflation* scenario where the inflaton persists after inflation to eventually become what we today experience as dark energy.[260–291] It is an appealing prospect as the unification of two of the biggest mysteries in cosmology could be solved within one theory, which, owing to their similarities as periods of accelerating expansion, does not seem unreasonable.

Despite the elegance and apparent simplicity of the idea, achieving it is challenging. While inflation occurs at immense energies close to or around the Planck scale in the very early universe, dark energy is comparably tiny. A hundred or more orders of magnitude between their energy scales is not a trivial problem, as simply introducing this vast hierarchy of energy scales in a theory by hand is questionable from a theoretical standpoint. The issue is then further compounded by the point that quantum corrections would render the introduction of such a small energy scale at the classical level futile anyway, without immense fine-tuning. Similarly, if one supposes a potential with a steep exponential decline to allow such a vast change in energy to occur dynamically as the field evolves, one typically finds that the field is displaced by a super-Planckian amount, a scale over which we cannot be confident in the real behaviour of without a concrete understanding of physics at such large energies, which we presently lack. It is in this latter detail that the GB effect might be useful, though. If the GB-sourced impedance of the field can prevent it undergoing a trans-Planckian excursion, then we could potentially avoid

this problem that plagues simpler quintessential inflation scenarios.

To model this, we need an inflationary potential which allows the field to continue to decrease in energy after inflation so that it can drop to the dark energy scale without reaching zero. This first ingredient makes it likely that conventional reheating will not be possible, so a process like instant preheating may be needed. Further to this, we also need a GB coupling that becomes large at late times to freeze the field so that once the radiation/matter produced by reheating later dilute away, there is a dark energy fluid waiting to dominate the universe in their place. To this end, let us consider the potential

$$V(\phi) = \frac{V_0}{2}\left[1 + \tanh\left(p\,\frac{\phi - \phi_c}{M_{\rm Pl}}\right)\right], \quad p > 0\,. \tag{5.3.1}$$

and the GB coupling function

$$G(\phi) = G_0 e^{-q\phi/M_{\rm Pl}}, \quad q > 0\,, \tag{5.3.2}$$

while again assuming $F = 1$ for simplicity. As shown in eq. (5.2.11), with exponential potential and coupling, one doesn't need to introduce the Jordan Frame function F to gain control over where the field freezes, unlike with power law coupling and eq. (5.2.9). While our potential here is technically tanh and not a straightforward exponential, consider that following an inflationary period where the field begins at large and positive $\phi \gg \phi_c$ and rolls down the potential towards negative field values, we require the field to freeze when it has rolled sufficiently far for its energy to be suppressed down to the level of dark energy. That is, when $p\phi$ is large and negative, at which point the potential can be approximated to leading order by

$$V(\phi) \approx V_0 e^{2p\phi/M_{\rm Pl}}\,. \tag{5.3.3}$$

In essence, then, when considering the static solution - which we will here call ϕ_s - we have the result of eq. (5.2.11), but with a potential exponent of $2p$, that is

$$\phi_s = \phi_c + \frac{M_{\rm Pl}}{q - 2p}\ln\alpha\,, \tag{5.3.4}$$

where

$$\alpha \equiv \frac{2qV_0G_0}{3pM_{\rm Pl}^2}\,. \tag{5.3.5}$$

and as discussed previously, freezing of the field occurs when we have $q > 2p$. For generality, we have also introduced the parameter ϕ_c in the potential, but by noting that under a field redefinition $\phi \to \phi + \phi_c$, we have the GB coupling prefactor behaving as $G_0 \to G_0 e^{q\phi_c}$. The value of ϕ_c can hence be set equal to 0 without loss of generality, as it can be absorbed into a rescaling of the GB coupling. We will henceforth neglect it. Also note that we have explicitly reinstated $M_{\rm Pl}$ into the above equations to make a point about the values of p and q. By re-interpreting, e.g. the GB coupling as

$$G(\phi) = G_0 e^{-\phi/M}\,, \tag{5.3.6}$$

where M is some mass-scale, what value might it have? One would like it to be of a sufficiently high energy scale that it represents new physics beyond the standard model and is feasibly stable under quantum corrections, but below the Planck scale, perhaps around the energy of grand unification theories, e.g. $M \sim M_{\rm Pl}/100$ or so. This would imply by comparison to the coupling function written in terms of q, that $q \approx O(10^2)$ would be ideal. A similar argument applies to p. As one goal of this approach is to achieve quintessential inflation while avoiding naturalness issues, it is important to bear in mind how realistic the numbers proposed in this context are. With that said, let us move on to the inflationary considerations of this model.

5.3.1. Inflation

As inflation is assumed to occur on the upper plateau of the tanh potential, when $p\phi$ and hence $q\phi$ is large (as $q > p$ for the static solution to exist, numerically), we expect the GB coupling to be negligible in this limit as it is exponentially suppressed by $q\phi$. While this is entirely an artefact of our arbitrary choice of coupling function, for now we do not worry about this. While it is of course true that one could consider more general scenarios where the GB coupling plays a role in inflation, we

are first interested in what role it can play later. It would be interesting to construct a similar scenario to this from a fundamental physical theory featuring the GB term like String Theory, as this might lead to the same parameters influencing inflationary parameters (e.g. spectral index, tensor-to-scalar ratio) and the properties (equation of state, etc) of dark energy. Here, though, we take a more simplistic approach of just having inflation proceed in a straightforward way and only invoking the GB coupling when it is needed for our main goal of achieving quintessential inflation.

As the potential is flat in this plateau region, the slow-roll approximation should suffice for computations. Using eq. (3.2.18) we find for the potential (5.3.1) that

$$\epsilon_0 = \frac{p^2}{2}\left[1 - \tanh\left(p \times \frac{\phi}{M_{\rm Pl}}\right)\right]^2 , \tag{5.3.7}$$

which, via solution of $\epsilon_0 = 1$ implies an end-point of inflation at field value

$$\phi_{\rm end} = \frac{M_{\rm Pl}}{p}\tanh^{-1}\left(1 - \frac{\sqrt{2}}{p}\right) . \tag{5.3.8}$$

To determine when inflation must begin to produce sufficient expansion before reaching the point $\phi_{\rm end}$, we perform the integral (3.2.24) to find that in this case

$$\begin{aligned} N &= \frac{1}{M_{\rm Pl}}\int_{\phi_{\rm end}}^{\phi}\frac{{\rm d}\phi}{\sqrt{2\epsilon}} \\ &\simeq \frac{1}{4p^2}e^{2p\phi/M_{\rm Pl}} + \frac{\phi}{2pM_{\rm Pl}} - \frac{1}{2p^2}\left[\frac{p}{\sqrt{2}} + \tanh^{-1}\left(1 - \frac{\sqrt{2}}{p}\right) - \frac{1}{2}\right] , \end{aligned} \tag{5.3.9}$$

which can be approximately inverted in the limit where the first term is dominant (which is expected, as inflation occurs when $p\phi$ is large and positive) to obtain

$$\phi(N) \approx \frac{M_{\rm Pl}}{2p}\log 4p^2 N . \tag{5.3.10}$$

This suggests an initial condition for a desired e-fold number (typically 50 – 60). We can determine spectral parameters, then, using the standard result (3.3.36) and derived expressions such as eq. (3.3.37) to find power spectra N e-folds before the end of inflation, giving the results

$$\mathcal{P}_{\mathcal{R}} = \frac{H^2}{8\pi^2\epsilon} = \frac{p^2 V_0 N^2}{3\pi^2 M_{\rm Pl}^4}\,, \tag{5.3.11}$$

where in the second equality we have used the Friedmann equation approximated as $3H^2M_{\rm Pl}^2 = V$ and the above results to rewrite e.g. ϵ_0 in terms of ϕ and then N. We also have, following a similar process to determine ϵ_1 in these terms, the result

$$n_s - 1 = -2\epsilon_0 - \epsilon_1 = -\frac{4p^2\left(1+8p^2N\right)}{\left(1+4p^2N_*\right)^2} \approx -\frac{2}{N}\,, \tag{5.3.12}$$

and

$$r = 16\epsilon = \frac{32p^2}{\left(1+4p^2N\right)^2} \approx \frac{2}{p^2N^2}\,. \tag{5.3.13}$$

These are generally good predictions for the spectral index and tensor-to-scalar ratio. The inverse-square dependence on N in eq. (5.3.13) is conducive to suppressing the tensor-to-scalar ratio over cases like the power law potential inflation discussed in Chapter 3, which has $r \propto 1/N$. Similarly, a fiducial value of $N = 60$ places $n_s \approx 1 - 2/N$ very close to the Planck best fit value. We also note that for a given model with a certain p value, eq. (5.3.11) entirely specifies V_0 by comparison to the experimentally measured amplitude.

5.3.2. Late time behaviour and reheating

The result (5.3.4), alongside numerical investigation, demonstrates that there will be no conventional perturbative reheating in this model, much like in Section 5.2.1. In that section, we saw a model which would usually be able to reheat but is impeded by the GB term and instead inflation does not end. Here, the situation is slightly different because event without the GB term, perturbative reheating would not occur anyway because of the non-oscillatory potential. Instead, instant preheating would have to be used from the start. As discussed in Section 3.2.5, instant preheating occurs when the non-adiabaticity condition on the mass of decay products χ, $|\dot{m}_\chi| > m_\chi^2$, is fulfilled, allowing particle production, and this occurs typically when the ϕ-dependent mass of the decay products rapidly changes. Or in other words, when

ϕ rapidly changes. Our tanh potential has the means to achieve this built in; with sufficiently large p (which we want anyway to be able to suppress the energy of the late-time inflaton enough to make it serve as dark energy later), the region around $\phi = 0$ is very steep and hence suitable for this. This also occurs much before we want the GB term to become important, so it will not interfere in this. Assuming the same simple inflaton-matter coupling discussed in Section 3.2.5, we can therefore use the standard result derived there in eq. (3.2.67). Assuming that $\nu = 0$ for simplicity, this result reduces to

$$\rho_\chi = \frac{g^{5/2}|\dot{\phi}|^{3/2}_{t=t_{\rm ip}}}{8\pi^3}|\phi_{\rm ip}|\,, \tag{5.3.14}$$

where $t_{\rm ip}$ is the time at which instant preheating occurs, at which point $\phi = \phi_{\rm ip}$. These values are found in numerical simulations of the post-inflationary dynamics by identifying the time at which the above adibaticity condition is first broken. The parameters of importance to determining the size of ρ_χ are the steepness of the potential, p, which affects the field's velocity at $t_{\rm ip}$, and the coupling constant between the inflaton and matter, g.

There are some complications to consider, however. We expect that over the very short amount of time that instant preheating occurs, energy is conserved, so that the field will be left with some energy ($\rho_{\phi,\rm a}$) equal to the difference between its energy immediately before $t_{\rm ip}$ ($\rho_{\phi,\rm b}$) and the ρ_χ calculated in eq. (5.3.14). To bring about the onset of radiation domination following $t_{\rm ip}$, it is essential that ρ_χ is greater than $\rho_{\phi,\rm a}$. This implies, using energy conservation, that the final radiation density should be half or more the initial scalar field density, or

$$\rho_\chi > \rho_{\phi,\rm a} \quad \rightarrow \quad \rho_\chi > \frac{1}{2}\rho_{\phi,\rm b}\,. \tag{5.3.15}$$

Similarly, we want to avoid the problem that we found with instant preheating in Section 5.2.1. That is, with a potential-dominated inflaton, even if it is initially sub-dominant, it will dilute less rapidly than matter/radiation and hence quickly bring about another inflationary epoch. This is of course the eventual goal; a realisation of another accelerating expansion to produce dark energy. However, we want to

avoid this being the case immediately following instant preheating as we need there to be extended radiation/matter-dominated epochs before this occurs. This means that the field must not be potential-dominated post-reheating else it may not dilute sufficiently fast to permit radiation domination to persist. In other words, the final scalar density should be more than double the scalar potential (such that the majority of its energy is kinetic). After some manipulation, and using the assumption that the field's potential energy is constant throughout instant preheating (that is, the energy being converted to radiation is purely of kinetic origin), this leads us to another inequality for the produced radiation density

$$\rho_{\phi,\mathrm{a}} > 2V(\phi_{\mathrm{ip}}) \quad \rightarrow \quad \rho_{\chi} < \rho_{\phi,\mathrm{b}} - 2V(\phi_{\mathrm{ip}})\,. \tag{5.3.16}$$

Combining these inequalities give us the following bounds on the acceptable values of ρ_{χ} produced by instant preheating as

$$\frac{1}{2}\rho_{\phi,\mathrm{b}} < \rho_{\chi} < \rho_{\phi,\mathrm{b}} - 2V(\phi_{\mathrm{ip}})\,. \tag{5.3.17}$$

The interpretation of this is that the radiation density must be sufficiently large to dominate over the final scalar density, but not so large as to sequester all of the field's kinetic energy so as to make it potential-dominated again. It is easier to meet these conditions if the field therefore comes into the instant preheating window with a small potential but plenty of kinetic energy. For some parameters, this range of allowed values may have zero size, which would indicate that the model is infeasible in those cases. This can be used to rule out some parameters, as we will see later. The set of parameters ruled out in this way is inextricably linked to the assumption we make as to what constitutes a sufficient overdensity of radiation over residual scalar, or a sufficient excess of kinetic energy over potential, in constructing the above inequalities, so here we have made an admittedly arbitrary choice for the sake of making progress and demonstrating the principle behind the model. It is however true that we could formally introduce a parameter, say β, representing the required ratio of quantities needed to constitute domination for the purpose of obtaining the correct subsequent evolution. That is, our constraints would become $\rho_{\chi} > \beta\rho_{\phi,\mathrm{a}}$ and

$\rho_{\phi,\mathrm{a}} > (\beta+1)V$, such that the total bounds would then be

$$\frac{\beta}{\beta+1}\rho_{\phi,\mathrm{b}} < \rho_\chi < \rho_{\phi,\mathrm{b}} - (\beta+1)V(\phi_{\mathrm{ip}})\,. \tag{5.3.18}$$

Then, results could be obtained in terms of β to parametrise our uncertainty in this value so that accompanying numerical work determining the β value actually necessary to give way to a radiation-dominated epoch could produce more precise constraints. One could even extend this further by allowing two different parameters such that each inequality can represent domination by a different ratio as they may not necessarily be equal. We do not however undertake this here, and merely note this detail as a point of interest for future work attempting similar things. We hence go forth assuming $\beta = 1$ as in eq. (5.3.17).

5.3.3. Post-reheating evolution of field

We restrict ourselves to parameter space in which the inequalities (5.3.17) are obeyed, and hence by construction the field is kinetically-dominated rather than potential-dominated in the period following instant preheating. Its equation of motion is then approximated by

$$\ddot{\phi} + 3H\dot{\phi} \approx 0\,, \tag{5.3.19}$$

where H is now determined primarily by the radiation (or later, dust) dominating the universe, so it will scale roughly as $H \sim k/t$. We call this time following preheating the kination period. It is in this period that conventional quintessential inflation[262,292] leads to a super-Planckian field displacement, as the unimpeded field obeys this equation indefinitely. We solve eq. (5.3.19) for $t > t_{\mathrm{ip}}$ as

$$\phi(t) = \phi_{\mathrm{ip}} - M_{\mathrm{Pl}}\sqrt{6\Omega_{\mathrm{ip}}}\left(\frac{k}{3k-1}\right)\left[1-\left(\frac{t_{\mathrm{ip}}}{t}\right)^{3k-1}\right], \quad (t < t_{\mathrm{gb}}) \tag{5.3.20}$$

where k is the exponent in eq. (3.1.14): $k = 1/2$ for radiation domination, or $2/3$ for the dust case. It is kept general for now just because it is easy to do so and it may be useful or informative to inspect some results with both values. We also define, here,

$\Omega_{\rm ip}$ as the density parameter of the inflaton at the time of instant preheating, which we will obtain numerically when needed. It appears in the above result because in kinetic domination, the Friedmann equation is $\dot{\phi}^2 = 6\Omega_{\rm ip}H^2M_{\rm Pl}^2$ and this is used to set a boundary condition for $\dot{\phi}(t_{\rm ip})$. The second boundary condition comes simply from specifying the field value at $t_{\rm ip}$ is called $\phi_{\rm ip}$.

Unlike in conventional quintessential inflation, this solution will only remain valid until the GB coupling becomes important. While the full Klein-Gordon equation (5.1.4) is too complex to solve exactly in a radiation-dominated background, we note that at late times when the field is strongly impeded by the large GB coupling, we could instead use the approximation

$$3H\dot{\phi} + 12M_{\rm Pl}^2H^2G_{,\phi}(\dot{H}+H^2) \approx 0\,. \tag{5.3.21}$$

That is, neglecting the second derivative *à la* slow-roll (and continuing to neglect the potential because it is heavily exponentially suppressed) but including now the GB term in the equation of motion, we can predict the behaviour of the field sufficiently long after the GB term becomes important. We estimate the time when the GB term first is significant enough to make the field approximately obey (5.3.21) rather than (5.3.19) as the time when the neglected terms in each limit are equal in magnitude, i.e. $|\ddot{\phi}| = |12M_{\rm Pl}^2H^2(\dot{H}+H^2)G_{,\phi}|$. We will call this time of the GB term's first significance $t_{\rm gb}$. Solving eq. (5.3.21) for $t > t_{\rm gb}$ we find

$$\phi(t) = \phi_{\rm gb} + \frac{M_{\rm Pl}}{q}\ln\left[1 + 2G_0q^2k^2(1-k)e^{-q\phi_{\rm gb}/M_{\rm Pl}}\left(\frac{1}{t^2}-\frac{1}{t_{\rm gb}^2}\right)\right]\,, \tag{5.3.22}$$

which, at late times $t \gg t_{\rm gb}$ is approximated as

$$\phi(t \gg t_{\rm gb}) \approx \phi_{\rm gb} + \frac{M_{\rm Pl}}{q}\ln\left(1 - \frac{\beta G_0q^2e^{-q\phi_{\rm gb}/M_{\rm Pl}}}{t_{\rm gb}^2}\right) \approx \phi_{\rm gb}\,, \tag{5.3.23}$$

where $\beta = 2k^2(1-k)$ is a constant.[2] We note from trying out some fiducial values of parameters that the second term in this expression is typically small, such that after $t_{\rm gb}$ when the GB term first becomes important in the field equations, the field does

[2]For reference, $\beta = 1/4$ for radiation and $8/27$ for matter.

not evolve much further and remains close to $\phi = \phi_{\rm gb}$. This is not unexpected based on results in previous sections as we know a large GB coupling tends to freeze the field. Regardless, this solution shows that the field's final value is dependent on the time $t_{\rm gb}$ at which the GB term is important. Our next step, then, is to compute $\phi_{\rm gb}$ and $t_{\rm gb}$. We can approximate this by solving $|\ddot{\phi}| = |12M_{\rm Pl}^2 H^2(\dot{H}+H^2)G_{,\phi}|$ where ϕ is given by eq. (5.3.20) to obtain the following expression for $t_{\rm gb}$

$$A t_{\rm gb}^{\nu} = \exp\left(-B t_{\rm gb}^{\mu}\right) , \tag{5.3.24}$$

where the four constants in this equation are given by combinations of model parameters and quantities derived from them as

$$A = \frac{1}{2qkG_0(1-k)}\sqrt{\frac{3\Omega_{\rm ip}}{2}}\exp\left(q\phi_{\rm ip}/M_{\rm Pl} - \frac{qk\sqrt{6\Omega_{\rm ip}}}{3k-1}\right) t_{\rm ip}^{3k-1} , \tag{5.3.25}$$

$$B = qk\sqrt{6\Omega_{\rm ip}}\left(\frac{t_{\rm ip}^{3k-1}}{3k-1}\right) , \tag{5.3.26}$$

$$\mu = 1-3k , \tag{5.3.27}$$

$$\nu = 3-3k . \tag{5.3.28}$$

This equation is nonlinear and not solvable with standard functions, but we can define a special function $W(x)$ that is the inverse function of xe^x such that $We^W = x$. This is often referred to as the Lambert W Function. In terms of this special function, we can solve for $t_{\rm gb}$ to find

$$t_{\rm gb} = \left[\frac{\nu}{B\mu}W\left(\frac{B\mu}{\nu}\left(\frac{1}{A}\right)^{\frac{\mu}{\nu}}\right)\right]^{\frac{1}{\mu}} , \tag{5.3.29}$$

Next, we can "stitch" together the two asymptotic solutions (5.3.22) and (5.3.20) such that the solution of the latter is used to set approximate initial conditions for the former at the crossover point $t_{\rm gb}$. It is important to note that the $W(x)$ function has two branches in the region $(-e^{-1} < x < 0)$, implying that there are two times at which equality between kinetic and GB contributions is achieved. Only the earlier of the two solutions (provided by the lower branch of W, denoted W_{-1}) is typically

valid, though, as the latter solution would occur at some later time at which our assumptions are violated (as the GB term has already become important once at the earlier time). We also require that $t_{\rm gb} > t_{\rm ip}$ due to our assumptions, so the later of the two solutions (W_0, the principle branch) for $t_{\rm gb}$ would instead be the correct physical solution when the first one is ruled out on such grounds. Additionally, the function W has no real values for $x < e^{-1}$, so such an argument would instead imply that there are no real solutions for $t_{\rm gb}$ which would rule out the parameters leading to this, as it either implies that conventional quintessential inflation proceeds unimpeded by the GB contribution, or that the GB term is dominant before instant preheating and acts too early to produce dark energy. This consideration imposes the constraint

$$\frac{B\mu}{\nu}\left(\frac{1}{A}\right)^{\frac{\mu}{\nu}} \geq -\frac{1}{e}\,, \tag{5.3.30}$$

on the parameters of the theory. Finally, we also note that it is possible that the physical value of $t_{\rm gb}$ is sufficiently large that it is not in practice reached within the present age of the universe. The physical meaning of this would be that the GB impedance slows the field down enough that it cannot reach its ultimate late-time state in the available time.

Evaluating eq. (5.3.23) with the $t_{\rm gb}$ value computed above, then, we obtain a quantity we shall call ϕ_m

$$\phi_m = \phi(t \gg t_{\rm gb}) \approx \phi_{\rm ip} + \frac{M_{\rm Pl}B}{q}\left(t_{\rm gb}^{\mu} - t_{\rm ip}^{\mu}\right) + \frac{M_{\rm Pl}}{q}\ln\left(1 + \frac{\mu B}{2}t_{\rm gb}^{\mu}\right)\,, \tag{5.3.31}$$

which is the final value ϕ will freeze in at during the later matter-dominated epoch. We want ϕ_m should be sub-Planckian to avoid the problems with this in conventional quintessential inflation, though this is a conservative bound if the scenario is the aforementioned one where $t_{\rm gb}$ is comparable to the age of the universe, as even if ϕ_m is super-Planckian, if it is not actually reached by the field then it's just an upper limit on how far the field might be displaced, rather than its achieved maximum displacement.

Here, as the field's velocity has been heavily suppressed by the GB coupling, we expect its equation of state to be close to -1 again, and hence suitable to eventually behave as dark energy. As right now its potential energy is $V(\phi_m)$, which, for large p, will be very small, it will remain subdominant until the remaining matter is diluted to a lower density. Then, at very late times, when $\Omega_m \ll 1$ and the universe is strongly dominated by dark energy, the field will obey the equations of motion in the matter-free static limit and tend to freeze at the value ϕ_s determined in eq. (5.3.4). We hence propose that today, we are somewhere between the field values ϕ_m and ϕ_s as present observations indicate that $\Omega_m \approx 0.3$. However, as the equation of state for dark energy is $w \approx -1$, this model predicts that the field could be not exactly frozen yet, but instead slowly rolling. This field value today, which we will determine next, and is somewhere between ϕ_m and ϕ_s, should be sub-Planckian to avoid the usual problems.

5.3.4. Producing dark energy

We expect that when $\Omega_m = 1$, $\phi = \phi_m$ and when $\Omega_m = 0$, $\phi = \phi_s$, but we are at present between these limits. Here, we will work out exactly where the field must therefore lie between these given the observational data. First, noting that eq. (3.2.17) implies

$$M_{\rm Pl}^2 \dot{H} = -\frac{1}{2}(\rho + p) = -\frac{1}{2}(1+w)\rho = -\frac{3}{2}(1+w)H^2 M_{\rm Pl}^2 \,, \tag{5.3.32}$$

we can rewrite the Klein-Gordon equation as

$$\ddot{\phi} + 3H\dot{\phi} + V_{,\phi} - 6H^4(1+3w)G_{,\phi}M_{\rm Pl}^2 = 0 \,. \tag{5.3.33}$$

Then, assuming $\ddot{\phi}$ remains negligible, we have

$$\dot{\phi} \approx 2H^3(1+3w)G_{,\phi}M_{\rm Pl}^2 - \frac{V_{,\phi}}{3H} \,. \tag{5.3.34}$$

The Friedmann equation, meanwhile, can be broken up into parts depending only on the field and only on matter using the definition of the density parameters, such

that we can write

$$3H^2M_{\rm Pl}^2\Omega_\Lambda = \frac{1}{2}\dot{\phi}^2 + V + 12M_{\rm Pl}^2H^3G_{,\phi}\dot{\phi}\,. \tag{5.3.35}$$

Substituting eq. (5.3.34) into this, then, yields a constraint equation

$$V+\frac{V_{,\phi}^2}{18H^2}+\left[3\Omega_\Lambda+\frac{2}{3}(7+3w)V_{,\phi}G_{,\phi}\right]M_{\rm Pl}^2H^2+2(1+3w)(13+3w)(M_{\rm Pl}^2G_{,\phi})^2H^6=0\,. \tag{5.3.36}$$

Or, in terms of our particular forms of V and G, we can solve this equation for $\phi_{\rm de}$, the value of ϕ today, as

$$\begin{aligned}V_0e^{2p\phi_{\rm de}/M_{\rm Pl}}+\frac{2p^2V_0^2}{9H^2M_{\rm Pl}^2}e^{4p\phi_{\rm de}/M_{\rm Pl}}+2q^2G_0^2M_{\rm Pl}^2H^6(1+3w)(13+3w)e^{-2q\phi_{\rm de}/M_{\rm Pl}}\\+\frac{4}{3}qpG_0V_0H^2(7+3w)e^{(2p-q)\phi_{\rm de}/M_{\rm Pl}}-3H^2M_{\rm Pl}^2\Omega_\Lambda=0\,.\end{aligned} \tag{5.3.37}$$

This is highly nonlinear and complex, but with the substitution

$$\phi_{\rm de}\to-\frac{M_{\rm Pl}}{2p}\log\chi\,, \tag{5.3.38}$$

it reduced to a polynomial in χ with terms

$$\lambda_0+\lambda_1\chi+\lambda_2\chi^2+\lambda_3\chi^{1+\frac{q}{2p}}+\lambda_4\chi^{2+\frac{q}{p}}=0\,, \tag{5.3.39}$$

such that for certain ratios q/p it is analytically solvable, and for others either approximately or numerically more tractable than the $\phi_{\rm de}$ constraint. We will not here give the precise forms of the λ_n coefficients but note that for typical parameters today, very small numbers such as e.g. $H = H_0 \approx 10^{-60}M_{\rm Pl}$ are present and this renders many of these coefficients of vastly different orders of magnitude, and hence one must be careful to use sufficiently high-precision arithmetic when numerically evaluating them.

We proceed to solve this using $\Omega_\Lambda = 0.7$, $w = \Omega_\Lambda w_\Lambda + \Omega_m w_m \approx -0.7$, V_0 given by inflation constraints (5.3.11), and a range of possible model parameters p, q

and G_0. This then tells us, for each set of parameters, what field value must be realised today in order for the observational data on Ω_Λ and such to make sense. Multiple solutions are technically possible, but many will be immediately ruled out by sign, or order of magnitude, for example. There may be some parameter space where no sensible solutions occur and that is in itself a constraint in principle. The requirement that the resulting $\phi_{\rm de}$ value is sub-Planckian will be the main physical constraint here, though. In what follows we will now summarise all the constraints we have accumulated and use them to constraint parts of the parameter space.

5.3.5. Constraints from cosmology

To summarise, then, we have the following cosmological history and resulting constraints.

1. Inflation occurs for $\phi > 0$. We fix V_0 using (5.3.11) and (5.3.12 – 5.3.13) imply limits on p.

2. Instant preheating occurs at $\phi_{\rm ip} \approx 0$. The inequalities (5.3.17) constrain a combination of model parameters (p, g).

3. The field undergoes kination and then the GB term becomes important later, giving an upper limit to the field's displacement ϕ_m (5.3.31) which should be $O(M_{\rm Pl})$ at worst. This constrains a combination of p, q and G_0.

4. The field is now rolling slowly between ϕ_m and ϕ_s, and the present day value (5.3.37) should be sub-Planckian, too, constraining p, q and G_0.

There are evidently not enough constraints to solely determine all the viable parameters, so we must in the definition of the model specify some relation between them. Fortunately we have something already approaching this in the statement that the matter-free static solution ϕ_s only exists when $q > 2p$, so we will consider different models defined by their q/p ratio.

Inflation

With eq. (5.3.11) and $\mathcal{P}_\mathcal{R} \approx 2.2 \times 10^{-9}$ from Planck,[39] we find

$$V_0 \approx \frac{6.5 \times 10^{-8}}{p^2 N^2} M_{\rm Pl}^4 \approx \frac{1.8 \times 10^{-11}}{p^2} M_{\rm Pl}^4 \,, \quad (N_* \approx 60) \,. \tag{5.3.40}$$

For 60 e-folds of inflation, the tensor-to-scalar ratio (5.3.13) has a maximum value of $r = 0.03$ no matter what p value is considered. As this is a factor of 3 or so below present observational limits, we cannot impose any limits on p via this. However, the full expression for the spectral index in eq. (5.3.12) requires $p \gtrsim 0.1$ to meet the Planck limits. This is already much smaller that what we intuitively want based on units (see eq. (5.3.6) and discussion) and the idea that we want the potential to be steep to avoid super-Planckian excursions anyway. For larger p, however, the spectral index is independent of p, and predicts $n_s = 0.9678$, which is near ideal, so we cannot say much more than this.

Given the V_0 from eq. (5.3.40) we can also see roughly what p value we might need to get a dark-energy level suppression of energy within an at-most Planckian field displacement. Using $\phi = M_{\rm Pl}$ and eq. (5.3.3), we see that $2p \approx \ln(V_0/\Lambda) \approx O(100)$, where $\Lambda \approx 10^{-120} M_{\rm Pl}^4$ is the dark energy scale. This is nice because then, (5.3.40) is roughly $V_0 \simeq 10^{-15} M_{\rm Pl}^4$, or $V_0^{1/4} \simeq 10^{14}\,\text{GeV}$, which is a typical Grand Unification energy scale.

Reheating and Dark Energy

Using a numerical integration of the equations of motion to determine the energy density after inflation at the point of instant preheating, the field velocity at this time, and so on, as needed to assess the inequalities in eq. (5.3.17), then using the values from this to similarly evaluate eq. (5.3.31) and eq. (5.3.37), for a range of models specified by their q/p ratio, their G_0 value, and their g coupling for preheating, we obtain the results in Table 5.1 constraining p for each case.

We can see that in each case, $p = O(100)$ as estimated from the discussion in Section 5.3.5. We have considered two different G_0 values: first a Planckian value of $G_0 M_{\rm Pl}^2 = 1$ (note the units, as defined in eq. (5.1.1) and the following discussion)

$G_0 M_{\rm Pl}^2$	q/p	g	p limits
1	4	0.8	$86 < p < 100$
		0.9	$86 < p < 238$
		1	$86 < p < 507$
	8	0.8	$51 < p < 100$
		0.9	$51 < p < 207$
		1.0	$51 < p < 370$
100	4	0.8	$85 < p < 100$
		0.9	$85 < p < 238$
		1.0	$85 < p < 507$
	8	0.8	$51 < p < 72$
		0.9	$51 < p < 155$
		1.0	$51 < p < 258$

Table 5.1.: Table of bounds for p in GB coupled quintessential inflation for various models specified by G_0, q/p and the g coupling to matter. For each example, we find that the lower bound on p is due to imposition of the sub-Planckian nature of $\phi_{\rm de}$ today. Similarly, the upper bounds on p arise are due to the reheating inequalities in eq. (5.3.17) being violated otherwise.

and then a more sub-Planckian value of 100. This choice barely affects the bounds for the $q = 4p$ models, but when instead $q = 8p$, the upper limits are altered by consideration of a different G_0 value; this can be interpreted as the GB term becoming too strong too early and affecting reheating. We also considered three values of the coupling g in each of these four cases, and from our results it is clear that allowing a larger g widens the acceptable parameter space, but for the models studied we saw that going below $g \approx 0.8$ makes it difficult to find successful models. In each case, the allowed range of p values quoted do not violate any of the discussed constraints, but as we go below or above these limits one or more constraints are violated. In practice, for overly small p, we find that $\phi_{\rm de}$ becomes super-Planckian as the potential is not steep enough to reach the scale of dark energy within a sub-Planckian field displacement, and for overly large p we instead find that reheating is the problem; most likely this is because the steeper potential allows the non-adiabaticity condition to be fulfilled at a point where the field still possesses large amounts of potential energy.

5.3.6. Tests of modified gravity as further constraints

As we have modified gravity to develop this model, there could in principle be observable deviations from GR in e.g. Solar System tests of gravity. Some pre-existing work that discuss limits on the size of a GB-coupled scalar for these purposes[293–295] has been done before, but critically is based on the assumption that $V_{,\phi} \approx V_\phi$, which is of course not true in our case, where the parameter p sets the ratio between these functions and is rather larger than $O(1)$. Nevertheless, in the absence of constraints more tuned to our situation, we will use this existing work as a starting point to get an approximate idea. Doing so, we find their strongest constraint coming from the Cassini spacecraft's measurements of time delay in a gravitational field, which implies the limit

$$M_{\rm Pl}|G_{,\phi}| \lesssim 1.6 \times 10^{20}\ {\rm m}^2 \approx 1.5 \times 10^{88} M_{\rm Pl}^{-2}\,, \tag{5.3.41}$$

The constraint is on the combination of parameters $G_{,\phi} = qG_0 e^{-q\phi/M_{\rm Pl}}$, which is much more strongly dependent on the super-exponential contribution of q than the linear G_0 factor, therefore a small change in q would easily cancel out a change of an order of magnitude or more in G_0. We hence apply this constraint to q to find, again, using the Lambert W function defined above, that for a given G_0 value and field displacement $\phi_{\rm de}$, q must obey

$$q \lesssim -\frac{M_{\rm Pl}}{\phi_{\rm de}}\, W\left(\frac{1.5\times 10^{88}}{G_0 M_{\rm Pl}^2}\right)\,. \tag{5.3.42}$$

Assuming a Planckian field displacement for $\phi_{\rm de}$, which corresponds to the smallest allowed p in each model in Table 5.1, and specialising to the $G_0 M_{\rm Pl}^2 = 1$ model, for example, this constraint is evaluated to $q \lesssim 200$. Meanwhile, the best case scenario in the table of results is $q \approx 300$. This is fairly typical of the constraints, in that we find our q values to be typically a factor of 2 or so too large to meet the Cassini constraint. While, of course, this is all subject to the disclaimer that these limits are derived based on an assumption that does not apply to our model, it does not bode well. We would require the corrected analysis to weaken the constraints in order to make them once again feasible. Failing this, the model may still be saved by e.g. a

screening mechanism but we will not address either of these questions here, instead leaving them to future work.

Finally, we note that the recent observation of a multi-messenger gravitational wave and gamma ray burst signal[6] also can be used to constrain our model. As shown in eq. (5.1.32), a GB coupling predicts a deviation from $c_t = 1$. That is, it predicts that gravitational waves will travel not at the speed of light, but at some other speed. The multi-messenger observation found that the gravitational waves and electromagnetic waves emitted by the same neutron star merger arrived at Earth at the same time, leaving very little uncertainty that $c_t = 1$ to very high precision. This, essentially, rules out all models that require a non-trivial GB coupling to be present in the universe today. Despite this disappointing result, we still believe that this is an interesting example of how using modified gravity to freeze a field may be able to achieve quintessential inflation, even if this exact realisation was, very shortly after its conception, proven wrong by this impressive new frontier in observational astronomy. We nonetheless believe that these results are useful as they could go on to inspire future model building efforts based on similar principles but without explicitly introducing a pathological coupling which affects the tensor speed; there is no a priori reason we would expect modification of the tensor speed to be a necessary condition in achieving a sub-Planckian frozen field.

CHAPTER 6

TESTING INFLATION WITH THE RUNNING OF THE RUNNING OF THE SPECTRAL INDEX

Compared to the previous two chapters which focused on models which realise inflation by modifying gravity, in this chapter we will change direction and look instead at testing inflation. In particular, testing it with higher order deviations from scale invariance in the power spectrum. Based on an article published with Carsten van de Bruck in Physical Review D Rapid Communications,[296] as well as a paper in a special issue of Universe containing the proceedings of the conference Varying Constants and Fundamental Cosmology,[297] we will discuss experimental analyses which motivate this approach before providing a theoretical framework with which to compute relevant quantities in multi-field inflation. This will then be used to discuss the prospect of finding models which fit the data available.

6.1. Motivations to study the Running of the Running

At present most inflation models in the literature, and indeed this thesis, are compared to data via computation of the spectral index n_s and the tensor-to-scalar ratio r. As in Chapter 4, sometimes non-Gaussianity is also utilised, but the existing bounds on this are too rough for it to be as precise a discriminator. Constraints on non-Gaussianity will presumably be improved with time as better data is accumulated, however, so it is widely considered an interesting and useful direction of investigation nonetheless. Higher order terms (collectively referred to as *runnings* of the spectral index) in the power spectrum's series expansion (3.3.28) such as α_s and β_s are of a similar status. To summarise, the basic Planck analysis[39] assumes $\beta_s \equiv 0$ alongside all higher order runnings, and finds that

$$n_s = 0.9655 \pm 0.0062\,, \tag{6.1.1}$$

$$\alpha_s = -0.0084 \pm 0.0082\,, \tag{6.1.2}$$

$$\beta_s \equiv 0\,. \tag{6.1.3}$$

Inflationary models which then predict n_s of around 0.96 and runnings of no more than $O(10^{-3})$ or so are hence favoured by the data. Many simple models of inflation predict just this, so it is unsurprising that very little work calculating α_s (for some examples, see[298–301]), and less still on β_s has been done. It is taken as a kind of common sense that the spectrum is close enough to scale invariant that these extra parameters are more or less negligible and the above approximation should suffice. However, a further analysis[39] by the Planck team which does not assume $\beta_s \equiv 0$ casts some doubt on this, as it finds

$$n_s = 0.9569 \pm 0.0077\,, \tag{6.1.4}$$

$$\alpha_s = 0.011^{+0.014}_{-0.013}\,, \tag{6.1.5}$$

$$\beta_s = 0.029^{+0.015}_{-0.016}\,. \tag{6.1.6}$$

It is worth explicitly noting that these results come with rather large error bars. This is essentially because runnings are hard to measure in CMB experiments which only have access to information on the power spectrum over a modest range of k values. As these running terms are proportional to higher powers of $\log k$ in the parametrisation used, the full extent of their possible influence would only be felt at larger k. While it is hence important to keep these limitations in mind we see that, here, β_s is consistent with a positive value of $O(10^{-2})$ at more than 1σ significance despite the sizeable uncertainty. Furthermore, its value is probably larger than that of α_s according to this result. This provides some motivation to question whether the standard assumption of a near-scale-invariant power spectrum which only significantly departs from scale-invariance in the linear regime, as in eqs. (6.1.1 – 6.1.3), is reasonable. Higher order deviations from scale-invariance would, if non-negligible, provide information of considerable use in testing inflationary models. We see in the second version of the constraints that the quadratic-order running α_s is still largely consistent with zero, but the data at present seems to support the possibility of a large and non-zero cubic deviation from scale invariance in β_s.
The mutability of the results under the inclusion of the next order term in the fit is suspicious. This could of course be a spurious result that with further data will be ruled out with considerable significance - the error bars are large for now and it is too soon to conclude this is definitely real - but it could also be the first hint that we should expect something other than the standard hierarchy of runnings. This is further supported by the more recent analysis of the Planck data by another group,[302] which found

$$n_s = 0.9582^{+0.0055}_{-0.0054}\,, \tag{6.1.7}$$

$$\alpha_s = 0.011 \pm 0.010\,, \tag{6.1.8}$$

$$\beta_s = 0.027 \pm 0.013\,, \tag{6.1.9}$$

further cementing the inconsistency of $\beta_s = 0$ now at more than 2σ. This analysis differs from the Planck in-house analysis in that some additional parameters; the

lensing amplitude A_L, the curvature density parameter Ω_k and the sum of the masses of standard model neutrinos, are taken to be independent. Doing so produces results more strongly consistent with the expectation that A_L and Ω_k are zero, strengthening the argument for this interpretation. Furthermore, the results including non-zero β_s have been found to better fit the Planck data at low multipoles.[39]

As noted, there are considerable uncertainties in these results thanks to the difficulty of measuring β_s, but the statistics do nevertheless suggest the very interesting possibility of non-trivial runnings. Between this and the further suggestions that the fit to the data may be improved in this case, we argue in this chapter that it is worth trying to understand the implications of a large β_s from a theoretical perspective in anticipation of the future confirmation or denial of this result, much like with the similarly-uncertain case of non-Gaussianity. Our goal is not to endorse the idea that the runnings are large, but instead to cautiously acknowledge the possible evidence for this scenario and speculatively investigate further. Before moving onto this theoretical work, we first give a quick overview of the prospects of improving the bounds we have on α_s and β_s given forecasts from future and/or proposed experiments.

6.1.1. Forecasts for the Runnings

Several future experiments give promising forecasts for measurements of the runnings. CMB spectral distortions - slight deviations from a perfect black body spectrum such as the presence of an effective chemical potential term - can be measured and depend on the power spectrum at larger k values than observable CMB anisotropies. This means they are correspondingly more sensitive to higher order terms in the series expansion (3.3.28). Future improvements of our constraints on spectral distortions, such as from the PIXIE[303–306] experiment, would be advantageous in improving our bounds on the runnings.

Future CMB surveys succeeding the very successful existing WMAP and Planck missions, such as CORE[307,308] or PRISM[309] would of course be helpful, but it is also noted that 21 cm mapping[310] experiments using e.g. the Square Kilometre Array[311] would provide useful data, as would propositions of using the Euclid satellite[312] to perform a highly detailed spectroscopic galaxy survey.

A combination of some or all of these propositions,[313] or perhaps equivalent/comparable alternative experiments with the same goals, could bring the size of the uncertainties in α_s and β_s down to as low as $O(10^{-3})$, an improvement of around an order of magnitude over present results. This would be invaluable in confirming or disproving the hints discussed above.

6.2. Spectral runnings in minimal single-field inflation

In Chapter 3 we found that at leading order in a slow-roll expansion, the power spectrum is given by

$$\mathcal{P}_\mathcal{R} = \frac{H^2}{8\pi^2\epsilon_0}\,, \tag{6.2.1}$$

and the spectral index is similarly

$$n_s - 1 = \frac{\mathrm{d}\ln\mathcal{P}_\mathcal{R}}{\mathrm{d}\ln k} = -2\epsilon_0 - \epsilon_1\,. \tag{6.2.2}$$

Extending this calculation to the next two terms in the series expansion (3.3.28), one finds

$$\alpha_s = \frac{\mathrm{d}n_s}{\mathrm{d}\ln k} = -2\epsilon_0\epsilon_1 - \epsilon_1\epsilon_2\,, \tag{6.2.3}$$

$$\beta_s = \frac{\mathrm{d}\alpha_s}{\mathrm{d}\ln k} = -2\epsilon_0\epsilon_1(\epsilon_1+\epsilon_2) - \epsilon_1\epsilon_2(\epsilon_2+\epsilon_3)\,. \tag{6.2.4}$$

It is clear from this that $\alpha_s \sim O(\epsilon^2) \sim (n_s-1)^2$ and $\beta_s \sim O(\epsilon^3) \sim (n_s-1)^3$. At the point of horizon crossing when observable anisotropies are generated, $\epsilon_n \ll 1$ and hence the general result of an almost scale-invariant power spectrum is ensured. For the same reason, however, each running is correspondingly smaller by a factor of $O(\epsilon)$ than the former one, and we consistently obtain for all kinds of potentials and slow-roll scenarios the hierarchy (6.1.1 – 6.1.3). That is, if one has $n_s - 1 \approx -4\times10^{-2}$ to match eq. (6.1.1), one would roughly expect $\alpha \approx 10^{-3}$ and $\beta_s \approx 10^{-5}$, the latter of which is largely consistent with the assumed $\beta_s = 0$ as it is all but undetectable

either way.[314] This is, however, considerably harder to reconcile with the analyses including β_s which predict it is three orders of magnitude larger than this.
Additionally, as one usually has $\epsilon_n \geq 0$, the slow-roll formalism generally predicts negative runnings. Meanwhile, the extended analyses somewhat favour positive α_s and strongly favour positive β_s. This clearly presents a problem should the $\beta_s \neq 0$ hierarchy be confirmed to higher significance; mainstream inflationary theory based on the pillar of slow-roll is fundamentally incompatible with it. This would open the door to more serious consideration of non-slow-roll, multi-field, and other non-standard inflationary scenarios. We hence are motivated to begin considering some of these options and work towards answering questions like which extensions of inflation are best suited to realising diverse hierarchies of runnings.

6.2.1. Slow-roll inflation with a sound speed

To extend the point we are making here, consider the scenario discussed in Section 3.3.8 where the field has a sound speed c_s. We saw there that the power spectrum is now

$$\mathcal{P}_\mathcal{R} = \frac{H^2}{8\pi^2\epsilon_0 c_s}\,, \tag{6.2.5}$$

where c_s is the sound speed of the adiabatic perturbation. If we define a series of slow-roll-like parameters in c_s such that,

$$s_0 = \frac{\dot{c_s}}{Hc_s}\,, \quad s_{n+1} = \frac{\dot{s_n}}{Hs_n}\,, \tag{6.2.6}$$

then, we find results for the spectral index and its runnings:

$$n_s = -2\epsilon_0 - \epsilon_1 - s_0\,, \tag{6.2.7}$$

$$\alpha_s = -2\epsilon_0\epsilon_1 - \epsilon_1\epsilon_2 - s_0 s_1\,, \tag{6.2.8}$$

$$\beta_s = -2\epsilon_0\epsilon_1(\epsilon_1+\epsilon_2) - \epsilon_1\epsilon_2(\epsilon_2+\epsilon_3) - s_0 s_1(s_1+s_2)\,. \tag{6.2.9}$$

We see, again, that the correction terms are correspondingly first, second and third

order in a slow-roll parameter. This kind of hierarchy is unavoidable in single-field slow-roll scenarios because the time derivatives of slow-roll parameters are second order in slow-roll, by construction, as their too-rapid growth would quickly cause them to cease being small and cause a premature end to inflation. In general, the point being made here is that to reconcile inflation with the non-standard running hierarchy including β_s, we must go beyond not just minimal slow-roll inflation, but also slow-roll models with non-minimal inclusions like sound speeds, or e.g. the $F(\phi)R$ and Gauss-Bonnet couplings in Chapter 5, as these all follow the pattern of increasingly small contribution at each order in the series expansion of runnings.

6.3. Multi-field scenarios and Runnings

As we have argued that we need to go beyond the limits of single-field slow-roll inflation, we choose here to see what happens if we relax the assumption of a single field. While instead relaxing the assumption of slow-roll and investigating e.g. local slow-roll violating features in potentials may produce interesting effects, they may have to be unnaturally fine-tuned to occur at the right time and have the right-sized effect on each spectral parameter. Therefore we focus instead on whether more general two-field phenomena may prove useful.

In multi-field inflation the power spectrum is given by

$$\mathcal{P}_{\mathcal{R}} = \mathcal{P}^*_{\mathcal{R}} \times (1 + \mathcal{T}^2_{\mathcal{RS}}) \,, \tag{6.3.1}$$

where $\mathcal{P}^*_{\mathcal{R}}$ is the power spectrum at horizon crossing (note that we will frequently specify or distinguish a quantity as being at horizon crossing with an asterisk in this fashion), and $\mathcal{T}_{\mathcal{RS}}$ is as defined in eqs. (3.3.50 – 3.3.51). Here, all of the inflationary dynamics from the beginning of inflation up to t^* is encoded in this first term, and $\mathcal{T}_{\mathcal{RS}}$ then evolves the result at t^* to the end of inflation. In single-field scenarios, $\mathcal{T}_{\mathcal{RS}} = 0$ as the power spectrum is unchanged on superhorizon scales due to the conservation of the curvature perturbation $\mathcal{R}$ in this regime. However, in multi-field scenarios the presence of a non-negligible isocurvature perturbation $\mathcal{S}$ changes this. The horizon crossing power spectrum $\mathcal{P}^*_{\mathcal{R}}$ is still, in multi-field scenarios, computed

via the same procedure as in single-field scenarios. That is, we use the result (6.2.1) for $\mathcal{P}^*_{\mathcal{R}}$. While the presence of multiple fields changes how matter sources curvature, the dependence of the power spectrum on background objects resulting from the curvature (H, ϵ_0) is unchanged.[1] The spectral index and runnings derived from $\mathcal{P}^*_{\mathcal{R}}$ will still behave the same way as in the standard case. However, the parameters of the power spectrum at the end of inflation will also contain a correction term deriving from $\mathcal{T}_{\mathcal{RS}}$, such that, using the standard definitions of the runnings and spectral index as in Chapter 3, we recursively find at leading order in slow-roll that

$$(n_s - 1) = \frac{\mathrm{d}\ln\mathcal{P}_{\mathcal{R}}}{\mathrm{d}\ln k} = (n_s^* - 1) + \frac{1}{H^*}\frac{\mathrm{d}\ln\left(1+\mathcal{T}^2_{\mathcal{RS}}\right)}{\mathrm{d}t^*}\,, \tag{6.3.2}$$

$$\alpha_s = \frac{\mathrm{d}n_s}{\mathrm{d}\ln k} = \alpha_s^* + \frac{1}{(H^*)^2}\frac{\mathrm{d}^2\ln\left(1+\mathcal{T}^2_{\mathcal{RS}}\right)}{\mathrm{d}(t^*)^2}\,, \tag{6.3.3}$$

$$\beta_s = \frac{\mathrm{d}\alpha_s}{\mathrm{d}\ln k} = \beta_s^* + \frac{1}{(H^*)^3}\frac{\mathrm{d}^3\ln\left(1+\mathcal{T}^2_{\mathcal{RS}}\right)}{\mathrm{d}(t^*)^3}\,. \tag{6.3.4}$$

Here, the first term in each expression is the usual horizon crossing result that will, in normal circumstances, behave much like the single-field result. The difference due to multi-field effects then arises in the second term of each expression, correcting the horizon-crossing value by an amount dependent on the derivatives of $\mathcal{T}_{\mathcal{RS}}$ with respect to the horizon crossing time t^*. It is helpful to apply the chain rule to see this explicitly as

$$n_s = n_s^* + \frac{2}{H^*}\left[\frac{\mathcal{T}_{\mathcal{RS}}}{1+\mathcal{T}^2_{\mathcal{RS}}}\dot{\mathcal{T}}_{\mathcal{RS}}\right]\,,$$

$$\alpha_s = \alpha_s^* + \frac{2}{(H^*)^2}\left[\frac{\mathcal{T}_{\mathcal{RS}}}{1+\mathcal{T}^2_{\mathcal{RS}}}\ddot{\mathcal{T}}_{\mathcal{RS}} + \frac{1-\mathcal{T}^2_{\mathcal{RS}}}{\left(1+\mathcal{T}^2_{\mathcal{RS}}\right)^2}\dot{\mathcal{T}}^2_{\mathcal{RS}}\right]\,,$$

$$\beta_s = \beta_s^* + \frac{2}{(H^*)^3}\left[\frac{\mathcal{T}_{\mathcal{RS}}}{1+\mathcal{T}^2_{\mathcal{RS}}}\dddot{\mathcal{T}}_{\mathcal{RS}} + 3\frac{1-\mathcal{T}^2_{\mathcal{RS}}}{\left(1+\mathcal{T}^2_{\mathcal{RS}}\right)^2}\dot{\mathcal{T}}_{\mathcal{RS}}\ddot{\mathcal{T}}_{\mathcal{RS}} + 2\frac{\mathcal{T}_{\mathcal{RS}}\left(\mathcal{T}^2_{\mathcal{RS}}-3\right)}{\left(1+\mathcal{T}^2_{\mathcal{RS}}\right)^3}\dot{\mathcal{T}}^3_{\mathcal{RS}}\right]\,.$$

Here, noting that the dotted variables indicate derivatives with respect to t^* specif-

[1] When the single-field power spectrum depends on matter-related quantities like c_s as in eq. (6.2.5) this is no longer generally the case, such as when two fields have different sound speeds. This is discussed in Chapter 4 and a related article.[148]

ically, we can use the definitions (3.3.50 – 3.3.51) of the transfer functions and the fundamental theorem of calculus to obtain the following[296]

$$\dot{\mathcal{T}}_{\mathcal{RS}} = -H^* \left[A^* + B^* \mathcal{T}_{\mathcal{RS}}\right] , \tag{6.3.5}$$

$$\ddot{\mathcal{T}}_{\mathcal{RS}} = (H^*)^2 \left[A^* B^* + (B^*)^2 \mathcal{T}_{\mathcal{RS}}\right] , \tag{6.3.6}$$

$$\dddot{\mathcal{T}}_{\mathcal{RS}} = -(H^*)^3 \left[A^* (B^*)^2 + (B^*)^3 \mathcal{T}_{\mathcal{RS}}\right] , \tag{6.3.7}$$

where A and B are model-dependent functions of background quantities that one obtains by recasting the perturbed equations of motion in the form (3.3.48 – 3.3.49) and comparing. Using these derivatives and explicitly substituting them into the above expressions for the spectral index and runnings, we could obtain expressions for the corrections to each parameter in terms of the three variables A^*, B^* and $\mathcal{T}_{\mathcal{RS}}$ (as it is easily seen that the factors of H^* will trivially cancel out). To make the resulting expressions a little bit more intuitive, however, we define the transfer angle Θ as

$$\mathcal{T}_{\mathcal{RS}} = \tan\Theta \, . \tag{6.3.8}$$

In this picture, $\Theta = 0$ corresponds to $\mathcal{T}_{\mathcal{RS}} = 0$, while the other limiting case of $\mathcal{T}_{\mathcal{RS}} \gg 1$ (such that the final spectrum is dominated by power derived from entropy transfer) is represented by $\Theta \to \pi/2$. This trigonometric description has the advantage of Θ hence having a finite domain of possible values, as well as the helpful feature of being able to use trigonometric identities to manipulate expressions written in terms of e.g. $\sin\Theta$ or $\cos\Theta$. Note, for example, that eq. (6.3.1) is now

$$\mathcal{P}_{\mathcal{R}} = \frac{\mathcal{P}^*_{\mathcal{R}}}{\cos^2\Theta} \, . \tag{6.3.9}$$

The value of Θ could be measured, for example, by a violation of the usual inflationary consistency relation between the tensor-to-scalar ratio and tensor spectral index, which for single-field slow-roll models is $r = -8n_t$. For a two-field model, Θ would be given by

$$\Theta = \cos^{-1}\left[\sqrt{-\frac{r}{8n_t}}\right] . \tag{6.3.10}$$

Similarly, the expressions for the corrections to the spectral parameters become

$$\begin{aligned}
n_s &= n_s^* + \frac{2}{H^*}\left[\dot{\Theta}\tan\Theta\right] , \\
\alpha_s &= \alpha_s^* + \frac{2}{(H^*)^2}\left[\ddot{\Theta}\tan\Theta + \dot{\Theta}^2\sec^2\Theta\right] , \\
\beta_s &= \beta_s^* + \frac{2}{(H^*)^3}\left[\dddot{\Theta}\tan\Theta + 3\ddot{\Theta}\dot{\Theta}\sec^2\Theta + 2\dot{\Theta}^2\tan\Theta\sec^2\Theta\right] .
\end{aligned}$$

We can also see from eq. (6.3.8) that derivatives of the transfer angle behave as e.g. $\dot{\Theta} = \dot{\mathcal{T}}_{\mathcal{RS}}\cos^2\Theta$ (with extensions to higher orders following naturally via the chain rule). Putting all of this together then yields our main result expressing these corrections in terms of A^*, B^* and the transfer angle Θ as

$$n_s - 1 = (n_s - 1)^* - 2\sin\Theta\left(A^*\cos\Theta + B^*\sin\Theta\right) , \tag{6.3.11}$$

$$\begin{aligned}
\alpha_s = \alpha_s^* &+ 2\cos\Theta\left(A^*\cos\Theta + B^*\sin\Theta\right) \\
&\times \left(A^*\cos 2\Theta + B^*\sin 2\Theta\right) ,
\end{aligned} \tag{6.3.12}$$

$$\begin{aligned}
\beta_s = \beta_s^* &- 2\cos\Theta\left(A^*\cos\Theta + B^*\sin\Theta\right) \\
&\times \left(B^*\cos 2\Theta - A^*\sin 2\Theta\right) \\
&\times \left(A^* + 2A^*\cos 2\Theta + 2B^*\sin 2\Theta\right) .
\end{aligned} \tag{6.3.13}$$

6.3.1. Analysis and Limiting Cases

We can look at the expressions (6.3.11 – 6.3.13) in particular limiting cases to gain useful insight into what qualitative behaviour to expect. First, in the limit of small Θ, the expressions reduce to

$$n_s - 1 = (n_s - 1)^* \,, \tag{6.3.14}$$

$$\alpha_s = \alpha_s^* + 2(A^*)^2 \,, \tag{6.3.15}$$

$$\beta_s = \beta_s^* - 6(A^*)^2 B^* \,. \tag{6.3.16}$$

Because the correction to n_s is proportional to $\sin\Theta$, it is uncorrected at leading order in the small transfer angle limit. Meanwhile, the factor of $\cos\Theta$ instead appearing in the runnings gives them a non-zero correction. Of course, when $\Theta \equiv 0$ due to the absence of isocurvature, this is because $A = 0$ in eq. (3.3.48), so none of the terms are corrected, but when Θ is small but non-zero these results are valid. We see that the correction to β_s differs from that to α_s by a factor of $-3B^*$. This implies two things for the small angle limit:

1. To obtain a positive correction for β_s, B^* should be negative.

2. To make the magnitude of the corrected β_s comparable to or greater than that of α_s, we need $-3B^* \geq 1$.

This could be promising. For an appropriate size A^* of any sign as well as a negative and $O(1)$ or greater B^*, this could feasibly match the constraints given, as similar-sized positive corrections to both runnings would be obtained. The spectral index continues to be well described by its horizon-crossing value, assuring that the corrections needed to generate large runnings do not move n_s into a disfavoured region.

In the opposite limit of $\Theta \to \pi/2$, representing substantial transfer of power from entropic to adiabatic fluctuations, we find leading order corrections of

$$(n_s - 1) = (n_s^* - 1) - 2B^* \,, \tag{6.3.17}$$

$$\alpha_s = \alpha_s^* \,, \tag{6.3.18}$$

$$\beta_s = \beta_s^* \,. \tag{6.3.19}$$

This is less useful as it does nothing to directly alter the usual hierarchy of runnings from horizon-crossing, and potentially ruins a perfectly good spectral index prediction.

We also note by inspection that specific transfer angles may set certain factors in the above expressions equal to zero. For example, in the case where $\Theta = \tan^{-1}(-A^*/B^*)$, the factor $(A^* \cos\Theta + B^* \sin\Theta) = 0$. As this factor appears in all three expressions, this would correspond to no corrections to the spectral index or runnings. This is , of course, yet again not useful for our purposes. However, by noting that the factor $(A^* \cos 2\Theta + B^* \sin 2\Theta)$ appears only in the correction to α_s and not in β_s, we could obtain a hierarchy of runnings consistent with small α_s while still generating a significant β_s in the case where $\Theta = \tan^{-1}(-A^*/B^*)/2$. In this case, we would find

$$(n_s - 1) = (n_s^* - 1) + B^* \sqrt{1 + \frac{(A^*)^2}{(B^*)^2}} - B^* \,, \tag{6.3.20}$$

$$\alpha_s = \alpha_s^* \,, \tag{6.3.21}$$

$$\beta_s = \beta_s^* - B^*(A^*)^2 \sqrt{1 + \frac{(A^*)^2}{(B^*)^2}} \,. \tag{6.3.22}$$

Then, for example, if $B^* \gg A^*$, n_s is approximately uncorrected while $\beta_s = \beta_s^* - B^*(A^*)^2$, which could again be a useful case in achieving concordance with the CMB data analyses discussed above.

6.3.2. Particular Models

In general we see that whether we inspect the unsimplified results or any of the above limiting cases, to obtain an interesting deviation from the horizon-crossing behaviour of the spectral parameters we still need A^* and B^* to be sufficiently large for the correction terms to be significant. All of the trigonometric factors simply set the sign and relative size of one correction to another, but it is the A^* and B^* which then set the maximum size of those corrections, given a suitable angle. As the nth order deviation from scale invariance is typically $O(\epsilon^n)$ at horizon crossing,

and the correction term at that order is also nth order in A^* and B^*, we can see that we typically will need these two functions to be greater than $O(\epsilon)$, i.e. not slow-roll suppressed, in a model for there to be a good chance of producing non-standard runnings. Otherwise, the correction terms will be of a comparable size to the horizon-crossing baselines. To this end, theories like eq. (2.2.20) with modified kinetic terms may be a good place to start. A well-studied subset of such theories of the form

$$S = \int \mathrm{d}^4x\sqrt{-g}\left[\frac{1}{2}R - \frac{1}{2}(\partial\phi)^2 + -\frac{1}{2}e^{2b(\phi)}(\partial\chi)^2 - V(\phi,\chi)\right], \tag{6.3.23}$$

provide a simple starting point.[206,207] This kind of action with particular forms of the two free functions V and b can arise physically from supergravity-motivated scenarios and from extended Starobinsky Inflation.[315] First, let us consider a special case where $b = 0$ and V is simply the sum of mass terms for the two fields:

$$V = \frac{1}{2}m_\phi^2\phi^2 + \frac{1}{2}m_\chi^2\chi^2\,, \quad b = 0\,. \tag{6.3.24}$$

Here, we find that (all quantities are assumed to be evaluated at t^* henceforth so we omit the superscripted asterisks for better readability)

$$A \approx \frac{4(1-R^2)}{(\phi^2+\chi^2)(\phi^2+R^2\chi^2)}\dot{\phi}\dot{\chi}\,, \tag{6.3.25}$$

$$B \approx -2\epsilon_0 + \frac{2(1-R^2)}{(\phi^2+\chi^2)(\phi^2+R^2\chi^2)}\left(\dot{\phi}^2 - \dot{\chi}^2\right), \tag{6.3.26}$$

where R is the mass ratio m_χ/m_ϕ. For near-equal masses $R \approx 1$, we see that $A \approx 0$ and $B \approx O(\epsilon)$. For unequal masses $R \neq 1$, the relevant factors in these terms could be sizeable but as they multiply $\dot{\phi}\dot{\chi}$ and $\dot{\phi}^2 - \dot{\chi}^2$, respectively, and these are $O(\epsilon)$, a simple deviation in the mass ratio from unity is not sufficient to generate large runnings regardless of Θ. To demonstrate this visually we present Figure 6.1, where for a given model we show $n_s(\Theta)$, $\alpha_s(\Theta)$ and $\beta_s(\Theta)$ calculated using eqs. (6.3.11 – 6.3.13) and the above expressions for A and B, obtained from a numerical integration of the equations of motion. For argument's sake, we do this

for $\Theta \in [-\pi/2, \pi/2]$, rather than just the single Θ value that would be achieved in reality. In the figure, we see that regardless of Θ, the usual hierarchy is obeyed and results largely consistent with the $\beta_s \equiv 0$ Planck analysis are found.
A less minimal choice of b and V, such as

$$V = \frac{1}{2}m_\phi^2\phi^2 + \frac{1}{2}m_\chi^2\chi^2 + \frac{1}{2}g^2\phi^2\chi^2\,, \quad b = -\xi\phi\,, \tag{6.3.27}$$

may however be able to do more. We find the new forms of A and B to be resultingly much more complex:

$$\begin{aligned} A \approx & \frac{4}{F^2(\phi^2 + e^{-2\xi\phi}\chi^2)}\Big[(\xi(\lambda^2+\phi^2)+2\phi)\chi e^{-2\xi\phi}\dot{\chi}^2 \\ & -(\mu^2 - \lambda^2 + \chi^2 - \phi^2)e^{-\xi\phi}\dot{\phi}\dot{\chi} - 2\phi\chi\dot{\phi}^2\Big]\,, \end{aligned} \tag{6.3.28}$$

$$\begin{aligned} B \approx & -2\epsilon_0 + \frac{2\xi(\lambda^2+\phi^2)\chi}{F^2} + \frac{2}{F^2(\phi^2 + e^{-2\xi\phi}\chi^2)}\Big[((1+\xi\chi)(\lambda^2+\phi^2)) \\ & -(\mu^2+\chi^2)e^{-2\xi\phi}\dot{\chi}^2 - (\xi(\lambda^2+\phi^2) - 8\phi)\chi e^{-\xi\phi}\dot{\phi}\dot{\chi} + (\mu^2 - \lambda^2 + \chi^2 - \phi^2)\dot{\phi}^2\Big]\,, \end{aligned} \tag{6.3.29}$$

where $F^2 = (\mu^2\phi^2 + (\lambda^2+\phi^2)\chi^2)$, $\mu = m_\phi/g$ and $\lambda = m_\chi/g$. Here, while many terms still contain $O(\epsilon)$ factors due to being second order in time derivatives of fields, many of them are now multiplied by an exponential factor coming from the non-zero choice of b. For certain parameters and initial conditions, it may be the case that these exponentials are large enough to make A^* and B^* significant even in a slow-roll trajectory with small field derivatives. In contrast to the plots shown in Figure 6.1, where regardless of Θ one always finds $|n_s - 1| > |\alpha_s| > |\beta_s|$, we might expect that in this generalised case we can find Θ values for some choices of g and ξ where this is not the case. An extreme example is shown in Figure 6.2 using the same methodology.
Here, we see that the size of A^* and B^* are large enough to cause quite dramatic oscillations in the runnings. In reality, this model predicts via numerical evaluation of eqs. (3.3.50 – 3.3.51) that $\Theta = 2.8 \times 10^{-2}$, and this point is shown on the figure as a dashed black line at which $\alpha_s = 1.4 \times 10^{-2}$, and $\beta_s = 2.7 \times 10^{-2}$. These values are largely concordant with the experimentally favoured values from the extended

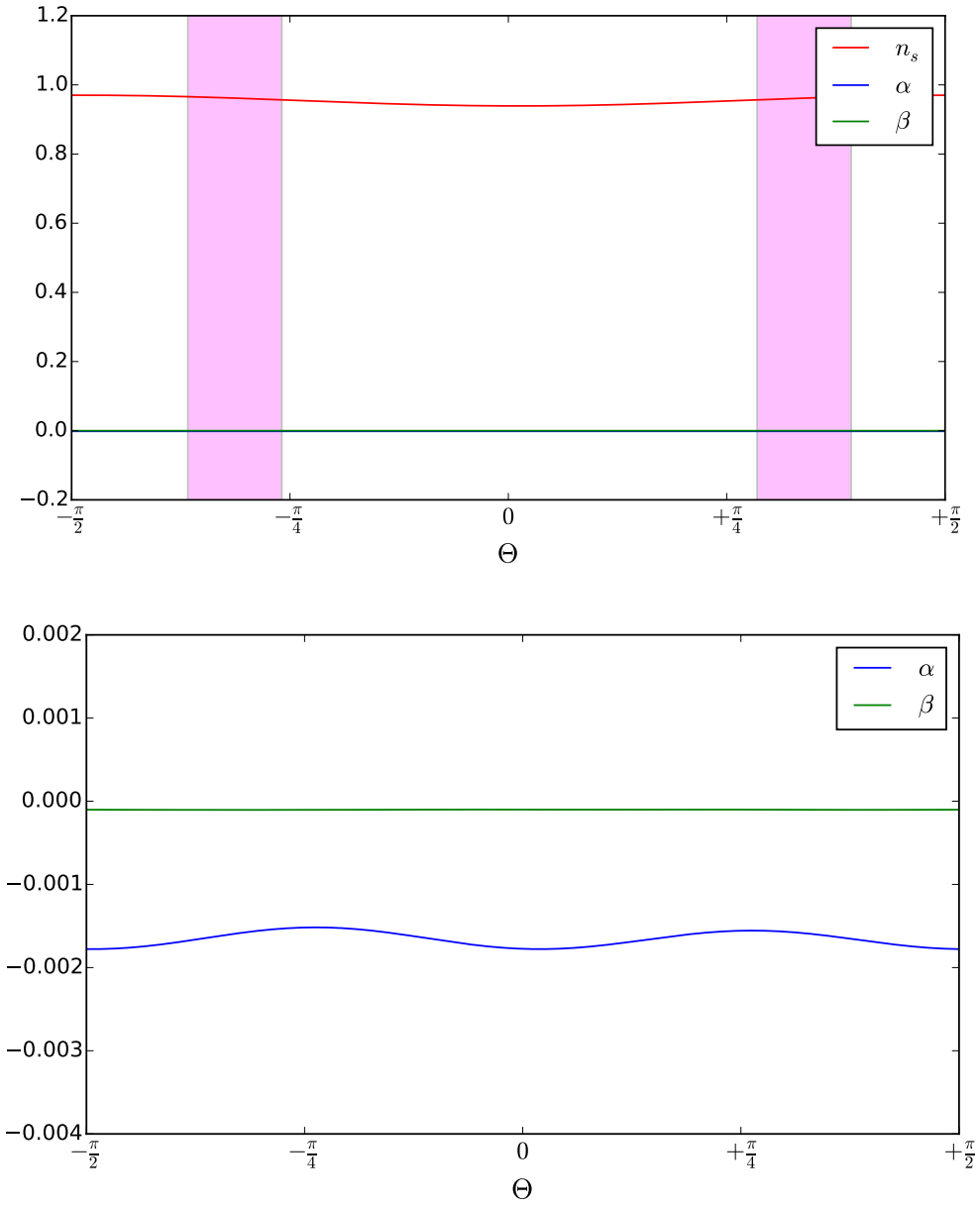

Figure 6.1.: Spectral parameters for the potential and kinetic function given by eq. (6.3.24), with $m_\phi = 5 \times 10^{-6} M_{\rm Pl} = 5 m_\chi$ such that $R = 5$, though the behaviour shown is considerably more general and typical than this. Initial conditions are chosen to give rise to a suitable amount of inflation. We first show n_s, α_s and β_s as a function of the transfer angle Θ together but given the smallness of the latter two parameters we also show them more clearly in the lower plot. The shaded region is where n_s falls within the Planck 1σ contours. The amplitude of oscillation as a function of Θ is consecutively smaller for each order deviation, such that one always has $|n_s - 1| > |\alpha_s| > |\beta_s|$.

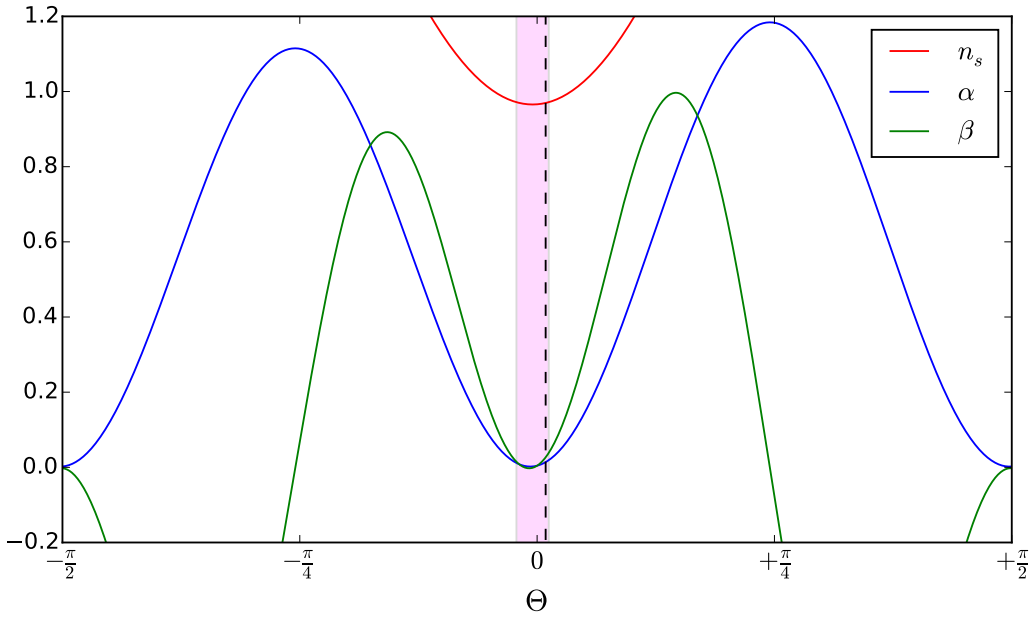

Figure 6.2.: Spectral parameters for the potential and kinetic function given by eq. (6.3.27), with $m_\phi/M_{\rm Pl} = 5m_\chi/M_{\rm Pl} = g = 4.8 \times 10^{-4}$ and $\xi = -0.125/M_{\rm Pl}$. This model predicts A^* and B^* which can be considerably larger than in the uncoupled case (6.3.24) and the oscillations in α_s and β_s as a function of Θ are hence amplified. Again, the range of favoured values of the runnings are shown as a shaded region. A black-dashed line within this shaded region represents the numerically computed value of $\Theta = 2.8 \times 10^{-2}$ for this particular trajectory, for which we find $\alpha_s = 1.4 \times 10^{-2}$, and $\beta_s = 2.7 \times 10^{-2}$.

analyses, though this is just one example that was achieved by trial and error with parameters for the sake of demonstrating the principles involved, not a statement about the general suitability of this particular model. For comparison, we find here that $\beta_s^* \approx -1 \times 10^{-3}$ which is negative and much smaller in magnitude, such that the final β_s value is clearly dominated by the superhorizon effects, as assumed.

Qualitatively, note that around $\Theta = 0$ we have $n_s \approx n_s^* \sim 1 - O(\epsilon)$ as expected from discussion in Section 6.3.1, but at larger Θ, large superhorizon corrections ruin the spectral index. Similarly, the runnings tend to approach near-zero values at $\Theta = \pi/2$ as the superhorizon corrections proportional to $\cos\Theta$ vanish in this limit. The running of the running approaches zero from negative values, which is not conducive to achieving a positive running of the running at large Θ, though as n_s is far too large in this limit it is not a feasible model anyway. The only

feasible transfer angles appear to be very small ones, as elsewhere α_s and β_s are never simultaneously of a comparable order and sufficiently small, as well as the fact that it is only at small Θ that n_s remains reasonable. We might hence expect that barring any coincidental special cases, it is in the small Θ limit that good results will typically be made possible. Unfortunately, via the consistency relation $r = -8n_t \cos^2\Theta$, it is in this limit that we do not obtain a consistency relation significantly different to the single-field case, making detection of such a deviation more challenging.

6.4. Alternatives to Inflationary Cosmology

As we argued that basic inflation is incompatible with the $\beta_s \neq 0$ hierarchy of runnings, it is reasonable to consider how alternatives to inflation fare in this scenario; confirmation of an unexpected set of runnings potentially motivates not just extensions of inflation, but perhaps could imply a different physical principle entirely is at work. Theories such as variable speed of light (VSL) models are popular with critics of inflation,[316] and quantum gravity (QG) scenarios may pave the way to early universe theories where suitable primordial perturbations are generated via novel and general high energy effects rather than the details of the inflationary model. Here, we briefly cover an example of each of these to compare and contrast with the standard inflationary approach and the multi-field formalism introduced above.

6.4.1. VSL and Runnings

VSL models involve a non-constant ratio of the speed of light to the speed of gravitational waves.[317–319] As mentioned, critics of inflation often favour it as an alternative as they claim it is more predictive, and relativiely free of fine-tuning issues.[320] VSL cosmology has also been studied outside the context of the early universe as e.g. an aspect of dark energy model building.[100,321] Bimetric theories of gravity are often used to construct VSL scenarios (a context in which much like the model of Chapter 4, disformal couplings may be useful). For example, in the VSL theory advocated by Moffat,[318,322] the power spectrum takes the general form

$$\mathcal{P}_{\mathcal{R}} \propto \ln^2\left(Ak^3\right) , \tag{6.4.1}$$

where A is a constant depending on model parameters whose precise form we shall not at present concern ourselves with. Proceeding with the standard definitions of the spectral index and its runnings, one obtains the following relations between them

$$\alpha_s = -\frac{1}{2}\left(n_s - 1\right)^2 , \tag{6.4.2}$$

$$\beta_s = \frac{1}{2}\left(n_s - 1\right)^3 , \tag{6.4.3}$$

such that $n_s \approx 0.96$ would imply $\alpha_s \approx -8 \times 10^{-4}$ and $\beta_s \approx -3 \times 10^{-5}$.
This is very similar to the standard hierarchy of runnings. As in slow-roll single-field inflation, $\alpha_s \propto (n_s - 1)^2$ and $\beta_s \propto (n_s - 1)^3$, and so once again the same process which allows the theory to make good scale-invariant predictions also dooms it to incompatibility with large runnings. Another similarity to standard inflation is that a prediction of $\beta_s < 0$ is made, contradictory to the extended analyses of the experimental data. We can see that a confirmation of $\beta_s \approx O(10^{-2})$ would not help distinguish VSL from inflation. If one is to take the predictivity of VSL as a main advantage over the wide range of models that inflation can be achieved by, then it would be contrary to the spirit of this to build arbitrary extensions to the theory as needed to produce a non-standard running hierarchy. One could even argue that a confirmation of large runnings would disfavour VSL when compared to extended models of inflation such as multi-field scenarios.

6.4.2. Quantum Gravity and Runnings

Quantum gravity may provide novel effects beyond those of the General Relativistic perturbation theory that has been used thus far to determine inflationary spectra. For example, it has been shown that in Canonical Quantum Gravity (CQG), one finds[323,324] a correction term to the basic inflationary power spectra arising from

QG effects in the form

$$\mathcal{P}_{\mathcal{R}} = \mathcal{P}_{\mathcal{R}}^{(0)}(1+\Delta)\,, \tag{6.4.4}$$

where $\mathcal{P}_{\mathcal{R}}^{(0)}$ is the base General Relativistic spectrum such as in eq. (6.2.1), and the correction term Δ is

$$\Delta = 0.988\frac{H^2}{M_{\rm pl}^2}\left(\frac{\bar{k}}{k}\right)^3 + O(\epsilon)\,. \tag{6.4.5}$$

Note that $\Delta > 0$. Here, $\bar{k}$ is an inverse length scale introduced by CQG. Proceeding to compute the spectral parameters from their usual definitions yields

$$n_s - 1 = (n_s-1)^{(0)} - \frac{3\Delta}{(1+\Delta)} + O(\epsilon)\,, \tag{6.4.6}$$

$$\alpha_s = \alpha_s^{(0)} + \frac{9\Delta}{(1+\Delta)^2} + O(\epsilon)\,, \tag{6.4.7}$$

$$\beta_s = \beta_s^{(0)} + \frac{27\Delta\,(\Delta-1)}{(1+\Delta)^3} + O(\epsilon)\,, \tag{6.4.8}$$

where symbols superscripted with a (0) again indicate those calculated from the uncorrected spectrum $\mathcal{P}_{\mathcal{R}}^{(0)}$. It is interesting to study these corrections in the small Δ limit, in which case one finds

$$n_s - 1 \approx (n_s-1)^{(0)} - 3\Delta\,, \tag{6.4.9}$$

$$\alpha_s = \alpha_s^{(0)} + 9\Delta\,, \tag{6.4.10}$$

$$\beta_s = \beta_s^{(0)} - 27\Delta\,, \tag{6.4.11}$$

revealing that each order's correction term is larger than the previous one. This is similar to findings in Loop Quantum Gravity[325] where runnings of comparable magnitude at all orders are found. In the above expressions, however, the correction to β_s is negative, such that while it may present a large deviation from the minimal hierarchy of runnings, it does so in the wrong direction to match the analyses

showing $\beta_s > 0$. We can similarly study the limit of large Δ, but here we find the uninteresting result that α_s and β_s are largely unchanged while $n_s - 1 \approx -3$ which is irreconcilable with data; this is not unexpected as we have in this limit $\mathcal{P}_\mathcal{R} \propto \Delta \propto k^{-3}$ which by eq. (3.3.28) implies this result. In less extreme cases, a large Δ can produce an appropriately sized positive correction to β_s, but in doing so also corrects n_s and α_s by undesirably large amounts. In summary, small CQG corrections are inappropriate as they are unfortunately negative, and larger CQG corrections tend to produce too great a difference in n_s and/or α_s for this approach to be successful. While QG corrections to spectra are perhaps an interesting approach in general to solving this problem, this particular realisation does not successfully produce concordant results with the $\beta_s \neq 0$ analyses.

6.4.3. Alternative Parametrisation of the Power Spectrum

The usual procedure of expanding the power spectrum as a Taylor series in $\log k$ and determining the coefficients of this expansion via eq. (3.3.28) would lead to the usual expectation that each subsequent term is roughly smaller than the previous one, such that one can truncate the power series at a certain order and have it still represent a reasonable approximation of the true function. The possibility of a deviation from this, where $\beta_s \gg \alpha_s$, for example, leads to serious questions such as "but what about the next order term, γ_s?". If, say, a further extended analysis found that the best fit values of α_s and β_s were rather different under the inclusion of a γ_s parameter, which was found to be comparable to or larger than β_s again, this would likely be a sign of a pathology in the choice of parametrisation itself.

If such a Taylor series representation of the curvature perturbation spectrum of inflation is not suitable, one could instead consider a Padé series. That is, an approximant that is a ratio of two Taylor series, e.g.

$$\log\left(\mathcal{P}_\mathcal{R}\right) = \log\left(A_s\right) + \frac{x_1 \log\left(\frac{k}{k^*}\right) + \frac{x_2}{2}\log\left(\frac{k}{k^*}\right)^2 + \ldots}{1 + y_1 \log\left(\frac{k}{k^*}\right) + \frac{y_2}{2}\log\left(\frac{k}{k^*}\right)^2 + \ldots}\,, \tag{6.4.12}$$

where the first term on the denominator is set to 1 without loss of generality. Padé series are widely used in numerical evaluation of special functions to high precision,

providing a better approximation than an equal-order Taylor series and being well behaved for certain functions where the Taylor series is undefined or problematic. The question we wish to ask here, then, is whether a well-behaved Padé series with decreasing coefficients could lead to an unexpectedly large β_s when we analyse the spectrum through the lens of a Taylor series parametrisation. First, let us note that the apparent values of n_s and so on one would find by projecting the Padé series (6.4.12) onto the usual Taylor expansion (3.3.28) would be

$$n_s - 1 = x_1 \,, \tag{6.4.13}$$

$$\alpha_s = x_2 - x_1 y_1 \,, \tag{6.4.14}$$

$$\beta_s = x_3 - \frac{3}{2} x_2 y_1 + \frac{3}{2} x_1 y_1^2 - x_1 y_2 \,. \tag{6.4.15}$$

From this, we see that α_s picks up a correction dependent on the denominator coefficient y_1 and the numerator coefficient x_1, which is just the spectral index. Similarly β_s picks up corrections proportional to $n_s - 1$ and α_s and combinations of the denominator coefficients. It is then feasible that for certain values of the denominator coefficients y_1 and y_2, these corrections could amount to e.g. $\beta_s \approx O(n_s - 1)$. Let us say, then, we take $x_1 = -0.04$ to impose $n_s = 0.96$, and assume that the numerator coefficients are $x_2 \sim x_1^2$, $x_3 \sim x_1^3$ and so on, as a prototype for their decreasing nature. Then, these expressions become

$$n_s = 0.96 \,, \tag{6.4.16}$$

$$\alpha_s = 1.6 \times 10^{-3} + 4 y_1 \times 10^{-2} \,, \tag{6.4.17}$$

$$\beta_s = -6.4 \times 10^{-5} - 2.4 y_1 \times 10^{-3} - 6 y_1^2 \times 10^{-2} + 4 y_2 \times 10^{-2} \,. \tag{6.4.18}$$

One can immediately see that most of the corrections to β_s are negative, leading to a negative observed β_s for many possible y_i values. Particularly, the y_1^2 term is always negative regardless of the sign of y_1. This immediately poses a problem for creating a hierarchy of runnings similar to that implied by the Planck data analysis

without resorting to $|y_2| > |y_1|$ in the denominator power series. For example, in the case where $y_2 \approx 1/4 \gg |y_1|$, we can obtain $\beta_s \approx 10^{-2}$, but at this point is this any better than just having a large running of the running in a normal power series expansion? In fact, maximising eq. (6.4.18) subject to the constraint $y_2 \leq |y_1|$ finds the best we can do in this case is $\beta_s = 7.4 \times 10^{-3}$ for $y_2 = -y_1 \approx 0.353$, for which $\alpha_s \approx -0.125$, which is rather inconsistent with the experimental constraints and seemingly too great a price to pay for an only moderately consistent β_s. With the stronger condition of $y_2 \leq |y_1|/2$, this reduces to a maximum running of the running of $\beta_s \approx 2 \times 10^{-3}$ with $\alpha_s \approx -5 \times 10^{-3}$, largely trivialised once again.

In summary, we see that the effects of a Padé parametrisation of the power spectrum may uplift the apparent Taylor series parameters n_s, α_s and β_s somewhat, but not enough to achieve e.g. β_s of $O(10^{-2})$ without requiring a non-decreasing set of coefficients in the denominator, thus failing to do any better than the questionable status of having such a series of coefficients in the original Taylor parametrisation.

CHAPTER 7

CONCLUSIONS

While cosmic inflation is widely accepted as the leading description of the early universe, as a necessary phenomenon to generate primordial curvature perturbations consistent with Cosmic Microwave Background radiation anisotropies, it is not known precisely how it happened and what caused it. The research projects presented in this thesis are hence motivated by the ongoing pursuit of an explanation of how cosmic inflation may have occurred. Standard model physics coupled to General Relativity provides a good description of most of the universe, but has been long ruled out as an inflationary theory, and so we look either at extensions of particle physics or gravity theory to provide possible mechanisms for this. In this thesis we focus primarily on the latter; how modified gravity may provide a framework for inflation. At the same time, the simplest models of inflation such as a simple massive scalar field slow-rolling have now been ruled out by improved limits on the tensor-to-scalar ratio, motivating in particular work on extended models of inflation with diverse and interesting phenomenology. As well as understanding inflation for its own sake, a comprehension of the physics of the early universe would also be a significant and useful step towards understanding high energy and beyond-standard-model physics in general.

Following a review of the necessary background material in gravity theory and phys-

ical cosmology, in this thesis we have seen the results of my research spanning three main topics relating to cosmic inflation in scenarios based on and inspired largely by modified gravity: the novel disformally coupled model of inflation, the effects of the Gauss-Bonnet term during and after inflation, and the computation of inflationary spectral parameters such as the running of the running in multi-field theories.

In the first of these, we described and analysed a model of two-field inflation whose noteworthy feature is that the second field is defined on an extra-dimensional brane whose induced metric is disformally related to the spacetime metric. The non-standard interactions of these two fields, elucidated by making a transformation to a frame in which the theory looks like it describes a non-standard field on the standard metric rather than a standard field on a non-standard metric, provide interesting phenomenology including the distinctive feature of having two distinct propagation speeds. We discussed how this was related to the kinetic structure of the theory and used this to define and quantise the fundamental degrees of freedom and subsequently compute the power spectra of the primordial fluctuations as well as the curvature bispectrum and its non-Gaussianity parameter. We found that a String Theory motivated realisation of this model was uninteresting due to its suppression of potentially new physics in the inflationary scenario, but found a different form of the theory provided more interesting behaviour to study. Effects of the two sound speeds, the isocurvature transfer function, and the size of the disformal coupling were discussed in relation to the spectra. It was found that one could obtain spectra consistent with the latest experimental constraints if one did not have the disformality parameter γ evolving too rapidly, and that successful models produced consistently smaller tensor-to-scalar ratios than the simplest models of inflation due to the amplified scalar power spectrum. These are some of the first results on the topic of multi-speed theories.

Secondly, we developed a generalisation of the ubiquitous slow-roll formalism for approximate computation of relevant quantities to inflation which accounts for the presence of a coupling of a scalar field to the Gauss-Bonnet combination of quadratic curvature scalars, and for generality did so in a Jordan Frame described by an arbitrary non-minimal coupling function to the Ricci scalar. Subsequently, we showed

that a Gauss-Bonnet coupling of the typical inverse power law form previously considered in the literature, while interesting in its generation of primordial perturbations, does not actually allow inflation to end due to its inhibition of the field's motion. Following a discussion of the dynamics of this we argued that it is infeasible to save the model via any of the major reheating processes and instead found a minimal extension of the model which does allow reheating to proceed. We determined the consequences of this extension and carried out extensive numerical simulations of the reheating phase to determine its influence on inflationary observations. We also took the ability of the GB term to freeze a scalar field and applied this to developing a model of quintessential inflation where the inflaton persists after inflation at low densities and goes on to become dark energy in the present universe, and found that while this was technically achievable with natural parameter choices, the resulting dark energy model is incompatible with recent observations that gravitational waves travel at the speed of light, but nevertheless demonstrates an interesting principle.
Our third topic involved a change of pace from the model building activities of previous chapters to instead think about tests of inflation. Reflecting on a recent experimental analysis which indicates that the so-called running of the running of the spectral index, β_s, may not be consistent with zero as was previously expected, we ask the question of what implications this has for the multitude of inflationary models. After showing that minimal slow-roll inflation is not suitable to achieve this, we looked at how multi-field models, with their superhorizon evolution of the curvature perturbation, are more suitable for predicting such large β_s values. In turn, the confirmation of this unexpected experimental result would cast serious doubt on most single-field realisations of inflation. Similarly, we looked at some theories such as variable speed of light scenarios, the effects of canonical quantum gravity on inflationary spectra, and alternative parametrisations of $\mathcal{P}_\mathcal{R}$ from the perspective of spectral runnings. A confirmation of the hints that the runnings of the spectral index may be non-trivial could change the landscape of inflationary theories dramatically, and here we have taken some of the first steps towards comprehending this in a theoretically-useful way.

APPENDIX A

APPENDICES

A.1. Useful derivatives of the P function of Disformally Coupled Inflation

Here we list, for convenience, all the different symmetrised derivatives that are needed to compute spectra and non-Gaussianities of Disformally Coupled Inflation. Where a difference is present between canonical and DBI models, this will be noted with a superscript of C or DBI.

A.1.1. Second order symmetrised derivatives

Out of a possible $2^4 = 16$ combinations of derivatives, only 6 of these are unique due to the symmetries $X^{\phi\chi} = X^{\chi\phi}$ and $f_{,xy} = f_{,yx}$ (standard reordering of partial derivatives). Of these, three are identically zero due to the structure of the Lagrangian.

$$P^{\rm C}_{<\phi\phi><\phi\phi>} = -\gamma^3 hD\left(X^{\chi\chi} - CV\right) + 6\gamma^5 h^2 D(X^{\phi\chi})^2\,,$$
$$P^{\rm DBI}_{<\phi\phi><\phi\phi>} = h\gamma^3 + P^{\rm C}_{<\phi\phi><\phi\phi>}\,,$$

$$P_{<\phi\phi><\chi\chi>} = P_{<\chi\chi><\phi\phi>} = -\gamma D\,,$$

$$P_{<\phi\phi><\phi\chi>} = P_{<\phi\phi><\chi\phi>} = P_{<\phi\chi><\phi\phi>} = P_{<\chi\phi><\phi\phi>} = 2\gamma^3 h D X^{\phi\chi}\,,$$

$$P_{<\phi\chi><\chi\chi>} = P_{<\chi\phi><\chi\chi>} = P_{<\chi\chi><\phi\chi>} = P_{<\chi\chi><\chi\phi>} = 0\,,$$

$$P_{<\chi\chi><\chi\chi>} = 0\,,$$

$$P_{<\phi\chi><\phi\chi>} = P_{<\phi\chi><\chi\phi>} = P_{<\chi\phi><\phi\chi>} = P_{<\chi\phi><\chi\phi>} = \gamma D\,.$$

A.1.2. Third order symmetrised derivatives

Out of a possible $2^6 = 64$ combinations of derivatives, only 10 of these are unique due to the symmetries $X^{\phi\chi} = X^{\chi\phi}$ and $f_{,xy} = f_{,yx}$ (standard reordering of partial derivatives). Of these, 6 are identically zero due to the structure of the Lagrangian.

$$P^{\mathrm{C}}_{<\phi\phi><\phi\phi><\phi\phi>} = -3\gamma^5 h^2 D\left(X^{\chi\chi} - CV\right) + 30\gamma^7 h^3 D (X^{\phi\chi})^2\,,$$
$$P^{\mathrm{DBI}}_{<\phi\phi><\phi\phi><\phi\phi>} = 3h^2\gamma^5 + P^{\mathrm{C}}_{<\phi\phi><\phi\phi>}\,,$$

$$P_{<\chi\chi><\chi\chi><\chi\chi>} = 0\,,$$

$$P_{<\phi\chi><\phi\chi><\phi\chi>} = P_{<\chi\phi><\phi\chi><\phi\chi>} = P_{<\phi\chi><\chi\phi><\phi\chi>} = P_{<\phi\chi><\phi\chi><\chi\phi>}$$
$$= P_{<\chi\phi><\chi\phi><\phi\chi>} = P_{<\chi\phi><\phi\chi><\chi\phi>} = P_{<\phi\chi><\chi\phi><\chi\phi>} = P_{<\chi\phi><\chi\phi><\chi\phi>} = 0\,,$$

$$P_{<\phi\phi><\phi\phi><\chi\chi>} = P_{<\phi\phi><\chi\chi><\phi\phi>} = P_{<\chi\chi><\phi\phi><\phi\phi>} = -\gamma^3 hD\,,$$

$$P_{<\phi\phi><\phi\phi><\phi\chi>} = P_{<\phi\phi><\phi\phi><\chi\phi>} = P_{<\phi\phi><\phi\chi><\phi\phi>}$$
$$= P_{<\phi\phi><\chi\phi><\phi\phi>} = P_{<\phi\chi><\phi\phi><\phi\phi>} = P_{<\chi\phi><\phi\phi><\phi\phi>} = 6\gamma^5 h^2 D X^{\phi\chi}\,,$$

$$P_{<\chi\chi><\chi\chi><\phi\phi>} = P_{<\chi\chi><\phi\phi><\chi\chi>} = P_{<\phi\phi><\chi\chi><\chi\chi>} = 0\,,$$

$$P_{<\chi\chi><\chi\chi><\phi\chi>} = P_{<\chi\chi><\chi\chi><\chi\phi>} = P_{<\chi\chi><\phi\chi><\chi\chi>}$$
$$= P_{<\chi\chi><\chi\phi><\chi\chi>} = P_{<\phi\chi><\chi\chi><\chi\chi>} = P_{<\chi\phi><\chi\chi><\chi\chi>} = 0\,,$$

$$P_{<\phi\phi><\phi\chi><\phi\chi>} = P_{<\phi\phi><\chi\phi><\phi\chi>} = P_{<\phi\phi><\phi\chi><\chi\phi>} = P_{<\phi\phi><\chi\phi><\chi\phi>}$$
$$= P_{<\phi\chi><\phi\phi><\phi\chi>} = P_{<\chi\phi><\phi\phi><\phi\chi>} = P_{<\phi\chi><\phi\phi><\chi\phi>} = P_{<\chi\phi><\phi\phi><\chi\phi>}$$
$$= P_{<\phi\chi><\phi\chi><\phi\phi>} = P_{<\chi\phi><\phi\chi><\phi\phi>} = P_{<\phi\chi><\chi\phi><\phi\phi>} = P_{<\chi\phi><\chi\phi><\phi\phi>} = \gamma^3 hD\,,$$

$$P_{<\chi\chi><\phi\chi><\phi\chi>} = P_{<\chi\chi><\chi\phi><\phi\chi>} = P_{<\chi\chi><\phi\chi><\chi\phi>} = P_{<\chi\chi><\chi\phi><\chi\phi>}$$
$$= P_{<\phi\chi><\chi\chi><\phi\chi>} = P_{<\chi\phi><\chi\chi><\phi\chi>} = P_{<\phi\chi><\chi\chi><\chi\phi>} = P_{<\chi\phi><\chi\chi><\chi\phi>}$$
$$= P_{<\phi\chi><\phi\chi><\chi\chi>} = P_{<\chi\phi><\phi\chi><\chi\chi>} = P_{<\phi\chi><\chi\phi><\chi\chi>} = P_{<\chi\phi><\chi\phi><\chi\chi>} = 0\,,$$

$$P_{<\phi\phi><\chi\chi><\phi\chi>} = P_{<\phi\phi><\chi\chi><\chi\phi>} = P_{<\chi\chi><\phi\phi><\phi\chi>} = P_{<\chi\chi><\phi\phi><\chi\phi>}$$
$$= P_{<\phi\phi><\phi\chi><\chi\chi>} = P_{<\phi\phi><\chi\phi><\chi\chi>} = P_{<\chi\chi><\phi\chi><\phi\phi>} = P_{<\chi\chi><\chi\phi><\phi\phi>}$$
$$= P_{<\phi\chi><\phi\phi><\chi\chi>} = P_{<\chi\phi><\phi\phi><\chi\chi>} = P_{<\phi\chi><\chi\chi><\phi\phi>} = P_{<\chi\phi><\chi\chi><\phi\phi>} = 0\,.$$

A.2. Perturbation Coefficients in Disformally Coupled Inflation

In this appendix we detail various coefficients used in the perturbation equations of disformally coupled inflation. These are background quantities that multiply the linearised perturbation equations and are needed to numerically solve the system. As in the main body of text, we use eq. (4.2.14) to encode differences between Canonical and DBI models.

A.2.1. Coefficients in the Perturbed Einstein Equations

The X_n, Y_n and Z_n coefficients appearing in eqs. (4.3.6 – 4.3.8) have some slight differences between Canonical and DBI cases, and are given by the expressions

$$
\begin{aligned}
X_1 &= 2U - \left(2\gamma^2 - 3\right)\rho_\chi - \gamma^4 p_\chi - \frac{C}{D}\left(\gamma_d^3 - 3\gamma_d + 2\right) , \\
X_2 &= U' - \frac{1}{2}\left(\left[\left(2\gamma^2 - 5\right)\rho_\chi + \gamma^4 p_\chi\right]\frac{C'}{C} - \left(\gamma^2 - 1\right)\left[2\rho_\chi + \gamma^2 p_\chi\right]\frac{D'}{D}\right) \\
&\quad - \frac{C}{2D}\left(\frac{C'}{C} - \frac{D'}{D}\right)\left(\gamma_d^3 - 3\gamma_d + 2\right) , \\
X_3 &= \left[\gamma_d^3 + \frac{D}{C}\gamma^2\left(2\rho_\chi + \gamma^2 p_\chi\right)\right]\dot{\phi} , \\
X_4 &= \gamma C^2 V' , \\
X_5 &= \gamma^3 C\dot{\chi} .
\end{aligned}
$$

$$
\begin{aligned}
Z_1 &= -2\left(\dot{\phi}^2 - U\right) - \left(\rho_\chi + 3p_\chi\right) - \frac{C}{D}\left(\gamma_d^3 - 3\gamma_d + 2\right) , \\
Z_2 &= -U' - \frac{1}{2}\left[\left(\rho_\chi - 3p_\chi\right)\frac{C'}{C} - \frac{\gamma^2 - 1}{\gamma^2}\rho_\chi\frac{D'}{D}\right] - \frac{C}{2\gamma D}\left(\frac{C'}{C} - \frac{D'}{D}\right)\left(\gamma_d - 1\right)^2 , \\
Z_3 &= -Y_1 = \left[\gamma_d + \frac{D}{C}\rho_\chi\right]\dot{\phi} , \\
Z_4 &= -\frac{C^2 V'}{\gamma} , \\
Z_5 &= -Y_2 = \gamma C\dot{\chi} .
\end{aligned}
$$

A.2.2. Coefficients in the Perturbed Klein Gordon Equation for χ

The β_n coefficients appearing in eq. (4.3.5) are the same regardless of ϕ's kinetic term and take the forms

$$
\begin{aligned}
\beta_1 &= \gamma^2 \frac{D}{C}\dot{\phi}\dot{\chi}\,, \quad \beta_2 = 1\,,\\
\beta_3 &= -\frac{D}{C}\dot{\phi}\dot{\chi}\,, \quad \beta_4 = -\frac{1}{\gamma^2}\,,\\
\beta_5 &= -\left(\gamma^2+3\right)\dot{\chi}\,,\\
\beta_6 &= \gamma^2\left(2\gamma^2-1\right)\frac{D}{C}\dot{\chi}\ddot{\phi} - 2D\dot{\phi}V' - \frac{1}{2}\left[\left(2\gamma^4-\gamma^2-3\right)\frac{C'}{C} - \left(2\gamma^4-\gamma^2-1\right)\frac{D'}{D}\right]\dot{\chi}\,,\\
\beta_7 &= 3H + \gamma^2\frac{D}{C}\dot{\phi}\ddot{\phi} - \frac{1}{2}\left[\left(\gamma^2-3\right)\frac{C'}{C} - \left(\gamma^2-1\right)\frac{D'}{D}\right]\dot{\phi}\,,\\
\beta_8 &= -2\gamma^2\left(\gamma^2\frac{D}{C}\dot{\phi}\dot{\chi}\ddot{\phi} - CV' - \frac{1}{2}\left[\frac{C'}{C} - \frac{D'}{D}\right]\left(\gamma^2-1\right)\dot{\phi}\dot{\chi}\right)\,,\\
\beta_9 &= \gamma^4\frac{D}{C}\dot{\phi}\dot{\chi}\ddot{\phi}\left(\frac{D'}{D} - \frac{C'}{C}\right) + \frac{CV'}{\gamma^2}\left[\gamma^2\frac{C'}{C} - \left(\gamma^2-1\right)\frac{D'}{D}\right]\\
&\quad + \frac{1}{2}\left[\left(\gamma^2-1\right)\frac{D''}{D} - \left(\gamma^2-3\right)\frac{C''}{C} + \left(\gamma^2\frac{C'}{C} - \left(\gamma^2-1\right)\frac{D'}{D}\right)^2 - 3\left(\frac{C'}{C}\right)^2\right]\dot{\phi}\dot{\chi}\,,\\
\beta_{10} &= \frac{CV''}{\gamma^2}\,.
\end{aligned}
$$

A.2.3. Coefficients in the Perturbed Klein Gordon Equation for ϕ

The α_n coefficients appearing in eq. (4.3.4) are the main element of the perturbed system that differs between DBI and Canonical cases, and are given by

$$
\begin{aligned}
\alpha_1 &= \gamma_d^3 + \frac{D}{C}\gamma^2\rho_\chi\,,\\
\alpha_2 &= 0\,,\\
\alpha_3 &= -\left(\gamma_d - \frac{D}{C}\gamma^2 p_\chi\right)\,,\\
\alpha_4 &= 0\,,\\
\alpha_5 &= -\dot\phi\left[\gamma\left(\gamma^2+3\right) + \frac{D}{C}\gamma^2\left(\rho_\chi - 3p_\chi\right)\right]\,,\\
\alpha_6 &= 3H\left[\gamma_d^3\left(1 - 3\frac{\gamma_d^2-1}{\gamma^2+\gamma+1}\right) - \frac{D}{C}\left(\gamma^4 p_\chi + \left(\gamma^2-1\right)\left(\rho_\chi + \gamma^2 p_\chi\right)\right)\right]\\
&\quad + \frac{D}{C}\gamma^2\dot\phi\left[\frac{D}{C}\gamma^2\left(4\rho_\chi + \gamma^2 p_\chi\right)\ddot\phi\right.\\
&\quad \left. -\frac{1}{2}\left(\left[\left(4\gamma^2-1\right)\rho_\chi + \left(\gamma^2+4\right)\gamma^2 p_\chi\right]\frac{C'}{C} - \left[\left(4\gamma^2-2\right)\rho_\chi + \left(\gamma^2-1\right)\gamma^2 p_\chi\right]\frac{D'}{D}\right)\right]\\
&\quad + \frac{3}{2}\left(\frac{C'}{C} - \frac{D'}{D}\right)\dot\phi\gamma^3\frac{1+\gamma_d - 2\gamma_d^2}{\gamma^2+\gamma+1}\,,\\
\alpha_7 &= D\gamma^3\left(\gamma^2\ddot\phi - 3H\dot\phi\right)\dot\chi - \frac{1}{2}C\gamma^3\left(\left(\gamma^2+1\right)\frac{C'}{C} - \left(\gamma^2-1\right)\frac{D'}{D}\right)\dot\chi\,,
\end{aligned}
$$

$$
\begin{aligned}
\alpha_8 = & -\left(2+\frac{D}{C}\gamma^2\left[\left(4\gamma^2-1\right)\rho_\chi+\gamma^4 p_\chi\right]\right)\ddot{\phi} \\
& -3H\dot{\phi}\left(2+\frac{\gamma\left(\gamma_d-1\right)^2\left(2\gamma^2+3\gamma+1\right)}{\gamma^2+\gamma+1}-\frac{D}{C}\gamma^2\left[\rho_\chi+\left(2\gamma^2-1\right)p_\chi\right]\right) \\
& +\frac{1}{2}\Bigg(\left[\left(4\gamma^4-4\gamma^2+2\right)\rho_\chi+\left(\gamma^4+4\gamma^2-3\right)\gamma^2 p_\chi\right]\frac{C'}{C} \\
& -\left[\left(4\gamma^4-5\gamma^2+1\right)\rho_\chi+\left(\gamma^2-1\right)\gamma^4 p_\chi\right]\frac{D'}{D}\Bigg) \\
& +\frac{1}{2}\frac{C}{D}\left(\frac{C'}{C}-\frac{D'}{D}\right)\frac{\left(\gamma_d-1\right)^3\left(4\gamma^2+7\gamma+4\right)}{\gamma^2+\gamma+1},
\end{aligned}
$$

$$
\begin{aligned}
\alpha_9 = & U''+\frac{1}{2}\left(\left[\left(\gamma^2-2\right)\rho_\chi+3\gamma^2 p_\chi\right]\frac{D''}{D}-\left[\left(\gamma^2-1\right)\rho_\chi\right]\frac{C''}{C}\right) \\
& +\frac{1}{4}\Bigg(\left[\frac{1}{2}\left(4\gamma^2-3\right)\frac{C'}{C}-2\left(\gamma^2-1\right)\frac{D'}{D}\right]^2\rho_\chi \\
& +\left[\left(\gamma^2+2\right)\frac{C'}{C}-\left(\gamma^2-1\right)\frac{D'}{D}\right]^2\gamma^2 p_\chi+\left[\frac{15}{4}\rho_\chi-13\gamma^2 p_\chi\right]\left(\frac{C'}{C}\right)^2\Bigg) \\
& +\frac{\gamma^2 D}{2C}\Bigg(\left(\left[\left(4\gamma^2-2\right)\ddot{\phi}-3H\frac{D}{C}\dot{\phi}^3\right]\rho_\chi+\left[\left(\gamma^2-1\right)\ddot{\phi}-6H\dot{\phi}\right]\gamma^2 p_\chi\right)\frac{D'}{D} \\
& -\left(\left[\left(4\gamma^2-5\right)\ddot{\phi}-3H\dot{\phi}\right]\rho_\chi+\left[\gamma^4\ddot{\phi}-3H\dot{\phi}\left(2\gamma^2-3\right)\right]p_\chi\right)\frac{C'}{C}\Bigg] \\
& +\frac{3}{2}H\dot{\phi}\left(\frac{C'}{C}-\frac{D'}{D}\right)\frac{\gamma\left(\gamma_d-1\right)^2\left(2\gamma^2+3\gamma+1\right)}{\gamma^2+\gamma+1} \\
& +\frac{3}{4}\frac{C}{D}\gamma^3\left(\frac{C'}{C}-\frac{D'}{D}\right)^2\frac{4\gamma_d^2+\gamma_d-2}{\gamma_d^2+\gamma_d+1} \\
& -\frac{C}{4D}\Bigg(3\gamma_d\left(2\gamma_d^2-1\right)\left(\frac{C'}{C}\right)^2+\left(10\gamma_d^2-15\gamma_d+8\right)\left(\frac{D'}{D}\right)^2 \\
& -2\frac{C'}{C}\frac{D'}{D}\left(8\gamma_d^3-9\gamma_d+4\right)\Bigg)-\frac{1}{2}\frac{C}{D}\left(\gamma_d^3-3\gamma_d+2\right)\left(\frac{C''}{C}-\frac{D''}{D}\right),
\end{aligned}
$$

$$
\alpha_{10} = \left(\frac{1}{2}\left[\left(\gamma^2-1\right)\frac{D'}{D}-\left(\gamma^2-5\right)\frac{C'}{C}\right]+\frac{D}{C}\left[\gamma^2\ddot{\phi}+3H\dot{\phi}\right]\right)\gamma C^2 V'.
$$

A.2.4. Coefficients following transformation to gauge-invariant Sasaki-Mukhanov variables

When transforming from eqs. (4.3.4 – 4.3.5) to eqs. (4.3.2 – 4.3.3), one eliminates the metric perturbations to obtain gauge invariant field equations, and in doing so, we define modified versions of some of the above coefficients as they appear in the gauge invariant system. These are

Transformation of α_n

$$
\begin{aligned}
\bar{\alpha}_6 &= \alpha_6 - \frac{1}{2H}\left[\left(\alpha_1\dot{\phi}+\alpha_2\dot{\chi}\right)Z_3 + \left(\alpha_3\dot{\phi}+\alpha_4\dot{\chi}\right)X_3\right] , \\
\bar{\alpha}_7 &= \alpha_7 - \frac{1}{2H}\left[\left(\alpha_1\dot{\phi}+\alpha_2\dot{\chi}\right)Z_5 + \left(\alpha_3\dot{\phi}+\alpha_4\dot{\chi}\right)X_5\right] , \\
\bar{\alpha}_9 &= \alpha_9 + \frac{Y_1}{2H}\left(\bar{\alpha}_6\dot{\phi}+\bar{\alpha}_7\dot{\chi}+2\left[\alpha_1\left(\ddot{\phi}-\frac{\dot{H}\dot{\phi}}{H}\right)+\alpha_2\left(\ddot{\chi}-\frac{\dot{H}\dot{\chi}}{H}\right)\right]\right. \\
&\quad \left. - H\left[\alpha_5+(4\alpha_1-3\alpha_3)\dot{\phi}+(4\alpha_2-3\alpha_4)\dot{\chi}\right]\right) \\
&\quad - \frac{Z_2}{2H}\left(\alpha_1\dot{\phi}+\alpha_2\dot{\chi}\right) - \frac{X_2}{2H}\left(\alpha_3\dot{\phi}+\alpha_4\dot{\chi}\right) , \\
\bar{\alpha}_{10} &= \alpha_{10} + \frac{Y_2}{2H}\left(\bar{\alpha}_6\dot{\phi}+\bar{\alpha}_7\dot{\chi}+2\left[\alpha_1\left(\ddot{\phi}-\frac{\dot{H}\dot{\phi}}{H}\right)+\alpha_2\left(\ddot{\chi}-\frac{\dot{H}\dot{\chi}}{H}\right)\right]\right. \\
&\quad \left. - H\left[\alpha_5+(4\alpha_1-3\alpha_3)\dot{\phi}+(4\alpha_2-3\alpha_4)\dot{\chi}\right]\right) \\
&\quad - \frac{Z_4}{2H}\left(\alpha_1\dot{\phi}+\alpha_2\dot{\chi}\right) - \frac{X_4}{2H}\left(\alpha_3\dot{\phi}+\alpha_4\dot{\chi}\right) .
\end{aligned}
$$

Transformation of β_n

$$
\begin{aligned}
\bar{\beta}_6 &= \beta_6 - \frac{1}{2H}\left[\left(\beta_1\dot{\phi}+\beta_2\dot{\chi}\right)Z_3 + \left(\beta_3\dot{\phi}+\beta_4\dot{\chi}\right)X_3\right] , \\
\bar{\beta}_7 &= \beta_7 - \frac{1}{2H}\left[\left(\beta_1\dot{\phi}+\beta_2\dot{\chi}\right)Z_5 + \left(\beta_3\dot{\phi}+\beta_4\dot{\chi}\right)X_5\right] , \\
\bar{\beta}_9 &= \beta_9 + \frac{Y_1}{2H}\Bigg(\bar{\beta}_6\dot{\phi}+\bar{\beta}_7\dot{\chi}+2\left[\beta_1\left(\ddot{\phi}-\frac{\dot{H}\dot{\phi}}{H}\right)+\beta_2\left(\ddot{\chi}-\frac{\dot{H}\dot{\chi}}{H}\right)\right] \\
&\quad - H\left[\beta_5+\left(4\beta_1-3\beta_3\right)\dot{\phi}+\left(4\beta_2-3\beta_4\right)\dot{\chi}\right]\Bigg) \\
&\quad - \frac{Z_2}{2H}\left(\beta_1\dot{\phi}+\beta_2\dot{\chi}\right) - \frac{X_2}{2H}\left(\beta_3\dot{\phi}+\beta_4\dot{\chi}\right) , \\
\bar{\beta}_{10} &= \beta_{10} + \frac{Y_2}{2H}\Bigg(\bar{\beta}_6\dot{\phi}+\bar{\beta}_7\dot{\chi}+2\left[\beta_1\left(\ddot{\phi}-\frac{\dot{H}\dot{\phi}}{H}\right)+\beta_2\left(\ddot{\chi}-\frac{\dot{H}\dot{\chi}}{H}\right)\right] \\
&\quad - H\left[\beta_5+\left(4\beta_1-3\beta_3\right)\dot{\phi}+\left(4\beta_2-3\beta_4\right)\dot{\chi}\right]\Bigg) \\
&\quad - \frac{Z_4}{2H}\left(\beta_1\dot{\phi}+\beta_2\dot{\chi}\right) - \frac{X_4}{2H}\left(\beta_3\dot{\phi}+\beta_4\dot{\chi}\right) .
\end{aligned}
$$

BIBLIOGRAPHY

[1] A. Einstein, *Die grundlage der allgemeinen relativitätstheorie*, *Annalen der Physik* **354** (1916), no. 7 769–822.

[2] **Particle Data Group** Collaboration, J. Beringer et al., *Review of Particle Physics (RPP)*, *Phys. Rev.* **D86** (2012) 010001.

[3] **Particle Data Group** Collaboration, K. A. Olive et al., *Review of Particle Physics*, *Chin. Phys.* **C38** (2014) 090001.

[4] **Particle Data Group** Collaboration, C. Patrignani et al., *Review of Particle Physics*, *Chin. Phys.* **C40** (2016), no. 10 100001.

[5] **Virgo, LIGO Scientific** Collaboration, B. P. Abbott et al., *Observation of Gravitational Waves from a Binary Black Hole Merger*, *Phys. Rev. Lett.* **116** (2016), no. 6 061102, [arXiv:1602.03837].

[6] **GROND, SALT Group, OzGrav, DFN, INTEGRAL, Virgo, Insight-Hxmt, MAXI Team, Fermi-LAT, J-GEM, RATIR, IceCube, CAASTRO, LWA, ePESSTO, GRAWITA, RIMAS, SKA South Africa/MeerKAT, H.E.S.S., 1M2H Team, IKI-GW Follow-up, Fermi GBM, Pi of Sky, DWF (Deeper Wider Faster Program), Dark Energy Survey, MASTER, AstroSat Cadmium Zinc Telluride Imager Team, Swift, Pierre Auger, ASKAP,**

VINROUGE, JAGWAR, Chandra Team at McGill University, TTU-NRAO, GROWTH, AGILE Team, MWA, ATCA, AST3, TOROS, Pan-STARRS, NuSTAR, ATLAS Telescopes, BOOTES, CaltechNRAO, LIGO Scientific, High Time Resolution Universe Survey, Nordic Optical Telescope, Las Cumbres Observatory Group, TZAC Consortium, LOFAR, IPN, DLT40, Texas Tech University, HAWC, ANTARES, KU, Dark Energy Camera GW-EM, CALET, Euro VLBI Team, ALMA Collaboration, B. P. Abbott et al., *Multi-messenger Observations of a Binary Neutron Star Merger*, *Astrophys. J.* **848** (2017), no. 2 L12, [arXiv:1710.05833].

[7] **ATLAS** Collaboration, G. Aad et al., *Observation of a new particle in the search for the Standard Model Higgs boson with the ATLAS detector at the LHC*, *Phys. Lett.* **B716** (2012) 1–29, [arXiv:1207.7214].

[8] **CMS** Collaboration, S. Chatrchyan et al., *Observation of a new boson at a mass of 125 GeV with the CMS experiment at the LHC*, *Phys. Lett.* **B716** (2012) 30–61, [arXiv:1207.7235].

[9] S. Dodelson, *Modern Cosmology*. Academic Press. Academic Press, 2003.

[10] V. Mukhanov, *Physical Foundations of Cosmology*. Cambridge University Press, 2005.

[11] J. Peacock, *Cosmological Physics*. Cambridge Astrophysics. Cambridge University Press, 1999.

[12] P. Peebles, *Principles of Physical Cosmology*. Princeton series in physics. Princeton University Press, 1993.

[13] R. A. Alpher, H. Bethe, and G. Gamow, *The origin of chemical elements*, *Phys. Rev.* **73** (Apr, 1948) 803–804.

[14] R. Durrer, *The Cosmic Microwave Background*. Cambridge University Press, 2008.

[15] **Supernova Search Team** Collaboration, A. G. Riess et al., *Observational evidence from supernovae for an accelerating universe and a cosmological constant*, *Astron. J.* **116** (1998) 1009–1038, [astro-ph/9805201].

[16] **Supernova Cosmology Project** Collaboration, S. Perlmutter et al., *Measurements of Omega and Lambda from 42 high redshift supernovae*, *Astrophys. J.* **517** (1999) 565–586, [astro-ph/9812133].

[17] **Supernova Search Team** Collaboration, A. G. Riess et al., *Type Ia supernova discoveries at $z > 1$ from the Hubble Space Telescope: Evidence for past deceleration and constraints on dark energy evolution*, *Astrophys. J.* **607** (2004) 665–687, [astro-ph/0402512].

[18] J. C. Kapteyn, *First Attempt at a Theory of the Arrangement and Motion of the Sidereal System*, *The Astrophysical Journal* **55** (May, 1922) 302.

[19] F. Zwicky, *On the Masses of Nebulae and of Clusters of Nebulae*, *The Astrophysical Journal* **86** (Oct., 1937) 217.

[20] V. C. Rubin and W. K. Ford, Jr., *Rotation of the Andromeda Nebula from a Spectroscopic Survey of Emission Regions*, *The Astrophysical Journal* **159** (Feb., 1970) 379.

[21] V. C. Rubin, N. Thonnard, and W. K. Ford, Jr., *Extended rotation curves of high-luminosity spiral galaxies. IV - Systematic dynamical properties, SA through SC*, *The Astrophysical Journal Letters* **225** (Nov., 1978) L107–L111.

[22] V. C. Rubin, W. K. Ford, Jr., and N. Thonnard, *Rotational properties of 21 SC galaxies with a large range of luminosities and radii, from NGC 4605 $R = 4$ kpc to UGC 2885 $R = 122$ kpc*, *The Astrophysical Journal* **238** (June, 1980) 471–487.

[23] M. Persic, P. Salucci, and F. Stel, *The universal rotation curve of spiral galaxies - i. the dark matter connection*, *Monthly Notices of the Royal Astronomical Society* **281** (1996), no. 1 27–47.

[24] **Planck** Collaboration, P. A. R. Ade et al., *Planck 2015 results. XIII. Cosmological parameters*, *Astron. Astrophys.* **594** (2016) A13, [arXiv:1502.01589].

[25] F. C. Adams and G. Laughlin, *A Dying universe: The Long term fate and evolution of astrophysical objects*, *Rev. Mod. Phys.* **69** (1997) 337–372, [astro-ph/9701131].

[26] I. Albarran, M. Bouhmadi-López, C.-Y. Chen, and P. Chen, *Doomsdays in a modified theory of gravity: A classical and a quantum approach*, *Phys. Lett.* **B772** (2017) 814–818, [arXiv:1703.09263].

[27] Y. Wang, J. M. Kratochvil, A. D. Linde, and M. Shmakova, *Current observational constraints on cosmic doomsday*, *JCAP* **0412** (2004) 006, [astro-ph/0409264].

[28] A. V. Yurov, A. V. Astashenok, and P. F. Gonzalez-Diaz, *Astronomical bounds on future big freeze singularity*, *Grav. Cosmol.* **14** (2008) 205–212, [arXiv:0705.4108].

[29] C. Misner, K. Thorne, J. Wheeler, and D. Kaiser, *Gravitation*. Princeton University Press, 2017.

[30] S. Hawking and W. Israel, *General Relativity; an Einstein Centenary Survey*. Cambridge University Press, 1979.

[31] R. Carrigan and W. Trower, *Magnetic Monopoles*. Nato Science Series B:. Springer US, 2012.

[32] A. H. Guth, *The Inflationary Universe: A Possible Solution to the Horizon and Flatness Problems*, *Phys. Rev.* **D23** (1981) 347–356.

[33] A. D. Linde, *A new inflationary universe scenario: A possible solution of the horizon, flatness, homogeneity, isotropy and primordial monopole problems*, *Physics Letters B* **108** (Feb., 1982) 389–393.

[34] E. Kolb and M. Turner, *The Early Universe*. Avalon Publishing, 1994.

[35] A. Liddle and D. Lyth, *Cosmological Inflation and Large-Scale Structure*. Cosmological Inflation and Large-scale Structure. Cambridge University Press, 2000.

[36] D. Lyth and A. Liddle, *The Primordial Density Perturbation: Cosmology, Inflation and the Origin of Structure*. Cambridge University Press, 2009.

[37] **WMAP** Collaboration, C. L. Bennett et al., *Nine-Year Wilkinson Microwave Anisotropy Probe (WMAP) Observations: Final Maps and Results*, *Astrophys. J. Suppl.* **208** (2013) 20, [arXiv:1212.5225].

[38] **WMAP** Collaboration, G. Hinshaw et al., *Nine-Year Wilkinson Microwave Anisotropy Probe (WMAP) Observations: Cosmological Parameter Results*, *Astrophys. J. Suppl.* **208** (2013) 19, [arXiv:1212.5226].

[39] **Planck** Collaboration, P. A. R. Ade et al., *Planck 2015 results. XX. Constraints on inflation*, arXiv:1502.02114.

[40] **BICEP2, Planck** Collaboration, P. A. R. Ade et al., *Joint Analysis of BICEP2/KeckArray and Planck Data*, *Phys. Rev. Lett.* **114** (2015) 101301, [arXiv:1502.00612].

[41] C. M. Will, *The Confrontation between General Relativity and Experiment*, *Living Rev. Rel.* **17** (2014) 4, [arXiv:1403.7377].

[42] R. P. Feynman, *Quantum theory of gravitation*, *Acta Phys. Polon.* **24** (1963) 697–722.

[43] G. W. Horndeski, *Second-order scalar-tensor field equations in a four-dimensional space*, *Int. J. Theor. Phys.* **10** (1974) 363–384.

[44] J. Ben Achour, D. Langlois, and K. Noui, *Degenerate higher order scalar-tensor theories beyond Horndeski and disformal transformations*, *Phys. Rev.* **D93** (2016), no. 12 124005, [arXiv:1602.08398].

[45] M. Zumalacárregui and J. García-Bellido, *Transforming gravity: from derivative couplings to matter to second-order scalar-tensor theories beyond*

the Horndeski Lagrangian, *Phys. Rev.* **D89** (2014) 064046, [arXiv:1308.4685].

[46] T. Clifton, P. G. Ferreira, A. Padilla, and C. Skordis, *Modified Gravity and Cosmology*, *Phys. Rept.* **513** (2012) 1–189, [arXiv:1106.2476].

[47] M. Escudero, H. Ramírez, L. Boubekeur, E. Giusarma, and O. Mena, *The present and future of the most favoured inflationary models after planck 2015*, *Journal of Cosmology and Astroparticle Physics* **2016** (2016), no. 02 020.

[48] J. Martin, C. Ringeval, and V. Vennin, *Encyclopædia Inflationaris*, *Phys. Dark Univ.* **5-6** (2014) 75–235, [arXiv:1303.3787].

[49] T. Kibble and F. Berkshire, *Classical Mechanics*. Imperial College Press, 2004.

[50] I. Newton, "Original letter from Isaac Newton to Richard Bentley." 189.R.4.47, ff. 7-8, Trinity College Library, Cambridge, UK, http://www.newtonproject.ox.ac.uk/view/texts/normalized/THEM00258, (1692).

[51] M. Born, *Einstein's Theory of Relativity*. Dover Books on Physics. Dover Publications, 2012.

[52] S. Carroll, *Spacetime and Geometry: An Introduction to General Relativity*. Pearson Education, Limited, 2013.

[53] R. D'Inverno, *Introducing Einstein's Relativity*. Clarendon Press, 1992.

[54] R. Wald, *General Relativity*. University of Chicago Press, 2010.

[55] J. Hartle, *Gravity: Pearson New International Edition: An Introduction to Einstein's General Relativity*. Pearson Education Limited, 2013.

[56] E. Poisson, *A Relativist's Toolkit: The Mathematics of Black-Hole Mechanics*. Cambridge University Press, 2004.

[57] H. Stephani, D. Kramer, M. MacCallum, C. Hoenselaers, and E. Herlt, *Exact Solutions of Einstein's Field Equations*. Cambridge Monographs on Mathematical Physics. Cambridge University Press, 2009.

[58] D. J. Kapner, T. S. Cook, E. G. Adelberger, J. H. Gundlach, B. R. Heckel, C. D. Hoyle, and H. E. Swanson, *Tests of the gravitational inverse-square law below the dark-energy length scale*, *Phys. Rev. Lett.* **98** (2007) 021101, [hep-ph/0611184].

[59] M. H. Goroff and A. Sagnotti, *The Ultraviolet Behavior of Einstein Gravity*, *Nucl. Phys.* **B266** (1986) 709–736.

[60] G. 't Hooft and M. J. G. Veltman, *One loop divergencies in the theory of gravitation*, *Ann. Inst. H. Poincare Phys. Theor.* **A20** (1974) 69–94.

[61] K. Koyama, *Cosmological Tests of Modified Gravity*, *Rept. Prog. Phys.* **79** (2016), no. 4 046902, [arXiv:1504.04623].

[62] R. Durrer and R. Maartens, *Dark Energy and Modified Gravity*, in *Dark Energy: Observational & Theoretical Approaches, ed. P Ruiz-Lapuente (Cambridge UP, 2010), pp48 - 91*, pp. 48 – 91, 2008. arXiv:0811.4132.

[63] F. S. N. Lobo, *The Dark side of gravity: Modified theories of gravity*, arXiv:0807.1640.

[64] S. Nojiri, S. D. Odintsov, and V. K. Oikonomou, *Modified Gravity Theories on a Nutshell: Inflation, Bounce and Late-time Evolution*, *Phys. Rept.* **692** (2017) 1–104, [arXiv:1705.11098].

[65] S. Capozziello and M. De Laurentis, *Extended Theories of Gravity*, *Phys. Rept.* **509** (2011) 167–321, [arXiv:1108.6266].

[66] C. P. Burgess, *Quantum gravity in everyday life: General relativity as an effective field theory*, *Living Rev. Rel.* **7** (2004) 5–56, [gr-qc/0311082].

[67] J. F. Donoghue, *General relativity as an effective field theory: The leading quantum corrections*, *Phys. Rev.* **D50** (1994) 3874–3888, [gr-qc/9405057].

[68] S. Weinberg, *Effective Field Theory, Past and Future*, *PoS* **CD09** (2009) 001, [arXiv:0908.1964].

[69] J. F. Donoghue, *The effective field theory treatment of quantum gravity*, *AIP Conf. Proc.* **1483** (2012) 73–94, [arXiv:1209.3511].

[70] H. A. Buchdahl, *Non-linear Lagrangians and cosmological theory*, *Monthly Notices of the Royal Astronomical Society* **150** (1970) 1.

[71] T. P. Sotiriou and V. Faraoni, *$f(R)$ Theories Of Gravity*, *Rev. Mod. Phys.* **82** (2010) 451–497, [arXiv:0805.1726].

[72] A. De Felice and S. Tsujikawa, *f(R) theories*, *Living Rev. Rel.* **13** (2010) 3, [arXiv:1002.4928].

[73] A. A. Starobinsky, *A New Type of Isotropic Cosmological Models Without Singularity*, *Phys. Lett.* **B91** (1980) 99–102.

[74] J. A. R. Cembranos, *Dark Matter from R^2-gravity*, *Phys. Rev. Lett.* **102** (2009) 141301, [arXiv:0809.1653].

[75] G. J. Olmo, *The Gravity Lagrangian according to solar system experiments*, *Phys. Rev. Lett.* **95** (2005) 261102, [gr-qc/0505101].

[76] C. P. L. Berry and J. R. Gair, *Linearized f(R) Gravity: Gravitational Radiation and Solar System Tests*, *Phys. Rev.* **D83** (2011) 104022, [arXiv:1104.0819]. [Erratum: Phys. Rev.D85,089906(2012)].

[77] A. W. Brookfield, C. van de Bruck, and L. M. H. Hall, *Viability of f(R) Theories with Additional Powers of Curvature*, *Phys. Rev.* **D74** (2006) 064028, [hep-th/0608015].

[78] Y. Fujii and K. Maeda, *The scalar-tensor theory of gravitation*. Cambridge University Press, 2007.

[79] G. Esposito-Farese and D. Polarski, *Scalar tensor gravity in an accelerating universe*, *Phys. Rev.* **D63** (2001) 063504, [gr-qc/0009034].

[80] R. V. Wagoner, *Scalar tensor theory and gravitational waves*, *Phys. Rev.* **D1** (1970) 3209–3216.

[81] D. Wands, *Extended gravity theories and the Einstein-Hilbert action*, *Class. Quant. Grav.* **11** (1994) 269–280, [gr-qc/9307034].

[82] E. E. Flanagan, *Higher order gravity theories and scalar tensor theories*, *Class. Quant. Grav.* **21** (2003) 417–426, [gr-qc/0309015].

[83] F. Bezrukov, *The Higgs field as an inflaton*, *Class. Quant. Grav.* **30** (2013) 214001, [arXiv:1307.0708].

[84] F. L. Bezrukov and M. Shaposhnikov, *The Standard Model Higgs boson as the inflaton*, *Phys. Lett.* **B659** (2008) 703–706, [arXiv:0710.3755].

[85] C. Brans and R. H. Dicke, *Mach's principle and a relativistic theory of gravitation*, *Phys. Rev.* **124** (Nov, 1961) 925–935.

[86] J. Alsing, E. Berti, C. M. Will, and H. Zaglauer, *Gravitational radiation from compact binary systems in the massive Brans-Dicke theory of gravity*, *Phys. Rev.* **D85** (2012) 064041, [arXiv:1112.4903].

[87] N. D. Birrell and P. Davies, *Quantum Fields in Curved Spacetime*. Cambridge University Press, 1982.

[88] T. P. Sotiriou, *$f(R)$ gravity and scalar tensor theory*, *Classical and Quantum Gravity* **23** (Sept., 2006) 5117–5128, [gr-qc/0604028].

[89] T. Faulkner, M. Tegmark, E. F. Bunn, and Y. Mao, *Constraining $f(R)$ Gravity as a Scalar Tensor Theory*, *Phys. Rev.* **D76** (2007) 063505, [astro-ph/0612569].

[90] D. F. Carneiro, E. A. Freiras, B. Goncalves, A. G. de Lima, and I. L. Shapiro, *On useful conformal tranformations in general relativity*, *Grav. Cosmol.* **10** (2004) 305–312, [gr-qc/0412113].

[91] A. S. Arapoglu, *Generalized Slow-roll Inflation in Non-minimally Coupled Theories*, arXiv:1504.02192.

[92] T. Chiba and M. Yamaguchi, *Conformal-Frame (In)dependence of Cosmological Observations in Scalar-Tensor Theory*, *JCAP* **1310** (2013) 040, [arXiv:1308.1142].

[93] V. Faraoni and S. Nadeau, *The (pseudo)issue of the conformal frame revisited*, *Phys. Rev.* **D75** (2007) 023501, [gr-qc/0612075].

[94] T. Qiu and J.-Q. Xia, *Perturbations of Single-field Inflation in Modified Gravity Theory*, *Phys. Lett.* **B744** (2015) 273–279, [arXiv:1406.5902].

[95] D. F. Torres, *Slow roll inflation in nonminimally coupled theories: Hyperextended gravity approach*, *Phys. Lett.* **A225** (1997) 13–17, [gr-qc/9610021].

[96] C. F. Steinwachs and A. Yu. Kamenshchik, *Non-minimal Higgs Inflation and Frame Dependence in Cosmology*, arXiv:1301.5543. [AIP Conf. Proc.1514,161(2012)].

[97] J. D. Bekenstein, *The Relation between physical and gravitational geometry*, *Phys. Rev.* **D48** (1993) 3641–3647, [gr-qc/9211017].

[98] M. Zumalacrregui, T. S. Koivisto, and D. F. Mota, *DBI Galileons in the Einstein Frame: Local Gravity and Cosmology*, *Phys. Rev.* **D87** (2013) 083010, [arXiv:1210.8016].

[99] E. Silverstein and D. Tong, *Scalar speed limits and cosmology: Acceleration from D-cceleration*, *Phys. Rev.* **D70** (2004) 103505, [hep-th/0310221].

[100] C. van de Bruck, C. Burrage, and J. Morrice, *Vacuum Cherenkov radiation and bremsstrahlung from disformal couplings*, *JCAP* **1608** (2016), no. 08 003, [arXiv:1605.03567].

[101] F. Arroja, N. Bartolo, P. Karmakar, and S. Matarrese, *The two faces of mimetic Horndeski gravity: disformal transformations and Lagrange multiplier*, *JCAP* **1509** (2015) 051, [arXiv:1506.08575].

[102] E. Bittencourt, I. P. Lobo, and G. G. Carvalho, *On the disformal invariance of the Dirac equation*, *Class. Quant. Grav.* **32** (2015) 185016, [arXiv:1505.03415].

[103] G. Domènech, A. Naruko, and M. Sasaki, *Cosmological disformal invariance*, arXiv:1505.00174.

[104] T. S. Koivisto and F. R. Urban, *Disformal vectors and anisotropies on a warped braneHulluilla on Halvat Huvit*, *JCAP* **1503** (2015), no. 03 003, [arXiv:1407.3445].

[105] M. Minamitsuji, *Disformal transformation of cosmological perturbations*, *Phys. Lett.* **B737** (2014) 139–150, [arXiv:1409.1566].

[106] H. Motohashi and J. White, *Disformal invariance of curvature perturbation*, arXiv:1504.00846.

[107] H. Y. Ip, J. Sakstein, and F. Schmidt, *Solar System Constraints on Disformal Gravity Theories*, *JCAP* **1510** (2015), no. 10 051, [arXiv:1507.00568].

[108] P. Brax and C. Burrage, *Constraining Disformally Coupled Scalar Fields*, *Phys. Rev.* **D90** (2014), no. 10 104009, [arXiv:1407.1861].

[109] C. van de Bruck and J. Morrice, *Disformal couplings and the dark sector of the universe*, *JCAP* **1504** (2015) 036, [arXiv:1501.03073].

[110] T. Koivisto, D. Wills, and I. Zavala, *Dark D-brane Cosmology*, *JCAP* **1406** (2014) 036, [arXiv:1312.2597].

[111] J. Sakstein, *Disformal Theories of Gravity: From the Solar System to Cosmology*, *JCAP* **1412** (2014) 012, [arXiv:1409.1734].

[112] M. Zumalacárregui, T. S. Koivisto, D. F. Mota, and P. Ruiz-Lapuente, *Disformal Scalar Fields and the Dark Sector of the Universe*, *JCAP* **1005** (2010) 038, [arXiv:1004.2684].

[113] D. G. Boulware and S. Deser, *Can gravitation have a finite range?*, *Phys. Rev.* **D6** (1972) 3368–3382.

[114] E. Papantonopoulos, *The Invisible Universe: Dark Matter and Dark Energy*. Lecture Notes in Physics. Springer Berlin Heidelberg, 2007.

[115] F. Sbisà, *Classical and quantum ghosts*, *Eur. J. Phys.* **36** (2015) 015009, [arXiv:1406.4550].

[116] K. S. Stelle, *Renormalization of Higher Derivative Quantum Gravity*, *Phys. Rev.* **D16** (1977) 953–969.

[117] K. S. Stelle, *Classical Gravity with Higher Derivatives*, *Gen. Rel. Grav.* **9** (1978) 353–371.

[118] R. P. Woodard, *Ostrogradsky's theorem on Hamiltonian instability*, *Scholarpedia* **10** (2015), no. 8 32243, [arXiv:1506.02210].

[119] A. De Felice, T. Kobayashi, and S. Tsujikawa, *Effective gravitational couplings for cosmological perturbations in the most general scalar-tensor theories with second-order field equations*, *Phys. Lett.* **B706** (2011) 123–133, [arXiv:1108.4242].

[120] A. De Felice and S. Tsujikawa, *Conditions for the cosmological viability of the most general scalar-tensor theories and their applications to extended Galileon dark energy models*, *JCAP* **1202** (2012) 007, [arXiv:1110.3878].

[121] T. Kobayashi, M. Yamaguchi, and J. Yokoyama, *Generalized G-inflation: Inflation with the most general second-order field equations*, *Prog. Theor. Phys.* **126** (2011) 511–529, [arXiv:1105.5723].

[122] C. Charmousis, E. J. Copeland, A. Padilla, and P. M. Saffin, *Self-tuning and the derivation of a class of scalar-tensor theories*, *Phys. Rev.* **D85** (2012) 104040, [arXiv:1112.4866].

[123] E. J. Copeland, A. Padilla, and P. M. Saffin, *The cosmology of the Fab-Four*, *JCAP* **1212** (2012) 026, [arXiv:1208.3373].

[124] W. T. Emond and P. M. Saffin, *Disformally self-tuning gravity*, *JHEP* **03** (2016) 161, [arXiv:1511.02055].

[125] X. Gao and D. A. Steer, *Inflation and primordial non-Gaussianities of 'generalized Galileons'*, *JCAP* **1112** (2011) 019, [arXiv:1107.2642].

[126] J. Gleyzes, D. Langlois, F. Piazza, and F. Vernizzi, *Healthy theories beyond Horndeski*, *Phys. Rev. Lett.* **114** (2015), no. 21 211101, [arXiv:1404.6495].

[127] N. Kaloper and M. Sandora, *Spherical Cows in the Sky with Fab Four*, *JCAP* **1405** (2014) 028, [arXiv:1310.5058].

[128] P. Martín-Moruno, N. J. Nunes, and F. S. N. Lobo, *Attracted to de Sitter: cosmology of the linear Horndeski models*, *JCAP* **1505** (2015), no. 05 033, [arXiv:1502.05878].

[129] S. Tsujikawa, *Dark energy in the most general scalar-tensor theories and their observational constraints*, *AIP Conf. Proc.* **1514** (2012) 118–127.

[130] J. Gleyzes, D. Langlois, F. Piazza, and F. Vernizzi, *Exploring gravitational theories beyond Horndeski*, *JCAP* **1502** (2015) 018, [arXiv:1408.1952].

[131] T. Biswas, E. Gerwick, T. Koivisto, and A. Mazumdar, *Towards singularity and ghost free theories of gravity*, *Phys. Rev. Lett.* **108** (2012) 031101, [arXiv:1110.5249].

[132] H. Lu, A. Perkins, C. N. Pope, and K. S. Stelle, *Black Holes in Higher-Derivative Gravity*, *Phys. Rev. Lett.* **114** (2015), no. 17 171601, [arXiv:1502.01028].

[133] T. Biswas, T. Koivisto, and A. Mazumdar, *Towards a resolution of the cosmological singularity in non-local higher derivative theories of gravity*, *JCAP* **1011** (2010) 008, [arXiv:1005.0590].

[134] I. Dimitrijevic, B. Dragovich, J. Grujic, and Z. Rakic, *On Modified Gravity*, *Springer Proc. Math. Stat.* **36** (2013) 251–259, [arXiv:1202.2352].

[135] D. Lovelock, *The Einstein tensor and its generalizations*, *J. Math. Phys.* **12** (1971) 498–501.

[136] M. Gurses, *Some solutions of the Gauss-Bonnet gravity with scalar field in four dimensions*, *Gen. Rel. Grav.* **40** (2008) 1825–1830, [arXiv:0707.0347].

[137] B. Zumino, *Gravity Theories in More Than Four-Dimensions*, *Phys. Rept.* **137** (1986) 109.

[138] C. Armendariz-Picon, V. F. Mukhanov, and P. J. Steinhardt, *Essentials of k essence*, *Phys. Rev.* **D63** (2001) 103510, [astro-ph/0006373].

[139] M. Malquarti, E. J. Copeland, A. R. Liddle, and M. Trodden, *A New view of k-essence*, *Phys. Rev.* **D67** (2003) 123503, [astro-ph/0302279].

[140] D. Langlois and S. Renaux-Petel, *Perturbations in generalized multi-field inflation*, *JCAP* **0804** (2008) 017, [arXiv:0801.1085].

[141] M. Alishahiha, E. Silverstein, and D. Tong, *DBI in the sky*, *Phys. Rev.* **D70** (2004) 123505, [hep-th/0404084].

[142] D. Wands, N. Bartolo, S. Matarrese, and A. Riotto, *An Observational test of two-field inflation*, *Phys. Rev.* **D66** (2002) 043520, [astro-ph/0205253].

[143] A. L. Berkin and R. W. Hellings, *Multiple field scalar - tensor theories of gravity and cosmology*, *Phys. Rev.* **D49** (1994) 6442–6449, [gr-qc/9401033].

[144] M. Rainer and A. Zhuk, *Tensor - multi - scalar theories from multidimensional cosmology*, *Phys. Rev.* **D54** (1996) 6186–6192, [gr-qc/9608020].

[145] V. Vardanyan and L. Amendola, *How can we tell whether dark energy is composed of multiple fields?*, *Phys. Rev.* **D92** (2015), no. 2 024009, [arXiv:1502.05922].

[146] S. Pi and D. Wang, *Cosmological perturbations in inflation with multiple sound speeds*, *Nucl. Phys.* **B862** (2012) 409–429, [arXiv:1107.0813].

[147] Y.-F. Cai and H.-Y. Xia, *Inflation with multiple sound speeds: a model of multiple DBI type actions and non-Gaussianities*, *Phys. Lett.* **B677** (2009) 226–234, [arXiv:0904.0062].

[148] C. Longden, *The adiabatic/entropy decomposition in $P(\phi^I, X^{IJ})$ theories with multiple sound speeds*, *Phys. Rev.* **D95** (2017), no. 2 023511, [arXiv:1611.03481].

[149] K. Becker, M. Becker, and J. Schwarz, *String Theory and M-Theory: A Modern Introduction*. Cambridge University Press, 2006.

[150] M. Green, J. Schwarz, and E. Witten, *Superstring Theory: Volume 1, Introduction*. Cambridge Monographs on Mathematical Physics. Cambridge University Press, 1988.

[151] M. Green, J. Schwarz, and E. Witten, *Superstring Theory: Volume 2, Loop Amplitudes, Anomalies and Phenomenology*. Cambridge Monographs on Mathematical Physics. Cambridge University Press, 1987.

[152] J. Polchinski, *String Theory: Volume 2, Superstring Theory and Beyond*. Cambridge Monographs on Mathematical Physics. Cambridge University Press, 1998.

[153] J. Polchinski, *String Theory: Volume 1, An Introduction to the Bosonic String*. Cambridge Monographs on Mathematical Physics. Cambridge University Press, 1998.

[154] D. Tong, *Lectures on string theory*, arXiv:0908.0333.

[155] D. Baumann and L. McAllister, *Inflation and String Theory*. Cambridge Monographs on Mathematical Physics. Cambridge University Press, 2015.

[156] D. G. Boulware and S. Deser, *String Generated Gravity Models*, *Phys. Rev. Lett.* **55** (1985) 2656.

[157] J. T. Wheeler, *Symmetric Solutions to the Gauss-Bonnet Extended Einstein Equations*, *Nucl. Phys.* **B268** (1986) 737–746.

[158] H. Yoshida and T. Yoshino, *EXPLICIT DERIVATION OF GAUSS-BONNET COMBINATION FROM STRING THEORIES*, .

[159] D. J. Gross and J. H. Sloan, *The Quartic Effective Action for the Heterotic String*, *Nucl. Phys.* **B291** (1987) 41–89.

[160] A. A. Tseytlin and C. Vafa, *Elements of string cosmology*, *Nucl. Phys.* **B372** (1992) 443–466, [hep-th/9109048].

[161] F. Quevedo, S. Krippendorf, and O. Schlotterer, *Cambridge Lectures on Supersymmetry and Extra Dimensions*, arXiv:1011.1491.

[162] P. Binétruy, *Supersymmetry: Theory, Experiment, and Cosmology*. Oxford Graduate Texts. OUP Oxford, 2006.

[163] H. Müller-Kirsten and A. Wiedemann, *Introduction to Supersymmetry*. World Scientific lecture notes in physics. World Scientific, 2010.

[164] C. Johnson, *D-Branes*. Cambridge Monographs on Mathematical Physics. Cambridge University Press, 2006.

[165] P. Brax and C. van de Bruck, *Cosmology and brane worlds: A Review*, *Class. Quant. Grav.* **20** (2003) R201–R232, [hep-th/0303095].

[166] A. Friedmann, *Über die krümmung des raumes*, *Zeitschrift für Physik* **10** (Dec, 1922) 377–386.

[167] G. Lemaître, *Un Univers homogène de masse constante et de rayon croissant rendant compte de la vitesse radiale des nébuleuses extra-galactiques*, *Annales de la Société Scientifique de Bruxelles* **47** (1927) 49–59.

[168] H. P. Robertson, *Kinematics and World-Structure*, *The Astrophysical Journal* **82** (Nov., 1935) 284.

[169] A. G. Walker, *On milne's theory of world-structure**, *Proceedings of the London Mathematical Society* **s2-42** (1937), no. 1 90–127.

[170] S. Weinberg, *GRAVITATION AND COSMOLOGY: PRINCIPLES AND APPLICATIONS OF THE GENERAL THEORY OF RELATIVITY*. Wiley India Pvt. Limited, 2008.

[171] **Planck** Collaboration, P. A. R. Ade et al., *Planck 2013 results. XVI. Cosmological parameters*, *Astron. Astrophys.* **571** (2014) A16, [arXiv:1303.5076].

[172] A. G. Riess et al., *Type Ia Supernova Distances at z ¿ 1.5 from the Hubble Space Telescope Multi-Cycle Treasury Programs: The Early Expansion Rate*, arXiv:1710.00844.

[173] N. Kaloper and A. Padilla, *Vacuum Energy Sequestering: The Framework and Its Cosmological Consequences*, *Phys. Rev.* **D90** (2014), no. 8 084023, [arXiv:1406.0711]. [Addendum: Phys. Rev.D90,no.10,109901(2014)].

[174] N. Kaloper and A. Padilla, *Sequestering the Standard Model Vacuum Energy*, *Phys. Rev. Lett.* **112** (2014), no. 9 091304, [arXiv:1309.6562].

[175] J. Khoury, *Theories of Dark Energy with Screening Mechanisms*, arXiv:1011.5909.

[176] R. Kimura, T. Kobayashi, and K. Yamamoto, *Vainshtein screening in a cosmological background in the most general second-order scalar-tensor theory*, *Phys. Rev.* **D85** (2012) 024023, [arXiv:1111.6749].

[177] T. S. Koivisto, D. F. Mota, and M. Zumalacarregui, *Screening Modifications of Gravity through Disformally Coupled Fields*, *Phys. Rev. Lett.* **109** (2012) 241102, [arXiv:1205.3167].

[178] J. Wheeler and K. Ford, *Geons, Black Holes, and Quantum Foam: A Life in Physics*. W. W. Norton, 2010.

[179] P. Peter and J. Uzan, *Primordial cosmology*. Oxford graduate texts. Oxford University Press, 2009.

[180] A. R. Liddle, P. Parsons, and J. D. Barrow, *Formalizing the slow roll approximation in inflation*, *Phys. Rev.* **D50** (1994) 7222–7232, [astro-ph/9408015].

[181] K. Bamba and S. D. Odintsov, *Inflationary cosmology in modified gravity theories*, *Symmetry* **7** (2015), no. 1 220–240, [arXiv:1503.00442].

[182] S. Nojiri and S. D. Odintsov, *Accelerating cosmology in modified gravity: from convenient $F(R)$ or string-inspired theory to bimetric $F(R)$ gravity*, *Int. J. Geom. Meth. Mod. Phys.* **11** (2014) 1460006, [arXiv:1306.4426].

[183] A. Ijjas, P. J. Steinhardt, and A. Loeb, *Inflationary paradigm in trouble after Planck2013*, *Phys. Lett.* **B723** (2013) 261–266, [arXiv:1304.2785].

[184] A. Ijjas, P. J. Steinhardt, and A. Loeb, *Inflationary schism*, *Phys. Lett.* **B736** (2014) 142–146, [arXiv:1402.6980].

[185] S. M. Carroll, *Beyond Falsifiability: Normal Science in a Multiverse*, 2018. arXiv:1801.05016.

[186] A. Linde, *Inflationary Cosmology after Planck 2013*, in *Proceedings, 100th Les Houches Summer School: Post-Planck Cosmology: Les Houches, France, July 8 - August 2, 2013*, pp. 231–316, 2015. arXiv:1402.0526.

[187] C. van de Bruck, K. Dimopoulos, and C. Longden, *Reheating in Gauss-Bonnet-coupled inflation*, *Phys. Rev.* **D94** (2016), no. 2 023506, [arXiv:1605.06350].

[188] L. Kofman, A. D. Linde, and A. A. Starobinsky, *Towards the theory of reheating after inflation*, *Phys. Rev.* **D56** (1997) 3258–3295, [hep-ph/9704452].

[189] R. Allahverdi, R. Brandenberger, F.-Y. Cyr-Racine, and A. Mazumdar, *Reheating in Inflationary Cosmology: Theory and Applications*, *Ann. Rev. Nucl. Part. Sci.* **60** (2010) 27–51, [arXiv:1001.2600].

[190] P. B. Greene, L. Kofman, A. D. Linde, and A. A. Starobinsky, *Structure of resonance in preheating after inflation*, *Phys. Rev.* **D56** (1997) 6175–6192, [hep-ph/9705347].

[191] G. N. Felder, L. Kofman, and A. D. Linde, *Instant preheating*, *Phys. Rev.* **D59** (1999) 123523, [hep-ph/9812289].

[192] G. N. Felder, L. Kofman, and A. D. Linde, *Inflation and preheating in NO models*, *Phys. Rev.* **D60** (1999) 103505, [hep-ph/9903350].

[193] A. Berera and T. W. Kephart, *The interaction structure and cosmological relevance of mass scales in string motivated supersymmetric theories*, *Phys. Lett.* **B456** (1999) 135–140, [hep-ph/9811295].

[194] R. Allahverdi, K. Enqvist, J. Garcia-Bellido, and A. Mazumdar, *Gauge invariant MSSM inflaton*, *Phys. Rev. Lett.* **97** (2006) 191304, [hep-ph/0605035].

[195] J. C. Bueno Sanchez, K. Dimopoulos, and D. H. Lyth, *A-term inflation and the MSSM*, *JCAP* **0701** (2007) 015, [hep-ph/0608299].

[196] K. Enqvist, A. Mazumdar, and P. Stephens, *Inflection point inflation within supersymmetry*, *JCAP* **1006** (2010) 020, [arXiv:1004.3724].

[197] D. H. Lyth, *MSSM inflation*, *JCAP* **0704** (2007) 006, [hep-ph/0605283].

[198] L. H. Ford, *Quantum field theory in curved space-time*, in *Particles and fields. Proceedings, 9th Jorge Andre Swieca Summer School, Campos do Jordao, Brazil, February 16-28, 1997*, pp. 345–388, 1997. gr-qc/9707062.

[199] E. J. Chun, S. Scopel, and I. Zaballa, *Gravitational reheating in quintessential inflation*, *JCAP* **0907** (2009) 022, [arXiv:0904.0675].

[200] L. H. Ford, *Gravitational Particle Creation and Inflation*, *Phys. Rev.* **D35** (1987) 2955.

[201] K. A. Malik and D. Wands, *Cosmological perturbations*, *Phys. Rept.* **475** (2009) 1–51, [arXiv:0809.4944].

[202] M. Sasaki, *Large scale quantum fluctuations in the inflationary universe*, *Progress of Theoretical Physics* **76** (1986), no. 5 1036–1046.

[203] V. F. Mukhanov, L. A. Kofman, and D. Yu. Pogosian, *Cosmological Perturbations in the Inflationary Universe*, *Phys. Lett.* **B193** (1987) 427–432.

[204] A. Riotto, *Inflation and the theory of cosmological perturbations*, *ICTP Lect. Notes Ser.* **14** (2003) 317–413, [hep-ph/0210162].

[205] C. Gordon, D. Wands, B. A. Bassett, and R. Maartens, *Adiabatic and entropy perturbations from inflation*, *Phys. Rev.* **D63** (2001) 023506, [astro-ph/0009131].

[206] F. Di Marco and F. Finelli, *Slow-roll inflation for generalized two-field Lagrangians*, *Phys. Rev.* **D71** (2005) 123502, [astro-ph/0505198].

[207] F. Di Marco, F. Finelli, and R. Brandenberger, *Adiabatic and isocurvature perturbations for multifield generalized Einstein models*, *Phys. Rev.* **D67** (2003) 063512, [astro-ph/0211276].

[208] J. Garcia-Bellido and D. Wands, *Metric perturbations in two field inflation*, *Phys. Rev.* **D53** (1996) 5437–5445, [astro-ph/9511029].

[209] D. Wands, *Primordial perturbations from inflation*, in *New trends in theoretical and observational cosmology. Proceedings, 5th RESCEU International Symposium, Tokyo, Japan, November 13-16, 2001*, pp. 1–10, 2002. astro-ph/0201541.

[210] D. Wands, K. A. Malik, D. H. Lyth, and A. R. Liddle, *A New approach to the evolution of cosmological perturbations on large scales*, *Phys. Rev.* **D62** (2000) 043527, [astro-ph/0003278].

[211] D. Polarski and A. A. Starobinsky, *Isocurvature perturbations in multiple inflationary models*, *Phys. Rev.* **D50** (1994) 6123–6129, [astro-ph/9404061].

[212] D. Langlois, S. Renaux-Petel, D. A. Steer, and T. Tanaka, *Primordial perturbations and non-Gaussianities in DBI and general multi-field inflation*, *Phys. Rev.* **D78** (2008) 063523, [arXiv:0806.0336].

[213] M. Nakashima, R. Saito, Y. Takamizu, and J. Yokoyama, *The Effect of Varying Sound Velocity on Primordial Curvature Perturbations*, *Progress of Theoretical Physics* **125** (May, 2011) 1035–1052, [arXiv:1009.4394].

[214] J. Garriga and V. F. Mukhanov, *Perturbations in k-inflation*, *Phys. Lett.* **B458** (1999) 219–225, [hep-th/9904176].

[215] N. Bartolo, E. Komatsu, S. Matarrese, and A. Riotto, *Non-Gaussianity from inflation: Theory and observations*, *Phys. Rept.* **402** (2004) 103–266, [astro-ph/0406398].

[216] D. Seery and J. E. Lidsey, *Primordial non-Gaussianities in single field inflation*, *JCAP* **0506** (2005) 003, [astro-ph/0503692].

[217] **Planck** Collaboration, P. A. R. Ade et al., *Planck 2015 results. XVII. Constraints on primordial non-Gaussianity*, *Astron. Astrophys.* **594** (2016) A17, [arXiv:1502.01592].

[218] C. M. Peterson and M. Tegmark, *Non-gaussianity in two-field inflation*, *Phys. Rev. D* **84** (Jul, 2011) 023520.

[219] F. Vernizzi and D. Wands, *Non-gaussianities in two-field inflation*, *JCAP* **0605** (2006) 019, [astro-ph/0603799].

[220] J. Emery, G. Tasinato, and D. Wands, *Local non-Gaussianity from rapidly varying sound speeds*, *JCAP* **1208** (2012) 005, [arXiv:1203.6625].

[221] J. M. Maldacena, *Non-Gaussian features of primordial fluctuations in single field inflationary models*, *JHEP* **05** (2003) 013, [astro-ph/0210603].

[222] C. van de Bruck, T. Koivisto, and C. Longden, *Disformally coupled inflation*, *JCAP* **1603** (2016), no. 03 006, [arXiv:1510.01650].

[223] C. van de Bruck, T. Koivisto, and C. Longden, *Non-Gaussianity in multi-sound-speed disformally coupled inflation*, *JCAP* **1702** (2017), no. 02 029, [arXiv:1608.08801].

[224] D. Bettoni and M. Zumalacárregui, *Kinetic mixing in scalar-tensor theories of gravity*, *Phys. Rev.* **D91** (2015) 104009, [arXiv:1502.02666].

[225] J. A. R. Cembranos, A. Dobado, and A. L. Maroto, *Brane world dark matter*, *Phys. Rev. Lett.* **90** (2003) 241301, [hep-ph/0302041].

[226] J. A. R. Cembranos and A. L. Maroto, *Disformal scalars as dark matter candidates: Branon phenomenology*, *Int. J. Mod. Phys.* **31** (2016), no. 14n15 1630015, [arXiv:1602.07270].

[227] D. Baumann, A. Dymarsky, S. Kachru, I. R. Klebanov, and L. McAllister, *D3-brane Potentials from Fluxes in AdS/CFT*, *JHEP* **06** (2010) 072, [arXiv:1001.5028].

[228] S. B. Giddings, S. Kachru, and J. Polchinski, *Hierarchies from fluxes in string compactifications*, *Phys. Rev.* **D66** (2002) 106006, [hep-th/0105097].

[229] I. R. Klebanov and M. J. Strassler, *Supergravity and a confining gauge theory: Duality cascades and chi SB resolution of naked singularities*, *JHEP* **08** (2000) 052, [hep-th/0007191].

[230] Y.-F. Cai and W. Xue, *N-flation from multiple DBI type actions*, *Phys. Lett.* **B680** (2009) 395–398, [arXiv:0809.4134].

[231] J. Emery, G. Tasinato, and D. Wands, *Mixed non-Gaussianity in multiple-DBI inflation*, *JCAP* **1305** (2013) 021, [arXiv:1303.3975].

[232] M.-x. Huang, G. Shiu, and B. Underwood, *Multifield DBI Inflation and Non-Gaussianities*, *Phys. Rev.* **D77** (2008) 023511, [arXiv:0709.3299].

[233] F. Arroja, S. Mizuno, and K. Koyama, *Non-gaussianity from the bispectrum in general multiple field inflation*, *JCAP* **0808** (2008) 015, [arXiv:0806.0619].

[234] X. Gao, D. Langlois, and S. Mizuno, *Oscillatory features in the curvature power spectrum after a sudden turn of the inflationary trajectory*, *JCAP* **1310** (2013) 023, [arXiv:1306.5680].

[235] M. Konieczka, R. H. Ribeiro, and K. Turzynski, *The effects of a fast-turning trajectory in multiple-field inflation*, *JCAP* **1407** (2014) 030, [arXiv:1401.6163].

[236] T. Noumi and M. Yamaguchi, *Primordial spectra from sudden turning trajectory*, *JCAP* **1312** (2013) 038, [arXiv:1307.7110].

[237] C. M. Peterson and M. Tegmark, *Testing Two-Field Inflation*, *Phys. Rev.* **D83** (2011) 023522, [arXiv:1005.4056].

[238] S. Tsujikawa, D. Parkinson, and B. A. Bassett, *Correlation-consistency cartography of the double-inflation landscape*, *Phys. Rev. D* **67** (Apr., 2003) 083516, [astro-ph/0210322].

[239] S. Yokoyama, K. Kamada, and K. Kohri, *Iso-curvature fluctuations in modulated reheating scenario*, in *Proceedings, 20th Workshop on General Relativity and Gravitation in Japan (JGRG20): Kyoto, Japan, September 21-25, 2010*, pp. 456–459, 2011.

[240] T. Suyama and M. Yamaguchi, *Non-Gaussianity in the modulated reheating scenario*, *Phys. Rev.* **D77** (2008) 023505, [arXiv:0709.2545].

[241] A. Mazumdar and K. P. Modak, *Constraints on variations in inflaton decay rate from modulated preheating*, *JCAP* **1606** (2016), no. 06 030, [arXiv:1506.01469].

[242] D. Langlois and T. Takahashi, *Density Perturbations from Modulated Decay of the Curvaton*, *JCAP* **1304** (2013) 014, [arXiv:1301.3319].

[243] K. Enqvist and S. Rusak, *Modulated preheating and isocurvature perturbations*, *JCAP* **1303** (2013) 017, [arXiv:1210.2192].

[244] B. A. Bassett, S. Tsujikawa, and D. Wands, *Inflation dynamics and reheating*, *Rev. Mod. Phys.* **78** (2006) 537–589, [astro-ph/0507632].

[245] M. Cicoli, G. Tasinato, I. Zavala, C. P. Burgess, and F. Quevedo, *Modulated Reheating and Large Non-Gaussianity in String Cosmology*, *JCAP* **1205** (2012) 039, [arXiv:1202.4580].

[246] K.-Y. Choi and O. Seto, *Modulated reheating by curvaton*, *Phys. Rev.* **D85** (2012) 123528, [arXiv:1204.1419]. [Erratum: Phys. Rev.D87,no.2,029902(2013)].

[247] F. Bernardeau, L. Kofman, and J.-P. Uzan, *Modulated fluctuations from hybrid inflation*, *Phys. Rev.* **D70** (2004) 083004, [astro-ph/0403315].

[248] N. Kobayashi, T. Kobayashi, and A. L. Erickcek, *Rolling in the Modulated Reheating Scenario*, *JCAP* **1401** (2014) 036, [arXiv:1308.4154].

[249] K. Karwan and P. Channuie, *Preheating in an inflationary model with disformal coupling*, *Phys. Rev.* **D96** (2017), no. 2 023524, [arXiv:1701.01267].

[250] C. van de Bruck and C. Longden, *Higgs Inflation with a Gauss-Bonnet term in the Jordan Frame*, *Phys. Rev.* **D93** (2016), no. 6 063519, [arXiv:1512.04768].

[251] C. van de Bruck, K. Dimopoulos, C. Longden, and C. Owen, *Gauss-Bonnet-coupled Quintessential Inflation*, arXiv:1707.06839.

[252] F. Bezrukov, A. Magnin, M. Shaposhnikov, and S. Sibiryakov, *Higgs inflation: consistency and generalisations*, *JHEP* **01** (2011) 016, [arXiv:1008.5157].

[253] F. Bezrukov, J. Rubio, and M. Shaposhnikov, *Living beyond the edge: Higgs inflation and vacuum metastability*, *Phys. Rev.* **D92** (2015), no. 8 083512, [arXiv:1412.3811].

[254] F. L. Bezrukov, A. Magnin, and M. Shaposhnikov, *Standard Model Higgs boson mass from inflation*, *Phys. Lett.* **B675** (2009) 88–92, [arXiv:0812.4950].

[255] A. O. Barvinsky, A. Yu. Kamenshchik, and A. A. Starobinsky, *Inflation scenario via the Standard Model Higgs boson and LHC*, *JCAP* **0811** (2008) 021, [arXiv:0809.2104].

[256] Z.-K. Guo and D. J. Schwarz, *Slow-roll inflation with a Gauss-Bonnet correction*, *Phys. Rev.* **D81** (2010) 123520, [arXiv:1001.1897].

[257] J.-c. Hwang and H. Noh, *Conserved cosmological structures in the one loop superstring effective action*, *Phys. Rev.* **D61** (2000) 043511, [astro-ph/9909480].

[258] C. Cartier, J.-c. Hwang, and E. J. Copeland, *Evolution of cosmological perturbations in nonsingular string cosmologies*, *Phys. Rev.* **D64** (2001) 103504, [astro-ph/0106197].

[259] M. Robinson, *Models of the very early universe with multiple scalar fields*. PhD thesis, University of Sheffield, 2015.

[260] P. J. E. Peebles and A. Vilenkin, *Quintessential inflation*, *Phys. Rev.* **D59** (1999) 063505, [astro-ph/9810509].

[261] K. Dimopoulos, *Towards a model of quintessential inflation*, *Nucl. Phys. Proc. Suppl.* **95** (2001) 70–73, [astro-ph/0012298]. [,70(2000)].

[262] K. Dimopoulos and J. W. F. Valle, *Modeling quintessential inflation*, *Astropart. Phys.* **18** (2002) 287–306, [astro-ph/0111417].

[263] S. C. C. Ng, N. J. Nunes, and F. Rosati, *Applications of scalar attractor solutions to cosmology*, *Phys. Rev.* **D64** (2001) 083510, [astro-ph/0107321].

[264] G. Huey and J. E. Lidsey, *Inflation, brane worlds and quintessence*, *Phys. Lett.* **B514** (2001) 217–225, [astro-ph/0104006].

[265] A. S. Majumdar, *From brane assisted inflation to quintessence through a single scalar field*, *Phys. Rev.* **D64** (2001) 083503, [astro-ph/0105518].

[266] N. J. Nunes and E. J. Copeland, *Tracking quintessential inflation from brane worlds*, *Phys. Rev.* **D66** (2002) 043524, [astro-ph/0204115].

[267] R. Rosenfeld and J. A. Frieman, *A Simple model for quintessential inflation*, *JCAP* **0509** (2005) 003, [astro-ph/0504191].

[268] R. Rosenfeld and J. A. Frieman, *Cosmic microwave background and large-scale structure constraints on a simple quintessential inflation model*, *Phys. Rev.* **D75** (2007) 043513, [astro-ph/0611241].

[269] M. Bastero-Gil, A. Berera, B. M. Jackson, and A. Taylor, *Hybrid Quintessential Inflation*, *Phys. Lett.* **B678** (2009) 157–163, [arXiv:0905.2937].

[270] M. C. Bento, R. G. Felipe, and N. M. C. Santos, *Brane assisted quintessential inflation with transient acceleration*, *Phys. Rev.* **D77** (2008) 123512, [arXiv:0801.3450].

[271] V. H. Cardenas, *Tachyonic quintessential inflation*, *Phys. Rev.* **D73** (2006) 103512, [gr-qc/0603013].

[272] M. Dias and A. R. Liddle, *On the possibility of braneworld quintessential inflation*, *Phys. Rev.* **D81** (2010) 083515, [arXiv:1002.3703].

[273] R. A. Frewin and J. E. Lidsey, *On identifying the present day vacuum energy with the potential driving inflation*, *Int. J. Mod. Phys.* **D2** (1993) 323–350, [astro-ph/9312035].

[274] C.-Q. Geng, M. W. Hossain, R. Myrzakulov, M. Sami, and E. N. Saridakis, *Quintessential inflation with canonical and noncanonical scalar fields and Planck 2015 results*, *Phys. Rev.* **D92** (2015), no. 2 023522, [arXiv:1502.03597].

[275] C.-Q. Geng, C.-C. Lee, M. Sami, E. N. Saridakis, and A. A. Starobinsky, *Observational constraints on successful model of quintessential Inflation*, *JCAP* **1706** (2017), no. 06 011, [arXiv:1705.01329].

[276] E. Guendelman, E. Nissimov, and S. Pacheva, *Quintessential Inflation, Unified Dark Energy and Dark Matter, and Higgs Mechanism*, arXiv:1609.06915.

[277] J. de Haro, *On the viability of quintessential inflation models from observational data*, *Gen. Rel. Grav.* **49** (2017), no. 1 6, [arXiv:1602.07138].

[278] J. de Haro and S. Pan, *Bulk viscous quintessential inflation*, arXiv:1512.03033.

[279] J. de Haro and L. Aresté Saló, *Reheating constraints in quintessential inflation*, *Phys. Rev.* **D95** (2017), no. 12 123501, [arXiv:1702.04212].

[280] M. W. Hossain, R. Myrzakulov, M. Sami, and E. N. Saridakis, *Variable gravity: A suitable framework for quintessential inflation*, *Phys. Rev.* **D90** (2014), no. 2 023512, [arXiv:1402.6661].

[281] M. W. Hossain, R. Myrzakulov, M. Sami, and E. N. Saridakis, *Unification of inflation and dark energy à la quintessential inflation*, *Int. J. Mod. Phys.* **D24** (2015), no. 05 1530014, [arXiv:1410.6100].

[282] A. R. Khalifeh, *Quintessential Inflation in Mimetic Dark Matter*, arXiv:1506.06250.

[283] A. Membiela and M. Bellini, *Quintessential inflation from a variable cosmological constant in a 5D vacuum*, *Phys. Lett.* **B641** (2006) 125–129, [gr-qc/0606119].

[284] I. P. Neupane, *Reconstructing a model of quintessential inflation*, *Class. Quant. Grav.* **25** (2008) 125013, [arXiv:0706.2654].

[285] J. Rubio and C. Wetterich, *Emergent scale symmetry: connecting inflation and dark energy*, arXiv:1705.00552.

[286] M. Sami and V. Sahni, *Quintessential inflation on the brane and the relic gravity wave background*, *Phys. Rev.* **D70** (2004) 083513, [hep-th/0402086].

[287] J. C. Bueno Sanchez and K. Dimopoulos, *Trapped Quintessential Inflation*, *Phys. Lett.* **B642** (2006) 294–301, [hep-th/0605258]. [Erratum: Phys. Lett.B647,526(2007)].

[288] J. C. Bueno Sanchez and K. Dimopoulos, *Trapped quintessential inflation in the context of flux compactifications*, *JCAP* **0710** (2007) 002, [hep-th/0606223].

[289] X.-h. Zhai and Y.-b. Zhao, *Dynamics of quintessential inflation*, *Chin. Phys.* **15** (2006) 2465, [astro-ph/0511512].

[290] S. Ahmad, R. Myrzakulov, and M. Sami, *Relic gravitational waves from Quintessential Inflation*, arXiv:1705.02133.

[291] M. C. Bento, R. G. Felipe, and N. M. C. Santos, *A simple quintessential inflation model*, *Int. J. Mod. Phys.* **A24** (2009) 1639.

[292] K. Dimopoulos and C. Owen, *Quintessential Inflation with α-attractors*, *JCAP* **1706** (2017), no. 06 027, [arXiv:1703.00305].

[293] T. P. Sotiriou and E. Barausse, *Post-Newtonian expansion for Gauss-Bonnet gravity*, *Phys. Rev.* **D75** (2007) 084007, [gr-qc/0612065].

[294] L. Amendola, C. Charmousis, and S. C. Davis, *Constraints on Gauss-Bonnet gravity in dark energy cosmologies*, *JCAP* **0612** (2006) 020, [hep-th/0506137].

[295] L. Amendola, C. Charmousis, and S. C. Davis, *Solar System Constraints on Gauss-Bonnet Mediated Dark Energy*, *JCAP* **0710** (2007) 004, [arXiv:0704.0175].

[296] C. van de Bruck and C. Longden, *Running of the Running and Entropy Perturbations During Inflation*, *Phys. Rev.* **D94** (2016), no. 2 021301, [arXiv:1606.02176].

[297] C. Longden, *Non-standard hierarchies of the runnings of the spectral index in inflation*, *Universe* **3** (2017), no. 1 [arXiv:1702.00206].

[298] J. Garcia-Bellido and D. Roest, *Large-N running of the spectral index of inflation*, *Phys. Rev.* **D89** (2014), no. 10 103527, [arXiv:1402.2059].

[299] S. Gariazzo, O. Mena, H. Ramirez, and L. Boubekeur, *Primordial power spectrum features in phenomenological descriptions of inflation*, arXiv:1606.00842.

[300] K. Kohri and T. Matsuda, *Ambiguity in running spectral index with an extra light field during inflation*, *JCAP* **1502** (2015) 019, [arXiv:1405.6769].

[301] M. Peloso, L. Sorbo, and G. Tasinato, *A falsely fat curvaton with an observable running of the spectral tilt*, *JCAP* **1406** (2014) 040, [arXiv:1401.7136].

[302] G. Cabass, E. Di Valentino, A. Melchiorri, E. Pajer, and J. Silk, *Constraints on the running of the running of the scalar tilt from CMB anisotropies and spectral distortions*, *Phys. Rev.* **D94** (2016), no. 2 023523, [arXiv:1605.00209].

[303] G. Cabass, A. Melchiorri, and E. Pajer, *μ distortions or running: A guaranteed discovery from CMB spectrometry*, *Phys. Rev.* **D93** (2016), no. 8 083515, [arXiv:1602.05578].

[304] J. Chluba, *Which spectral distortions does ΛCDM actually predict?*, arXiv:1603.02496.

[305] J. Chluba, J. Hamann, and S. P. Patil, *Features and New Physical Scales in Primordial Observables: Theory and Observation*, *Int. J. Mod. Phys.* **D24** (2015), no. 10 1530023, [arXiv:1505.01834].

[306] A. Kogut, D. J. Fixsen, D. T. Chuss, J. Dotson, E. Dwek, M. Halpern, G. F. Hinshaw, S. M. Meyer, S. H. Moseley, M. D. Seiffert, D. N. Spergel, and E. J. Wollack, *The Primordial Inflation Explorer (PIXIE): a nulling polarimeter for cosmic microwave background observations*, *JCAP* **7** (July, 2011) 025, [arXiv:1105.2044].

[307] **CORE** Collaboration, E. Di Valentino et al., *Exploring Cosmic Origins with CORE: Cosmological Parameters*, arXiv:1612.00021.

[308] **CORE** Collaboration, F. Finelli et al., *Exploring Cosmic Origins with CORE: Inflation*, arXiv:1612.08270.

[309] **PRISM** Collaboration, P. André et al., *PRISM (Polarized Radiation Imaging and Spectroscopy Mission): An Extended White Paper*, *JCAP* **1402** (2014) 006, [arXiv:1310.1554].

[310] R. A. Battye, R. D. Davies, and J. Weller, *Neutral hydrogen surveys for high redshift galaxy clusters and proto-clusters*, *Mon. Not. Roy. Astron. Soc.* **355** (2004) 1339–1347, [astro-ph/0401340].

[311] **SKA Cosmology SWG** Collaboration, R. Maartens, F. B. Abdalla, M. Jarvis, and M. G. Santos, *Overview of Cosmology with the SKA*, *PoS* **AASKA14** (2015) 016, [arXiv:1501.04076].

[312] L. Amendola et al., *Cosmology and Fundamental Physics with the Euclid Satellite*, arXiv:1606.00180.

[313] A. Pourtsidou, *Synergistic tests of inflation*, arXiv:1612.05138.

[314] J. B. Muñoz, E. D. Kovetz, A. Raccanelli, M. Kamionkowski, and J. Silk, *Towards a measurement of the spectral runnings*, arXiv:1611.05883.

[315] C. van de Bruck and L. E. Paduraru, *Simplest extension of Starobinsky inflation*, *Phys. Rev.* **D92** (2015) 083513, [arXiv:1505.01727].

[316] J. W. Moffat, *Superluminary universe: A Possible solution to the initial value problem in cosmology*, *Int. J. Mod. Phys.* **D2** (1993) 351–366, [gr-qc/9211020].

[317] N. Afshordi and J. Magueijo, *The critical geometry of a thermal big bang*, *Phys. Rev.* **D94** (2016), no. 10 101301, [arXiv:1603.03312].

[318] J. W. Moffat, *Variable speed of light cosmology and bimetric gravity: An Alternative to standard inflation*, *Int. J. Mod. Phys.* **A20** (2005) 1155–1162, [gr-qc/0404066].

[319] J. Magueijo, *New varying speed of light theories*, *Rept. Prog. Phys.* **66** (2003) 2025, [astro-ph/0305457].

[320] J. W. Moffat, *Variable speed of light cosmology: An Alternative to inflation*, hep-th/0208122.

[321] V. Salzano and M. P. Dabrowski, *Statistical hierarchy of varying speed of light cosmologies*, arXiv:1612.06367.

[322] J. W. Moffat, *Bimetric Gravity, Variable Speed of Light Cosmology and Planck2013*, arXiv:1306.5470.

[323] D. Brizuela, C. Kiefer, and M. Kraemer, *Quantum-gravitational effects on gauge-invariant scalar and tensor perturbations during inflation: The de Sitter case*, *Phys. Rev.* **D93** (2016), no. 10 104035, [arXiv:1511.05545].

[324] D. Brizuela, C. Kiefer, and M. Kraemer, *Quantum-gravitational effects on gauge-invariant scalar and tensor perturbations during inflation: The slow-roll approximation*, *Phys. Rev.* **D94** (2016), no. 12 123527, [arXiv:1611.02932].

[325] M. Bojowald, G. Calcagni, and S. Tsujikawa, *Observational test of inflation in loop quantum cosmology*, *JCAP* **1111** (2011) 046, [arXiv:1107.1540].